

THE ROLE OF THE FLAVODIIRON PROTEINS IN NITRIC OXIDE DETOXIFICATION

João Filipe Bogalho Vicente

*Dissertation presented to obtain the European Label PhD degree in Biochemistry
at the Instituto de Tecnologia Química e Biológica, Universidade Nova de Lisboa,
and at the Dipartimento di Scienze Biochimiche "A. Rossi Fanelli",
Università degli Studi di Roma, "La Sapienza"*

Supervisors

Prof. Miguel Teixeira (ITQB)
Prof. Paolo Sarti (Univ. di Roma)

Opponents

Prof. Paolo Sarti (Univ. di Roma)
Dr. Alessandro Giuffrè (Univ. di Roma)



Instituto de Tecnologia Química e Biológica,
Universidade Nova de Lisboa



Dipartimento di Scienze Biochimiche
"A. Rossi Fanelli",
Università degli Studi di Roma, "La Sapienza"

First Edition, January 2007

Metalloproteins and Bioenergetics Laboratory
Instituto de Tecnologia Química e Biológica, Universidade Nova de Lisboa
Av. da República (EAN), 2781-901 Oeiras, PORTUGAL

Dipartimento di Scienze Biochimiche "A. Rossi Fanelli"
Università degli Studi di Roma, "La Sapienza"
Piazzale Aldo Moro 5, 00185 Roma, ITALIA

Foreword

This dissertation comprises research work performed under the supervision of Prof. Miguel Teixeira, in the Metalloproteins and Bioenergetics Laboratory from the Instituto de Tecnologia Química e Biológica, Universidade Nova de Lisboa, and Prof. Paolo Sarti, in the Dipartimento di Scienze Biochimiche "A. Rossi Fanelli" from the Università degli Studi di Roma, "La Sapienza". This close collaboration was formalized by an agreement of the two Universities by transforming this dissertation in a European Label PhD.

The work here reported concerns recent developments on the knowledge about the family of flavodiiron proteins, and describes the steps that led to the establishment of a role for these proteins in nitric oxide detoxification. The initially proposed role of these proteins in oxygen scavenging in anaerobes should still be considered, as suggested by recent reports. Therefore, this dissertation focuses not only on the growing evidence for a role of flavodiiron proteins in nitric oxide detoxification, but also on the ambiguity of NO vs. O₂ reductase activities of these proteins.

The thesis is organized as follows: the introduction is split in two chapters, one focusing on general aspects of nitric oxide biochemistry, and a second one concerning the flavodiiron proteins family. The introduction is followed by several chapters based on original publications, and the thesis closes with a discussion chapter that integrates the described results.

Acknowledgements

I want to express my deepest gratitude to the following people, for what is within and beyond this work.

My supervisor at ITQB, Prof. Miguel Teixeira, to whom I am greatly indebted for the opportunity to grow to be a scientist and to develop my research in the best environment I can imagine. His passion for science, extended knowledge, broadness of interests and eagerness for discovery, were, are, and will always be a source of inspiration. I am thankful for the freedom to pursue the research where it took me, and the opportunities to visit other laboratories. With him I witnessed and learned the “simple” pleasure of finding things out.

My supervisor in Università di Roma “La Sapienza”, Prof. Paolo Sarti, for accepting me as his PhD student and providing me the means to develop part of my research studies in a friendly and positively challenging environment. I learned a lot from our most interesting discussions, and felt compelled to seek an understanding of the physiological integration of everything.

My early co-supervisor at ITQB, Dr. Cláudio M. Gomes, for his friendship and for his committed dedication to my introduction to science, in a dynamic and passionate way, continuously challenging me to devise the means to provide answers to my questions. His contribution to my development as a researcher is invaluable and many of the lessons I learned from him still hold as guiding lights.

Dr. Alessandro Giuffrè from Università di Roma “La Sapienza”, for his friendship, and for some of the most valuable scientific training I had. Alessandro shared with me his deep knowledge on many scientific subjects and I learned immensely from his pondered and rational approach towards experimental planning, data analysis, data validation and interpretation. He is an inspiring example of a committed and passionate scientist, who also provided me a home far from my home.

Dr. Lígia M. Saraiva at ITQB, for the support, learning opportunities, enthusiasm in pursuing a novel research field against many obstacles, and for allowing me to participate in several of the interesting ongoing research projects.

Prof. Maurizio Brunori from Università di Roma “La Sapienza”, for welcoming me to perform the kinetics studies on flavorubredoxin in a fantastic environment, and for sharing with me his research experience and deep scientific knowledge through fruitful discussions.

Francesca M. Scandurra, my good lab friend with whom I shared a PhD “label” and more importantly many good moments, in and out of the lab. I learned a lot from the mutual learning experience and gained a good friend for life.

Prof. Claudina Rodrigues-Pousada, Dr. Solange Oliveira and Rute Rodrigues, for the ongoing collaboration in the understanding of the oxygen detoxification mechanisms in *Desulfovibrio gigas*. I want to specially thank Rute for the perseverance and hard work, not only in the molecular genetics studies, but also in the purifications and characterisation steps done at our lab.

Prof. Cláudio Soares and Bruno Victor, for their interest in the protein modelling studies of flavodiiron proteins, and for interesting and fruitful discussions. I want to thank Bruno for continuously sharing his latest findings regarding this project, and for the laughs we have about everything.

Prof. Maria Arménia Carrondo, for her continuous interest in the structural studies of flavodiiron proteins, for the support, and for allowing me to get a hands-on first taste of protein crystallization and protein crystallography.

João Carita, for the friendship and valuable support in my first steps of cell mass production and several other microbiology techniques.

My colleagues and friends at the Metalloproteins and Bioenergetics Laboratory, for the friendly and dynamic environment, the availability and support, and interesting discussions: Manuela Pereira, Ana Melo, Andreia Fernandes, Smilja Todorovic, Andreia Veríssimo, Filipa Sousa, Ana Batista, Ana Refojo, Vera Gonçalves, Filipa Pinto, and previous members of our group: Susana Lobo, Rita Lemos, Isabel Abreu. I feel especially indebted to Manuela, Rita and Isabel for the patience to teach me many things at the early stages of my research.

João V. Rodrigues, my lab mate, for his support in the kinetics studies of flavorubredoxin, for his inspiring drive to devise gadgets from waste, and for the fun we have in and out of the lab.

Célia Romão, my lab mate since 1999, for the enthusiastic involvement and continuous efforts on the structural side of the research here described (and for the initial support in my research training).

Everyone in the Group of Dr. Lígia Saraiva, especially Marta Justino, for the collaborative and interesting work regarding the transcriptional response of NO-

challenged *E. coli*, but more importantly for the enthusiasm and dedication to this project. Cláudia Almeida and Vera Gonçalves, for their kindness and permanent availability to help me, by performing molecular biology tasks. Vera and Lígia Nobre for the collaborative work on *S. aureus* Hmp.

My lab mates in Roma, who created a fantastic environment for me to do my research work and to have the greatest fun possible: Elena, Daniela, Cecilia, Antonella, Emilio, Alessandra, Marzia, Fabrizio, and everyone else in the department that I had the pleasure to meet (a special mention to the soon-to-be champions Lokomotiv Mordor).

Everyone in the groups of Dr. Cláudio Gomes (Sónia, Hugo, Raquel, Vesna and Bárbara), and Dr. Inês Pereira (Filipa, Sofia, Sofia and Tiago), for the friendly and mutually helpful environment in the “3rd floor” of ITQB II.

My colleagues and friends from the early days at ITQB I, scattered among several groups: Ricardo Pires, Filipa Valente, Patrícia Pereira, Ilídio Correia and Catarina Paquete, for the companionship and discussions.

Vitor Teixeira and Vanessa Morais, my fellow “SCANners”, with whom I had much fun and the pleasure to work together in the organization of the SCAN seminars.

Prof. Simon de Vries, from the Delft University of Technology, for the opportunity to visit his lab and perform kinetics studies, using the fabulous microsecond freeze-hyperquenching machine, with the valuable support of Marc Strampaad. I am also grateful for the many interesting conversations about science, the world and our common passion for football.

Dr. Wolfram Meyer-Klaucke and Dr. Maud Achard-Joris, from EMBL, Hamburg, for the EXAFS studies on the flavodiiron domain of flavorubredoxin.

Prof. Miguel de la Rosa, Dr. José Navarro and Dr. Manuel Hervás, from the Instituto de Bioquímica Vegetal y Fotosíntesis, Universidad de Sevilla, for kindly receiving me for two research visits, to perform kinetics studies using laser flash photolysis and to learn cyanobacterial growth techniques.

Tim Urich and Fabian Müller, two special people that I met in visits to my lab, that grown to be good friends, and with whom I shared great moments in and out of the lab(s).

Tiago Bandeiras, my Friend and school/university/lab mate for more than 15 years, who is the proof that brotherhood means more than sharing blood. As a hard-working scientist and a person, he is a permanent and shining example to me.

All my true friends, you know who you are.

All my family, especially **Avó Zeca**, for her undying love and dedication to her “Prof. Pardal”, and for her continuous curiosity about everything.

Élia for her love, support, patience, for being an example of hard-work, perseverance, sacrifice, and for being a shining light in dark days.

My parents, **Zé e Luísa**, for their love and support, permanent encouragement, understanding and interest in my development as a person and as a scientist. For letting me know from my very first interest in science that, as a career, it required passion, dedication, hard work and honesty, and for propelling me over every obstacle with dedication and pride. You’re the best.

Fundação para a Ciência e Tecnologia is acknowledged for financial support, by awarding a PhD Grant (SFRH/ BD/2002/9136).

Thesis Publications

The dissertation is based on original publications, listed by chronological order:

1 – Gomes, C.M., Vicente, J.B., Wasserfallen, A. and Teixeira, M. (2000) “Spectroscopic studies and characterization of a novel electron-transfer chain from *Escherichia coli* involving a flavorubredoxin and its flavoprotein reductase partner” *Biochemistry* 39(51):16230-7.

2 – Vicente, J.B., Gomes, C.M., Wasserfallen, A., Teixeira, M. (2002) “Module fusion in an A-type flavoprotein from the cyanobacterium *Synechocystis* condenses a multiple-component pathway in a single polypeptide chain” (2002) *Biochem Biophys Res Commun* 294(1):82-7.

3 – Gomes, C.M., Giuffrè, A., Forte, E., Vicente, J.B., Saraiva, L.M., Brunori, M., and Teixeira, M. (2002) “A novel type of nitric-oxide reductase. *Escherichia coli* flavorubredoxin” *J Biol Chem* 277(28):25273-6.

4 – Victor, B.L., Vicente, J.B., Rodrigues, R., Oliveira, S., Rodrigues-Pousada, C., Frazao, C., Gomes, C.M., Teixeira, M., Soares, C.M. (2003) “Docking and electron transfer studies between rubredoxin and rubredoxin:oxygen oxidoreductase” *J Biol Inorg Chem* 8(4):475-88.

5 – Saraiva, L.M., Vicente, J.B., Teixeira, M. (2004) “The role of the flavodiiron proteins in microbial nitric oxide detoxification” *Adv Microb Physiol* 49:77-129.

6 – Vicente, J.B., Teixeira, M. (2005) “Redox and spectroscopic properties of the *Escherichia coli* nitric oxide-detoxifying system involving flavorubredoxin and its NADH-oxidizing redox partner” *J Biol Chem* 280(41):34599-608.

7 – Rodrigues, R., Vicente, J.B., Felix, R., Oliveira, S., Teixeira, M., Rodrigues-Pousada, C. (2006) “*Desulfovibrio gigas* flavodiiron protein affords protection against nitrosative stress in vivo” *J Bacteriol* 188(8):2745-51.

8 – Vicente, J.B., Scandurra, F.M., Rodrigues, J.V., Brunori, M., Sarti, P., Teixeira, M., and Giuffrè, A. (2006) “Kinetics of electron transfer from NADH to the *Escherichia coli* nitric oxide reductase flavorubredoxin” *FEBS J*, in press

Dissertation Abstract

This dissertation portrays recent developments on the knowledge of a protein family whose once elusive role is presently clearer, although still prone to discussion. The family of Flavodiiron Proteins (FDPs), initially thought to protect anaerobes from oxygen exposure, have been proposed to have a role in nitric oxide detoxification. The main object of study of this dissertation, *Escherichia coli* Flavorubredoxin (FIRd) made a large contribution to establish this role. FIRd was the first member of the FDP family to be assigned as an NO reductase, followed by the demonstration of the same activity in other FDPs, although a role in oxygen scavenging by other FDP family members has to be considered.

On the basis of its primary structure, *E. coli* flavorubredoxin is a modular protein, composed by the flavodiiron structural core and a rubredoxin (Rd) domain fused at the C-terminus. The flavodiiron core, which defines this protein family, is built by a C-terminal FMN-binding flavodoxin domain fused with a β -lactamase domain, that harbours a non-haem diiron centre (the active site of NO/O₂ reduction), with carboxylate and histidine residues in the first coordination sphere. Consistent with the cofactor content inferred from the protein sequence, homologously-expressed recombinant FIRd is isolated (as a homotetramer, ~54 kDa/monomer) with ~3 Fe/monomer (one from the [Fe-Cys₄] centre in the rubredoxin domain and two from the non-haem diiron centre), and ~1 mol FMN/monomer. The complexity of FIRd's modular arrangement led to the construction of two truncated versions of FIRd: one consisting on its flavodiiron core (thus named FDP-D) and another consisting of the rubredoxin domain (Rd-D).

Spectroscopic studies on flavorubredoxin were consistent with the cofactor content. The visible spectrum of FIRd is dominated by the flavin moiety and the [Fe-Cys₄] centre from the Rd domain, yielding bands with maxima at ~380 nm and ~470 nm. A broader and less intense band at $\lambda > 550$ nm is almost exclusively

attributed to the Rd domain. Apparently, no signature in the visible spectrum of FIRd can be assigned to the non-haem diiron centre. Despite the conservation of the diiron ligands in FIRd and the iron quantifications, undisputable evidence for the non-haem diiron centre arose from EPR studies, where resonances characteristic of a mixed valence $\text{Fe}^{\text{III}}\text{-Fe}^{\text{II}}$ centre (rhombic signal with g values <2) was detected by mild chemical reduction and in the course of redox titrations, of both FIRd and its FDP domain.

Flavorubredoxin is part of an electron transfer (eT) chain that couples NADH oxidation to NO reduction and includes an FAD-binding NADH oxidase, thus named NADH:flavorubredoxin oxidoreductase (FIRd-Red). As the name indicates, FIRd-Red accepts electrons from NADH (as the primary source of reducing equivalents for this eT chain) and transfers those to FIRd, the rubredoxin domain being the electron entry point. With the spectroscopic footprints assigned to the FIRd and FIRd-Red cofactors, the functional properties of the electron transfer chain were studied in terms of its thermodynamic and kinetic parameters. The redox (thermodynamic) properties were studied by a combination of potentiometric and spectroscopic techniques, namely UV-visible and EPR spectroscopies. Studies on the truncated domains were essential to deconvolute part of the results obtained for the full-length FIRd. To test the effect of the interacting partners on the properties of each other, redox titrations were performed with the as isolated proteins and in stoichiometric mixtures. Interestingly, whereas the reduction potentials of the flavin cofactors in both proteins (FAD in FIRd-Red and FMN in FIRd) remained essentially unaltered ($E_m'_{\text{FAD}_{\text{ox}}/\text{FAD}_{\text{red}}}$: -240 mV; $E_o'_{\text{FMN}_{\text{ox}}/\text{FMN}_{\text{sq}}}$: -40 mV, $E_o'_{\text{FMN}_{\text{sq}}/\text{FMN}_{\text{red}}}$: -130 mV), the reduction potentials of the iron centres in FIRd were significantly altered, with possible functional implications. The reduction potential of Rd's $[\text{Fe-Cys}_4]$ centre increased from -123 mV to -65 mV in the presence of the reductase partner, and the diiron centre reduction potentials increased from -20 mV to +20 mV (for the

$\text{Fe}^{\text{III}}\text{-Fe}^{\text{III}}/\text{Fe}^{\text{III}}\text{-Fe}^{\text{II}}$ step) and -90 to -50 mV (for the $\text{Fe}^{\text{III}}\text{-Fe}^{\text{II}}/\text{Fe}^{\text{II}}\text{-Fe}^{\text{II}}$ step). On the basis of the observed modulation of FIRd's reduction potentials by its interacting partner, it could be envisaged an eT mechanism where electrons entering at the rubredoxin site could be shuttled in consecutive one-electron steps to the diiron active site *via* partially reduced FMN (FMN semiquinone, FMN_{sq}), possibly without achieving full reduction of FMN. This would imply a 4-electron load for the "fully" reduced enzyme, sufficient to catalyze either NO or oxygen reduction to N_2O or water, respectively.

The proposed intra-molecular eT mechanism was further assessed through kinetics studies, by performing stopped-flow absorption spectroscopy experiments. In these studies, the reaction of NADH with oxidized FIRd-Red, and the interaction between reduced FIRd-Red and oxidized FIRd, were investigated. NADH (but not NADPH) was shown to efficiently reduce FIRd-Red ($k = 5.5 \pm 2.2 \times 10^6 \text{ M}^{-1}\text{s}^{-1}$ at 5°C), with a limiting rate of $255 \pm 17 \text{ s}^{-1}$, in a process essentially pH independent (in the 5-8 pH range) and slightly ionic strength dependent. Furthermore, reduced FIRd-Red quickly reduced FIRd ($k \sim 1 \times 10^7 \text{ M}^{-1}\text{s}^{-1}$), with the reaction being significantly dependent on both pH and ionic strength. Interestingly, the combined kinetic and spectroscopic data point for the end-point of FIRd reduction by FIRd-Red to be in fact the semiquinone state of FMN, i.e., in accordance with the above mentioned thermodynamic properties. Moreover, the corresponding 4-electron load of reduced FIRd is corroborated by the reaction rates working on the truncated protein consisting only of the rubredoxin domain. Altogether, these observations point for a finely tuned eT chain, where FIRd-Red efficiently shuttles electrons from NADH to the Rd domain of FIRd, the FMN semiquinone acting as a one-electron shuttle between the Rd centre and the diiron site, the three centres being in very fast redox equilibration. Preclusion of FMN full reduction during the reaction cycle may contribute to prevent enzyme inactivation, as it has been observed in other modular proteins where FMN_{sq} acts

as one-electron shuttle.

Flavorubredoxin and its reductase partner are encoded in a dicistronic transcriptional unit, which is under the regulation of the adjacent yet divergently transcribed NorR, harbouring an NO-sensing non-haem Fe. This observation led to the proposal of a role of FIRd in NO detoxification, on the basis of molecular genetics studies and further confirmed by the *in vitro* reconstitution of the eT chain coupling NADH oxidation to NO reduction. By amperometric measurements with an NO-specific electrode, FIRd was shown to be an efficient NO reductase, with an activity ($\sim 15 \text{ s}^{-1}$) in the range of respiratory haem *b*₃-non-haem Fe NO reductases. The relevance of FIRd in NO detoxification in anaerobically-grown *E. coli* (as well as other FDPs and their respective organisms) was further demonstrated by transcriptional studies.

Studies were performed also on FDPs from other organisms, namely the *Desulfovibrio gigas* rubredoxin:oxygen oxidoreductase (Dg_ROO, the first member of this protein family to be characterized and whose structure revealed the flavodiiron core), and the FDP from the cyanobacterium *Synechocystis* sp. PCC6803.

The nature of the interaction between Dg_ROO and its rubredoxin redox partner was investigated by steady-state kinetics to correlate with modelling studies. The bell-shaped dependence of eT rates between Rd and Dg_ROO suggest a non-trivial electrostatic interaction, which the modelling results assign to a contribution of acidic residues from Rd and basic residues from Dg_ROO (at their surfaces), as well as to non-polar interactions. The initially proposed role of Dg_ROO in oxygen detoxification was assayed in a comparative fashion with a possible role in nitric oxide detoxification. The recombinant enzyme was shown to be an efficient *in vitro* NO and oxygen reductase (with reduced rubredoxin as the electron donor), the latter activity being far greater than the former.

On the basis of sequence analyses, it is observed that the FDP from *Synechocystis*

sp. PCC6803 (Ss_ATF) has a C-terminal NADH:flavin oxidoreductase module fused to the flavodiiron core. This extra module is common to the other 3 FDPs encoded in the genome of this organism, similarly to other cyanobacteria that also have multiple copies of FDPs in their genomes. Ss_FDP was heterologously over-expressed and its biochemical and spectroscopic characterization revealed the sub-stoichiometric presence of two flavins per monomer (the analyses revealed the presence of both FMN and FAD), one for each flavin binding domain, and ~1.9 Fe/monomer, consistent with a fully loaded diiron site. Ss_FDP displays a preference for NADH in comparison with NADPH, and it catalyzes the reduction of oxygen to water.

The results herein presented for the different flavodiiron proteins, with special emphasis on the *E. coli* flavorubredoxin, are discussed in the perspective of a role in nitric oxide detoxification with possible implications in the subversion of the host immune system by pathogenic microbes. The ambiguity of nitric oxide versus oxygen reduction by FDPs is framed with the available structural and functional data for different members of this protein family.

Resumo da Dissertação

Esta dissertação retrata desenvolvimentos recentes no conhecimento de uma família proteica cuja função outrora desconhecida é presentemente mais clara, embora ainda sendo alvo de discussão. Inicialmente, pensava-se que a família de Proteínas Flavodiférricas (FDPs) protegia organismos anaeróbicos da exposição a oxigénio, tendo sido mais tarde proposto um papel na destoxificação de óxido nítrico (NO). O principal objecto de estudo desta dissertação, a flavorubredoxina (FIRd) de *Escherichia coli*, contribuiu significativamente para a atribuição desta função à família das FDPs. A FIRd foi o primeiro membro da família das FDPs a ser considerado uma redutase do NO, seguida da demonstração da mesma actividade noutras FDPs, embora um papel na destoxificação de oxigénio deva ser considerado.

Com base na estrutura primária, a FIRd de *E. coli* é uma proteína modular, composta pela unidade estrutural flavodiférrica e um domínio rubredoxina (Rd) fundido no *C-terminus*. O domínio flavodiférrico, que define esta família de proteínas, é composto por um domínio flavodoxina C-terminal (que liga FMN), fundido com um domínio metalo- β -lactamase, que liga um centro diférrico não-hémico (o centro activo de redução de NO e/ou O₂) com resíduos carboxilato e histidina na primeira esfera de coordenação do Fe. De acordo com o conteúdo em cofactores deduzido pela sequência proteica, a FIRd recombinante, sobre-expressa homologamente, é isolada (como um homo-tetrâmero, ~54kDa/monómero) com ~3 Fe/monómero (um do centro [Fe-Cis₄] do domínio rubredoxina e dois do centro binuclear de ferro não-hémico), e ~1 FMN/monómero. A complexidade da disposição modular da FIRd levou à construção de duas versões truncadas da mesma: uma consistindo do seu domínio flavodiférrico (chamada FDP-D) e outra consistindo do seu domínio rubredoxina (Rd-D).

Estudos espectroscópicos da FIRd estão de acordo com os cofactores determinados para esta proteína. O espectro de visível da FIRd é dominado pelo

cofactor flavínico e pelo centro [Fe-Cis₄] do domínio Rd, resultando em bandas com máximos a $\lambda \sim 380$ nm e $\lambda \sim 470$ nm. Uma banda alargada e de menor intensidade a $\lambda > 550$ nm é atribuída quase exclusivamente ao domínio Rd. Aparentemente, nenhuma evidência no espectro de visível da FIRd pode ser atribuída ao centro binuclear de ferro não-hémico. Apesar da conservação dos ligandos do centro binuclear e das quantificações de ferro, provas irrefutáveis da presença do centro foram obtidos com estudos espectroscópicos de ressonância paramagnética electrónica (EPR). Por redução química e no decorrer de titulações redox, detectaram-se ressonâncias características de um centro de valência mista Fe^{III}-Fe^{II} (sinal rômbico com valores de $g < 2$).

A flavorubredoxina faz parte de uma cadeia de transferência electrónica que acopla a oxidação de NADH à redução de NO, que inclui uma NADH oxidase (que liga FAD) denominada NADH:flavorubredoxina oxidoreductase (FIRd-Red). A FIRd-Red aceita electrões do NADH e transfere-os para a FIRd, sendo que o domínio Rd é o ponto de entrada de electrões na FIRd. Com as características espectrais de cada cofactor da FIRd e da FIRd-Red atribuídas, estudaram-se as propriedades funcionais desta cadeia de transferência electrónica, nomeadamente os parâmetros termodinâmicos e cinéticos. As propriedades redox foram determinadas por uma combinação de técnicas potenciométricas e espectroscópicas (UV-visível e EPR). Estudos com os domínios truncados foram essenciais para a desconvolução dos resultados obtidos com a FIRd intacta. Para testar o efeito de cada parceiro redox em interacção nas propriedades do outro, titulações redox foram efectuadas com as proteínas isoladas e com uma mistura estequiométrica de ambas. É com interesse que se verifica que os potenciais dos cofactores flavínicos de ambas as proteínas (FAD na FIRd-Red e FNM na FIRd) se mantêm praticamente inalterados ($E_m' FAD_{ox}/FAD_{red}$: -240 mV; $E_o' FMN_{ox}/FMN_{sq}$: -40 mV, $E_o' FMN_{sq}/FMN_{red}$: -130 mV), ao passo que os potenciais dos dois centros de ferro da FIRd sofrem alterações com possíveis implicações funcionais. O potencial de

redução do centro [Fe-Cys₄] aumentou de -123 mV para -65 mV na presença do parceiro FIRd-Red, e os potenciais do centro binuclear de ferro aumentaram de -20 mV para +20 mV (para o passo Fe^{III}-Fe^{III}/Fe^{III}-Fe^{II}) e de -90 mV para -50 mV (para o passo Fe^{III}-Fe^{II}/Fe^{II}-Fe^{II}). Com base na modulação pela FIRd-Red dos potenciais de redução da FIRd, um mecanismo de transferência electrónica pode ser idealizado, em que os electrões que entram na FIRd pelo domínio Rd são transferidos em passos consecutivos de um electrão para o centro binuclear de ferro, através do FMN parcialmente reduzido (semiquinona de FMN, FMNsq), possivelmente sem atingir redução completa do FMN. Tal implicaria uma carga total de 4 electrões para a FIRd “totalmente” reduzida, suficiente para catalizar a redução de NO ou O₂ a N₂O ou H₂O, respectivamente.

O mecanismo de transferência electrónica intra-molecular foi analisado através de estudos cinéticos, por espectroscopia de absorção de fluxo interrompido. Nestes estudos, estudaram-se a reacção do NADH com a FIRd-Red, e a interacção entre FIRd-Red reduzida e FIRd oxidada. Demonstrou-se a eficiência com que o NADH (mas não o NADPH) reduz a FIRd-Red ($k = 5.5 \pm 2.2 \times 10^6 \text{ M}^{-1}\text{s}^{-1}$ at 5°C), num processo independente do pH na gama de 5.0 a 8.0 e relativamente dependente da força iónica. Paralelamente, demonstrou-se que a FIRd-Red reduz eficientemente a FIRd ($k \sim 1 \times 10^7 \text{ M}^{-1}\text{s}^{-1}$), sendo que a reacção depende significativamente do pH e força iónica. Os dados cinéticos e espectroscópicos combinados apontam para que o estado semiquinona do FMN da FIRd seja o ponto-final da redução da FIRd pela FIRd-Red, corroborando desta forma a proposta mecanística baseada apenas nas propriedades redox. Em suma, os resultados dos estudos termodinâmicos e cinéticos demonstram uma cadeia de transferência electrónica afinada, em que a FIRd-Red transfere eficientemente electrões para o domínio Rd da FIRd, onde o estado semiquinona do FMN transfere um electrão de cada vez do domínio Rd para o centro binuclear de ferro, sendo que os três cofactores estarão em rápido equilíbrio redox.

A flavorubredoxina e a sua parceira redutase estão codificadas por dois genes que formam uma unidade transcripcional dicistrónica, sob a regulação do produto do gene adjacente (*norR*), que é transcrito na direcção oposta. Esta observação levou à proposta de um papel da FIRd na destoxificação de NO, com base em estudos de genética molecular, posteriormente confirmados pela medição *in vitro* da actividade NO redutase da FIRd (com electrões provenientes do NADH, via FIRd-Red). Por ensaios amperométricos, demonstrou-se que a FIRd é uma NO redutase eficiente, com uma actividade ($\sim 15 \text{ s}^{-1}$) dentro da gama de valores para as NO redutases respiratórias. A relevância da FIRd na destoxificação de NO em *E. coli* crescendo em anaerobiose foi subseqüentemente confirmada por estudos transcripcionais, assim como foi observado para outras FDPs de diferentes organismos.

Estudos foram realizados com as FDPs de *Desulfovibrio gigas* (denominada por ROO, rubredoxina:oxigénio oxidoreductase) e da cianobactéria *Synechocystis* sp. PCC6803 (denominada Ss_ATF).

A base molecular da interacção entre a ROO de *D. gigas* e a rubredoxina (o seu parceiro redox) foi estudada pela correlação de dados de cinéticas de estado estacionário e de simulações e modelação proteica. A forma da dependência das taxas de transferência electrónica entre a Rd e a ROO sugerem uma interacção electrostática não trivial, que os resultados de modelação atribuem a uma contribuição de resíduos ácidos à superfície da Rd e resíduos básicos à superfície da ROO e a uma contribuição de interacções não polares. A ROO recombinante é dotada de actividades NO e O₂ redutase significativas, sendo mais eficiente com oxigénio como substrato.

Com base em análises de sequências, observa-se que as FDPs da cianobactéria *Synechocystis* sp. PCC6803 têm um módulo C-terminal com características de proteínas do tipo NAD(P)H:flavina oxidoreductase fundido à unidade estrutural flavodiférrica. A Ss_ATF sobre-expressa heterologamente é isolada com ~ 1.9

Fe/monómero e um conteúdo sub-estequiométrico de dois tipos de flavina: FMN e FAD. A Ss_ATF demonstra a capacidade de oxidar *per se* NAD(P)H, com preferência para o NADH, catalizando a redução de oxigénio a água.

Os resultados expostos nesta dissertação para as diferentes FDPs, com especial ênfase relativamente à flavorubredoxin de *E. coli*, são discutidos na perspectiva de um papel na destoxificação de NO, com possíveis implicações na subversão do sistema imunitário por parte de microrganismos patogénicos. A ambiguidade da redução de NO e de O₂ catalizadas por FDPs são enquadradas com os dados estruturais e funcionais presentemente disponíveis.

Table of Contents

1	CHEMISTRY AND BIOLOGY OF NITRIC OXIDE	
1.1	Historic Background of Nitric Oxide	3
1.2	Physical-Chemical Properties of Nitric Oxide	4
1.3	Reactions and Reactivity of Nitric Oxide	6
	Autoxidation of NO	6
	Reaction of NO with Superoxide	7
	Radical Chemistry of NO	8
	Reactions of NO with Metals	8
	Reactions of NO with Thiols	10
	Chemistry of the Nitroxyl Anion, NO ⁻ /HNO	11
1.4	Biological Aspects of Nitric Oxide	12
	Sources of Nitric Oxide in Biological Systems	12
	<i>Denitrification</i>	12
	<i>NO Synthases</i>	19
	“Good” and “Bad” Nitric Oxide: the Threshold Between Signalling and Toxicity	23
	Nitric Oxide in the Host-Pathogen Interaction	28
	Microbial Defence Mechanisms Against Nitric Oxide	30
	Genetic Responses to Nitrosative Stress	32
	Prokaryotic Defence Systems Against Nitrosative Stress	35
	Other Enzymatic Systems	38
	References	40
2	THE FAMILY OF THE FLAVODIIRON PROTEINS	
2.1	Oxygen Biochemistry in “Anaerobes”	48
2.2	Establishment of a Novel Family of Flavodiiron Proteins	54
	Structure of <i>Desulfovibrio gigas</i> Rubredoxin:Oxygen Oxidoreductase	55
	A Novel Type of Non-Haem Diiron Centre in a β -Lactamase Fold	57
	Modular Nature of Flavodiiron Proteins – Structural Classification	59
	Diversity of Electron Transfer Chains	61
2.3	Basis for a Role in Nitric Oxide Detoxification	64
	References	67

3	Spectroscopic studies and characterisation of a novel electron transfer chain from <i>Escherichia coli</i> involving a flavorubredoxin and its flavoprotein reductase partner	
3.1	Introduction	75
3.2	Materials and Methods	76
3.3	Results and Discussion	79
3.4	Conclusions	89
3.5	References	91
4	A novel type of nitric oxide reductase: <i>Escherichia coli</i> flavorubredoxin	
4.1	Introduction	97
4.2	Materials and Methods	99
4.3	Results and Discussion	100
4.4	Conclusions	103
4.5	References	105
5	Redox and Spectroscopic Properties of the <i>Escherichia coli</i> Nitric Oxide Detoxifying System Involving Flavorubredoxin and its NADH Oxidizing Redox Partner	
5.1	Introduction	111
5.2	Materials and Methods	114
5.3	Results and Discussion	115
5.4	Conclusions	128
5.5	References	130
6	Kinetics of Electron Transfer from NADH to the <i>Escherichia coli</i> Nitric Oxide Reductase Flavorubredoxin	
6.1	Introduction	137
6.2	Materials and Methods	139
6.3	Results	141
6.4	Discussion	148
6.5	References	152

7	Functional properties of <i>Desulfovibrio gigas</i> Flavodiiron Protein: interaction with rubredoxin and NO vs. O₂ reduction	
7.1	Introduction	157
7.2	Materials and Methods	159
7.3	Results and Discussion	164
7.4	Conclusions	170
7.5	References	171

8	Module fusion in an A-Type Flavoprotein from the cyanobacterium <i>Synechocystis</i> condenses a multiple component pathway in a single polypeptide chain	
8.1	Introduction	177
8.2	Materials and Methods	179
8.3	Results and Discussion	181
8.4	Conclusions	188
8.5	References	189

9 | **DISCUSSION**

9.1	Structural and Functional Properties of Flavodiiron Proteins	192
	<i>Primary structure, domain arrangement and electron transfer chains</i>	192
	<i>Molecular properties</i>	193
	<i>Spectroscopic properties</i>	194
	<i>Redox properties</i>	196
	<i>Kinetic properties</i>	198
	<i>Structural properties</i>	200
9.2	Role of <i>Escherichia coli</i> Flavorubredoxin in Nitric Oxide Detoxification	201
	<i>Genetic basis for a role in nitric oxide detoxification</i>	201
	<i>Nitric oxide reductase activity of flavodiiron proteins</i>	203
	<i>Nitric oxide reduction mechanism</i>	204
	<i>Nitric oxide vs. oxygen reduction by flavodiiron proteins</i>	206
	References	209



CHEMISTRY AND BIOLOGY OF NITRIC OXIDE

1.1	Historic Background of Nitric Oxide	3
1.2	Physical-Chemical Properties of Nitric Oxide	4
1.3	Reactions and Reactivity of Nitric Oxide	6
	Autoxidation of NO	6
	Reaction of NO with Superoxide	7
	Radical Chemistry of NO	8
	Reactions of NO with Metals	8
	Reactions of NO with Thiols	10
	Chemistry of the Nitroxyl Anion, NO ⁻ /HNO	11
1.4	Biological Aspects of Nitric Oxide	12
	Sources of Nitric Oxide in Biological Systems	12
	<i>Denitrification</i>	12
	<i>NO Synthases</i>	19
	“Good” and “Bad” Nitric Oxide: the Threshold Between Signalling and Toxicity	23
	Nitric Oxide in the Host-Pathogen Interaction	28
	Microbial Defence Mechanisms Against Nitric Oxide	30
	Genetic Responses to Nitrosative Stress	32
	Prokaryotic Defence Systems Against Nitrosative Stress	35
	Other Enzymatic Systems	38
	References	40

1. CHEMISTRY AND BIOLOGY OF NITRIC OXIDE

1.1 HISTORIC BACKGROUND OF NITRIC OXIDE

The discovery of nitric oxide (NO) is associated with various incidents at the chemistry laboratories of some of the eminent “giants” on whose shoulders scientists now stand. The first to report its preparation was Jan Baptist van Helmont in 1620 whereas, in the 1660s, Boyle and Hooke generated NO by heating “nitre” (potassium nitrate) with glowing charcoal in the absence of air, describing it as a “volatile nitre” in the air, or nitrous air. In 1772, the gifted Joseph Priestley significantly contributed to the knowledge on NO, while studying the properties of “nitrous air”, generated by adding “spirit of nitre” (nitric acid) to various metals. Among other observations, Priestley reported that “nitrous air” did not support plant growth, it reduced putrefaction and that water impregnated with it had an acid taste. His studies led to the development of a



Figure 1.1 – caricature of Joseph Priestley

device for measuring the “purity” of air. All of this only added to Priestley’s long list of achievements concerning studies with gases, such as his discovery of oxygen and carbon dioxide. Nitric oxide gained its present designation in 1806, according to J. A. Murray’s description “nitrous air”. In the 1840s Walter Crum described the production of pure NO by shaking together nitric acid, concentrated sulphuric acid and mercury (1). The intrinsically complex chemistry of NO reflects itself in the intricate biological processes in which NO is involved, that ultimately led to its nomination as Molecule of the Year in 1992, and to the attribution of the 1998 Nobel Prize of Medicine to R. Furchgott, L. Ignarro and F. Murad.

1.2 PHYSICAL-CHEMICAL PROPERTIES OF NITRIC OXIDE

Nitric oxide (NO) displays the behaviour of an atypical molecule due to several of its physical-chemical properties, part of which are listed in table 1.1.

Table 1.1 - Physical-Chemical Properties of Nitric Oxide

Boiling Point, T_b	-151.74 °C
Enthalpy of Vaporization, $\Delta_{\text{vap}}H$ (at T_b)	13.83 kJ/mol
Dielectric Constant or Permittivity, ϵ	1.00060
Permanent Dipole Moment, μ	0.159 D
Solubility in Water (Molar Fraction expression, valid between 273.15 and 358.15°C)	$\ln X_1 = -62.81 + 82.34/T^* + 22.81 \ln T^*$ ($T^* = T/100$ K)

At room temperature and pressure, NO is a colourless gas, with a relatively low solubility in water (~2 mM at room temperature), as expected from its essentially apolar nature. In fact, no hydration reaction occurs with NO. Its solubility is higher in organic solvents ranging from ~3 mM.atm⁻¹ (in DMSO) to 15 mM.atm⁻¹ (in cyclohexane) (2).

The hydrophobicity of nitric oxide is crucial for its physiological functions, since it allows NO to freely diffuse through the cell boundaries, the hydrophobic milieu of cell and organelle membranes. In the cytoplasm, it moves with a diffusion coefficient of 4.8×10^{-5} cm².s⁻¹ in aqueous solution, at 37° C. Alike oxygen, NO is lipo-soluble, which contributes to higher rates for reactions involving NO occurring in hydrophobic environments.

Nitric oxide has eleven valence shell electrons, as illustrated in the molecular orbital diagram (Fig. 1.3), hence its radical nature.

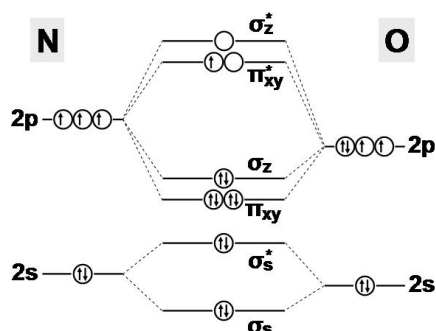


Figure 1.2 – Molecular orbital diagram for NO.

The electronic structure of nitric oxide is $KK(\sigma_s)^2(\sigma_s^*)^2(\pi_{xy})^4(\sigma_z)^2(\pi_{xy}^*)^1$, according to the molecular orbital terminology. Because of the single electron located at the anti-bonding π_{xy}^* , NO has a net bond order of 2.5, which is consistent with a bond length of 1.150 Å, intermediate between the double bond of oxygen (O_2) and the triple bond of nitrogen (N_2).

Theoretical studies confirm the localization of the unpaired electron in a π^* orbital. The radical is shared between the nitrogen and the oxygen, although the N atom has a higher orbital coefficient, hence why most of the observed radical chemistry takes place at the N atom. Despite of its radical nature, NO does not readily dimerize at room temperature and pressure. Although dimerization would satisfy the octet rule regarding the Lewis notation (Fig 1.3), in this process there is no net bond order gain (the overall bond order becomes 5) and entropy favours the monomer over the dimer.

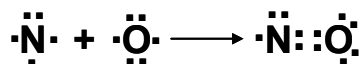


Figure 1.3 – Lewis dot structure of nitric oxide.

NO is the second in the IUPAC series of nitrogen gases, assigned according to the oxidation state of the N atom.

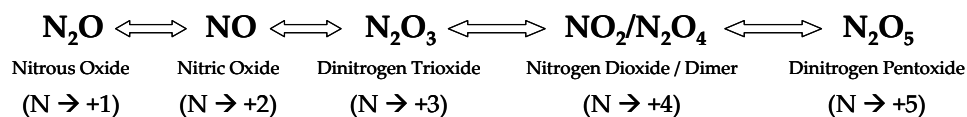


Figure 1.4 – IUPAC series of N_yO_x gases with different oxidation states of the N atom.

Nitrite (NO_2^-) has the same oxidation state as N_2O_3 , whereas nitrate (NO_3^-) has the same oxidation state of N_2O_5 . Nitrogen is a versatile element in the sense that it can harbour several other oxidation states, such as in molecular nitrogen (N_2 , 0),

hydroxylamine (NH₂OH, -1), hydrazine (N₂H₄, -2) and ammonia (NH₃, -3). This range of oxidation states gives nitrogen and its intricate chemistry a relevant role in many biological processes.

1.3 REACTIONS AND REACTIVITY OF NITRIC OXIDE

As mentioned above, NO has a number of properties that make this molecule reactive towards a diversity of organic and inorganic compounds. In this section some of these reactions are described, with special emphasis on those that are relevant for biological processes, either through the direct action of the NO molecule or by NO-derived products.

Autoxidation of NO

The oxygen molecule O₂ has two unpaired electrons, corresponding to a ground state triplet, therefore having properties of a biradical, and reacting with other radical species. In the gas phase, the reaction of NO with O₂ involves two equivalents of NO and yields two equivalents of nitrogen dioxide, NO₂. Since O₂ has two unpaired electrons and NO has one, the product NO₂ has still one unpaired electron and can thus react further, being in fact a potent oxidant, unlike NO. NO₂ reacts with ascorbate, phenol and thiols, with rate constants in the order of 10⁷-10⁸ M⁻¹.s⁻¹., and as an example, it generates nitrotyrosine by primarily producing the phenoxyl radical followed by a second NO₂ molecule completing the nitration reaction (3). The production of NO₂ by the reaction of NO with O₂ can ultimately lead to the formation of higher N-oxides such as dinitrogen trioxide and dinitrogen dioxide.

In aqueous solution, the reaction of NO with oxygen yields nitrite, according to the reaction scheme:



The kinetics of this reaction have been the subject of diverse studies and rate expressions have been established for the loss of O_2 ($-d[O_2]/dt = k[NO]^2[O_2]$) and NO ($-d[NO]/dt = 4k[NO]^2[O_2]$), with $k \sim 2 \times 10^6 \text{ M}^{-2}\cdot\text{s}^{-1}$ (at 25°C).

Nitrite has important chemical features with physiological implications (apart from being an intermediate of microbial denitrification), mainly in two different processes. On the one hand, under mild acidic conditions, nitrite can be protonated yielding N_2O_3 , which is a strong electrophile able to nitrosate several nucleophiles at high rates, such as amines and thiols. On the other hand, the reaction of nitrite with oxyhemoproteins is of physiological relevance due to the formation of highly reactive intermediates, both higher N-oxides and high valent metaloxo species. Whereas nitrite (and nitrate) metabolism by denitrifying commensals was considered in the past a source of carcinogenic compounds, it is now proposed that the resulting RNS intermediates are in fact beneficial for the host (4).

Reaction of NO with superoxide

The superoxide anion, O_2^- , is a reactive oxygen species (see Chapter 2) that has one unpaired electron occupying a π^* antibonding orbital, which accounts for the readiness of its reaction with nitric oxide, yielding peroxyxynitrite ($ONOO^-$) with a rate constant close to the diffusion limit (5). The generation of peroxyxynitrite is physiologically relevant in the perspective that simultaneous formation of significant amounts of NO and O_2^- is associated with certain pathophysiological conditions.

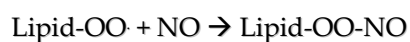


The ability of NO to bind and react with metal-bound O_2 can be formally viewed as the reaction of NO with O_2^- (as observed in the reaction of NO with oxyhemoglobin and oxymyoglobin), since the O_2 bound to the ferrous globins can be more accurately described as ferric- O_2^- complexes.

The reported pK_a of 6.8 for peroxynitrite/peroxynitrous acid (ONOO-/ONOOH) implies that at physiological pH, a significant fraction of ONOOH is present. The source of the high oxidizing power of both species is a matter of debate, although one common proposal is the formation of the highly cytotoxic species nitrogen dioxide (NO_2) and hydroxyl radical ($\cdot OH$) upon decomposition of both ONOO- and ONOOH to nitrate (NO_3^-). The pathways and targets of peroxynitrite cytotoxicity are described in the section devoted to the cytotoxic effects of NO.

Radical chemistry of NO

Due to its radical nature, NO reacts rapidly with species having unpaired electrons, such as O_2 , O_2^- and NO_2 , a property that allows NO to terminate radical chain reactions by “quenching” other radical species. In fact, NO is somewhat regarded as antioxidant in the sense that it can prevent lipid peroxidation by oxygen, by acting as a chain terminating species, according to the reaction scheme:



By blocking the chain initiating species (Lipid-OO \cdot), NO prevents further damage to the lipids. The effect of NO on metals that also catalyze this type of reactions is described below.

Reactions of NO with metals

NO binding to metals can assume two different geometries, regarding the M–N=O bond, which is explained by different types of interaction of NO with the metal ion (2). Likewise, bound NO can be formally viewed as nitrosonium cation NO^+ or nitroxyl anion NO^- , depending on the interaction type. The most common bonding mode for metal nitrosyls corresponds to a linear geometry, where the metal-NO bond consists of σ donation from NO to the metal and π

backbonding from the metal occupied d orbitals to the NO π^* antibonding orbital. The bound NO in this geometry donates one electron to the metal and is thus considered as NO⁺ in electron counting terms. As for the bent geometry, the metal is considered

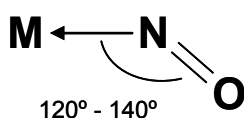
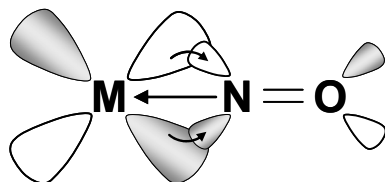


Fig 1.5 – Metal-NO bond geometry

to donate an electron to NO, yielding NO⁻, that binds to the metal in a σ interaction, placing an electron pair localized in an sp^2 orbital at the nitrogen atom. Although the metal-bound NO is merely formally considered as NO⁻ in the bent geometry and NO⁺ in the linear geometry, these different bonding modes may account for different properties and reactivities, namely linearly

metal-bound NO is more susceptible to nucleophilic attack, whereas the bent geometry may favor electrophilic reactions. In both geometries, it is noteworthy that the backbonding phenomenon accounts for a considerable portion of the metal-NO bond strength. Due to its reactivity with metal centers, NO is regarded both as a pro-oxidant and anti-oxidant, since it can reduce metal centers to a state where these can trigger damaging reactions (e.g., the Fenton reaction), or it can react with reduced metal centers and thus prevent other harmful processes.

Of notable importance in biological processes is the reaction of NO with the haem-iron centers of haem proteins. Besides being an efficient ligand for ferrous haems, NO can also bind – although with a lower affinity – to ferric haem, unlike other diatomic ligands such as O₂ and CO. Another distinct feature of NO binding to haem iron as compared to other diatomic ligands is that it labilizes the *trans* axial ligand, a property that accounts for the elegance of NO mediated biological processes. Due to the higher affinity of NO to ferrous haems in comparison with ferric ones, the NO binding kinetics to haems depends on the

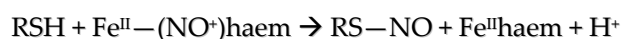
iron oxidation state, but also on the surrounding environment of the haem moiety. As an example, NO irreversibly binds to the ferrous form of myoglobin with a rate constant of $1.7 \times 10^7 \text{ M}^{-1}\cdot\text{s}^{-1}$, to be compared with $1.9 \times 10^5 \text{ M}^{-1}\cdot\text{s}^{-1}$ for NO binding to the ferric metmyoglobin (and 13.6 s^{-1} for the reverse reaction). The many reactions of NO with haem proteins, either in beneficial signaling processes or as a damaging molecule, will be discussed below in the appropriate sections. The reaction of NO with iron-sulfur centers is more often than not a damaging one and results in the disruption of the Fe-S center and the formation of a dinitrosyl-iron-dithiol complex. These reactions and the resulting damages will be discussed further below.

Reactions of NO with thiols

Physiological processes involving thiol chemistry are closely related to NO-mediated processes. The direct oxidation of thiols by NO in anaerobic conditions produces the corresponding di-sulfides, according to the reaction scheme:



Thiols can also be nitrosylated indirectly by NO in aerobic conditions (yielding S-nitrosothiols), where higher N-oxides (such as N_2O_3) are formed, or through the action of a ferric haem nitrosyl, as depicted in the reaction schemes.



Nitrosylated thiols (RSNO) can act as NO storage compounds that can give back a sulfhydryphilic compound, the electron-deficient nitrosonium cation (NO^+). An important aspect to take into account, when working with S-nitrosothiols, is the photolability of the RS-NO bond, which results in the release of NO and the corresponding thiyl radical.

Chemistry of the nitroxyl anion, NO⁻/HNO

Nitroxyl was first proposed by Angeli to be the product of decomposition of trioxodinitrate, Na₂N₂O₃, nowadays designated as Angeli's salt (6).



HNO has also been proposed to be generated in the process of bacterial denitrification. The base of HNO is nitroxyl anion, NO⁻, which is isoelectronic with dioxygen and likewise can exist as an electronic triplet (³NO⁻) or a singlet (¹NO⁻), the triplet being the electronic ground state, lower in energy than the singlet. The p*K_a* for HNO/³NO⁻ is 11.4 (7) (initially reported to be 4.7 and later on 7.2) and therefore the predominating and relevant species at physiological pH is HNO.

One aspect to take into consideration when dealing with HNO chemistry is its dimerization which



proceeds with a rate of 8 × 10⁶ M⁻¹.s⁻¹ (8), lower than initially reported and thus HNO is prone to be involved in physiologically relevant reactions prior to dimerization. The reported reduction potential for the NO/³NO⁻ pair is -0.8 V, but since the predominating form at physiological pH is HNO, this causes an upshift in this potential up to between -0.5 and -0.6V.

To determine the relevance of HNO reacting with biologically relevant molecules, kinetics studies have been performed and the following series has been established in decreasing rate constants:

oxymyoglobin (1 × 10⁷ M⁻¹.s⁻¹) > glutathione (GSH), horseradish peroxidase (2 × 10⁶ M⁻¹.s⁻¹) > N-acetyl cysteine, CuZn-SOD, Mn-SOD, metmyoglobin, catalase (3-10 × 10⁵ M⁻¹.s⁻¹) > ferricytochrome c (8 × 10⁴ M⁻¹.s⁻¹) > oxygen (3 × 10³ M⁻¹.s⁻¹).

Noteworthy, the efficiency with which HNO reacts with deoxymyoglobin, resulting in the formation of the HNO-Fe(II) complex, provides a valuable tool to detect HNO, due to the characteristic spectral features.

1.4 BIOLOGICAL ASPECTS OF NITRIC OXIDE

This section provides an overview on 1) the sources of nitric oxide and related species in living systems, 2) the biological and physiological effects of NO and 3) the role of NO in the host-pathogen interaction.

Sources of Nitric Oxide in Biological Systems

Nitric oxide is produced abiotically in living systems by mild acidification of nitrite, a process that is considered to be relevant in medical terms, since intracellular acidosis often occurs after ischemia or shock, together with hypoxia, leading to NO concentrations that can be higher than those produced enzymatically (9). Biotically, nitric oxide is produced by two main routes: as an intermediate in dissimilatory denitrification in certain microorganisms and as the product of specialized enzymes for its synthesis and thus named NO synthases (NOS). Each of this biotic NO sources are dealt with separately.

Denitrification is a most relevant process in the global nitrogen cycle carried out by prokaryotes, which is depicted in figure 1.6 (reviewed in (10)).

This scheme is a simple representation of the chemical and biological processes whereby nitrogen is introduced and removed from the biosphere. Whereas dinitrogen fixation introduces nitrogen into the cycle, the process known as denitrification is responsible for its removal. Denitrification is defined as the dissimilatory conversion of nitrate and/or nitrite to gaseous species coupled to energy conservation, in opposition to the assimilatory reduction (non-

electrogenic) of the same anions to ammonia for biosynthetic pathways, allowing at the same time to detoxify excess nitrite. In denitrifying organisms, the denitrification enzymatic machinery is part of the bioenergetic apparatus, where the several substrates and intermediates (nitrate, nitrite, nitric oxide and nitrous oxide) serve as electron acceptors. An N-oxide, instead of oxygen as in respiratory chains, is used

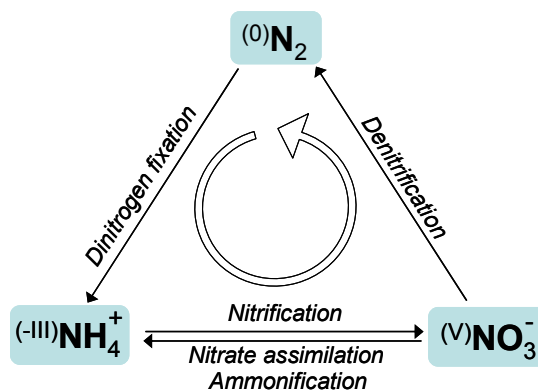


Fig. 1.6 – Biological nitrogen cycle.

as electron acceptor, contributing in some cases to the generation of the electrochemical gradient. In this sense, denitrification can be seen as the respiration of nitrate and nitrite, coupled to the reduction of NO and N_2O . Denitrification is a widespread process among prokaryotes, present both in bacteria and archaea (including extremophilic branches). Since nitric oxide is only an intermediate of dissimilatory denitrification, only this process shall be dealt with from this point on. The cartoon in Figure 1.7 (adapted from (10)) depicts the enzymatic complexes involved in dissimilatory denitrification.

Two types of dissimilatory **nitrate reductases** are known, a respiratory one embedded in the membrane and a periplasmic one ((10) and references therein). The respiratory enzyme is only expressed in anaerobic conditions, whereas the periplasmic one is expressed also in aerobiosis. The respiratory nitrate reductase (known as NAR, its corresponding operon being *narGHJI*) binds a molybdenum cofactor as the active site of nitrate reduction, whereto electrons are shuttled through the redox cofactors from the other sub-units: a haem b that accepts electrons from quinol and a “wire” of Fe-S centers. NAR uses quinol generated by the membrane-bound NADH dehydrogenase.

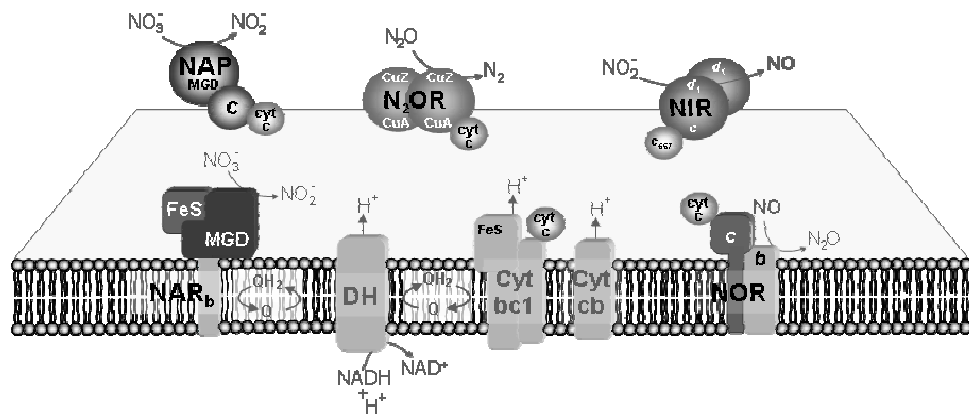


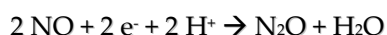
Figure 1.7 – Cartoon depicting the several enzymes involved in denitrification (adapted from (10))

The periplasmic soluble nitrate reductase (termed NAP, encoded by the *napEDABC* operon) also reduces nitrate through a molybdenum cofactor, using electrons delivered by soluble c-type cytochromes (which keep being reduced by the *bc1* cytochrome). Since the nitrate reduction machinery is located at the opposite site of where nitrite reduction takes place, transport systems for both oxyanions are required.

As for **nitrite reduction**, two types of dissimilatory enzymes have been described, although the two types are never present within the same cell (as opposed to nitrate reductases, where the several types may co-exist) ((10) and references therein). In both cases, the reaction product is nitric oxide, although their active sites and reaction mechanisms are different. The tetra-haem *cd1* NIR is located in the periplasm. It is composed by two identical subunits, each one harbouring one haem c and one haem d₁. The haem c is bound by two histidines and the haem D₁ is bound by one histidine and one tyrosine, which is provided by a protruding loop of the haem c domain. This NIR accepts electrons both from azurin and cytochrome *c*₅₅₁. The other type of dissimilatory nitrite reductase is a copper-binding nitrite enzyme termed as CuNIR, having two types of copper centers: a type-1 center that is the electron entry point of the enzyme (with azurin and pseudoazurin as the main electron donors) and a type-2 center, which is the site

of nitrite reduction. The next step in dissimilatory denitrification is the reduction of nitric oxide (NO) to nitrous oxide (N₂O), which is accomplished by a membrane-bound NO reductase.

Since nitric oxide reduction by a novel family of nitric oxide reductases is the scope of this thesis, it is appropriate to exploit at this point the properties of the respiratory nitric oxide reductases. The reaction catalyzed by NORs involves dimerization of NO and formation of an N,N bond, the overall reaction requiring 2 electrons (and two protons), since the formal oxidation states of nitrogen in NO and N₂O are +2 and +1, respectively.



Respiratory **NO reductases (NOR)** (10-13) have been isolated from several bacteria (such as *Pseudomonas stutzeri* and *Paracoccus denitrificans*) and genes encoding for NORs can be found in the genomes of organisms capable of dissimilatory denitrification (14). Since NO is generated in the periplasm during the denitrification process, the fact that NOR is located in the inner membrane prevents NO from reaching the cytoplasm. Therefore, NOR may act as a protective enzyme, on top of contributing to the cellular metabolism in bioenergetic terms. NOR was the last of the denitrification enzymes whose molecular properties were determined. An important step for its isolation was the understanding that it is not produced in aerobic cultures and that it has to be isolated from cells grown under oxygen-limited or anaerobic conditions. NOR activities are within turnover numbers of 61-70 s⁻¹(15,16).

Protein sequence analysis of NORs leads to their division into two classes: short-chain NORs (scNOR) with approximately 450 residues (comprising two subunits) and long-chain NORs (lcNOR) of about 760 aminoacids (13). This classification finds a parallel in the literature, where NORs are divided according to their electron donor, since scNOR accept electrons from reduced cytochrome c and lcNOR have quinol as their electron donor. Therefore, scNOR match the common

terminology of cNOR and lcNOR is commonly referred to as qNOR. Regarding the gene organization, the two subunits from scNORs are encoded by the genes *norB* (encoding the catalytic subunit) and *norC* (the electron-accepting subunit), while lcNORs single subunit is encoded by the gene *norZ*. Whereas the *norZ* gene is usually isolated in a given genome, the *norCB* genes are usually associated with ancillary genes in diverse manners (some of which with regulatory roles), the most common one being *norEFCBQD*. scNOR is composed by the NorB catalytic subunit and the c-type cytochrome NorC subunit, with sequence-deduced molecular masses of 53 and 17 kDa, respectively. The high degree of hydrophobicity of NorB, which is due to its predicted 12 trans-membrane helical segments, makes its apparent mass (determined by electrophoresis) to be around 34-38 kDa. While the spectroscopic properties of scNOR revealed the presence of haems B and C, the chemical analysis yielded more Fe than expected from the haem content; possible FeS centers were ruled out due to the absence of an EPR signal. An important development for the understanding of this enzyme was the finding of the structural homology between the NorB subunit and the CcOx1 subunit of cytochrome oxygen:oxidoreductase, the terminal enzyme of the oxygen respiratory chain. Indeed, structural models of NorB, generated by using the crystallographic structure of Cox1 as a template, place three conserved histidines (His207 from helix VI and His258 and His259 from helix VII) as a putative metal binding site, analogous to the active site copper Cu_B in cytochrome oxidase. Altogether, these observations allowed to postulate that the active site of NO reduction in NorB is constituted by a high-spin haem *b* and a non-haem iron, similarly to the haem-

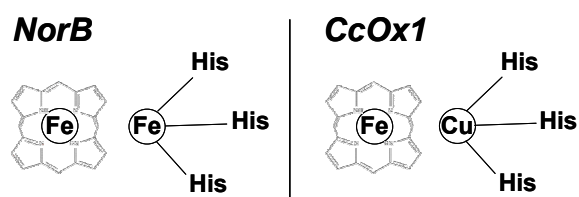


Figure 1.8 – Comparison of the binuclear centers of scNOR NorB subunit (haem-Fe non-haem Fe) and subunit 1 of CcOX (haem-Fe Cu_B).

copper active site in respiratory oxygen reductases (Fig. 1.8) (17). The stoichiometry of non-haem Fe with respect to haems *b* and *c* is thus 1:2:1. The non-haem Fe in NorB makes a μ -(hydr)oxo bridge with the high-spin haem *b*. scNOR accepts electrons from cytochrome *c* or (pseudo)azurin at the haem *c* domain, which are shuttled to the low-spin haem *b* and further to the high-spin haem : non-haem Fe active site, where NO reduction takes place. Proposed reaction mechanisms will be dealt with in the *Discussion* section, in a comparative fashion with the putative mechanisms of NO reduction by flavodiiron proteins. lcNORs differ structurally from scNOR by several aspects. They lack the cytochrome *c* subunit, binding instead quinol as their electron donor, possibly at the N-terminal extension corresponding to two extra trans-membrane helical segments, in addition to their 12 helices that are similar to the scNOR NorB subunit. The binuclear active site constituted by haem *b*₃ Fe and non-haem Fe is also present in lcNOR, with the single exception of *Pyrobaculum aerophilum* NorZ (18), which has haem *o* instead of haem *b*₃ at the diiron site.

The structural homology between NO reductases and oxygen reductases has been the subject of some evolutionary theories concerning an early atmosphere rich in N-oxides, where oxygen was absent and Fe²⁺ was available for bioactivity. The atmosphere gradually became aerobic, oxidizing Fe²⁺ to Fe³⁺ (much less soluble and thus unavailable for biological systems) and Cu¹⁺ to Cu²⁺ (in this case, the change in oxidation state increasing the solubility and bio-availability). Although attractive, these theories have some "loose threads" concerning the evolution of the super-family of haem-copper oxidases *per se*. Another open issue also related to oxygen reductases vs. NORs concerns proton pumping mechanisms. Although NORs were considered non-electrogenic for a long time - unlike oxygen reductases, which not only uptake protons to complete oxygen reduction to water, but also translocate protons through across the membrane - there is growing evidence for proton pumping in NORs (19-21). This creates a pitfall for

the longstanding idea that the reduction of NO in denitrifiers was a non-profitable reaction in energetic terms. Expression of NORs is mainly under the regulation of Dnr and NnrR, both of which are members of the CRP (cyclic AMP-receptor protein)-FNR (fumarate nitrate reductase protein) superfamily. One exception is the *Ralstonia eutropha* NOR, which is regulated by NorR, an observation that is at the genesis of the bulk of the work of this thesis, as described in the next chapter.

Besides scNOR and lcNOR, another type of denitrifying NOR has been identified in fungi, with molecular properties completely different from the former. In 1991, Shoun and co-workers (22) isolated a flavocytochrome from *Fusarium oxysporum* with molecular and spectroscopic properties similar to those of P450 cytochromes, capable of efficiently coupling NADH oxidation to NO reduction (to N₂O). The active site of NO reduction in P450nor is a haem ligated by a cysteine thiolate, with a low redox potential (E_m -307 mV in *F. oxysporum* P450nor). The redox and structural features of the haem pocket result in a strong binding of NO in the first step, eventually forming Fe(II)-NO⁺, where to a second NO molecule binds to yield N₂O. It is proposed that their occurrence in fungi results from lateral gene transfer from bacteria in very early steps of evolution.

The final step in dissimilatory denitrification consists of the reduction of nitrous oxide to dinitrogen, catalyzed by a copper enzyme named **nitrous oxide reductase** (N₂OR).



N₂O reductase is a soluble enzyme located in the periplasm, which can be isolated in different forms, depending on the presence of oxygen: form I, a purple species, is isolated in the absence of oxygen, whereas the aerobically purified enzyme, form II, is a pink species with decreased activity. In molecular terms, N₂OR is composed of two identical subunits, harboring two types of copper centers: a mixed-valent dinuclear Cu(A), which is the electron entry point, and a

tetranuclear Cu(Z) center, the active site of N₂O reduction and the first catalytically active Cu-sulfur complex reported.

As mentioned above, microorganisms may face nitric oxide, not only as an intermediate of denitrification pathways, but also as a product of specialized enzymes for its synthesis, named *NO synthases* (NOS). Since the discovery of the many physiological processes involving NO, much research efforts were directed to the study of the enzymes responsible for its synthesis (reviewed in (23)).

Three different forms of NO synthases have been identified, highly homologous within the human isoforms (51-57% sequence identity), although with different localization, regulation and catalytic properties. Despite their differences, each NOS isoform is encoded in a single copy gene in the haploid human genome. The first to be identified was the neuronal NOS, nNOS (NOS-1). Then, the inducible NOS, iNOS (NOS-2) was identified as being present in a wide variety of cells and tissues. Later, the endothelial NOS, eNOS (NOS-3) was the first to be discovered in vascular endothelial cells. Initially, the three types of NOS were divided in a shallow manner based on the fact that nNOS and eNOS were constitutive and calcium-dependent, whereas iNOS was inducible and calcium-independent.

In general terms, NO synthases are regarded as homodimers, although a functional dimeric NOS will require the binding of two calmodulins (CaM), making the enzyme a hetero-tetramer. Each monomer is composed of a reductase domain, with relatively tightly bound FAD and FMN, and an oxygenase domain that binds (6R)-5,6,7,8-tetrahydrobiopterin (BH₄) and a haem *b* (iron protoporphyrin IX). NOS catalyze the reaction of NADPH, L-arginine and O₂, yielding nitric oxide and citrulline. NADPH oxidation occurs at the reductase domain and electrons are subsequently transferred from the flavin moieties to the haem in the oxygenase domain, where arginine and O₂ react to give NO and

citrulline. The two domains within each monomer are linked by a calmodulin binding site.

The scheme in figure 1.9 depicts the reason for the homodimeric form (regardless of CaM binding) being the functional unit, i.e., electrons are shuttled from the reductase domain of one monomer to the oxygenase domain of the other monomer. The structure of the human iNOS oxygenase domain (24,25) revealed that the haem is penta-coordinate, with the proximal Cys₂₀₀ residue acting as an axial ligand. The same structure revealed that the BH₄ cavity is buried in the protein and removed from solvent, although being near the dimer interface. Unexpectedly, a zinc tetrathiolate was found at the dimer interface, proposed to contribute to dimer stability (26). This stability factor is relevant for iNOS, since only the oxygenase domain is involved in dimer formation in this NOS isoform, whereas in nNOS and eNOS also the reductase domains may be involved in dimerization.

As depicted by the scheme in Figure 1.9, the role of the flavin moieties (FAD and FMN) from the reductase domain is to accept electrons from NADPH and transfer them to the haem domain, essentially allowing a two electron donor to donate electrons to a mono-electronic center, by stabilizing their flavin one-electron reduced semiquinones.

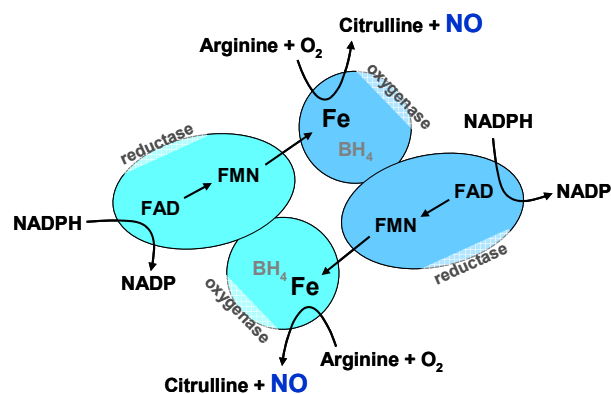
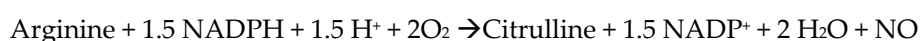


Fig. 1.9 - Domain arrangement and cofactor localization in the functional nitric oxide synthase homodimer.

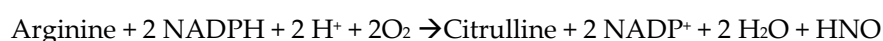
It has been proposed that eT between the two flavins may be where CaM thermodynamically modulates NOS activity, with eT being slower in the absence of Ca²⁺-CaM. The oxygenase domain shares similarities with

P450 cytochromes in the sense that the haems in each of these protein families have a thiolate ligand (from a cysteine). Indeed the two enzymes have been proposed to operate with similar reaction mechanisms. However, a distinct structural feature is that NOSs have a tryptophan hydrogen-bonded to the haem thiolate, which may have mechanistic implications.

Although it is widely accepted that nitric oxide is the reaction product of NO synthases – hence their name – this is still a matter of debate, with growing and disputed evidence for different reaction products, such as nitroxyl (in fact, its protonated form, HNO) or peroxynitrite, which are still reactive nitrogen species endowed with cytotoxic activities (23). This does not however change the observation that cells and tissues where NOS are located can produce NO, in spite of the enzymes' reaction product. It should be noted that if it becomes accepted that different isoforms with different localizations can generate distinct reactive nitrogen species, it is then essential to understand the physiological implications of this assumption. One difficulty to assess this issue relates to the fact that most of the detection systems for NO production in cells and tissues are indirect methods and can therefore suffer from interference of HNO (bio)chemistry, in some ways mistakable with NO (bio)chemistry. One way to sort out this matter would be the stoichiometry of the overall reaction which for NO production is:



and for nitroxyl production is:



Unfortunately, several experimental caveats make these subtle differences in NADPH/arginine consumption ratios technically difficult to measure. This open question may however simply be enlightened by the fact that probably, under different conditions, NOS can generate *in vitro* either reaction product, which may or not translate into physiological differences. Another point of divergence

concerning the NOS reaction product regards the possible formation of peroxynitrite. This is supported by the fact that all isoforms have been shown to perform an uncoupled NADPH oxidation reaction which generates superoxide (a reaction common to most NAD(P)H-oxidizing flavoproteins, related to a direct reduction of oxygen by the flavin moieties (27). Since NO promptly reacts with O_2^- to give peroxynitrite, it may be possible that under certain conditions the enzyme is producing both radicals leading to the formation of this reactive nitrogen species. Another possibility is that if HNO is the reaction product and there is available oxygen, the two can combine to give peroxynitrite. In either case, peroxynitrite is not the direct enzymatic product, but an adventitious side product. The regulation of NOS is intricate and takes place at several levels (23). A significant aspect of NOS regulation concerns its auto-inhibition mechanism by NO. In fact, any enzyme which generates a ferrous haem as part of its catalytic cycle is prone to bind NO (excess NO in the case of NOS), resulting in a ferrous nitrosyl. Another possibility is that the proposed intermediate Fe^{3+} -NO gets reduced, also generating a ferrous nitrosyl. Either way, this inhibition may be reverted by its reaction with oxygen, which yields nitrate. NOS are also regulated in terms of their activity, expression and localization by protein-protein interactions, alternative mRNA splicing and covalent modifications. The activity of NOS is regulated by calmodulin binding, which improves electron transfer steps, from NADPH to the flavin moieties and between the two domains, an effect that is more significant for nNOS and eNOS with respect to iNOS. Other examples of regulation at the activity level are the phosphorylation of nNOS and eNOS, and the heat-shock protein 90 (Hsp90) acting as an allosteric modulator of eNOS activity. The localization of eNOS is regulated by acylation of eNOS by myristate and palmitate. An emerging aspect of NOS regulation concerns its splice variants, resulting from alternative mRNA splicing. This feature has been exploited essentially for nNOS, which is encoded by one of the most structurally

diverse human genes. At least four splice variants of human nNOS have been detected so far. Regarding iNOS, although alternatively spliced mRNAs have been isolated, no protein variants were detected.

In summary, for the purpose of the work described in this thesis, NO derived from NOS activity (or any other reactive nitrogen species) presents a serious challenge for microbes invading a mammalian host. Most relevant is the inducible iNOS which is used by specialized cells of the host immune system – macrophages and neutrophils – to produce high concentrations of NO against invading microbes, at the sites of infection and inflammation.

“Good” and “Bad” Nitric Oxide: the threshold between signaling and toxicity

The functional properties of nitric oxide as a biologically active molecule in a wide range of physiological processes caused appall to chemists and biologists, since it was not envisaged that a toxic pollutant could be so elegantly used by living organisms. However, revising its chemistry, this now seems very convenient and logic due to several of its properties, as it continues to happen

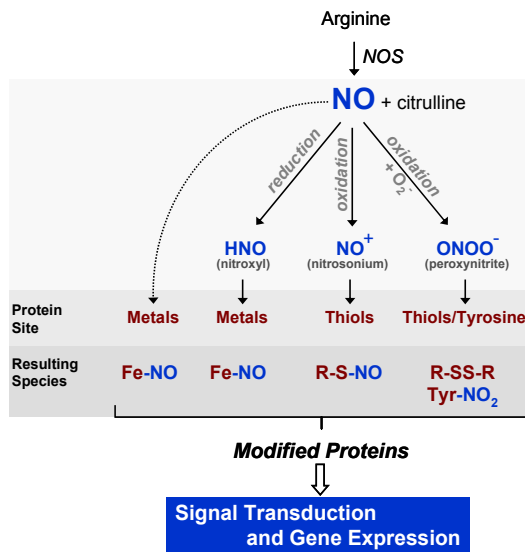


Figure 1.10 – Schematic representation of protein modifications by NO and RNS related with signaling processes and gene expression.

with other diatomic molecules, such as carbon monoxide and hydrogen sulfide, at present. One must bear in mind that the functional properties of nitric oxide in living systems are concentration dependent, since each tissue or cell (eukaryotic or prokaryotic), has an NO concentration threshold from which NO turns from beneficial to deleterious.

At low concentrations (nM range), *NO is an important signaling molecule*, essentially in mammalian systems. Signaling processes associated with NO may be mediated directly by NO *per se* or by other NO-derived reactive nitrogen species (Fig. 1.10), with different molecular targets and consequently different physiological implications (for example (28-30)). These species exert their effects mostly by modifying protein sites that ultimately trigger signaling processes and alter gene regulation. A major advantage of NO over other compounds as a signaling molecule is based on its membrane permeability and ease of diffusion both in hydrophobic and aqueous media. In essence, signaling processes attributed to NO are related to the activation of guanylate cyclase, resulting from a conformational change upon NO binding to the haem active site that enhances cyclic guanosine monophosphate (cGMP) production. This nucleotide in turn regulates a number of cellular functions, namely related to the cardiovascular and nervous systems, which are nevertheless intertwined with themselves and with most (if not all) physiological processes. The production of cGMP in the endothelial smooth muscle cells leads to activation of cGMP-dependent protein kinases, resulting in calcium sequestration and vasodilation. Initial evidence for a *role of nitric oxide in cardiovascular processes* – namely vasodilation – arose from the seminal work of R. Furchgott on the endothelial-derived relaxation factor (EDRF) (31) and the discovery that EDRF is in fact NO (32,33). This discovery eventually granted Robert Furchgott, together with Louis Ignarro and Ferid Murad, the 1998 Nobel Prize in Physiology or Medicine (Fig. 1.11). This observation also provided a physiological rationale for the empirical usage of nitroglycerin to treat cardiovascular disorders such as angina. When awarded the Nobel Prize in 1998, Furchgott reminded in his banquet speech (http://nobelprize.org/nobel_prizes/medicine/laureates/1998/furchgott-speech.html) the spirituous remark made by Alfred Nobel (notable for the development of dynamite, with

nitroglycerin as its active substance) when his doctor prescribed him nitroglycerin for his angina pectoris: "It sounds like the irony of fate that I should be ordered by my doctor to take nitroglycerin internally". Besides affecting the vascular smooth muscle, NO also acts on blood cells themselves, most importantly exerting an anti-aggregative and anti-adhesive effect on platelets, in a process also regulated by cGMP. Other cardiovascular effects of NO are the decrease in rolling and adhesion of leukocytes and a possible role in maintaining micro-vascular integrity and permeability, among others.

An interesting development was the finding that cardiovascular regulation involving a stimulated release of signalling agents from HNO follows a

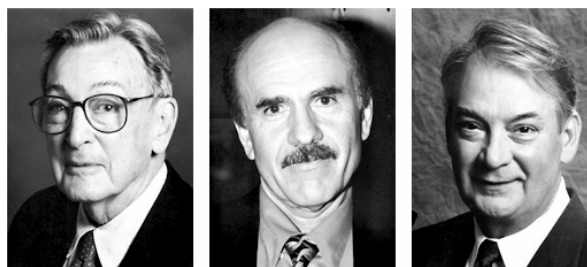


Figure 1.11 – Laureates of the 1998 Nobel Prize for Medicine or Physiology, "for their discoveries concerning nitric oxide as a signalling molecule in the cardiovascular system". Left to right: Robert Furchgott, Louis Ignarro and Ferid Murad.

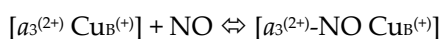
pathway different from NO-mediated processes (28). The two pathways are mutually exclusive and the HNO-mediated one is characterised by enhanced cAMP production (instead of cGMP) and possible modification of thiol and metal sites (to be compared with NO binding to the guanylate cyclase haem). The two pathways are thus named "orthogonal", having the same origin but diverging routes, and again emphasize the duality of NO vs. HNO physiology (28).

The role of NO in regulating the nervous system affects differently the central and peripheral systems, despite both also resulting mainly from the activation of guanylate cyclase by NO (34). In the central nervous system, due to the fact that the distribution of iNOS-bearing neurons in the brain is not uniform, NO is proposed to regulate diverse functions, which have in common being related with production of glutamate. Whereas NO signaling in the central nervous system is known to regulate / affect memory, spatial learning, task acquisition and

behavioral and sexual responses, in the peripheral nervous system NO is involved in signaling processes that influence the gastrointestinal tract, the airways and the genitourinary tract.

As the concentration of NO deviates from its beneficial range, it may result in physiological disorders, both above and below the beneficial threshold. On the one hand, a number of pathologies are associated with NO concentrations below the basal levels. Examples of disorders resulting from impaired NO production are the serious pathologies atherosclerosis and hypertension. On the other hand, when the NO concentration increases to the micro-molar range and above the beneficial threshold, NO becomes deleterious, being cytotoxic, cytostatic, and triggering cellular processes that culminate in pathological conditions. At these concentrations, NO is cytotoxic both for eukaryotes and prokaryotes, with common cellular targets, and the sensitivity of microbes to NO is used by higher eukaryotes in the immune response to microbial invasion (revised in the next section). The cytotoxicity of NO results from the multiple cellular components that react or are chemically modified by NO. As described at the beginning of the chapter, NO binds with ease to metal and thiol sites in proteins, besides also exerting (directly or indirectly, i.e., through NO-derived reactive nitrogen species) damage to other biomolecules such as lipids and DNA. At a physiological level, excess NO production induces disturbances in the regulation of many processes, being thus related to several pathologies, such as septic shock (triggered by over-production of NO to counteract microbial infection), cerebral ischaemia, and neurodegeneration (multiple sclerosis), to name a few (34). The dual effects of NO with respect to inflammatory diseases, illustrates the ambiguity of this species as a signaling molecule. Whereas the eNOS-derived NO is endowed with a protective role to tackle inflammatory processes, the iNOS-derived NO subsequently produced is partially responsible for certain aspects of chronic inflammation.

At the threshold of NO concentrations that are no longer beneficial for signalling purposes and start reaching cytotoxic levels, lies an important physiological role of NO, which concerns its *inhibition of respiratory oxygen reductases* (cytochrome oxidase – CcOX - in higher organisms and several prokaryotes) (reviewed in (35,36)). At the molecular level, inhibition of CcOX occurs within milliseconds at physiological NO concentrations and depends on several factors such as the electron flux through the respiratory chain and the relative concentrations of oxygen and NO. The inhibitory reaction takes place at the binuclear haem a_3 - Cu_B active site, NO binding to either metal in different redox states; both types of inhibition are ultimately reversible. Whereas NO binds quickly to the reduced haem a_3 to produce a ferrous nitrosyl adduct, it binds to Cu_B in its oxidized state (+2), which oxidizes NO to nitrite, possibly through an NO⁺ intermediate.



The occurrence of one inhibition route or the other is strongly related to the electron flux along the electron transport chain, i.e., the availability of reducing equivalents that are supplied to CcOX. At lower electron fluxes, the most significant inhibition mechanism is the formation of the nitrite-bound adduct, while at higher electron fluxes it is the haem a_3 -nitrosyl adduct that prevails. The reaction of NO with the haem-copper binuclear active site of oxygen reductases has ambiguous physiological implications. The extent of the inhibition is critical for this reaction to switch from a regulatory process to a pathophysiological condition. While low NO concentrations are believed to modulate respiration under normal metabolic conditions (e.g., to ensure proper oxygen availability in peripheral capillaries), at high concentrations its inhibition of respiration is related to apoptotic and necrotic events. Comparatively, haem-copper oxygen reductases from the respiratory chains invading (and possibly pathogenic)

microbes are part of the cellular targets of the high NO levels produced and released by the host immune system.

Nitric Oxide in the Host-Pathogen Interaction

The interaction between higher eukaryotes and microbes, either commensal or invading/infecting ones, is managed by the host's immune system. As elegantly described by Nathan and Shiloh (37), "immunity is the ability of the largest inherited genome in a body to restrict the replication of the smaller, non-inherited genomes in the same body". There are several strategies by which the immune system copes with invading microbes, one of which uses the cytotoxic and cytostatic properties of nitric oxide produced by the inducible form of NO synthases (iNOS, see above) (23,38). The process by which the host immune response triggers the induction of iNOS is controlled by a myriad of immunological stimuli and the enzyme is then regulated both at the transcriptional and post-transcriptional levels (mRNA stability, mRNA translation and protein stability). In these processes a number of signal transduction pathways and molecules are involved, such as lipopolysaccharides, multiple cytokines (such as interferon γ and interleukins), transforming growth factor, tumor necrosis factor α , and several phosphatases and kinases (37-39). iNOS induction is observed in many cells involved in the immune response, such as: macrophages, microglia, Kupffer cells, neutrophils, eosinophils, mast cells, dendritic cells, natural killer cells, fibroblasts, endothelial and epithelial cells, among others. The sustained production of NO by phagocytes in general confers these cells effective cytotoxic activity towards bacteria, viruses, fungi, protozoa, helminthes and tumor cells (37-39).

Under the same infection/inflammation regimes that enhance iNOS expression, another important phagocytical enzyme is induced, an NADPH oxidase (phox, from phagocyte oxidase) that reduces molecular oxygen to the superoxide anion

radical, a reactive species, cytotoxic *per se* and in synergy with other RNS and ROS. As described above, NO and superoxide readily react yielding peroxynitrite (ONOO⁻), a powerful oxidant and nitrating agent, which induces damage onto many cellular components. In fact, since macrophages produce simultaneously equivalent amounts of NO and superoxide, it is likely that part of the cytotoxicity attributed to either species may in fact result from a direct damage from peroxynitrite (Fig. 1.12) (37,38). For simplicity, it appears more correct to use the term RNS for NO-derived reactive nitrogen species in the perspective of the host-pathogen interaction. An important aspect that characterizes this strategy of the host

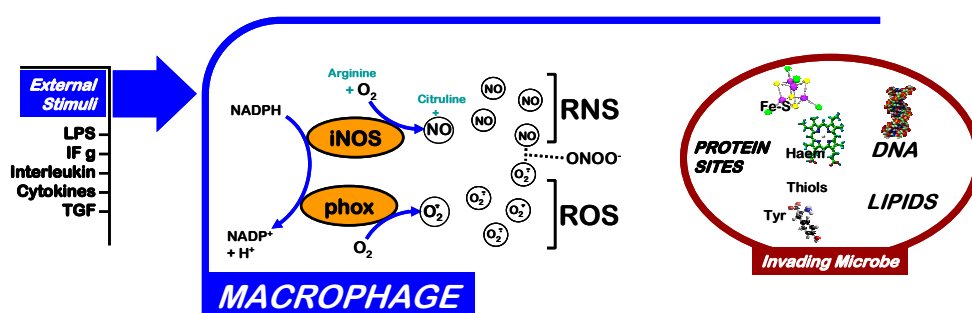


Figure 1.12 – Schematic representation of external stimuli that lead to the induction of macrophageal enzymes that produce cytotoxic species (NO, RNS and ROS) to target invading microbes, whose major cellular targets are depicted, namely iron centres, thiol groups, protein tyrosine residues, DNA and lipids.

immune system is its non-specificity in the sense that the cytotoxic species released to target the invading/infecting microbes are also damaging to the host's uninfected cells, since the molecular targets of RNS and ROS are the same in either type of cell: protein Fe sites (Fe-S, haem and non-haem Fe), thiol groups, tyrosyls, DNA and lipids, among others. As examples, nitrosylation of Fe-S centers is a key event in the inhibition of critical metabolic enzymes (of which aconitase is the best studied case (40)) and NO binding in an inhibitory fashion to the non-haem diiron centre of ribonucleotide reductase precludes DNA replication (41).

This aspect reflects the ability of the multi-cellular host to sacrifice part of its healthy cells to prevent microbial development (damaging to the whole organism), hence the formation of abscesses, a process that finds its equivalent in the plants' hyper-sensitivity reaction. The relevance of RNS in the host defense against microbial invasion is not restricted to their cytotoxic properties, since they are also immuno-regulatory, with inhibition/activation effects on G proteins, kinases and phosphatases, caspases, metalloproteases, etc., and affecting also (in either way) apoptosis (39). The ubiquity of the immune response by an infected host that uses the combined RNS-ROS cytotoxicity against the invading microbes creates a serious barrier for microbial survival in the host. Microbes have therefore evolved their own strategies to cope with the nitrosative and oxidative stress resulting from the host immune response and thus subvert it. Apart from the host-pathogen interaction, microbes can face nitrosative stress and encounter RNS as part of the nitrogen cycle, mostly in the process of dissimilatory denitrification (either if they are performing denitrification themselves or simply co-existing with denitrifiers). Analogously, anaerobic or microaerophilic organisms may be challenged with oxygen and its reactive intermediates, and thus have evolved appropriate detoxifying systems. The bulk of the microbial RNS detoxifying strategies are described below, whereas a glance is taken at ROS detoxification in the next chapter.

Microbial Defence Mechanisms Against Nitric Oxide

It should be noted that the interplay between the effects and the metabolism of RNS and ROS are not the sole factors to take into account when nitrosative and oxidative stresses come into play. Whatever is the physiological outcome of these types of stress, it is intimately related with the redox balance of the cells (also conditioned by the external medium) and the iron homeostasis. Thus, the prokaryotic responses to nitrosative stress, which are not yet completely

established, include at least five distinct types of enzymes/proteins: i) enzymes that directly detoxify NO, S-nitrosothiols or other RNS; ii) enzymes that detoxify ROS, thus avoiding the formation of RNS that are formed as a result of cross-reactions of NO with ROS; iii) enzymes that allow regeneration of reduced pyridine nucleotides, thus counteracting the effects of oxidative and nitrosative stress; iv) DNA-repairing enzymes; v) regulators of iron homeostasis (decreasing the formation of iron-nitrosyl species, that may act as catalysts of nitrosylation reactions). The enzymatic systems above mentioned are subject to tight regulatory processes, which are intricate and most likely differ from organism to organism. Interestingly, detoxification of RNS and denitrifying pathways share common regulatory routes (Fig. 1.13 and Fig. 1.14), which may imply that an adaptation to a certain type of metabolism may have endowed organisms with resistance to a certain type of stress.

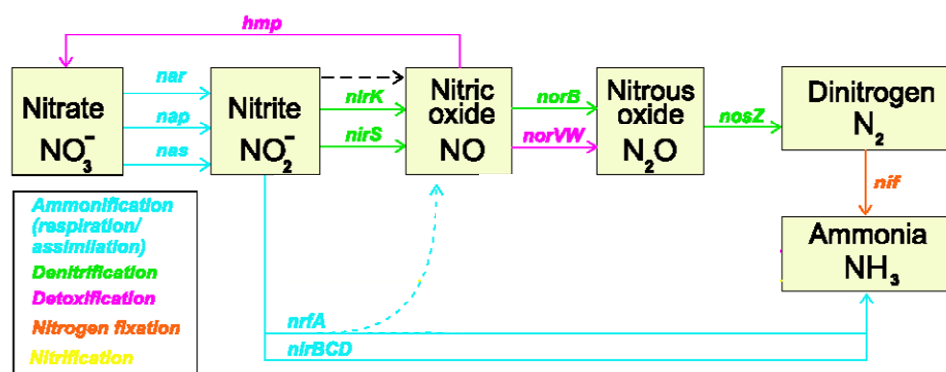


Fig. 1.13 – Bacterial inorganic cycle and corresponding enzymes (adapted from (14)).

The microbial resistance to nitrosative stress is characterized by an intricate regulation and it is thus important to understand the genetic responses in parallel with the knowledge of the enzymatic machinery. Moreover, the response involves not only detoxification and metabolic enzymes but also damage-repair machinery, as well as other cellular processes that altogether build a robust defence mechanism to nitrosative stress. As most biochemical pathways, nitrosative stress resistance machinery (including the regulatory processes) has

common features among certain groups of microorganisms. Redundancy is a major issue in microbial physiology, since one system that is important for certain organisms may be less relevant for others, or they can be under different regulatory processes in different organisms. On the other hand, distinct systems that perform the same function in different organisms may also be subjected to the same regulation. This is indeed the case in what concerns the relationship between nitrosative stress response and denitrification, as well as with oxidative stress. To illustrate the broadness of the nitrosative stress response, the *Escherichia coli* systems will be described with greater detail. *E. coli* is probably the organism for which the nitrosative stress response has been more thoroughly investigated. Studies have covered both the genetic response mediated by a number of regulons and the most relevant enzymatic systems involved in the microbial resistance to this type of stress.

Genetic Responses to Nitrosative Stress

The regulation of NO and RNS metabolism in *E. coli* is controlled by several regulons, specific for RNS (NorR and NsrR), common to oxidative and nitrosative stress response (SoxRS and OxyR), and related to iron metabolism (Fur). Considering the two prominent families of NO-detoxifying enzymes, the flavohemoglobins and the flavodiiron proteins, their regulation is of great importance in the concerted response to nitrosative stress. Whether nitrosative stress is exerted onto the cells by NO or the trans-nitrosating GSNO (an NO releaser under reducing conditions), two RNS-specific regulators are responsible for the induction of the NO-detoxifying enzymes. **NorR** is a homologue of *Ralstonia eutropha* NorR, a regulator of this organism's respiratory NOR. In *E. coli*, it has been shown to induce the expression of the NO reductase flavorubredoxin (also designated as NorV) (42-44), this organism's flavodiiron protein, which is the key subject of this thesis. The molecular basis of flavorubredoxin's regulation

by NorR will be detailed in the next chapter. NsrR (14) regulates the expression of *E. coli* flavohemoglobin (Hmp, detailed below), an NO-detoxifying enzyme that oxidizes NO to nitrate and constitutes the most relevant line of defence against NO for aerobically-grown *E. coli*. Moreover, NsrR regulates other genes that were demonstrated to be related to nitrosative stress response, whose roles were elusive but recently became clearer. Briefly, YtfE was shown to be involved in Fe-S clusters assembly (45) (a major target of nitrosative stress) and the hybrid-cluster protein (Hcp) was demonstrated to respond to oxidative stress, possibly as a new type of peroxidase (46) (scavenging of ROS is a key issue to avoid cross reactivity with RNS on top of the nitrosative stress).

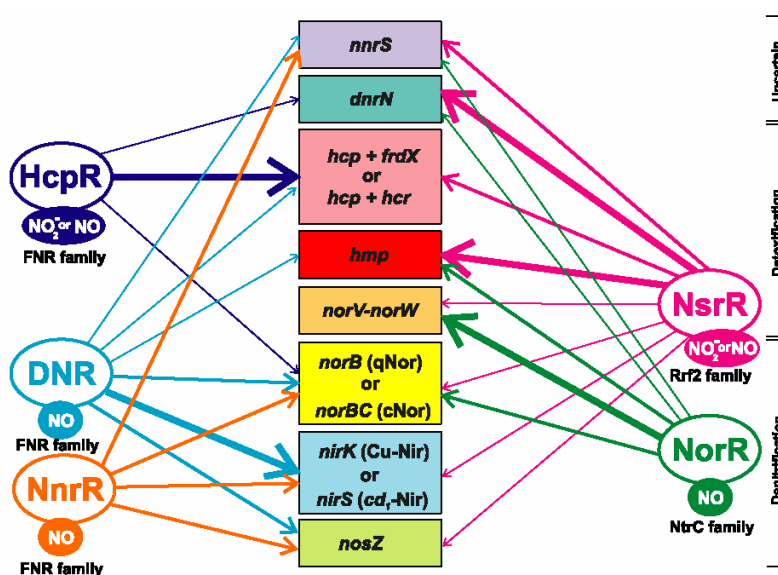


Fig. 1.14 – Major regulatory pathways of enzymes involved in denitrification and detoxification of reactive nitrogen species (taken from (14)). The combined regulatory network is based on a thorough multi-genome analysis combined with experimental data for DNR, NnrR, NsrR, and NorR. Arrows denote regulatory interactions, with the thickness reflecting the frequency of the interaction in the analyzed genomes.

To understand the intricate regulation regimes that govern multiple systems, the scheme in figure 1.14 (taken from (14)) illustrates common regulatory features of denitrification and NO detoxification pathways, observed from a thorough and integrative inspection of available data and genome sequences carried out by

Rodionov et al (14). Redundancy of systems coupled with independent regulatory pathways is a key strategy for survival of prokaryotes under certain stress conditions.

On the other hand, the two main regulons of *E. coli* related to oxidative stress aggressions, the SoxRS and OxyR systems, are also sensitive to nitrosative stress, through the attachment of NO to a metal or thiol centre, a common theme in regulation of cellular functions (47). SoxRS and OxyR mutants induce a higher sensitivity of *E. coli* to NO produced by macrophages, or to S-nitrosothiols (48,49). Under oxidative stress, the **SoxRS** system works in two steps: upon oxidation of the SoxR dinuclear FeS centre ($[2\text{Fe-2S}]^{2+/1+}$) from its transcriptionally inactive reduced (1+) state to the oxidized (2+) state, the transcription of SoxS is triggered, which then stimulates the transcription of about 65 other genes encoding for key defence enzymes such as manganese superoxide dismutase (SOD) and endonuclease IV. This regulon is also activated by nitric oxide, thus providing *E. coli* with some resistance to NO: NO binds to the binuclear centre of SoxR, forming a dinitrosyl-iron dithiol complex, which becomes active in activating soxS (50). The induction of enzymes such as SOD is quite important, since it contributes to avoid the formation of peroxynitrite, by the reaction of the superoxide anion with NO. **OxyR**, which contains cysteine redox centres, is activated by S-nitrosylation, S-hydroxylation and S-glutathionylation, and induces the expression of multiple genes that protect from oxidative and nitrosative stress, such as catalases, glutathione reductase, and alkylhydroperoxide reductase (49,51). The relation between iron homeostasis and NO stress is well exemplified by the effect of NO on the **Fur** (ferric uptake regulator) protein. Fur regulates not only the transcription of genes encoding for proteins of iron metabolism, but also for oxidative and acid stress, including more than 90 genes (52). At low intracellular iron contents, Fur loses its iron ion, thus releasing the transcriptional repression of multiple genes. Fur is under the control

of the OxyR and SoxRS systems (53). In the presence of NO, an iron-nitrosyl species is formed, which inactivates its repressor activity (54), causing a general derepression of Fur regulated genes. The general oxygen regulator **FNR** (Fumarate Nitrate Regulator) contains a $[4\text{Fe-4S}]^{2+/1}$ centre that is oxygen and NO labile. Since the cluster controls the protein dimerisation and its DNA binding capability, nitrosylation of the centre leads to an inactivated form of FNR (55). Although inactivation of FNR by NO was, so far, only shown to affect *E. coli* hmp regulation, all FNR-regulated genes are expected to respond to NO.

Prokaryotic Defence Systems Against Nitrosative Stress

Besides the regulatory aspects of the microbial response to nitrosative stress, at least three families of enzymes were shown to be undoubtedly relevant for nitric oxide metabolism: the newly identified family of flavodiiron NO reductases, which will be discussed at length in the next chapter, the membrane-bound haem-iron NO reductases of denitrifiers (described in detail above), and the globins, a family of cytoplasmatic proteins present in a wide range of organisms.

The function of prokaryotic **globins** (reviewed in (56-58)) remained elusive for a long time, but there is growing evidence that they are involved in NO detoxification. The globins can be divided into two classes: those that are built by a single B-type haem containing globin domain (hemoglobins), and those which have an extra NADP⁺:ferredoxin oxidoreductase like domain, containing an FAD moiety and an NAD(P)H binding motif (known as **flavo-hemoglobins**). When expressed in *E. coli*, the single domain hemoglobins of *Vitreoscilla* and *Mycobacterium tuberculosis* protected against nitrosative stress (57,59,60). Furthermore, fusion of *Vitreoscilla* hemoglobin with a heterologous reductase domain not only increased significantly the rates of NO consumption but also avoided the formation of thionitrosyls or peroxy-nitrite derivatives at the haem

domain. However, the *Vitreoscilla* hemoglobin gene expression was not enhanced by RNS or ROS (58), contrary to what is generally observed for flavohemoglobins (see below). Flavohemoglobins (Hmp) are widespread among bacteria, as well as in yeasts and other fungi, and in protozoa. In the presence of oxygen, Hmp oxidizes NO to nitrate, probably through a denitrosylase mechanism, with a turnover of $\sim 94 \text{ s}^{-1}$ at 200 μM oxygen and 1 μM NO, for the *E. coli* enzyme. The actual mechanism is a matter of debate regarding whether oxygen first binds to the haem and then NO binds to haem-bound O_2 , or if it is NO that binds to the haem and then O_2 to haem-bound NO. Recently, the flavohaemoglobin from *Staphylococcus aureus* has been shown to afford protection against nitric oxide in microaerophilic conditions, favouring an oxygen denitrosylase mechanism (61). The range of activities reported varies from 7.4 to 128 s^{-1} , at 20° C (58,62-64). Anaerobically, HMP reduced NO to N_2O , with a much lower activity of ca 0.14 to 0.5 s^{-1} (58,65). Nevertheless, a *Salmonella typhimurium* strain with a deletion on the hmp gene was more sensitive to NO and S-nitrothiols, even anaerobically, than the wild type strain (66). Thus, it has been proposed that Hmps are active mainly under aerobic conditions, although a function under anaerobiosis can not be completely excluded. Several experimental evidences indicate a role for Hmp in the resistance of pathogens to their hosts. For example, deletion of *hmp* in *Erwinia chrysanthemi*, a plant pathogen, decreased significantly its pathogenicity (67). In *Salmonella typhimurium*, Hmp was reported to contribute to the microbial protection from killing mediated by NO-released from human macrophages (68). Besides their function as NO scavengers, bacterial globins - either single- or two-domain - have since their discovery been suggested to play an important role in aerobic metabolism, due to its ability of reversibly binding O_2 , as the canonical hemoglobins. For example, heterologously expressed *Vitreoscilla* globin increased the cell yield of the host bacterium grown aerobically, concomitant with a higher level of protein synthesis, ATP production and a higher proton flux per reduced

oxygen molecule (58). A direct interaction between the *Vitreoscilla* globin and the haem-copper oxygen reductases was also proposed (58). Other studies showed that stimuli such as oxygen deprivation or oxidative stress increased the expression of the *hmp* gene: *hmp* was induced by paraquat, protecting against superoxide effects (69). In *Salmonella typhimurium* *hmp*-minus strain was shown to be more sensitive to oxygen stress than the wild type strain (68). It was also observed that the presence of Hmp was required for full induction of oxidative stress response enzymes, such as NADPH:ferredoxin oxidoreductase, a member of the SoxRS regulon. More recently, *E. coli* Hmp was proposed to act as an alkylhydroperoxide reductase (70), which is in accordance to previous results that suggest that Hmp has a peroxidase-like active site structure (71). Furthermore, Hmp from *Ralstonia eutrophus* and *E. coli* were reported to interact with membranes lipids (72) through conserved regions, therefore suggesting participation in lipid membrane regeneration. Thus, in summary, at present, the role of Hmp in oxidative stress response and/or as an oxygen delivery system appears to be important. It still remains to be clarified whether these enzymes have diverse functions in different organisms, or are indeed multifunctional. The mechanisms of *hmp* regulation are quite complex and not yet fully understood. In *E. coli*, *hmp* was found to be independent of the OxyR and SoxRS regulators (62,69,73), although Hmp expression is needed for full activation of the SoxRS system and for resistance to paraquat, as well as for full expression of SodA in response to paraquat (74). *E. coli* *hmp* was found to be induced by nitrate and, more effectively, by nitrite, apparently independent of the NarLP regulatory systems (73). Several studies showed that *E. coli* *hmp* was also up regulated by NO through, at least, three factors: FNR, Fur and MetR, the global regulator of the methionine biosynthesis pathway. In fact, it was shown that the repression caused by FNR and Fur on *E. coli* *hmp* could be relieved by addition of NO, which directly inhibits FNR and Fur through nitrosylation of the respective iron

centres (54,55). Also, it was observed that SNP and GSNO causes nitrosation of homocysteine, the cofactor of MetR, and that the binding of MetR to the intergenic glyA-hmp region that occurs under these conditions results in an up-regulation of hmp expression (75). The regulation of Hmp is still an open field, and its relevance as an NO detoxifying agent is continuously confirmed by its up-regulation in batch cultures under nitrosative stress, both aerobically (76) and anaerobically (77), and also in chemostat conditions (78,79). The ubiquity of Hmp as a prokaryotic defence mechanism against nitrosative stress makes it suitable for inhibition studies and antibiotic targeting and recent reports have demonstrated its sensitivity to imidazole antibiotics (80).

Other enzymatic systems

Besides the flavodiiron proteins and flavohaemoglobins, the two prominent families of NO-detoxifying enzymes, other enzymatic systems have been proposed to act as NO scavengers (81).

Additionally, the pentahaem nitrite reductase (Nrf) of *E. coli* seems to be able to perform NO detoxification, since the nrf minus strain cultured anaerobically with 20 mM of sodium nitrate and exposed to 150 μ M of NO suffered a significant growth inhibition (82). It remains to be clarified if that behaviour is indeed a response mechanism, or just a reflection of the fact that these nitrite reductases fully reduce nitrite to ammonia, being also capable of reducing intermediates of this six electron process, such as hydroxylamine (83,84) or nitric oxide (85). Cytochromes *c'* may also play a role in NO metabolism, as judged by the example of *Rhodobacter capsulatus*. In this organism cytochrome *c'* was shown to confer resistance to NO (86). Microbes may use other strategies to respond to the presence of nitrosative stress, although their general relevance is less well known. A process for detoxification of S-nitrosothiols was recently identified in *Arabidopsis* (87), *E. coli*, *Saccharomyces cerevisiae* and mouse macrophages (88): S-

nitrosoglutathione and S-nitrosated proteins are metabolised by the glutathione-dependent formaldehyde dehydrogenase, with the formation of GSNH₂, and, ultimately, formation of ammonia with the concomitant oxidation of NADH. The catalytic rate constant for GSNO is close to the diffusion limit. The glutathione-dependent formaldehyde dehydrogenases are widely present in living organisms and highly conserved, from bacteria to higher eukaryotes. These observations strongly suggest that besides the role of glutathione as a redox buffer, it plays also a major role in controlling the intracellular levels of nitrosylated species. Homocysteine was also proposed to act as an endogenous NO antagonist. In *Salmonella typhimurium*, a mutation in *metL*, whose gene product catalyses metabolic steps required for homocysteine biosynthesis, conferred hypersusceptibility to S-nitrosothiol and lowered the virulence of this pathogen in mice (89). Bacterial defences against peroxynitrite-mediated damage of methionine residues in proteins were reported as involving the peptide methionine sulfoxide reductase. The deletion in *E. coli* of this enzyme, which catalyses the reduction of methionine sulfoxide in proteins to methionine, made this organism hypersensitive to GSNO and nitrite in aerobic conditions (90). Another strategy used by bacteria to escape NO was revealed in *Helicobacter (H.) pylori* (91). In this system, bacterial resistance occurs indirectly by preventing the NO production by macrophages through scavenging of arginine, the common substrate of arginase and NOS. It was shown that while wild type *H. pylori* inhibits the NO produced by activated mice macrophages, inactivation of the arginase gene restored NO production.

REFERENCES

1. Beckman, J., Wink, D., and Crow, J. (1996). In: Feelisch, M., and Stamler, J. (eds). *Methods in Nitric Oxide Research*, John Wiley & Sons Ltd., Chichester
2. Ford, P. C., and Lorkovic, I. M. (2002) Mechanistic aspects of the reactions of nitric oxide with transition-metal complexes, *Chem Rev* **102**(4), 993-1018
3. Prutz, W. A., Monig, H., Butler, J., and Land, E. J. (1985) Reactions of nitrogen dioxide in aqueous model systems: oxidation of tyrosine units in peptides and proteins, *Arch Biochem Biophys* **243**(1), 125-134
4. Lundberg, J. O., Weitzberg, E., Cole, J. A., and Benjamin, N. (2004) Nitrate, bacteria and human health, *Nat Rev Microbiol* **2**(7), 593-602
5. Pryor, W. A., and Squadrito, G. L. (1995) The chemistry of peroxynitrite: a product from the reaction of nitric oxide with superoxide, *Am J Physiol* **268**(5 Pt 1), L699-722
6. Fukuto, J. M., Switzer, C. H., Miranda, K. M., and Wink, D. A. (2005) Nitroxyl (HNO): chemistry, biochemistry, and pharmacology, *Annu Rev Pharmacol Toxicol* **45**, 335-355
7. Bartberger, M. D., Liu, W., Ford, E., Miranda, K. M., Switzer, C., Fukuto, J. M., Farmer, P. J., Wink, D. A., and Houk, K. N. (2002) The reduction potential of nitric oxide (NO) and its importance to NO biochemistry, *Proc Natl Acad Sci U S A* **99**(17), 10958-10963
8. Shafirovich, V., and Lymar, S. V. (2002) Nitroxyl and its anion in aqueous solutions: spin states, protic equilibria, and reactivities toward oxygen and nitric oxide, *Proc Natl Acad Sci U S A* **99**(11), 7340-7345
9. Zweier, J. L., Samouilov, A., and Kuppasamy, P. (1999) Non-enzymatic nitric oxide synthesis in biological systems, *Biochim Biophys Acta* **1411**(2-3), 250-262
10. Zumft, W. G. (1997) Cell biology and molecular basis of denitrification, *Microbiol Mol Biol Rev* **61**(4), 533-616
11. Wasser, I. M., de Vries, S., Moenne-Loccoz, P., Schroder, I., and Karlin, K. D. (2002) Nitric oxide in biological denitrification: Fe/Cu metalloenzyme and metal complex NO(x) redox chemistry, *Chem Rev* **102**(4), 1201-1234
12. Hendriks, J., Oubrie, A., Castresana, J., Urbani, A., Gemeinhardt, S., and Saraste, M. (2000) Nitric oxide reductases in bacteria, *Biochim Biophys Acta* **1459**(2-3), 266-273
13. Zumft, W. G. (2005) Nitric oxide reductases of prokaryotes with emphasis on the respiratory, heme-copper oxidase type, *J Inorg Biochem* **99**(1), 194-215
14. Rodionov, D. A., Dubchak, I. L., Arkin, A. P., Alm, E. J., and Gelfand, M. S. (2005) Dissimilatory metabolism of nitrogen oxides in bacteria: comparative reconstruction of transcriptional networks, *PLoS Comput Biol* **1**(5), e55
15. Fujiwara, T., and Fukumori, Y. (1996) Cytochrome cb-type nitric oxide reductase with cytochrome c oxidase activity from *Paracoccus denitrificans* ATCC 35512, *J Bacteriol* **178**(7), 1866-1871
16. Suharti, Strampraad, M. J., Schroder, I., and de Vries, S. (2001) A novel copper A containing menaquinol NO reductase from *Bacillus azotoformans*, *Biochemistry* **40**(8), 2632-2639

17. Hendriks, J., Warne, A., Gohlke, U., Haltia, T., Ludovici, C., Lubben, M., and Saraste, M. (1998) The active site of the bacterial nitric oxide reductase is a dinuclear iron center, *Biochemistry* **37**(38), 13102-13109
18. de Vries, S., Strampraad, M. J., Lu, S., Moenne-Loccoz, P., and Schroder, I. (2003) Purification and characterization of the MQH2:NO oxidoreductase from the hyperthermophilic archaeon *Pyrobaculum aerophilum*, *J Biol Chem* **278**(38), 35861-35868
19. Thorndycroft, F. H., Butland, G., Richardson, D. J., and Watmough, N. J. (2007) A new assay for nitric oxide reductase reveals two conserved glutamate residues form the entrance to a proton-conducting channel in the bacterial enzyme, *Biochem J* **401**(1), 111-119
20. Flock, U., Watmough, N. J., and Adelroth, P. (2005) Electron/proton coupling in bacterial nitric oxide reductase during reduction of oxygen, *Biochemistry* **44**(31), 10711-10719
21. Flock, U., Reimann, J., and Adelroth, P. (2006) Proton transfer in bacterial nitric oxide reductase, *Biochem Soc Trans* **34**(Pt 1), 188-190
22. Shoun, H., and Tanimoto, T. (1991) Denitrification by the fungus *Fusarium oxysporum* and involvement of cytochrome P-450 in the respiratory nitrite reduction, *J Biol Chem* **266**(17), 11078-11082
23. Alderton, W. K., Cooper, C. E., and Knowles, R. G. (2001) Nitric oxide synthases: structure, function and inhibition, *Biochem J* **357**(Pt 3), 593-615
24. Li, H., Raman, C. S., Glaser, C. B., Blasko, E., Young, T. A., Parkinson, J. F., Whitlow, M., and Poulos, T. L. (1999) Crystal structures of zinc-free and -bound heme domain of human inducible nitric-oxide synthase. Implications for dimer stability and comparison with endothelial nitric-oxide synthase, *J Biol Chem* **274**(30), 21276-21284
25. Fischmann, T. O., Hruza, A., Niu, X. D., Fossetta, J. D., Lunn, C. A., Dolphin, E., Prongay, A. J., Reichert, P., Lundell, D. J., Narula, S. K., and Weber, P. C. (1999) Structural characterization of nitric oxide synthase isoforms reveals striking active-site conservation, *Nat Struct Biol* **6**(3), 233-242
26. Hemmens, B., Goessler, W., Schmidt, K., and Mayer, B. (2000) Role of bound zinc in dimer stabilization but not enzyme activity of neuronal nitric-oxide synthase, *J Biol Chem* **275**(46), 35786-35791
27. Mattevi, A. (2006) To be or not to be an oxidase: challenging the oxygen reactivity of flavoenzymes, *Trends Biochem Sci* **31**(5), 276-283
28. Miranda, K. M., Paolocci, N., Katori, T., Thomas, D. D., Ford, E., Bartberger, M. D., Espey, M. G., Kass, D. A., Feelisch, M., Fukuto, J. M., and Wink, D. A. (2003) A biochemical rationale for the discrete behavior of nitroxyl and nitric oxide in the cardiovascular system, *Proc Natl Acad Sci U S A* **100**(16), 9196-9201
29. Stamler, J. S. (1994) Redox signaling: nitrosylation and related target interactions of nitric oxide, *Cell* **78**(6), 931-936
30. Schopfer, F. J., Baker, P. R., and Freeman, B. A. (2003) NO-dependent protein nitration: a cell signaling event or an oxidative inflammatory response?, *Trends Biochem Sci* **28**(12), 646-654
31. Furchgott, R. F., Carvalho, M. H., Khan, M. T., and Matsunaga, K. (1987) Evidence for endothelium-dependent vasodilation of resistance vessels by acetylcholine, *Blood Vessels* **24**(3), 145-149

32. Palmer, R. M., Ferrige, A. G., and Moncada, S. (1987) Nitric oxide release accounts for the biological activity of endothelium-derived relaxing factor, *Nature* **327**(6122), 524-526
33. Ignarro, L. J., Buga, G. M., Wood, K. S., Byrns, R. E., and Chaudhuri, G. (1987) Endothelium-derived relaxing factor produced and released from artery and vein is nitric oxide, *Proc Natl Acad Sci U S A* **84**(24), 9265-9269
34. Moncada, S., and Higgs, A. (2001) Nitric Oxide: Role in Human Disease. In: *Encyclopedia of Life Sciences*, MacMillan Publishers Ltd, Nature Publishing Group / www.els.net
35. Brunori, M., Giuffre, A., Forte, E., Mastronicola, D., Barone, M. C., and Sarti, P. (2004) Control of cytochrome c oxidase activity by nitric oxide, *Biochim Biophys Acta* **1655**(1-3), 365-371
36. Cooper, C. E. (2003) Competitive, reversible, physiological? Inhibition of mitochondrial cytochrome oxidase by nitric oxide, *IUBMB Life* **55**(10-11), 591-597
37. Nathan, C., and Shiloh, M. U. (2000) Reactive oxygen and nitrogen intermediates in the relationship between mammalian hosts and microbial pathogens, *Proc Natl Acad Sci U S A* **97**(16), 8841-8848
38. MacMicking, J., Xie, Q. W., and Nathan, C. (1997) Nitric oxide and macrophage function, *Annu Rev Immunol* **15**, 323-350
39. Bogdan, C., Rollinghoff, M., and Diefenbach, A. (2000) Reactive oxygen and reactive nitrogen intermediates in innate and specific immunity, *Curr Opin Immunol* **12**(1), 64-76
40. Cooper, C. E. (1999) Nitric oxide and iron proteins, *Biochim Biophys Acta* **1411**(2-3), 290-309
41. Lepoivre, M., Fieschi, F., Coves, J., Thelander, L., and Fontecave, M. (1991) Inactivation of ribonucleotide reductase by nitric oxide, *Biochem Biophys Res Commun* **179**(1), 442-448
42. Justino, M. C., Goncalves, V. M., and Saraiva, L. M. (2005) Binding of NorR to three DNA sites is essential for promoter activation of the flavorubredoxin gene, the nitric oxide reductase of *Escherichia coli*, *Biochem Biophys Res Commun* **328**(2), 540-544
43. Spiro, S. (2006) Nitric oxide-sensing mechanisms in *Escherichia coli*, *Biochem Soc Trans* **34**(Pt 1), 200-202
44. Tucker, N. P., D'Autreaux, B., Spiro, S., and Dixon, R. (2006) Mechanism of transcriptional regulation by the *Escherichia coli* nitric oxide sensor NorR, *Biochem Soc Trans* **34**(Pt 1), 191-194
45. Justino, M. C., Almeida, C. C., Goncalves, V. L., Teixeira, M., and Saraiva, L. M. (2006) *Escherichia coli* YtfE is a di-iron protein with an important function in assembly of iron-sulphur clusters, *FEMS Microbiol Lett* **257**(2), 278-284
46. Almeida, C. C., Romao, C. V., Lindley, P. F., Teixeira, M., and Saraiva, L. M. (2006) The role of the hybrid cluster protein in oxidative stress defense, *J Biol Chem* **281**(43), 32445-32450
47. Demple, B., Ding, H., and Jorgensen, M. (2002) *Escherichia coli* SoxR protein: sensor/transducer of oxidative stress and nitric oxide, *Methods Enzymol* **348**, 355-364
48. Nunoshiba, T., deRojas-Walker, T., Wishnok, J. S., Tannenbaum, S. R., and Demple, B. (1993) Activation by nitric oxide of an oxidative-stress response that

- defends *Escherichia coli* against activated macrophages, *Proc Natl Acad Sci U S A* **90**(21), 9993-9997
49. Hausladen, A., Privalle, C. T., Keng, T., DeAngelo, J., and Stamler, J. S. (1996) Nitrosative stress: activation of the transcription factor OxyR, *Cell* **86**(5), 719-729
 50. Ding, H., and Demple, B. (1997) In vivo kinetics of a redox-regulated transcriptional switch, *Proc Natl Acad Sci U S A* **94**(16), 8445-8449
 51. Kim, S. O., Merchant, K., Nudelman, R., Beyer, W. F., Jr., Keng, T., DeAngelo, J., Hausladen, A., and Stamler, J. S. (2002) OxyR: a molecular code for redox-related signaling, *Cell* **109**(3), 383-396
 52. Hantke, K. (2001) Iron and metal regulation in bacteria, *Curr Opin Microbiol* **4**(2), 172-177
 53. Zheng, M., Doan, B., Schneider, T. D., and Storz, G. (1999) OxyR and SoxRS regulation of fur, *J Bacteriol* **181**(15), 4639-4643
 54. D'Autreaux, B., Touati, D., Bersch, B., Latour, J. M., and Michaud-Soret, I. (2002) Direct inhibition by nitric oxide of the transcriptional ferric uptake regulation protein via nitrosylation of the iron, *Proc Natl Acad Sci U S A* **99**(26), 16619-16624
 55. Cruz-Ramos, H., Crack, J., Wu, G., Hughes, M. N., Scott, C., Thomson, A. J., Green, J., and Poole, R. K. (2002) NO sensing by FNR: regulation of the *Escherichia coli* NO-detoxifying flavohaemoglobin, Hmp, *Embo J* **21**(13), 3235-3244
 56. Poole, R. K., and Hughes, M. N. (2000) New functions for the ancient globin family: bacterial responses to nitric oxide and nitrosative stress, *Mol Microbiol* **36**(4), 775-783
 57. Frey, A. D., Farres, J., Bollinger, C. J., and Kallio, P. T. (2002) Bacterial hemoglobins and flavohemoglobins for alleviation of nitrosative stress in *Escherichia coli*, *Appl Environ Microbiol* **68**(10), 4835-4840
 58. Frey, A. D., and Kallio, P. T. (2003) Bacterial hemoglobins and flavohemoglobins: versatile proteins and their impact on microbiology and biotechnology, *FEMS Microbiol Rev* **27**(4), 525-545
 59. Pathania, R., Navani, N. K., Gardner, A. M., Gardner, P. R., and Dikshit, K. L. (2002) Nitric oxide scavenging and detoxification by the *Mycobacterium tuberculosis* haemoglobin, HbN in *Escherichia coli*, *Mol Microbiol* **45**(5), 1303-1314
 60. Pathania, R., Navani, N. K., Rajamohan, G., and Dikshit, K. L. (2002) *Mycobacterium tuberculosis* hemoglobin HbO associates with membranes and stimulates cellular respiration of recombinant *Escherichia coli*, *J Biol Chem* **277**(18), 15293-15302
 61. Goncalves, V. L., Nobre, L. S., Vicente, J. B., Teixeira, M., and Saraiva, L. M. (2006) Flavohemoglobin requires microaerophilic conditions for nitrosative protection of *Staphylococcus aureus*, *FEBS Lett* **580**(7), 1817-1821
 62. Hausladen, A., Gow, A. J., and Stamler, J. S. (1998) Nitrosative stress: metabolic pathway involving the flavohemoglobin, *Proc Natl Acad Sci U S A* **95**(24), 14100-14105
 63. Gardner, P. R., Gardner, A. M., Martin, L. A., and Salzman, A. L. (1998) Nitric oxide dioxygenase: an enzymic function for flavohemoglobin, *Proc Natl Acad Sci U S A* **95**(18), 10378-10383

64. Hausladen, A., Gow, A., and Stamler, J. S. (2001) Flavohemoglobin denitrosylase catalyzes the reaction of a nitroxyl equivalent with molecular oxygen, *Proc Natl Acad Sci U S A* **98**(18), 10108-10112
65. Kim, S. O., Orii, Y., Lloyd, D., Hughes, M. N., and Poole, R. K. (1999) Anoxic function for the Escherichia coli flavohaemoglobin (Hmp): reversible binding of nitric oxide and reduction to nitrous oxide, *FEBS Lett* **445**(2-3), 389-394
66. Crawford, M. J., and Goldberg, D. E. (1998) Regulation of the Salmonella typhimurium flavohemoglobin gene. A new pathway for bacterial gene expression in response to nitric oxide, *J Biol Chem* **273**(51), 34028-34032
67. Favey, S., Labesse, G., Vouille, V., and Boccara, M. (1995) Flavohaemoglobin HmpX: a new pathogenicity determinant in Erwinia chrysanthemi strain 3937, *Microbiology* **141** (Pt 4), 863-871
68. Stevanin, T. M., Poole, R. K., Demoncheaux, E. A., and Read, R. C. (2002) Flavohemoglobin Hmp protects Salmonella enterica serovar typhimurium from nitric oxide-related killing by human macrophages, *Infect Immun* **70**(8), 4399-4405
69. Membrillo-Hernandez, J., Kim, S. O., Cook, G. M., and Poole, R. K. (1997) Paraquat regulation of hmp (flavohemoglobin) gene expression in Escherichia coli K-12 is SoxRS independent but modulated by sigma S, *J Bacteriol* **179**(10), 3164-3170
70. Bonamore, A., Gentili, P., Ilari, A., Schinina, M. E., and Boffi, A. (2003) Escherichia coli flavohemoglobin is an efficient alkylhydroperoxide reductase, *J Biol Chem* **278**(25), 22272-22277
71. Mukai, M., Mills, C. E., Poole, R. K., and Yeh, S. R. (2001) Flavohemoglobin, a globin with a peroxidase-like catalytic site, *J Biol Chem* **276**(10), 7272-7277
72. Bonamore, A., Farina, A., Gattoni, M., Schinina, M. E., Bellelli, A., and Boffi, A. (2003) Interaction with membrane lipids and heme ligand binding properties of Escherichia coli flavohemoglobin, *Biochemistry* **42**(19), 5792-5801
73. Poole, R. K., Anjum, M. F., Membrillo-Hernandez, J., Kim, S. O., Hughes, M. N., and Stewart, V. (1996) Nitric oxide, nitrite, and Fnr regulation of hmp (flavohemoglobin) gene expression in Escherichia coli K-12, *J Bacteriol* **178**(18), 5487-5492
74. Membrillo-Hernandez, J., Ioannidis, N., and Poole, R. K. (1996) The flavohaemoglobin (HMP) of Escherichia coli generates superoxide in vitro and causes oxidative stress in vivo, *FEBS Lett* **382**(1-2), 141-144
75. Membrillo-Hernandez, J., Coopamah, M. D., Channa, A., Hughes, M. N., and Poole, R. K. (1998) A novel mechanism for upregulation of the Escherichia coli K-12 hmp (flavohaemoglobin) gene by the 'NO releaser', S-nitrosoglutathione: nitrosation of homocysteine and modulation of MetR binding to the glyA-hmp intergenic region, *Mol Microbiol* **29**(4), 1101-1112
76. Mukhopadhyay, P., Zheng, M., Bedzyk, L. A., LaRossa, R. A., and Storz, G. (2004) Prominent roles of the NorR and Fur regulators in the Escherichia coli transcriptional response to reactive nitrogen species, *Proc Natl Acad Sci U S A* **101**(3), 745-750
77. Justino, M. C., Vicente, J. B., Teixeira, M., and Saraiva, L. M. (2005) New genes implicated in the protection of anaerobically grown Escherichia coli against nitric oxide, *J Biol Chem* **280**(4), 2636-2643

78. Pullan, S. T., Gidley, M. A., Jones, R. A., Barrett, J., Stevanin, T. M., Read, R. C., Green, J., and Poole, R. K. (2006) Nitric Oxide in Chemostat-Cultured *Escherichia coli* is Sensed by Fnr and Other Global Regulators; Unaltered Methionine Biosynthesis Indicates Lack of S-Nitrosation, *J Bacteriol*
79. Flatley, J., Barrett, J., Pullan, S. T., Hughes, M. N., Green, J., and Poole, R. K. (2005) Transcriptional responses of *Escherichia coli* to S-nitrosoglutathione under defined chemostat conditions reveal major changes in methionine biosynthesis, *J Biol Chem* **280**(11), 10065-10072
80. Gardner, P. R. (2005) Nitric oxide dioxygenase function and mechanism of flavohemoglobin, hemoglobin, myoglobin and their associated reductases, *J Inorg Biochem* **99**(1), 247-266
81. Poole, R. K. (2005) Nitric oxide and nitrosative stress tolerance in bacteria, *Biochem Soc Trans* **33**(Pt 1), 176-180
82. Poock, S. R., Leach, E. R., Moir, J. W., Cole, J. A., and Richardson, D. J. (2002) Respiratory detoxification of nitric oxide by the cytochrome c nitrite reductase of *Escherichia coli*, *J Biol Chem* **277**(26), 23664-23669
83. Rudolf, M., Einsle, O., Neese, F., and Kroneck, P. M. (2002) Pentaheme cytochrome c nitrite reductase: reaction with hydroxylamine, a potential reaction intermediate and substrate, *Biochem Soc Trans* **30**(4), 649-653
84. Einsle, O., Messerschmidt, A., Huber, R., Kroneck, P. M., and Neese, F. (2002) Mechanism of the six-electron reduction of nitrite to ammonia by cytochrome c nitrite reductase, *J Am Chem Soc* **124**(39), 11737-11745
85. Costa, C., Macedo, A., Moura, I., Moura, J. J., Le Gall, J., Berlier, Y., Liu, M. Y., and Payne, W. J. (1990) Regulation of the hexaheme nitrite/nitric oxide reductase of *Desulfovibrio desulfuricans*, *Wolinella succinogenes* and *Escherichia coli*. A mass spectrometric study, *FEBS Lett* **276**(1-2), 67-70
86. Cross, R., Aish, J., Paston, S. J., Poole, R. K., and Moir, J. W. (2000) Cytochrome c' from *Rhodobacter capsulatus* confers increased resistance to nitric oxide, *J Bacteriol* **182**(5), 1442-1447
87. Sakamoto, A., Ueda, M., and Morikawa, H. (2002) Arabidopsis glutathione-dependent formaldehyde dehydrogenase is an S-nitrosoglutathione reductase, *FEBS Lett* **515**(1-3), 20-24
88. Liu, L., Hausladen, A., Zeng, M., Que, L., Heitman, J., and Stamler, J. S. (2001) A metabolic enzyme for S-nitrosothiol conserved from bacteria to humans, *Nature* **410**(6827), 490-494
89. De Groote, M. A., Testerman, T., Xu, Y., Stauffer, G., and Fang, F. C. (1996) Homocysteine antagonism of nitric oxide-related cytostasis in *Salmonella typhimurium*, *Science* **272**(5260), 414-417
90. St John, G., Brot, N., Ruan, J., Erdjument-Bromage, H., Tempst, P., Weissbach, H., and Nathan, C. (2001) Peptide methionine sulfoxide reductase from *Escherichia coli* and *Mycobacterium tuberculosis* protects bacteria against oxidative damage from reactive nitrogen intermediates, *Proc Natl Acad Sci U S A* **98**(17), 9901-9906
91. Gobert, A. P., McGee, D. J., Akhtar, M., Mendz, G. L., Newton, J. C., Cheng, Y., Mobley, H. L., and Wilson, K. T. (2001) *Helicobacter pylori* arginase inhibits nitric oxide production by eukaryotic cells: a strategy for bacterial survival, *Proc Natl Acad Sci U S A* **98**(24), 13844-13849

2

THE FAMILY OF THE FLAVODIIRON PROTEINS

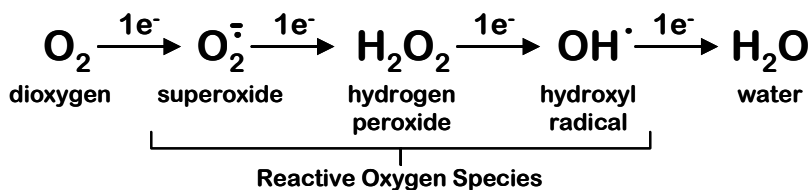
2.1	Oxygen Biochemistry in “Anaerobes”	48
2.2	Establishment of a Novel Family of Flavodiiron Proteins	54
	Structure of <i>Desulfovibrio gigas</i> Rubredoxin:Oxygen Oxidoreductase	55
	A Novel Type of Non-Haem Diiron Centre in a β -Lactamase Fold	57
	Modular Nature of Flavodiiron Proteins – Structural Classification	59
	Diversity of Electron Transfer Chains	61
2.3	Basis for a Role in Nitric Oxide Detoxification	64
	References	67

2. THE FAMILY OF FLAVODIIRON PROTEINS

2.1 OXYGEN BIOCHEMISTRY IN “ANAEROBES”

Oxygen metabolism in aerobic and anaerobic (strict and facultative) organisms has distinct physiological significances. Whereas aerobes mainly profit energetically from oxygen breakdown to water, anaerobes are sensitive to this diatomic molecule. However, both aerobes and anaerobes may have to cope with reactive oxygen species (ROS) and the resulting oxidative stress, under certain conditions. The cellular responses to oxidative stress resulting from ROS have some parallel pathways among aerobic and anaerobic organisms but differ in a number of routes.

There are two main routes by which aerobic organisms may have to cope with reactive oxygen species: one is related to malfunction of respiratory chains and the other has to do with the host immune response to microbial invasion/infection exploiting the cytotoxicity of ROS for the foreign organisms (which ultimately also harms the host). Reduction of oxygen to water is the terminal process of aerobic respiratory chains, which is accomplished by haem-copper oxygen reductases (Complex IV), using electrons provided by electron transfer complexes that primarily use reducing equivalents from NADH (deriving essentially from carbohydrates metabolism). In terminal oxidases, oxygen reduction is coupled to proton translocation across the membrane, which generates an electrochemical potential that is essential to drive ATP synthesis. Although eukaryotic and prokaryotic respiratory complexes differ in some of their properties (with increasing complexity from the prokaryotic to the eukaryotic world), the basic functional principles are conserved throughout evolution. Electron flow through the electron transfer chain from NADH to oxygen is prone to involve malfunctions which impair full reduction of oxygen and thus lead to the generation of partially reduced reactive oxygen species. As described in the



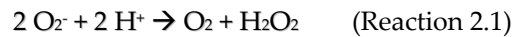
Scheme 2.1 – Oxygen reduction to water and its intermediate reactive oxygen species

previous chapter for reactive nitrogen species, also reactive oxygen species have cytotoxic effects at high concentrations both for eukaryotes and prokaryotes, and regulatory and signalling effects at low concentrations for higher eukaryotes. In fact, another way ROS enter living systems is related to their production as a weapon of the host immune system against microbial invasion and infection. Superoxide anion is generated by an NADPH oxidase that catalyzes the one-electron reduction of oxygen and released against the invading organisms. The released superoxide is cytotoxic *per se* and also gives rise to other superoxide-derived ROS (such as H₂O₂ and hydroxyl radical) and RNS (such as peroxyntirite, see previous chapter). This poses a challenge not only for the invading microbes, but also for the host cells, part of which are sacrificed in this process for the sake of the whole organism.

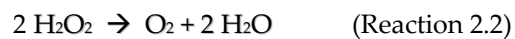
Anaerobic organisms are challenged with oxidative stress upon exposure to dioxygen and also as part of the above mentioned host immune response. Anaerobic microbial mats are often exposed temporarily to oxygen pressure. Oxygen is an apolar molecule and thus promptly diffuses across biological membranes. The anoxic environments and the cellular milieu of anaerobes are regarded as highly reductive media, where spurious oxygen partial reduction may occur non-enzymatically through its reaction with reduced cellular components, yielding partially reduced reactive oxygen species. The challenge of ROS / oxidative stress imposed onto anaerobes gains special relevance taking into account that many pathogens are anaerobes or microaerophiles and that

infection/inflammation sites are associated with low oxygen tensions (release of ROS by immune system specialized cells is localized).

Both in aerobic and anaerobic organisms, a number of specialized enzymes allow these organisms to cope (to some extent) with the cytotoxicity of ROS. In aerobes, superoxide is scavenged by the almost ubiquitous superoxide dismutases (SODs) that disproportionate superoxide to hydrogen peroxide and dioxygen (Reaction 2.1).



Eukaryotic SODs have typically a Cu-Zn active site, and although bacterial SODs have mainly Fe or Mn at their active sites, there are also cases of bacterial SODs with Cu-Zn or Ni sites. Hydrogen peroxide is detoxified in aerobes mainly by catalases, haem proteins which catalyze the disproportionation of H_2O_2 to dioxygen and water (Reaction 2.2).



Due to the high K_M of catalases for H_2O_2 , most aerobic bacteria use another strategy to cope with lower concentrations of H_2O_2 , which involves its reduction to water catalyzed by a class of enzymes named peroxidases (H_2O_2 reductases).

Besides the above mentioned classical enzymes for superoxide and hydrogen peroxide scavenging in aerobes, other cellular mechanisms may contribute to the aerobic concerted response to oxidative stress, which will not be described here.

In contrast with the finite number of available enzymatic responses of aerobes to oxidative stress, anaerobes have a myriad of enzymes and pathways that necessarily include dioxygen scavenging, since this is a toxic species for the latter. Indeed, redundancy of systems to cope with oxygen and its ROS is an aspect that characterizes the anaerobic response to oxidative stress, which contributes to its robustness. Oxygen metabolism in anaerobes is also intimately related with the iron metabolism, since it is at the organisms' convenience to prevent free ferrous

ions from catalyzing ROS formation through the Fenton reaction, which creates direct damages onto cellular components, such as DNA. Since the history of the FlavoDiiron Proteins (the scope of this thesis) has its roots in the seminal work exploring the survival mechanisms of anaerobic prokaryotes under oxidative stress, essentially in sulphate-reducing bacteria of the *Desulfovibrio* genus (figure 2.1), these organisms shall be taken as a case-study from this point on. In fact, organisms that were once considered strict anaerobes are now being shown to be endowed with the appropriate cellular machinery to cope with exposure to oxygen and its reactive species, and possibly even profiting energetically from oxygen metabolism.

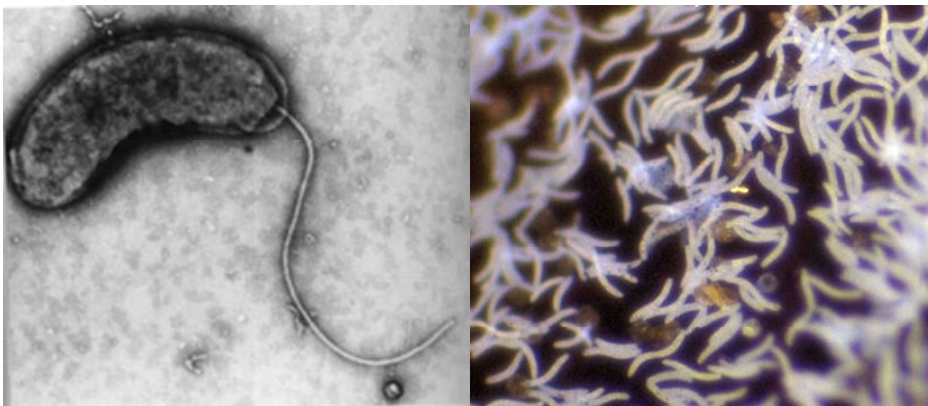


Fig 2.1 – Bacterial cells of the *Desulfovibrio* genus.

Under non-limiting growth conditions, *Desulfovibrio* strains have been shown to accumulate polyglucose (1). The observation that the “anaerobe” *Desulfovibrio* (*D.*) *gigas* was capable of utilizing its internal polyglucose reserves upon oxygen exposure (2) (as well as in anoxic conditions) was associated with the discovery of a soluble enzyme responsible for oxygen consumption. *D.gigas* rubredoxin:oxygen oxidoreductase (ROO) was described as a homodimeric flavohemoprotein (3), containing per 43 kDa monomer one FAD and two different types of hemes: protoporphyrin IX and uroporphyrin I. This enzyme was the first flavodiiron protein to be characterized and for a long time it

constituted the primary prototype of this protein family (see below). ROO was shown to be the terminal enzyme of an electron transfer chain that

includes an FAD- and FMN-binding NADH:rubredoxin oxidoreductase (Nro) (4) and a rubredoxin (Rd), a small (~6 kDa) soluble electron transfer protein containing one [Fe-S(Cys)₄] center. Electrons for oxygen reduction arrive at ROO via Rd (5), whose reduction is accomplished by reduced Nro, which accepts electrons from NADH (Figure 2.2). The demonstration that in *D. gigas* the genes encoding ROO and Rd form a

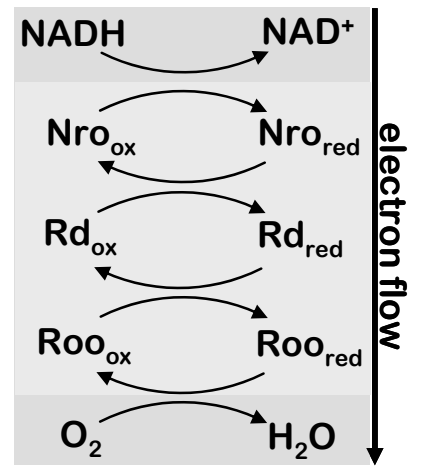


Fig.2.2 - Soluble electron transfer chain from *Desulfovibrio gigas* that couples NADH oxidation to oxygen reduction.

dicystronic transcriptional unit enforced the possible redox partnership of these two proteins, which was demonstrated spectroscopically (5). With the discovery of this electron transfer chain, it was proposed that it sustained *D. gigas* survival upon transient exposures to dioxygen. However, with the evergrowing number of available genome sequences, a striking observation was that sequenced *Desulfovibrio* strains encode for classical haem-copper oxygen reductases, as well as for the cyanide-insensitive *bd*-type oxidases (6,7), which was in fact isolated from *D. gigas* (8). Moreover, there appears to be an elusive role of hydrogenases and their associated soluble cytochromes in the periplasmatic reduction of oxygen. Therefore, the classification of *Desulfovibrio* strains as obligate anaerobes should be withdrawn and these organisms should probably be regarded as facultative anaerobes. Quite recently, growth of a pure culture of a *Desulfovibrio* species at almost atmospheric oxygen concentrations was reported (9). Moreover, to deal with other reactive oxygen species and the possibly resulting damages, *Desulfovibrio* strains are endowed with a multitude of enzymes and pathways,

which are represented schematically in Figure 2.3. Generally speaking, damage repair systems include alkyl hydroperoxide reductase (to clear damage onto lipids) and enzymes that metabolize disulfides (resulting from oxidative stress) generating thiol groups. Enzymatic machinery for the detoxification of ROS is unequally divided between the periplasmatic and cytoplasmatic spaces. Superoxide is scavenged in *Desulfovibrio* strains by two prominent families of proteins, the periplasmatic Fe-SODs and the cytoplasmatic Fe superoxide reductases (Fe-SORs), which contrarily to SODs catalyze only the one-electron reduction of superoxide to H_2O_2 (10). Fe-SORs are present in the genomes of many anaerobes and, although a significant part of these genomes also encode for SODs, some organisms rely solely on Fe-SORs to scavenge superoxide. Hydrogen peroxide is detoxified in the cytoplasm by catalases (which disproportionate H_2O_2 to water and oxygen) and rubrerythrins and nigerythrins,

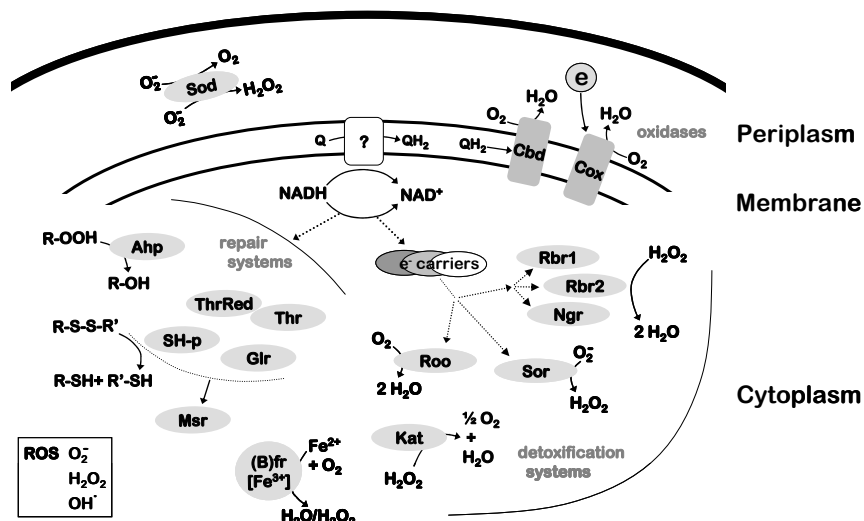


Fig. 2.3 – Schematic model of oxygen defence systems in *Desulfovibrio*. Sod – superoxide dismutase, Cbd – bd oxidase, Cox – cytochrome oxidase, Rbr – rubrerythrin, Ngr – nigerythrin, Sor – superoxide reductase, Roo – rubredoxin:oxygen oxidoreductase, Kat – catalase, (B)fr – (bactero)ferritin, Ahp – alkyl hydroperoxide reductase, ThrRed – thioredoxin reductase, Thr – thioredoxin, Glr – glutaredoxin, SH-p – protein-bound redox active thiol groups. (Adapted from (11))

which catalyze the reduction of H_2O_2 to water (12). The role of ROO (and possibly other Flavodiiron Proteins - see below) as an oxygen reductase, together with Fe-

SORs and rubrerythrins/nigerythrins, led to the proposal of an apparent “non-haem iron reductive paradigm” to cope with dioxygen and its derived reactive species (12). An interesting observation is that rubredoxins appear to be ubiquitous and somehow “promiscuous” electron donors for O₂/ROS-scavenging non-haem iron proteins (5,13,14).

2.2 ESTABLISHMENT OF A NOVEL FAMILY OF FLAVODIIRON PROTEINS

The proposed role of ROO as an oxygen reductase which afforded protection to the “anaerobe” *D. gigas* opened a new field of research, as reports began to sprout on enzymes homologous to ROO. Almost simultaneously, preliminary studies on flavoprotein ROO homologues from two different strains of *Methanothermobacterium thermoautotrophicum* suggested elusive roles related to methanogenesis (15) and iron or nitrogen metabolism (16). In the latter study, the aforementioned flavoprotein (then called Flavoprotein A, FprA) was one of the most expressed proteins in cells grown under iron limitation. The number of genome projects being sequenced in the mid-to-late 90s eventually led Wasserfallen and co-workers (17) to propose a family of A-type Flavoproteins (ATF, the former name given to FlavoDiiron Proteins), widespread in Bacteria and Archaea. This family of proteins was at this time mainly analysed in terms of the primary structures and available biochemical data, while the first steps for the characterization of the homologues from *Rhodobacter (R.) capsulatus*, *Escherichia (E.) coli* and *Synechocystis* sp. PCC6803 were undertaken. From the sequence analysis, it became evident that a core of 385-400 aminoacids was common to all the members, where a flavodoxin (soluble, FMN-binding, electron transfer protein) signature was present, starting at residues 245-285 of the core sequence. At the time, no other properties of the common core could be envisaged solely from the sequence analysis. However, one evident observation was that some

members of this protein family had C-terminal extensions beyond the common core, which could be identified as extra structural modules, upon analysing their separate sequences. It was then noticed that the C-terminal extension of the *E. coli* ATF was homologous to rubredoxins, whereas the C-terminus of the *Synechocystis* ATF was a homologue of NAD(P)H-oxidizing flavoproteins. On the basis of these observations, four types of ATFs could already be identified from a relatively small number of sequences: “simple” flavoproteins (the ones having simply the common core), diflavin flavoproteins (the *Synechocystis* ATF), a flavorubredoxin (the *E. coli* ATF) and a flavohemoprotein (*D. gigas* ROO). Interestingly, although major breakthroughs were to come to this field of research, this primordial classification still holds in most of its rationale (see below).

Structure of Desulfovibrio gigas Rubredoxin:Oxygen Oxidoreductase

A landmark in the history of the Flavodiiron Proteins was the resolution of the crystallographic 3-D structure of *D. gigas* ROO (18), which shed light onto the possible mechanisms and function of ROO and its homologues. Two main observations, which are described in detail below, were the most appalling upon unraveling ROO's structure: the *N-terminal* module is structurally homologous to *metallo-β-lactamases* and it harbours a novel type of *non-haem diiron centre*. Surprisingly, the haem moieties reported by Chen and coworkers (3) were absent from the ROO dimer in the crystallographic structure. The fact that these haems were far less than sub-stoichiometric and their absence from the crystallographic structure suggests that they are in fact unspecifically bound to ROO and thus co-purified (18). The structure of *D. gigas* ROO was not only the first available for this family of enzymes (PDB entry 1e5d, (18)), but also the only one for a considerable amount of time. The enzyme was isolated as a functional homodimer and the X-ray crystal structure, solved at 2.5 Å resolution confirmed this quaternary structure: the enzyme crystallises as a dimer, in which the two

monomers have a head-to tail arrangement (Figure 2.4). Two structurally distinct domains build up each monomer. The N-terminal domain (up to Gln249 - unless otherwise stated, the aminoacid numbering of the *D. gigas* enzyme will be used) has an $\alpha\beta/\beta\alpha$ arrangement, with the two inner β -sheets surrounded by solvent exposed helices towards the external faces (Figure 2.4). The fold is very similar to

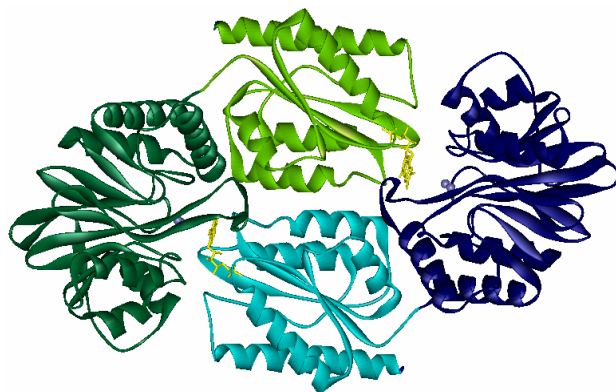


Figure 2.4 – Cartoon representation of homodimeric *D. gigas* ROO crystallographic structure. The two monomers (one in two shades of blue and the other in two shades of green) are arranged in a head-to-tail configuration, bringing the FMN of each monomer in close contact with the non-haem diiron centre of the other monomer.

that of class B Zn- β -lactamases, (r.m.s. values of C α atoms of 1.4 to 1.7 Å), although the amino-acid sequence identities are lower than 15%. But, in contrast with the lactamases, which contain a mono- or a di-zinc centre, ROO has a diiron centre, which

nevertheless occupies essentially the same spatial position as the zinc centre in the lactamases. Furthermore, the substrate binding residues and cavity required for the lactamase activity are not conserved in ROO: this space is occupied by an additional two-stranded β -sheet, the first helix of the C-half of the sandwich and its preceding extra loop, and contacts with the other monomer (Fig. 2.4), which altogether cover the metal site. The second domain (which starts at Lys250) has a typical $\alpha\beta\alpha$ flavodoxin-fold (Fig. 2.4) and contains one flavin mononucleotide (FMN). The FMN cofactor is located on one edge of the β -sheet. Although in each monomer the xylene ring from the FMN isoalloxazine ring is pointing to the surface of the flavodoxin module, the dimeric conformation of the as-isolated functional protein ends up covering the flavin moiety from bulk solvent exposure. The FMN isoalloxazine ring is parallel to the aromatic ring of Trp347.

In comparison to flavodoxins, the FMN pocket displays a greater preponderance of basic over acidic residues, which may account for a modulation of this cofactor's redox properties (discussed below).

A novel type of non-haem diiron centre in a β -lactamase fold

The iron ions are coordinated by histidines, glutamates and aspartates (H79-X-E81-X-D83-X₆₂-H146-X₁₈-D165-X₆₀-H226, Figure 2.5), and bridged by a μ -(hydr)oxo species and by the carboxylate of Asp165. Fe1, with a square pyramidal geometry, is further bound to His79, Glu81, and His 146, while Fe2 assumes a quadrangular planar geometry, being bound to Asp 83 and His 226.

Close to Fe2 there is a water molecule, which is at a non-bonding distance. The carboxylate oxygen OD1 of Asp83 is within hydrogen bonding distance to the μ -(hydr)oxo species. Further electron density close to Fe2 was interpreted as an oxygen molecule at H-bonding distance to the carboxylate oxygen OE2 of Glu81. The iron-to-iron distance (3.4 Å) is compatible with those determined for diferric centres. This set of ligands places the ROO iron centre in the family of the carboxylate/histidine diiron centres, present in a variety of enzymes, such as methane monooxygenase (MMOH), Type I ribonucleotide reductases (RNR), (hemo)ferritins (19) and hemerythrin (20,21) In these enzymes, the diiron centre is involved in oxygen binding (hemerythrin, the oxygen carrier in nematodes), or in

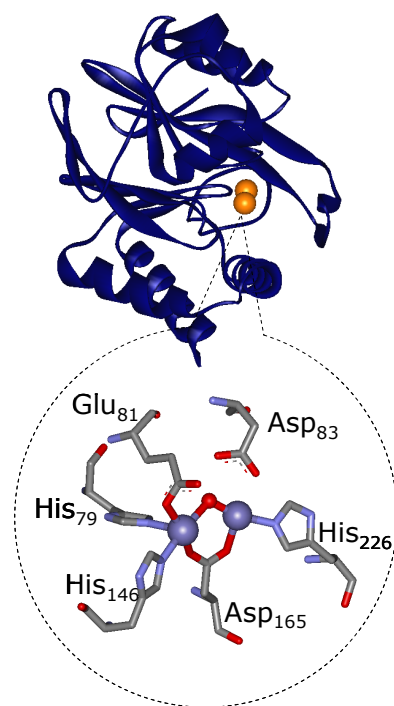


Figure 2.5 – β -lactamase domain of *D. gigas* ROO zoomed at the first coordination sphere of the non-haem diiron site.

oxygen activation, as a first step to perform their function (e.g., oxidation of methane to methanol by MMOH, oxidation of ferrous to ferric iron in ferritins, radical generation in RNR). However, in structural terms these enzymes are characterized by a four-helix bundle structural motif, quite distinct from the lactamase fold of ROO. The dimeric head-to tail arrangement has a strong functional implication. In fact, within each monomer, the two redox centres (the diiron site and the FMN) are quite far apart, at ca 35 Å, which limits considerably an efficient electron transfer between them. However, in the dimer, the diiron centre from one monomer is very close to the FMN of the other monomer (Figure 2.4). Indeed, the FMN methyl group C8M is in van der Waals contact with the carboxylate from Glu81, one of the ligands to Fe1, assuring a quite efficient electron transfer pathway between the two redox centres (18). More recently, the crystallographic structure of *Moorella thermoacetica* flavodiiron protein (Mt_FDP) was solved, in different states: as isolated, reduced and reduced/NO-reacted states (22). Although the majority of the above mentioned structural features of *D. gigas* ROO are conserved in the Mt_FDP structure, a significant difference is observed in the first coordination sphere. A histidine residue which is strictly conserved in this protein family (His86 in Mt_FDP and His84 in *D. gigas* ROO) is a diiron ligand in the Mt_FDP (22), whereas in ROO it is placed apart from the centre, being replaced by a crystallographic water molecule (18). The possible implications of this substitution are discussed in Chapter 10.

The metallo- β -lactamase structural domain is found in a large number of very diverse enzymes, from the three life domains: Eukarya, Bacteria and Archaea (23,24): glyoxalases II, which catalyse the hydrolysis of the thioester of S-D lactoglutathione to glutathione and lactic acid, arylsulfatases, DNA and RNA processing enzymes, among others. All these enzymes contain extra domains, besides the β -lactamase one. A total of 16 subfamilies have been proposed until now based on extensive sequence and structural comparisons (23), made for

already classified enzymes. However, Dayasu and co-workers indicated that a large number of still unassigned open reading frames in the sequenced genomes are also probably members of this large protein family. With the exception of the flavodiiron proteins, all other enzymes appear to contain a mono or di-zinc site, or, in the case of glyoxalases, a mixed iron-zinc centre (25). The metal site is always located at one edge of the internal $\alpha\beta\alpha$ sandwich; therefore, the larger aminoacid conservation occurs in aminoacid stretches that include the metal ligands. An analysis of the nature of those suggested that very minor substitutions led from a di-zinc to a diiron site, passing by a mixed-metal centre, keeping the same structural fold. This change is proposed to correlate with the activity of the enzymes, on going from a mainly Lewis-acid catalysis by the zinc site (in β -lactamases) to a redox active diiron site, capable of reducing dioxygen or nitric oxide (in the flavodiiron proteins). This proposal has been challenged by EXAFS studies on the β -lactamase domain of *E. coli* flavorubredoxin that demonstrated equivalently high affinities for both zinc and iron (26). Altogether, these analyses point to a possible evolutionary link between these proteins, being a paradigmatic example not only of divergent evolution but also of how nature can assemble diverse structural motifs and cofactors to achieve different functions. These enzymes are also a clear case where simple extrapolation of fold to function leads to wrong assignments of enzymatic functions, and calls for the need of extensive biochemical studies after the overwhelming amount of genomic data now available.

Modular Nature of Flavodiiron Proteins – Structural Classification

As above mentioned, Wasserfallen and co-workers (17) initially proposed a common sequence core for the flavodiiron proteins which the structure of *D. gigas* ROO (18) revealed to be a two-domain structural core, composed by a lactamase and a flavodoxin modules. However, as the same authors also noticed, several

members of this family have extra domains, fused at the C-terminal. Thus,

the initial proposal and the current extended knowledge on the modular composition of this protein family, it can be divided into three classes, A to C (Figure 2.6):



Figure 2.6 – Structural modules of flavodiiron proteins and respective classification.

. Class A, having only the two domain core, which so far

includes the largest number of members;

. Class B, which have a rubredoxin-like domain, containing a [FeCys₄]-binding motif, similar to those of Type I rubredoxins (two sets of cysteines, with the spacing –CysXXCys–). The recombinant enzyme from *E. coli* K12 was indeed shown to contain an extra rubredoxin-type centre, and was named flavorubredoxin (FlRd) (the central subject of this thesis, see next chapters). Genes encoding for Class B enzymes are so far found only in the genomes of enterobacteria (which contain only this type of flavodiiron proteins) and in *Erwinia chrysanthemi* (27).

. Class C, which have an additional module (of ca. 170 residues) with significant similarities to NAD(P)H:flavin oxidoreductases, and were only detected in cyanobacteria. The recombinant enzyme from *Synechocystis* sp. PCC6803 was purified and contains two flavin moieties, in agreement with this domain organisation (described in Chapter 8 of this thesis) (28). Within this class, two subgroups can be distinguished, according to the conservation of the iron binding residues (see below).

A possible fourth class may exist, since open reading frames in the genomes of *Clostridium perfringens* (29) and the protozoan parasite *Trichomonas vaginalis* (30) appear to encode for a flavodiiron protein, fused to a rubredoxin domain,

followed by an extra NADH:oxidoreductase domain. To clarify this possible new class of enzymes, biochemical data on it is needed. With the growing availability of genome sequences, and with the mosaic nature of this protein family, it is probable that even more classes of these enzymes may come to our knowledge.

Diversity of Electron Transfer Chains

The domain composition of these enzymes and in part the genomic organisation of the respective genes, reflect the different types of electron transfer chains operative in each organism. The studied chains have always in common the oxidation of NAD(P)H coupled to the reduction of the terminal electron acceptor (discussed in the next chapters) (Figure 2.7). Its variability is also reflected on the nature of the physiological partners, either already established or hypothesised on the basis of the genomic data.

. Class A

As mentioned above, *D. gigas* ROO has been shown to accept electrons directly from the one-electron reduced rubredoxin (Rd) partner (3,5), an electron transfer process which appears to be governed mainly but not exclusively by electrostatics (see chapter 7) (31). This electron transfer chain provided the first clear example of a function for a rubredoxin in anaerobes. In the genomes of *Clostridia* species, genes encoding for flavodiiron proteins are present. For example, the genome of *Clostridium perfringens* (29) has three loci coding for different flavodiiron proteins, one of which is contiguous to a rubredoxin-encoding gene and transcribed in the same direction. Interestingly, studies on *Clostridia* species revealed the presence of rubredoxin reductases in these organisms (32). In fact, the gene encoding the NADH:rubredoxin oxidoreductase in *Clostridium acetobutylicum* was identified (33), and it is contiguous to one of the genes coding for a flavodiiron protein in this organism, and transcribed in the same direction (34). Altogether these observations suggest that in *Clostridia* species the same type of electron transfer

chain, as the one observed in *D. gigas*, may be operative (Figure 2.7). In *Moorella thermoacetica*, the C-terminal modules from Class B and Class C flavodiiron proteins, i.e., the Rd and NAD(P)H:flavin oxidoreductase modules, are fused together in a single polypeptide chain, which was named by the authors as high molecular weight rubredoxin (Hrb) (35,36). The genes encoding for both Hrb and the flavodiiron protein are part of the same operon, which includes also a putative oxidative stress response protein, rubrerythrin. In the same locus, but divergently transcribed, there is a dicistronic unit, encoding for a two-iron superoxide reductase (desulfoferrodoxin) and its putative electron donor, a rubredoxin (35). Moreover, it was shown that Hrb efficiently reduces the flavodiiron protein at the expense of NADH oxidation (36). The Hrb NADH:flavin oxidoreductase module, which also displays a significant degree of similarity towards *Archaeoglobus fulgidus* ferric reductase (28), was proposed to accept electrons from NADH and to internally transfer them to the Rd module, which acts as the donor site for the flavodiiron protein (36). While in many genomes the flavodiiron genes are in loci containing genes that apparently do not encode for their physiological partners, analyses of other genomes suggest that other possibilities are plausible in terms of electron transfer chains involving flavodiiron proteins. Such is the case of *Archaeoglobus fulgidus*: this hyperthermophilic archaeon expresses two rubredoxins and has several NADH oxidases as candidates to act as NADH:rubredoxin oxidoreductases (37,38); nevertheless, the flavodiiron protein is encoded contiguously and in the same direction as the gene coding for an Fe-S flavoprotein, exactly as observed in the *Methanocaldococcus janaschii* genome (39). Moreover, in *Methanosarcina acetovorans* (40), this gene is present two genes downstream of the gene coding for the flavodiiron protein. These observations suggest the possible involvement of these uncharacterised Fe-S flavoproteins in electron transfer chains having flavodiiron proteins as the terminal acceptors (Figure 2.7).

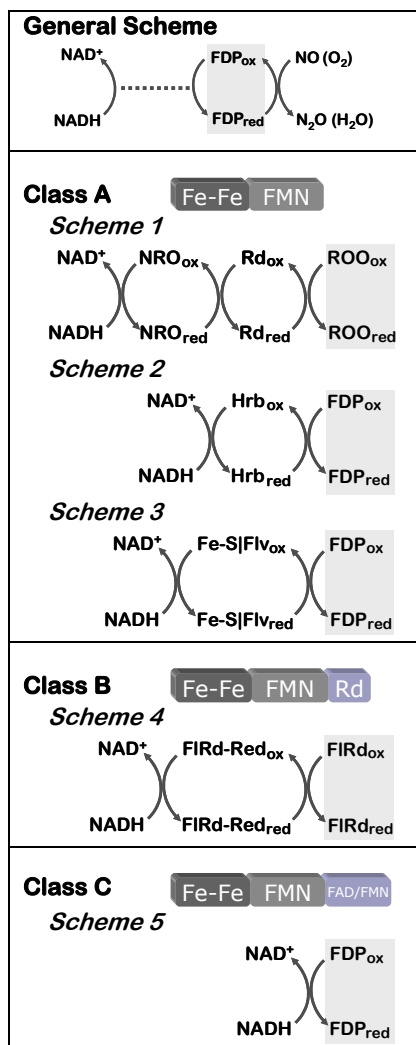


Figure 2.7 – Diversity of electron transfer chains involving flavodiiron proteins.

Synechocystis sp. PCC 6803 (See Chapter 8) (28) and the remainder multiple copies found in all the cyanobacterial sequenced genomes. In this case, the multi-component electron transfer chains are completely abolished, as the fusion of the NAD(P)H:flavin oxidoreductase module to the flavodiiron core allows the protein to accept electrons directly from NAD(P)H and perform several intramolecular electron transfer steps onto the diiron centre, which ultimately reduces the diatomic substrate (Figure 2.7).

. *Class B*

In *E. coli*, the flavodiiron protein, flavorubredoxin, was shown to interact directly with an NADH-dependent (flavo)rubredoxin reductase (FIRd-Red) (See chapters 3 to 6) (41) (Figure 2.7). The same type of gene organisation was observed in all enterobacterial genomes so far sequenced. The direct reduction of the terminal enzyme component FIRd by an NADH-dependent partner was a result of an interesting evolutionary event, which fused the Rd component to the flavodiiron structural core. Preliminary studies determined that the flavorubredoxin reductase is a monomeric NADH oxidase, containing one FAD, which efficiently reduces FIRd (Chapter 3) (41).

. *Class C*

An even more extreme module fusion is observed in the cyanobacterial flavodiiron proteins, both in the studied member of

2.3 BASIS FOR A ROLE IN NITRIC OXIDE DETOXIFICATION

Another landmark in the history of Flavodiiron Proteins was the groundbreaking seminal paper of Gardner and co-workers (42), reporting the induction of *E. coli* flavorubredoxin (this organism's FDP) by NO, and proposing a role for FIRd in NO detoxification, as an NO reductase.

A search for putative regulators related to NO metabolism led to the discovery of an unknown gene (*ygaA*) encoding for a protein sharing ~42% of sequence identity with NO-modulated *Ralstonia eutropha* transcriptional regulators NorR1 and NorR2. Genes encoding for homologues of these regulators are adjacent to flavohaemoglobin-encoding genes in the genomes of *Vibrio cholerae* and *Pseudomonas aeruginosa*, which put forward the idea of a possible role of *E. coli* *ygaA* in NO metabolism regulation. Moreover, it was noticed that adjacent to *ygaA* (*norR* in Fig. 2.8) were the divergently transcribed genes *ygaK* and *ygbD* (respectively *norV* and *norW* in Fig. 2.8), encoding flavorubredoxin (FIRd) and its cognate reductase, respectively. Since the *norRVW* nomenclature is the currently accepted one for this gene cluster, it will be used from this point on, for simplification. The observation that NO could bind to the non-haem diiron centre

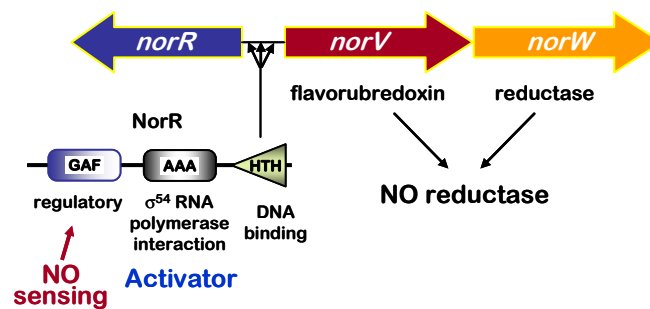


Figure 2.8 – Top: gene cluster comprising the genes encoding for flavorubredoxin (*norV*), its reductase (*norW*) and its regulator (*norR*). Bottom: domain arrangement of NorR and putative functions in the regulatory activity (adapted from (43)).

of FIRd (41) (See chapter 3) led the authors to envisage a possible role of FIRd in NO metabolism, possibly regulated by *norR*. *E. coli* mutant strains deleted in the *norR*, *norV* and *norW*

genes were generated and their phenotype analysed. The strains deleted in *norR* and *norV* were devoid of anaerobic NO consumption activity, contrarily to the

parental strain; the strain deleted in *norW* retained ~60% of the activity. It should be noted that both the anaerobic and aerobic NO consumption activity of the parental strain requires induction by exposure to NO. However, inducible NO consumption in aerobic conditions was not affected by the mutations, as compared to the parental strain. It was further shown that in anaerobic conditions *norR* and *norV* afford protection against NO to important metabolic enzymes, such as aconitase and 6-phosphogluconate dehydratase. Altogether, the reported results indicated unequivocally a role for *E. coli* flavorubredoxin in the protection of anaerobically-grown *E. coli* against NO, complementing the protection afforded by flavohaemoglobin to cells grown in aerobic and microaerophilic conditions. It was proposed that flavorubredoxin acts as an NO reductase, and that its expression is induced by NO, in a regulatory process probably mediated by *norR*.

The NO reductase activity of *Escherichia coli* flavorubredoxin was further confirmed *in vitro*; electrons for NO reduction by flavorubredoxin derived from NADH, via the *norW* gene product, NADH:flavorubredoxin oxidoreductase (44) (See Chapter 4).

Further studies on the regulation of flavorubredoxin (FIRd) pointed out several clues to further understand the role of FIRd in NO detoxification. A protective role against reactive nitrogen intermediates derived from the NO⁺-releaser nitroprusside was proposed (45). The induction of FIRd mediated by NorR was shown to be a σ^{54} -dependent process and upon deleting the N-terminal domain of NorR, induction of NO reductase activity became independent of NO exposure (46). An important observation was that the *norVW* form a di-cistronic transcriptional unit, shown to be induced by nitrite and repressed by nitrate (47). A deeper understanding of the molecular basis of the regulation of FIRd expression by NorR (recently reviewed in (48,49)) was achieved in 2005, with the identification of the three binding sites for NorR on FIRd's promoter region

(43,50) and the discovery of a non-haem mononuclear iron centre as the NO-sensing element in NorR (51). The role of each of the NorR domains is crucial for the overall regulatory activity of NorR (figure 2.9): the N-terminal GAF domain (named after cyclic GMP-specific and stimulated phosphodiesterases) harbours the NO-sensing non-haem iron centre, the central AAA⁺ domain is essential to couple nucleotide hydrolysis to formation of open promoter complexes by σ^{54} -RNA polymerase (52), and the C-terminal HTH domain is the DNA-binding region of NorR. It is thus proposed

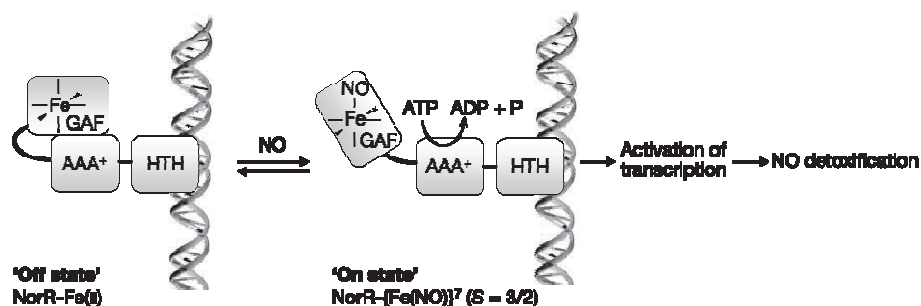


Figure 2.9 – Scheme depicting the mechanism of transcriptional activation of *norV* (encoding flavorubredoxin NO reductase) expression by NorR (taken from (51)).

that binding of NO to the GAF-domain non-haem iron centre generates an iron-nitrosyl $\{\text{Fe}(\text{NO})\}^7$ species, characterized by an EPR spectrum corresponding to an $S=3/2$ system. This NO-binding event induces a conformational change in the GAF domain, derepressing the AAA⁺ domain which in the absence of NO is in a resting “off state”. The resulting “on state” allows enhancer-stimulated ATPase activity and transcription initiation of the FIRD gene (*norV*) by σ^{54} -RNA polymerase. Binding of NorR’s HTH domain to all three binding sites on the *norV* promoter region is required for transcription initiation (43,50). Altogether, this mechanism couples the NO signalling event to the up-regulation of the appropriate NO detoxification systems, such as flavorubredoxin.

While great efforts were undertaken to understand the regulation of flavorubredoxin by NorR and to establish the role of FIRD in nitric oxide

detoxification, other regulatory strategies are expected for genes encoding for flavodiiron proteins in many organisms, since NorR is only present in part of the genomes bearing FDP-encoding genes. Moreover, the ambiguity of this protein family with respect to NO vs. O₂ reductase activity leaves space for possible regulation regimes by oxidative stress / oxygen metabolism regulons.

REFERENCES

1. van Niel, E. W., and Gottschal, J. C. (1998) Oxygen Consumption by Desulfovibrio Strains with and without Polyglucose, *Appl Environ Microbiol* **64**(3), 1034-1039
2. Santos, H., Fareleira, P., Xavier, A. V., Chen, L., Liu, M. Y., and LeGall, J. (1993) Aerobic metabolism of carbon reserves by the "obligate anaerobe" Desulfovibrio gigas, *Biochem Biophys Res Commun* **195**(2), 551-557
3. Chen, L., Liu, M. Y., LeGall, J., Fareleira, P., Santos, H., and Xavier, A. V. (1993) Rubredoxin oxidase, a new flavo-hemo-protein, is the site of oxygen reduction to water by the "strict anaerobe" Desulfovibrio gigas, *Biochem Biophys Res Commun* **193**(1), 100-105
4. Chen, L., Liu, M. Y., Legall, J., Fareleira, P., Santos, H., and Xavier, A. V. (1993) Purification and characterization of an NADH-rubredoxin oxidoreductase involved in the utilization of oxygen by Desulfovibrio gigas, *Eur J Biochem* **216**(2), 443-448
5. Gomes, C. M., Silva, G., Oliveira, S., LeGall, J., Liu, M. Y., Xavier, A. V., Rodrigues-Pousada, C., and Teixeira, M. (1997) Studies on the redox centers of the terminal oxidase from Desulfovibrio gigas and evidence for its interaction with rubredoxin, *J Biol Chem* **272**(36), 22502-22508
6. Das, A., Silaghi-Dumitrescu, R., Ljungdahl, L. G., and Kurtz, D. M., Jr. (2005) Cytochrome bd oxidase, oxidative stress, and dioxygen tolerance of the strictly anaerobic bacterium Moorella thermoacetica, *J Bacteriol* **187**(6), 2020-2029
7. Machado, P., Felix, R., Rodrigues, R., Oliveira, S., and Rodrigues-Pousada, C. (2006) Characterization and expression analysis of the cytochrome bd oxidase operon from Desulfovibrio gigas, *Curr Microbiol* **52**(4), 274-281
8. Lemos, R. S., Gomes, C. M., Santana, M., LeGall, J., Xavier, A. V., and Teixeira, M. (2001) The 'strict' anaerobe Desulfovibrio gigas contains a membrane-bound oxygen-reducing respiratory chain, *FEBS Lett* **496**(1), 40-43
9. Lobo, S. A. L., Melo, A. M. P., Carita, J. N., Teixeira, M., and Saraiva, L. M. (2007) The anaerobe Desulfovibrio desulfuricans ATCC 27774 grows at nearly atmospheric oxygen levels, *FEBS Lett* (in press)
10. Jenney, F. E., Jr., Verhagen, M. F., Cui, X., and Adams, M. W. (1999) Anaerobic microbes: oxygen detoxification without superoxide dismutase, *Science* **286**(5438), 306-309
11. Dolla, A., Kurtz, D. M., Jr., Teixeira, M., and Voordow, G. (2007) Biochemical,

- proteomic and genetic characterization of oxygen survival mechanisms in sulphate-reducing bacteria of the genus *Desulfovibrio*. In: Barton, L. L., and Hamilton, W. A. (eds). *Sulphate-Reducing Bacteria: Environmental and Engineered Systems*, Cambridge Univ. Press
12. Kurtz, D. M., Jr. (2004) Microbial detoxification of superoxide: the non-heme iron reductive paradigm for combating oxidative stress, *Acc Chem Res* **37**(11), 902-908
 13. Rodrigues, J. V., Abreu, I. A., Saraiva, L. M., and Teixeira, M. (2005) Rubredoxin acts as an electron donor for neelaredoxin in *Archaeoglobus fulgidus*, *Biochem Biophys Res Commun* **329**(4), 1300-1305
 14. Auchere, F., Pauleta, S. R., Tavares, P., Moura, I., and Moura, J. J. (2006) Kinetics studies of the superoxide-mediated electron transfer reactions between rubredoxin-type proteins and superoxide reductases, *J Biol Inorg Chem* **11**(4), 433-444
 15. Nolling, J., Ishii, M., Koch, J., Pihl, T. D., Reeve, J. N., Thauer, R. K., and Hedderich, R. (1995) Characterization of a 45-kDa flavoprotein and evidence for a rubredoxin, two proteins that could participate in electron transport from H₂ to CO₂ in methanogenesis in *Methanobacterium thermoautotrophicum*, *Eur J Biochem* **231**(3), 628-638
 16. Wasserfallen, A., Huber, K., and Leisinger, T. (1995) Purification and structural characterization of a flavoprotein induced by iron limitation in *Methanobacterium thermoautotrophicum* Marburg, *J Bacteriol* **177**(9), 2436-2441
 17. Wasserfallen, A., Ragetti, S., Jouanneau, Y., and Leisinger, T. (1998) A family of flavoproteins in the domains Archaea and Bacteria, *Eur J Biochem* **254**(2), 325-332
 18. Frazao, C., Silva, G., Gomes, C. M., Matias, P., Coelho, R., Sieker, L., Macedo, S., Liu, M. Y., Oliveira, S., Teixeira, M., Xavier, A. V., Rodrigues-Pousada, C., Carrondo, M. A., and Le Gall, J. (2000) Structure of a dioxygen reduction enzyme from *Desulfovibrio gigas*, *Nat Struct Biol* **7**(11), 1041-1045
 19. Macedo, S., Romao, C. V., Mitchell, E., Matias, P. M., Liu, M. Y., Xavier, A. V., LeGall, J., Teixeira, M., Lindley, P., and Carrondo, M. A. (2003) The nature of the di-iron site in the bacterioferritin from *Desulfovibrio desulfuricans*, *Nat Struct Biol* **10**(4), 285-290
 20. Wallar, B. J., and Lipscomb, J. D. (1996) Dioxygen Activation by Enzymes Containing Binuclear Non-Heme Iron Clusters, *Chem Rev* **96**(7), 2625-2658
 21. Solomon, E. I., Brunold, T. C., Davis, M. I., Kemsley, J. N., Lee, S. K., Lehnert, N., Neese, F., Skulan, A. J., Yang, Y. S., and Zhou, J. (2000) Geometric and electronic structure/function correlations in non-heme iron enzymes, *Chem Rev* **100**(1), 235-350
 22. Silaghi-Dumitrescu, R., Kurtz, D. M., Jr., Ljungdahl, L. G., and Lanzilotta, W. N. (2005) X-ray crystal structures of *Moorella thermoacetica* FprA. Novel diiron site structure and mechanistic insights into a scavenging nitric oxide reductase, *Biochemistry* **44**(17), 6492-6501
 23. Daiyasu, H., Osaka, K., Ishino, Y., and Toh, H. (2001) Expansion of the zinc metallo-hydrolase family of the beta-lactamase fold, *FEBS Lett* **503**(1), 1-6
 24. Gomes, C. M., Frazao, C., Xavier, A. V., Legall, J., and Teixeira, M. (2002) Functional control of the binuclear metal site in the metallo-beta-lactamase-like fold by subtle amino acid replacements, *Protein Sci* **11**(3), 707-712
 25. Zang, T. M., Hollman, D. A., Crawford, P. A., Crowder, M. W., and Makaroff, C. A.

- (2001) Arabidopsis glyoxalase II contains a zinc/iron binuclear metal center that is essential for substrate binding and catalysis, *J Biol Chem* **276**(7), 4788-4795
26. Schilling, O., Vogel, A., Kostecky, B., Natal da Luz, H., Spemann, D., Spath, B., Marchfelder, A., Troger, W., and Meyer-Klaucke, W. (2005) Zinc- and iron-dependent cytosolic metallo-beta-lactamase domain proteins exhibit similar zinc-binding affinities, independent of an atypical glutamate at the metal-binding site, *Biochem J* **385**(Pt 1), 145-153
 27. Okinaka, Y., Yang, C. H., Perna, N. T., and Keen, N. T. (2002) Microarray profiling of *Erwinia chrysanthemi* 3937 genes that are regulated during plant infection, *Mol Plant Microbe Interact* **15**(7), 619-629
 28. Vicente, J. B., Gomes, C. M., Wasserfallen, A., and Teixeira, M. (2002) Module fusion in an A-type flavoprotein from the cyanobacterium *Synechocystis* condenses a multiple-component pathway in a single polypeptide chain, *Biochem Biophys Res Commun* **294**(1), 82-87
 29. Shimizu, T., Ohtani, K., Hirakawa, H., Ohshima, K., Yamashita, A., Shiba, T., Ogasawara, N., Hattori, M., Kuhara, S., and Hayashi, H. (2002) Complete genome sequence of *Clostridium perfringens*, an anaerobic flesh-eater, *Proc Natl Acad Sci U S A* **99**(2), 996-1001
 30. Sarti, P., Fiori, P. L., Forte, E., Rappelli, P., Teixeira, M., Mastronicola, D., Sanciu, G., Giuffre, A., and Brunori, M. (2004) *Trichomonas vaginalis* degrades nitric oxide and expresses a flavorubredoxin-like protein: a new pathogenic mechanism?, *Cell Mol Life Sci* **61**(5), 618-623
 31. Victor, B. L., Vicente, J. B., Rodrigues, R., Oliveira, S., Rodrigues-Pousada, C., Frazao, C., Gomes, C. M., Teixeira, M., and Soares, C. M. (2003) Docking and electron transfer studies between rubredoxin and rubredoxin:oxygen oxidoreductase, *J Biol Inorg Chem* **8**(4), 475-488
 32. Petitdemange, H., Blusson, H., and Gay, R. (1981) Detection of NAD(P)H--rubredoxin oxidoreductases in Clostridia, *Anal Biochem* **116**(2), 564-570
 33. Guedon, E., and Petitdemange, H. (2001) Identification of the gene encoding NADH-rubredoxin oxidoreductase in *Clostridium acetobutylicum*, *Biochem Biophys Res Commun* **285**(2), 496-502
 34. Nolling, J., Breton, G., Omelchenko, M. V., Makarova, K. S., Zeng, Q., Gibson, R., Lee, H. M., Dubois, J., Qiu, D., Hitti, J., Wolf, Y. I., Tatusov, R. L., Sabathe, F., Doucette-Stamm, L., Soucaille, P., Daly, M. J., Bennett, G. N., Koonin, E. V., and Smith, D. R. (2001) Genome sequence and comparative analysis of the solvent-producing bacterium *Clostridium acetobutylicum*, *J Bacteriol* **183**(16), 4823-4838
 35. Das, A., Coulter, E. D., Kurtz, D. M., Jr., and Ljungdahl, L. G. (2001) Five-gene cluster in *Clostridium thermoaceticum* consisting of two divergent operons encoding rubredoxin oxidoreductase- rubredoxin and rubrerythrin-type A flavoprotein-high-molecular-weight rubredoxin, *J Bacteriol* **183**(5), 1560-1567
 36. Silaghi-Dumitrescu, R., Coulter, E. D., Das, A., Ljungdahl, L. G., Jameson, G. N., Huynh, B. H., and Kurtz, D. M., Jr. (2003) A flavodiiron protein and high molecular weight rubredoxin from *Moorella thermoacetica* with nitric oxide reductase activity, *Biochemistry* **42**(10), 2806-2815
 37. Abreu, I. A., Saraiva, L. M., Carita, J., Huber, H., Stetter, K. O., Cabelli, D., and Teixeira, M. (2000) Oxygen detoxification in the strict anaerobic archaeon *Archaeoglobus fulgidus*: superoxide scavenging by neelaredoxin, *Mol Microbiol*

- 38(2), 322-334
38. Abreu, I. A., Xavier, A. V., LeGall, J., Cabelli, D. E., and Teixeira, M. (2002) Superoxide scavenging by neelaredoxin: dismutation and reduction activities in anaerobes, *J Biol Inorg Chem* **7**(6), 668-674
 39. Bult, C. J., White, O., Olsen, G. J., Zhou, L., Fleischmann, R. D., Sutton, G. G., Blake, J. A., FitzGerald, L. M., Clayton, R. A., Gocayne, J. D., Kerlavage, A. R., Dougherty, B. A., Tomb, J. F., Adams, M. D., Reich, C. I., Overbeek, R., Kirkness, E. F., Weinstock, K. G., Merrick, J. M., Glodek, A., Scott, J. L., Geoghagen, N. S., and Venter, J. C. (1996) Complete genome sequence of the methanogenic archaeon, *Methanococcus jannaschii*, *Science* **273**(5278), 1058-1073
 40. Galagan, J. E., Nusbaum, C., Roy, A., Endrizzi, M. G., Macdonald, P., FitzHugh, W., Calvo, S., Engels, R., Smirnov, S., Atnoor, D., Brown, A., Allen, N., Naylor, J., Stange-Thomann, N., DeArellano, K., Johnson, R., Linton, L., McEwan, P., McKernan, K., Talamas, J., Tirrell, A., Ye, W., Zimmer, A., Barber, R. D., Cann, I., Graham, D. E., Grahame, D. A., Guss, A. M., Hedderich, R., Ingram-Smith, C., Kuettner, H. C., Krzycki, J. A., Leigh, J. A., Li, W., Liu, J., Mukhopadhyay, B., Reeve, J. N., Smith, K., Springer, T. A., Umayam, L. A., White, O., White, R. H., Conway de Macario, E., Ferry, J. G., Jarrell, K. F., Jing, H., Macario, A. J., Paulsen, I., Pritchett, M., Sowers, K. R., Swanson, R. V., Zinder, S. H., Lander, E., Metcalf, W. W., and Birren, B. (2002) The genome of *M. acetivorans* reveals extensive metabolic and physiological diversity, *Genome Res* **12**(4), 532-542
 41. Gomes, C. M., Vicente, J. B., Wasserfallen, A., and Teixeira, M. (2000) Spectroscopic studies and characterization of a novel electron-transfer chain from *Escherichia coli* involving a flavorubredoxin and its flavoprotein reductase partner, *Biochemistry* **39**(51), 16230-16237
 42. Gardner, A. M., Helmick, R. A., and Gardner, P. R. (2002) Flavorubredoxin, an inducible catalyst for nitric oxide reduction and detoxification in *Escherichia coli*, *J Biol Chem* **277**(10), 8172-8177
 43. Tucker, N., D'Autreaux, B., Spiro, S., and Dixon, R. (2005) DNA binding properties of the *Escherichia coli* nitric oxide sensor NorR: towards an understanding of the regulation of flavorubredoxin expression, *Biochem Soc Trans* **33**(Pt 1), 181-183
 44. Gomes, C. M., Giuffre, A., Forte, E., Vicente, J. B., Saraiva, L. M., Brunori, M., and Teixeira, M. (2002) A novel type of nitric-oxide reductase. *Escherichia coli* flavorubredoxin, *J Biol Chem* **277**(28), 25273-25276
 45. Hutchings, M. I., Mandhana, N., and Spiro, S. (2002) The NorR protein of *Escherichia coli* activates expression of the flavorubredoxin gene *norV* in response to reactive nitrogen species, *J Bacteriol* **184**(16), 4640-4643
 46. Gardner, A. M., Gessner, C. R., and Gardner, P. R. (2003) Regulation of the nitric oxide reduction operon (*norRVW*) in *Escherichia coli*. Role of NorR and sigma54 in the nitric oxide stress response, *J Biol Chem* **278**(12), 10081-10086
 47. da Costa, P. N., Teixeira, M., and Saraiva, L. M. (2003) Regulation of the flavorubredoxin nitric oxide reductase gene in *Escherichia coli*: nitrate repression, nitrite induction, and possible post-transcription control, *FEMS Microbiol Lett* **218**(2), 385-393
 48. Spiro, S. (2006) Nitric oxide-sensing mechanisms in *Escherichia coli*, *Biochem Soc Trans* **34**(Pt 1), 200-202
 49. Tucker, N. P., D'Autreaux, B., Spiro, S., and Dixon, R. (2006) Mechanism of

- transcriptional regulation by the *Escherichia coli* nitric oxide sensor NorR, *Biochem Soc Trans* **34**(Pt 1), 191-194
50. Justino, M. C., Goncalves, V. M., and Saraiva, L. M. (2005) Binding of NorR to three DNA sites is essential for promoter activation of the flavorubredoxin gene, the nitric oxide reductase of *Escherichia coli*, *Biochem Biophys Res Commun* **328**(2), 540-544
 51. D'Autreaux, B., Tucker, N. P., Dixon, R., and Spiro, S. (2005) A non-haem iron centre in the transcription factor NorR senses nitric oxide, *Nature* **437**(7059), 769-772
 52. Cannon, W. V., Gallegos, M. T., and Buck, M. (2000) Isomerization of a binary sigma-promoter DNA complex by transcription activators, *Nat Struct Biol* **7**(7), 594-601

3

Spectroscopic studies and characterisation of a novel electron transfer chain from *Escherichia coli* involving a flavorubredoxin and its flavoprotein reductase partner ‡

3.1	Introduction	75
3.2	Materials and Methods	76
3.3	Results and Discussion	79
3.4	Conclusions	89
3.5	References	91

SUMMARY

A novel two-component enzyme system from *Escherichia coli* involving a flavorubredoxin (FIRd) and its reductase was studied in terms of spectroscopic, redox and biochemical properties of its constituents. FIRd contains one FMN and one rubredoxin (Rd) centre per monomer. To assess the role of the Rd domain, FIRd and a truncated form lacking the Rd domain (FIRd Δ Rd), were characterised. FIRd contains 2.9 ± 0.5 iron atoms/subunit, whereas FIRd Δ Rd contains 2.1 ± 0.6 iron atoms/subunit. While for FIRd one iron atom corresponds to the Rd-centre, the other two irons, also present in FIRd Δ Rd, are most probably due to a diiron site. Redox titrations of FIRd using EPR and visible spectroscopies allowed to determine that the Rd site has a reduction potential of -140 ± 15 mV, whereas the FMN undergoes reduction via a red-semiquinone, at -140 ± 15 mV (Fl_{ox}/Fl_{sq}) and -180 ± 15 mV (Fl_{sq}/Fl_{red}), at pH 7.6. The rubredoxin site has the lowest potential ever reported for a rubredoxin centre, which may be correlated with specific amino acid substitutions close to both cysteine clusters. The gene adjacent to that encoding FIRd was found to code for an FAD-containing protein, (flavo)rubredoxin reductase (FIRd-reductase), which is capable of mediating electron transfer from NADH to *Desulfovibrio gigas* Rd as well as to *E. coli* FIRd. Further, electron donation was found to proceed through the Rd domain of FIRd, as the Rd-truncated protein does not react with FIRd-reductase. *In vitro*, this pathway links NADH oxidation with dioxygen reduction. The possible function of this chain is discussed considering the presence of FIRd homologues in all known genomes of anaerobes and facultative aerobes.

‡ **This Chapter was published in the following article:**

Gomes, C.M., Vicente, J.B., Wasserfallen, A. and Teixeira, M. (2000) "Spectroscopic studies and characterisation of a novel electron transfer chain from *Escherichia coli* involving a flavorubredoxin and its flavoprotein reductase partner", *Biochemistry* 26;39(51):16230-7

The molecular biology procedures undertaken to clone the target proteins for over-expression were performed in the Institut für Mikrobiologie, Eidgenössische Technische Hochschule, ETH, Zürich, Switzerland, with the help of S. Ragetti. João Carita performed cell growth for over-expression of target proteins and Manuela Regalla (both from ITQB) helped with the HPLC analysis of extracted flavins.

3.1 INTRODUCTION

Flavoproteins are catalytically extremely versatile, as their flavin coenzymes are able to perform a wide variety of enzymatic reactions comprising one-electron and two-electron transfers (1,2). The recently described recombinant flavorubredoxin (FIRd) from *Escherichia coli* is an example of a novel complex flavoprotein (3). It consists of a unique arrangement of structural modules in which a large, partly flavodoxin-like module, is fused to a rubredoxin-like one. The flavoprotein domain of FIRd exhibits extensive sequence similarity towards other proteins, which were established as a protein superfamily originally designated by A-type flavoproteins (ATF) (3). This group was recently expanded in terms of additional members and characteristic sequence fingerprints (4)). The rubredoxin domain of FIRd is found as an extension at the protein C-terminus. Rubredoxins (Rd) are small (~6 kDa), mononuclear iron-sulfur proteins whose role remains largely elusive except in few well documented cases such as in the *Pseudomonas*-type alkane hydroxylation system (5) and in the *Desulfovibrio gigas* oxygen-utilising pathway (6,7). Quite recently, the first example of a Rd from an eukaryote was established (8). This novel type of Rd was found to be attached to photosystem II, (9) which shows an unexpected wide relevance for these small electron transfer proteins. Flavorubredoxin is a novel example of a protein having a Rd-domain, after the case of rubrerythrin (10). Interestingly, in the genome of *Campylobacter jejuni* the putative product of gene Cj0012c contains several non-heme iron binding domains, including a Rd-like one (11).

The *Pseudomonads* and *D. gigas* pathways exploit the ability of flavoproteins to act as *in vivo* redox mediators, transferring electrons to other redox proteins. In both electron transfer chains a flavoprotein is reduced by NADH, and catalyses electron transfer to a rubredoxin which is reoxidised by the terminal component of the pathway. Particularly interesting is the finding that a large domain of *E. coli*

FIRd is identical to *D. gigas* rubredoxin:oxygen oxidoreductase (ROO) (4), the last element of the *D. gigas* oxygen utilising pathway, which was shown to interact with a rubredoxin (6,7). Thus, the *E. coli* flavorubredoxin appears to be a fusion of a flavoprotein with its redox partner (rubredoxin). This possibility was thoroughly investigated and here we report a novel electron transfer chain operating in *E. coli* which mediates electron transfer between NADH and the flavorubredoxin redox cofactors, as well as a characterisation of the spectroscopic and redox properties of its components. This pathway also involves a flavorubredoxin reductase (FIRd-reductase) which reduces the FIRd at the expense of NADH. Interaction and kinetic studies performed using both intact and Rd-domain truncated FIRd demonstrated that the flavorubredoxin reductase specifically reduces the Rd moiety of FIRd.

3.2 MATERIALS AND METHODS

Amplification, cloning and expression – All genes were amplified from genomic DNA of *E. coli* strain XL-1 Blue (F':Tn10 *proA*⁺*B*⁺ *lacI*^q Δ (*lacZ*)M15/*recA1 endA1 gyrA96* (Nal^r) *thi hsdR17* (r_Km_K⁺) *supE44 relA1 lac*) with no His tag(s) attached. Gene *orf479*, which encodes for FIRd, was amplified, cloned and expressed as described previously (3). The following primers were used for the amplification of *orf412* (encoding for FIRd Δ Rd) and *orf377* (encoding for FIRd-reductase) (restriction sites are underlined): 5'-TGAGGTTCATATGTCTATTG-3' (5' primer) and 5'-GTGGCAAAGCTTTATTCTTT-3' (3' primer, *orf412*) and 5'-GGAGGCCCATATGAGTAACG-3' (5' primer) and 5'-ATCCGAAAGCTTAGGCAC-3' (3' primer, *orf377*). Amplified DNA was isolated from agarose gels, digested with restriction enzymes *NdeI* and *HindIII* and cloned in vector pUC28 (12). After verifying the amplified sequence, the genes were recloned in the expression vector pET24a (Novagen) and overexpressed overnight after induction by IPTG (20 μ M final concentration), according to the

manufacturer's instructions. Recombinant *E. coli* growth medium was supplemented with 10 μ M Fe when the flavorubredoxin or its Rd-truncated form were expressed. The recombinant plasmids used were: pME2337 (*orf479*), pME2359 (*orf412*), and pME2540 (*orf377*).

Protein purification – Recombinant *E. coli* cells were broken using a French-press at 6000 PSI. The soluble extract was separated from membranes after 6 hour ultracentrifugation at 42000 rpm, at 4°C, and dialysed overnight against 10 mM Tris-HCl pH 7.6. All subsequent purification steps were performed in a HiLoad Pharmacia system. The first purification step is identical for the proteins studied. Typically, soluble extracts were applied to a Q-Sepharose ($v=30$ ml) previously equilibrated with 10 mM Tris-HCl pH 7.6. The overexpressed proteins were eluted with NaCl (FIRd at ~ 450 mM and FIRd-reductase at ~ 200 mM). FIRd was subsequently applied to a 70-ml gel filtration Superdex S-200 column, equilibrated and eluted with 10 mM Tris-HCl pH 7.6, 200 mM NaCl, 0.5 ml/min. The pink fraction was collected, dialysed overnight and finally applied to a Mono-Q (Pharmacia) column equilibrated with 10 mM Tris-HCl pH 7.6 and eluted with 400 mM NaCl. FIRd Δ Rd was purified on 3-ml custom-packed columns eluted by stepwise salt gradients. In step 1, on Q-Sepharose (Pharmacia) equilibrated in 20 mM KPi at pH 7, FIRd Δ Rd eluted with ca. 400 mM KCl. The pooled, yellowish fractions were diluted five-fold in 10 mM Tris-HCl, pH 8.3 and applied on Fractogel EMD TMAE (Merck); the protein eluted with ca. 250 mM NaCl as pure protein as judged by SDS-PAGE gel electrophoresis. After the initial Q-Sepharose, FIRd-reductase was applied to a 5-ml pre-packed Blue-Sepharose column (Pharmacia) equilibrated with 10 mM Tris-HCl pH 7.6 and eluted with NaCl. After dialysis, the yellow fraction was run on a Mono-Q, in a procedure similarly to that described for FIRd. Pure FIRd-reductase is an FAD-containing protein. In this work the interaction of this protein with FIRd was studied; its detailed biochemical characterisation will be reported elsewhere. The purified

proteins were divided in aliquots and stored at -70 °C.

Spectroscopic methods - Room temperature Ultra-violet/Visible spectra were recorded on a UV 1603 or Multispec 1501 diode-array Shimadzu spectrophotometers. EPR spectra were obtained on a Bruker ESP 380 spectrometer equipped with an ESR 900 continuous-flow helium cryostat from Oxford Instruments.

Analytical methods - The protein concentration was determined by the Bradford and Microbiuret methods (13), and iron by the 2,4,6-tripyridyl-1,3,5-triazine method (14). Flavin HPLC analysis was done as described in (15). The protein N-terminal sequence was determined using an Applied Biosystem Model 470A.

Enzymatic assays - In kinetic assays, NAD(P)H oxidation was followed at 340 nm in 10 mM Tris-HCl pH 7.6 ($\epsilon^{340}_{\text{NADH}}=6.2 \text{ mM}\cdot\text{cm}^{-1}$). Ferricyanide reduction (0.5 mM) was followed at 420 nm ($\epsilon^{420}_{\text{Ferricyanide}}=1.0 \text{ mM}\cdot\text{cm}^{-1}$). Oxygen consumption was measured in a YSI-Micro cell Clark-type oxygen electrode.

Redox titrations and analysis - Proteins were titrated anaerobically in 50 mM Tris/HCl pH 7.6 by stepwise addition of buffered sodium dithionite (250 mM Tris-HCl at pH 8.0). The following compounds were used as redox mediators (typically 0.25-0.5 μM for visible titrations and 30-40 μM for EPR titrations): methylene blue ($E'_{\circ} = 11 \text{ mV}$), indigo-tetrasulfonate ($E'_{\circ} = -30 \text{ mV}$), indigo-trisulfonate ($E'_{\circ} = -70 \text{ mV}$), indigo disulfate ($E'_{\circ} = -182 \text{ mV}$), anthraquinone 2,7 disulfonate ($E'_{\circ} = -182 \text{ mV}$), safranine ($E'_{\circ} = -280 \text{ mV}$), neutral red ($E'_{\circ} = -325 \text{ mV}$), benzyl viologen ($E'_{\circ} = -359 \text{ mV}$), methyl viologen ($E'_{\circ} = -446 \text{ mV}$). A silver chloride and a platinum electrode or a silver/silver chloride electrodes were used, calibrated against a saturated quinhydrone solution. The reduction potentials are quoted against the standard hydrogen electrode. The experimental data was manipulated and analyzed using MATLAB (Mathworks, South Natick, MA, USA) for Windows which was also used for optical deconvolution and data fitting calculations. All data was adjusted to monoelectronic Nernst equations, not

taking into consideration possible homotropic (electron-electron) interactions between the redox centres.

3.3 RESULTS AND DISCUSSION

Gene locus and proteins - Analysis of the complete *E. coli* genome (16) showed that the flavorubredoxin (FIRd) is encoded in a two cistron transcriptional unit, consisting of two consecutive open reading frames, *orf479* and *orf377*, forming a putative operon (Fig. 3.1, panel A). Upstream of *orf479* a putative promoter and a RBS sequence are found, and downstream of *orf377* a consensus terminator

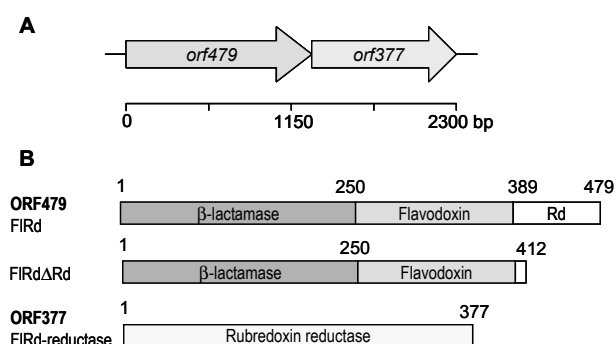


Figure 3.1 – The *E. coli* flavorubredoxin coding region (A) and domain structure (B). Panel A: The coding region was retrieved from NCBI Genebank. Panel B: Grey shaded boxes represent distinct domains inferred from aminoacid sequence analysis ((3) and this work).

sequence analysis of ORF377 shows that it exhibits a significant degree of identity with rubredoxin reductases (21-37% amino acid identity). Thus, the product of *orf377* is a potential redox partner for the flavorubredoxin, from here on named FIRd-reductase (Fig. 3.1, panel A and B).

The *E. coli* flavorubredoxin is a multidomain protein: sequence analysis and fold prediction using Genthreader (17) show that it contains a zinc β-lactamase module (residues 1 to 250), followed by a flavodoxin-like domain (residues 256 to 389) and a Rd-like extension (residues 423 to 479) (3,4,7). The Rd centre binding motif (Fig. 3.2) indicates it is a member of the type-1 family (18), *i.e.*, both cysteine

sequence is present. The coordinates of *orf479* and *orf377* are 2830499-2831938 and 2831935-2833068, respectively, in the sequence stored under accession number U00096. The FIRd is encoded by *orf479*, whereas the amino acid

motifs have the more usual CxxC spacing. An additional cofactor can be

anticipated to be present in *E. coli* FIRd on the basis of recent structural data obtained for *D. gigas* ROO (4). The N-terminus domain of this protein was found to contain a binuclear iron site, in a β -lactamase fold, coordinated by a H-X-E-D-X_n-H-X_m-D-H motif (4). In fact, pairwise sequence comparisons of the first

ROO	MQATKIIDGFHLUGAIDWNSRDFHGYTL .SPMGTTVNAVLUDEKTTLFD	49
FIRd	M .SIUUKNNIHWUGQRDWEURDFHGYTEYKTLRGSSVNSVLTREEKNULID	49
ROO	TUKAEYKGEELLCGIASUIDPKKIDVLUIQ ^{ELD} HAGALPALIEACOPEK	99
FIRd	TUDHKFSREFUQNLRNEIDLADIDYIUI ^{HAED} HAGALTELMAQIPDTP	99
ROO	I ^F TSSLGQKAMESHFHYKDW ^{PUQUUKHGETLSLG} .KRTUTFYETRML ^{HP}	148
FIRd	IYCTANAIDSINGHHHP ^{EMNFNUUKTGD} LDIGNGKQLIFUE ^{TPMLHP}	149
ROO	DSMUSWFAD ^E KULIS ^{NQ} IFGQ ^{NI} AASERFSDQIPUHTLERAMRE ^{VY} VANI ^U	198
FIRd	DSMMTYLTGDAULF ^{SNQ} AFGQ ^{HY} CDEHLFNDEVDQTELFEGCQR ^{YV} YANIL	199
ROO	NPYPQTLKAIETLUGAGUAPEFICPD ^{IGUI} FRGADQCTFAUQKYUEYAE	248
FIRd	TPFSRLUTPKITEILGFNLPUDMIATS ^{IGU} UWRDNPQT ^{QI} UEL ^Y LK ^W AA ^{DY}	249
ROO	QKPTNKUUIFYDSM ^{WH} STEK ^{MA} RULAESFRDE .GCTU ^{KLM} WCKACH ^{HS} Q	296
FIRd	. .QEDRITIF ^{YD} TMSN ^{TR} MMAD ^{AI} AQ ^{GI} AETDPRVAUKIF ^{NU} ARS ^D KNE	297
ROO	IMSEISDAGAUIUGSP TH NNGILPYUAGTLQYIKGLR ^{PQ} NKIDGAF ^{GS} FG	346
FIRd	ILTNUFRSKGULUG ^{TS} TMNNUMPKIAGLVEEMTGLR ^{FR} NKRASAF ^{GS} SHG	347
ROO	WSGESTKULAEWLTGMGF ^{DM} PATP ^{UK} PK ^{NU} PTHADYEQ ^{LK} TMAQT ^I ARAL	396
FIRd	WSGGAUDRLSTR ^{LQ} DAGFEM ^{SL} .L ^K AKWR ^{PD} QDAL ^K CREHG ^{RE} IARAL	396
ROO	KAKLAA	402
FIRd	ALAPLPQSTUNTUUKEETSATTTADLGRPMQ ^{SU} Q ^W IYDPAKGE ^{PM} QDU	446
FIRd	APGTPWSEUPDNFL ^{PE} SLGKDVFEELASEAK	479

Fig. 3.2 – Pairwise amino acid sequence comparison between *E. coli* FIRd (accession U29579) and *D. gigas* ROO (accession AF218053). Black shaded boxes indicate the conserved residues that bind the binuclear iron site present in ROO; grey shaded boxes with white coloured letters highlight the cysteine residues involved in binding of the Rd site in FIRd; other grey shaded boxes denote identical residues.

250 amino acids of these two proteins show that they are very similar to each other (34% identity and 54% similarity) and that the bimetallic site coordinating residues are strictly conserved in *E. coli* FIRd (Fig. 3.2). In respect to the flavodoxin-like domain of FIRd, it is interesting to note that the similarity of this region towards the flavodoxin from *E. coli* is substantially lower (13% identity and 25% similarity) than it is in respect to other flavodoxins from other sources (typically 19-36% identity and 42-61% similarity). This indicates that the flavodoxin domain of FIRd is not a result of a gene fusion event in the *E. coli* genome, and that it arose by an independent evolutionary pathway.

In order to investigate the possible interaction between these *E. coli* proteins and

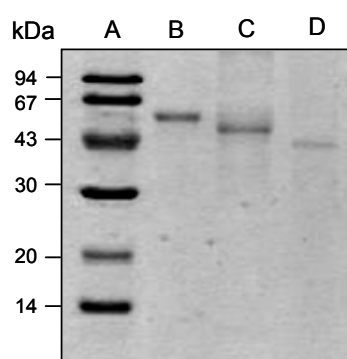


Figure 3.3 – SDS-PAGE analysis of purified proteins. Lane A, molecular mass markers (Amersham/Pharmacia); lane B, FIRd (ORF479, 54.2 kDa); lane C, FIRd Δ Rd (ORF412, 46.8 kDa); lane C, FIRd-reductase (ORF377, 41.4 kDa).

their involvement in a putative electron transfer system, they were purified, as well as a truncated protein made from FIRd, which lacks the rubredoxin-like domain (Fig. 3.1, panel B). The recombinant proteins were successfully overexpressed in *E. coli* and purified to homogeneity in considerable amounts, as evaluated by clean N-terminal sequences and by 12% SDS-PAGE gel electrophoresis (Fig. 3.3).

Flavorubredoxin spectroscopic characterisation - Recombinant FIRd is a tetrameric protein (4x54 kDa) which contains one FMN/subunit (3). Iron quantitation of intact FIRd gives a value of 2.9 ± 0.5 iron atoms/subunit. One iron atom corresponds to the Rd-centre; the other two iron atoms belong most probably to the diiron centre. Consistently, the Rd truncated form of FIRd, which nevertheless comprises the residues involved in coordination of the diiron site, has 2.1 ± 0.6 iron atoms/subunit.

The visible spectrum of *E. coli* FIRd shows features typical of flavin and rubredoxin (Fig. 3.4, trace a), with λ_{\max} at 340, 378, and 478 nm and a broader band at 570 nm. The visible spectrum of the Rd-domain truncated FIRd (FIRd Δ Rd) (Fig. 3.4, trace d) lacks the typical rubredoxin bands and solely contains pure flavinic fingerprints, with λ_{\max} at 445 and 372 nm. By subtraction of these two spectra, the rubredoxin component is obtained, with λ_{\max} at 575, 490 and 390 nm and a shoulder at 340 nm. (Fig. 3.4, trace b). For comparison, the spectrum of *D. gigas* rubredoxin (18) is also shown (Fig. 3.4, trace c).

The EPR spectrum of native *E. coli* FIRd is consistent with the presence of a rubredoxin-type metal centre (Fig. 3.5). Two different sets of resonances are observed, corresponding to two slightly distinct conformations of the Rd centre: resonances at $g \sim 9.3$ and at $g = 4.8$ and 4.3 ; corresponding to a high-spin ($S = 5/2$) ferric site with $E/D \sim 0.3$ ($g_{\max} = 9.6$, $|\pm 1/2\rangle$ doublet, $g_{\text{med}} = 4.30$, $|\pm 3/2\rangle$ doublet) and with $E/D = 0.24$ ($g_{\max} = 9.35$, $|\pm 1/2\rangle$ doublet, $g_{\text{med}} = 4.8$, $|\pm 3/2\rangle$ doublet). At $g = 2.00$, a radical type resonance is also observed, attributable to the flavin. Upon reduction with dithionite, these features

disappear as in these conditions the Rd centre has an integer spin; further, no other resonances develop (not shown). Native FIRd Δ Rd is EPR silent, apart from the minor radical signal at $g = 2.00$ (not shown). No signature for a diiron centre was detected in the EPR spectrum of native (oxidised) or dithionite reduced FIRd, as expected for an antiferromagnetically spin-coupled system, as observed for *D. gigas* ROO (4,7). No conditions could yet be found to detect the putative Fe(III)-

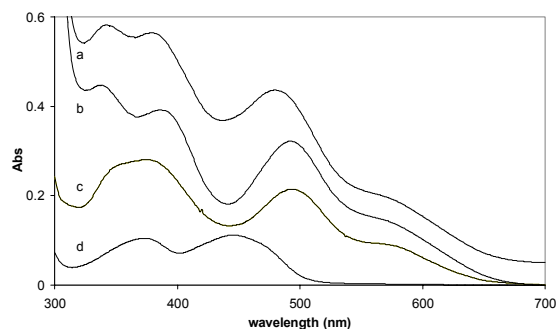


Figure 3.4 – UV-visible spectra of as purified proteins

Trace a, *E. coli* FIRd ($\approx 46 \mu\text{M}$); trace b, spectrum of the Rd domain of FIRd, obtained subtracting (1:1) the spectrum of FIRd to that of FIRd Δ Rd; trace c, *D. gigas* Rd ($\approx 29 \mu\text{M}$); trace d, FIRd Δ Rd ($\approx 9 \mu\text{M}$). All proteins in 50 mM Tris-HCl pH 7.6.

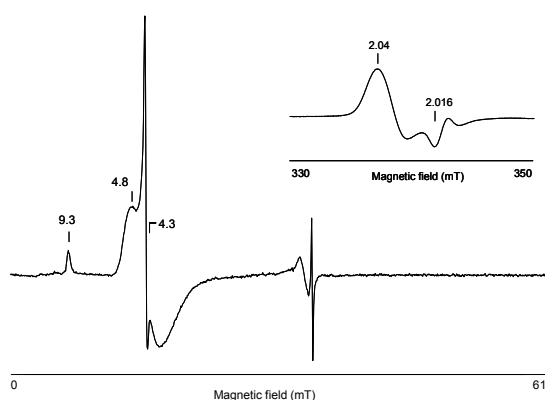


Figure 3.5 – EPR spectra of *E. coli* flavorubredoxin

EPR spectrum of as prepared FIRd at 10K. Inset, spectrum of NO-reacted, dithionite-reduced FIRd, at 50K. For both spectra: microwave power, 2.4 mW; microwave frequency, 9.44 GHz; modulation amplitude, 1 mT; protein concentration, $\approx 170 \mu\text{M}$, buffer: 50 mM Tris-HCl pH 7.6.

Fe(II) species, a situation also found for *D. gigas* ROO (4,7) and, *e.g.*, for bacterioferritins (19,20). However, nitric oxide can bind to the ferrous form of iron sites. The dithionite-reduced *E. coli* FIRd reacted with NO exhibits a high intensity EPR signal due to an $S=1/2$ spin ground state with features at $g=2.04$ and $g=2.0016$ (Fig. 3.5, inset). Similarly, the truncated FIRd displays an identical set of resonances, indicating that it also holds this metallic centre (not shown). In the oxidised (as isolated) states neither the intact nor the truncated proteins reacted with NO, suggesting that the di-iron centre was in the oxidised, di-ferric state, thus EPR silent.

Redox properties - The midpoint reduction potentials of the redox cofactors of flavorubredoxin were determined by redox titrations followed by visible and EPR spectroscopies. The stepwise reduction of *E. coli* FIRd in anaerobic conditions was followed by visible spectroscopy at pH 7.6 (Fig. 3.6, panel A). Major spectral changes occur upon reduction, with the almost simultaneous bleaching of the flavin and rubredoxin bands, which overlap below 550 nm (Fig. 3.4). The absorbance change at 475 nm *minus* the pseudo-isosbestic point at 425 nm was plotted against the reduction potential (Fig. 3.6, panel B) and fitted to a Nernst curve comprising a one-electron transfer step and two consecutive one-electron transfer steps. The observed transitions were tentatively assigned to the rubredoxin transition (Rd_{ox}/Rd_{red} , $E^0=-140\pm 15$ mV) and to the flavin transitions (Fl_{ox}/Fl_{sq} , $E^0=-140\pm 15$ mV and $Fl_{sq}/Fl_{red}=-180\pm 15$ mV), respectively.

An EPR-monitored titration allowed to assign unequivocally one of the -140 mV transitions to rubredoxin. The amplitude of the $g=4.3$ resonance and the height of the $g=9.3$ signal, which decrease upon anaerobic reduction with sodium dithionite, were measured as a function of the redox potential at pH 7.6, and

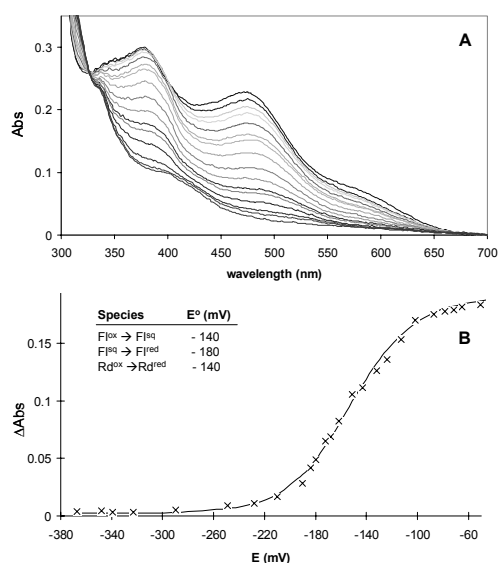


Figure 3.6 – Redox titration of *E. coli* flavorubredoxin at pH 7.6. **Panel A:** Visible spectra of FIRd (27 μ M) in 50 mM Tris-HCl pH 7.6 obtained along the redox titration. **Panel B.** Titration curve followed at 475-425 nm. The line corresponds to a fitting to the sequential equilibrium of three one-electron transfer steps, with E^0 = -140, -140 and -180 mV, respectively. Each transition was weighted in respect to the relative contribution of each component at the working wavelength.

found to fit to a one-electron process, with E^0 = -140 \pm 15 mV (Fig. 3.7, panel A), which completely agrees with the value obtained by following the absorbance changes at 590 nm taken from the redox titration monitored by visible spectroscopy (Fig. 3.7, panel A). Indeed, at this wavelength the major component in FIRd is due to the Rd centre (Cf. Fig. 3.4). The midpoint reduction potential of the Rd centre (-140 \pm 15 mV) is significantly lower than those generally found in rubredoxins, which range from \sim -50 mV to \sim 30 mV, with the exception of the Rd centre in rubrerythrin (\sim +250 mV) (10) and the rubredoxin from the eukaryotic alga *Guillardia theta* (+125 mV) (8,9). Extensive studies on the reduction potentials of Rds led to the division of Rds in two classes, distinguished by the presence of a valine or alanine after the second cysteine cluster (CPxCGX, X=A or V) (21). Those having a valine would have a reduction potential \sim 50 mV lower than those with the alanine. This change has been attributed to the influence of the dipole of the GA(V) peptide amide bond, and to the strength of its hydrogen bond to the γ -S of a cysteine ligand to the iron (22,23). In *E. coli* FIRd (E^0 = -140 mV, this work) this residue is a leucine, consistent with the lower reduction potential. However, other residues have been shown to affect the reduction potential of Rds: in most of these proteins, the residues after the second cysteine of each cysteine cluster are

glycines, and it has been predicted that the substitution of this residue by a bulkier aminoacid with a α -carbon, would change the hydrogen bonds to the cysteines

and affect the reduction potential (24). In fact, mutations in *Clostridium pasteurianum* Rd, have shown that the reduction potential decreases upon substituting the glycine by valine or alanine (25). Quite interestingly, the FIRd Rd domain has in these positions a glutamine (Gln⁴³²) and a serine (Ser⁴⁶⁵), substituting for glycine (Fig. 3.2). There are other important differences in other residues, namely at the protein surface, which may affect also the reduction potential. In summary, the Rd site in *E. coli* FIRd shows multiple aminoacid substitutions that may account for its lower reduction potential. The remaining two consecutive one-electron transfer steps

observed in the flavorubredoxin titration are attributable to FMN reduction through a semiquinone radical species. Spectral deconvolution of the FIRd titration data clearly identified the formation of a red (anionic) type flavin semiquinone during FIRd reduction (Fig. 3.7, panels B and C). This resulted from

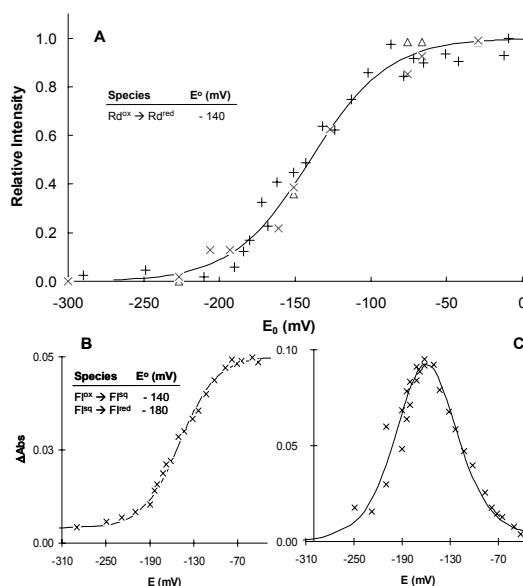


Figure 3.7 – Redox titrations of FIRd constituent cofactors at pH 7.6. Panel A. Titration of the FIRd Rdcentre followed by EPR and visible spectroscopies. The symbols (Δ) and (\times) represent the normalised amplitudes of the $g=4.3$ and $g=9.3$ EPR signals, whereas (+) denotes the normalised absorbance at 590 nm. Both titrations done in 50 mM Tris-HCl pH 7.6. Other conditions as in Figures 3.5 and 3.6. The solid line corresponds to a Nernst process with an $E^0=-140$ and $n=1$. Panels B and C. Titration of the flavin domain of FIRd. Plots were derived from data in figure 3.6, except that the contribution from Rd was removed by subtracting at each working redox potential the fraction of Rd that was reduced at that potential. The spectrum of *D. gigas* Rd (Fig. 3.4, trace c) was used in these calculations. The titrations were followed at 475-425nm (B) and at 380 nm (C). The lines correspond to a sequential two-step, one-electron equilibrium, with $E^0=-140$ mV (F_{lox}/F_{lsq}) and -180 mV (F_{lsq}/F_{lred}).

subtracting the basic Rd spectrum from several FIRd spectra along the titration, poisoning its intensity at each working redox potential, assuming a $E^0 = -140$ mV for the rubredoxin site. The resulting curves exhibit characteristic features of flavin reduction via a red-type semiquinone, namely the transient formation of absorption bands at ~ 380 nm and ~ 500 nm during reduction. The absorbance decay at $475 \text{ minus } 425$ nm follows a stepwise one-electron reduction process (Fig. 3.7, panel B), whereas a typical bell-shaped curve is obtained when the intensity of the band at 380 nm is plotted versus the reduction potential (Fig. 3.7, panel C). Fitting of the data gives midpoint reduction potentials identical to those previously estimated, $E^0 = -140 \pm 15$ mV ($\text{Fl}_{\text{ox}}/\text{Fl}_{\text{sq}}$) and $E^0 = -180 \pm 15$ mV ($\text{Fl}_{\text{sq}}/\text{Fl}_{\text{red}}$).

The Rd-truncated FIRd also undergoes reduction via a red type semiquinone (Fig. 3.8, panel A). However, in this case the determined midpoint redox potentials for

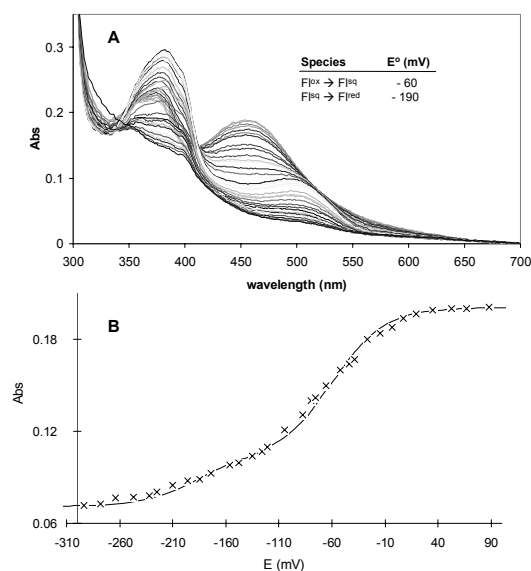


Figure 3.8 - Redox titration of the rubredoxin-truncated FIRd at pH 7.6. Panel A. Visible spectra of rubredoxin-truncated FIRd ($15 \mu\text{M}$) in 50 mM Tris-HCl pH 7.6, obtained along the redox titration. Panel B. Titration curve followed at $475\text{-}425$ nm. The line corresponds to a sequential two steps one-electron equilibrium, with $E^0 = -60$ mV ($\text{Fl}_{\text{ox}}/\text{Fl}_{\text{sq}}$) and -190 mV ($\text{Fl}_{\text{sq}}/\text{Fl}_{\text{red}}$).

be -170 ± 15 mV. This protein is reduced via two consecutive steps with $E^0 = -140 \pm 15$

the two flavin transitions are different from those determined in the intact protein: -60 ± 15 mV ($\text{Fl}_{\text{ox}}/\text{Fl}_{\text{sq}}$) and -190 ± 15 mV ($\text{Fl}_{\text{sq}}/\text{Fl}_{\text{red}}$) (Fig. 3.8, panel B). As in this protein the Rd site is absent, it appears that in intact flavorubredoxin, either the iron-sulfur centre or some of the truncated amino acid residues modulate the oxidation-reduction properties of the flavin.

The average reduction potential of the (flavo)rubredoxin reductase flavin cofactor was determined to

mV (E_{ox}/E_{red}) and $E^0 = -195 \pm 15$ mV (E_{ox}/E_{red}) (not shown).

The (flavo)rubredoxin reductase is the redox partner of flavorubredoxin – The product of *orf377* has been tentatively assigned as a rubredoxin reductase, considering its extensive amino acid sequence identity towards these proteins. Kinetically, it

receives electrons from NADH at a rate of 10 min^{-1} using molecular oxygen as electron acceptor, but not from NADPH. Using an oxygen electrode, the NADH-driven oxygen consumption rates measured at 25°C in the presence and absence of externally added catalase indicated that the product of dioxygen reduction is H_2O_2 (see below and Fig. 3.10). Ferricyanide could also be used as electron acceptor and, in this case, the K_m of the enzyme for NADH was $23 \mu\text{M}$. The ability of FIRd-reductase to reduce a rubredoxin centre was investigated (Fig. 3.9) using

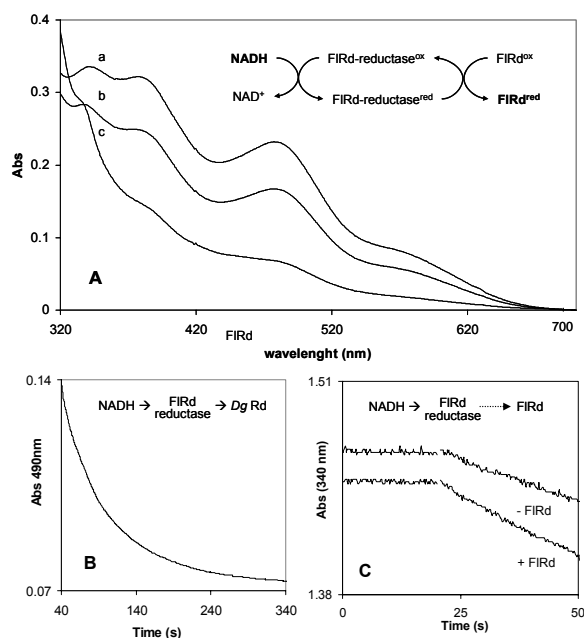


Figure 3.9 - The (flavo)rubredoxin reductase is the redox partner of flavorubredoxin and electron transfer to FIRd proceeds via the Rd-centre. Panel A. Trace a: anaerobic FIRd (28 μM) prepared in 50 mM Tris-HCl pH 7.6, in the presence of NADH (0.3 mM). This spectrum is superimposable to that of as prepared FIRd. Trace b: partially reduced FIRd, 1 minute after addition of a catalytic amount of FIRd-reductase (2.8 μM). Trace C: reduced FIRd, 4 minutes after recording spectrum B. **Panel B.** *D. gigas* Rd (10 μM) was anaerobically reduced by FIRd-reductase (0.6 μM) and NADH (50 μM) as followed by the decay of its 490 nm band. **Panel C.** The NADH consumption rate by FIRd-reductase (0.71 μM) in the presence of 0.24 mM NADH is increased ~1.5 fold by the presence of 14 μM FIRd (from 27 to ~40 min^{-1}). In all panels, schemes highlight the electron transfer pathways under study.

D. gigas rubredoxin as electron acceptor (Fig. 3.9, panel B). Indeed, the product of *E. coli* ORF377 can be assigned as a true rubredoxin reductase as the protein

catalyses electron transfer from NADH to *D. gigas* Rd (20 min^{-1}) (Fig. 3.9, panel B), but more importantly, also to *E. coli* FIRd at a higher rate (40 min^{-1}) (Fig. 3.9, panel C). These data thus provide the first indication that these two proteins interact with each other. In this context it is worth mentioning that no rubredoxin is encoded in the *E. coli* genome. Another set of experiments was performed in order to clearly demonstrate the interaction between the FIRd-reductase and FIRd. Anaerobic incubation of *E. coli* FIRd with NADH does not result in any spectral changes, indicating that the protein is not reducible by this compound (Fig. 3.9, Panel A, trace a). In agreement, FIRd shows no NAD(P)H oxidase activity. However, upon addition of a catalytic amount of FIRd-reductase, the FIRd spectra starts bleaching immediately, and full reduction is achieved within minutes, showing that the added protein is mediating electron transfer between NADH and FIRd (Fig. 3.9, Panel A, traces b and c). The Rd centre of FIRd was found to be the electron entry point in FIRd, as FIRd Δ Rd is not reduced by NADH/FIRd-reductase. Furthermore, *D. gigas* rubredoxin was able to mediate electron transfer between the reductase and the truncated FIRd, thus substituting the missing cofactor. Anaerobic incubation of *D. gigas* Rd with NADH and catalytic amounts of FIRd-reductase resulted in Rd reduction, as followed by the decrease of the intensity at 490 nm (Fig. 3.9, Panel B). However, upon anaerobic addition of FIRd Δ Rd, the exogenous Rd was reoxidised, showing that Rd had donated electrons to the redox cofactors present in the truncated protein (not shown).

These interaction experiments were reproduced in the oxygen electrode. Interestingly, it was observed that the NADH driven oxygen consumption rate by FIRd-reductase increased in the presence of FIRd (from 60 min^{-1} to 130 min^{-1}) (Fig. 3.10), thus suggesting that the latter could also be reducing molecular oxygen. This possibility was investigated in a set of experiments done in the presence of excess NADH, catalytic amounts of FIRd-reductase and FIRd (Fig. 3.10, trace a). It

could be observed that *in vitro*, the FIRd reduces dioxygen directly to water, as the addition of catalase and/or superoxide dismutase do not alter the oxygen

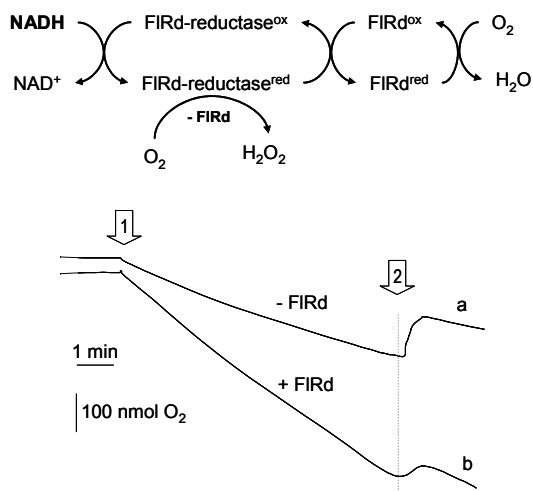


Figure 3.10 - The FIRd-reductase/FIRd system *in vitro* mediates electron transfer from NADH to oxygen and fully reduces it to water. Reaction medium contains 0.8 mM NADH in Tris/HCl 10 mM pH 7.6 buffer. Trace a, assay in the absence of FIRd. After addition of 1.1 μ M of FIRd-reductase (arrow 1) oxygen is uptaken at 62 min^{-1} by the FIRd-reductase, and is reduced to hydrogen peroxide, as shown by the production of an amount of oxygen equivalent to ~25% of total consumed after addition of catalase (arrow 2). Trace b, assay in the presence of FIRd (23 μ M) in the presence of the same amount of FIRd-reductase in trace a, and in the same conditions, results in uptake at a rate of 130 min^{-1} . In this case, oxygen reduction proceeds directly to water, as addition of catalase (arrow 2) or SOD (not shown) do not result in a significant oxygen production or rate change.

with oxygen occurs much slower, as electrons are more efficiently transferred to the terminal component of the pathway, the flavorubredoxin, a situation similar to that observed in *D. gigas* pathway (6,7).

3.4 CONCLUSIONS

A novel electron transfer pathway in *E. coli*, involving a flavorubredoxin and its flavoprotein reductase partner is here described (scheme 1).

consumption rate nor result in the production of oxygen (Fig. 3.10, trace b). This activity is likely to be associated to the diiron site, similarly to what is observed in *D. gigas* ROO (4). In the absence of FIRd, oxygen is consumed by the FIRd-reductase, at a slower rate, and with production of hydrogen peroxide (Fig. 3.10, trace a). In this particular case, our finding unequivocally further demonstrates that the studied proteins constitute in fact an electron transfer chain: in the presence of FIRd, the reaction of the flavorubredoxin-reductase

Scheme 1

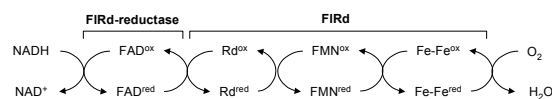


Table 1 – Redox potentials of the cofactors involved in the *E. coli* FIRd electron transfer chain

	E° (mV)
Flavorubredoxin reductase (FIRd Red)	
$FAD_{ox/sq}$ and $FAD_{sq/red}$	-140/-195
Flavorubredoxin (FIRd)	
$Rd_{ox/red}$	-140
$FMN_{ox/sq}$ and $FMN_{sq/red}$	-140/-180

The genes encoding for these proteins cluster together in the *E. coli* genome, in a putative two-cistron transcriptional unit, indicating their possible involvement in a common pathway. This was found to be the case on the basis of

the redox characterisation of the cofactors involved in this chain, and by spectroscopic demonstration of their interactions. Indeed, the midpoint reduction potentials of these electron carriers adequately mediate electron transfer from NADH ($E^{\circ}_{NADH/NAD^+} = -340$ mV) to the FIRd centres (Table 1). The Rd centre of FIRd, with the lowest reduction potential so far reported (-140 ± 15 mV), is a paradigmatic example of the influence of the protein backbone in adjusting the reduction potentials of a metal centre.

The terminal element of this chain, FIRd, is a particularly interesting example of the modular nature of a complex flavoprotein, harbouring distinct redox cofactors in a single polypeptide chain. Surprisingly, its sequence comprises a rubredoxin domain (which is not found elsewhere in the organism's genome) which is the electron entry point in this protein. Similarly to what is observed on *D. gigas* ROO structure (4), it can be anticipated that in FIRd the electrons proceeding from Rd are transferred to the FMN moiety and then to the binuclear iron site, which in ROO are in van der Waals contact. Together, the flavin cofactor and the diiron centre provide the four electrons necessary to reduce dioxygen to water. The FIRd is a member of a highly conserved superfamily of proteins that are found in all known genomes of strict anaerobic archaea and bacteria, presently comprising 21 members (3). The pathway described here resembles the one reported for *D. gigas*,

which involves a NADH:rubredoxin oxidoreductase (26), a rubredoxin and rubredoxin:oxygen oxidoreductase (ROO) as the terminal element. In this sulfate-reducing bacterium this pathway has been shown to be involved in the response to oxygen stress, linking NAD⁺ regeneration to oxygen reduction to water by ROO, and thus resulting in energy conservation by substrate-level phosphorylation (6,7,26,27). Thus, it constitutes an especially safe pathway to scavenge dioxygen in an anaerobe. It was not the aim of the present work to elucidate whether or not a similar role is played in *E. coli* by the flavorubredoxin electron transfer pathway. However, it may be speculated that it would play a similar function considering the need to scavenge transient oxygen species during anaerobic growth or even as a means to regenerate NAD⁺ during aerobiosis. Nevertheless, a distinct function for this pathway cannot be excluded at this stage.

3.5 REFERENCES

1. Massey, V. (1995) Introduction: flavoprotein structure and mechanism, *Faseb J* **9**(7), 473-475
2. Massey, V., and Hemmerich, P. (1980) Active-site probes of flavoproteins, *Biochem Soc Trans* **8**(3), 246-257
3. Wasserfallen, A., Ragettli, S., Jouanneau, Y., and Leisinger, T. (1998) A family of flavoproteins in the domains Archaea and Bacteria, *Eur J Biochem* **254**(2), 325-332
4. Frazao, C., Silva, G., Gomes, C. M., Matias, P., Coelho, R., Sieker, L., Macedo, S., Liu, M. Y., Oliveira, S., Teixeira, M., Xavier, A. V., Rodrigues-Pousada, C., Carrondo, M. A., and Le Gall, J. (2000) Structure of a dioxygen reduction enzyme from *Desulfovibrio gigas*, *Nat Struct Biol* **7**(11), 1041-1045
5. Ruettinger, R. T., Griffith, G. R., and Coon, M. J. (1977) Characterization of the omega-hydroxylase of *Pseudomonas oleovorans* as a nonheme iron protein, *Arch Biochem Biophys* **183**(2), 528-537
6. Chen, L., Liu, M. Y., LeGall, J., Fareleira, P., Santos, H., and Xavier, A. V. (1993) Rubredoxin oxidase, a new flavo-hemo-protein, is the site of oxygen reduction to water by the "strict anaerobe" *Desulfovibrio gigas*, *Biochem Biophys Res Commun* **193**(1), 100-105
7. Gomes, C. M., Silva, G., Oliveira, S., LeGall, J., Liu, M. Y., Xavier, A. V., Rodrigues-Pousada, C., and Teixeira, M. (1997) Studies on the redox centers of the terminal

- oxidase from *Desulfovibrio gigas* and evidence for its interaction with rubredoxin, *J Biol Chem* **272**(36), 22502-22508
8. Wastl, J., Sticht, H., Maier, U. G., Rosch, P., and Hoffmann, S. (2000) Identification and characterization of a eukaryotically encoded rubredoxin in a cryptomonad alga, *FEBS Lett* **471**(2-3), 191-196
 9. Wastl, J., Duin, E. C., Iuzzolino, L., Dorner, W., Link, T., Hoffmann, S., Sticht, H., Dau, H., Lingelbach, K., and Maier, U. G. (2000) Eukaryotically encoded and chloroplast-located rubredoxin is associated with photosystem II, *J Biol Chem* **275**(39), 30058-30063
 10. LeGall, J., Prickril, B. C., Moura, I., Xavier, A. V., Moura, J. J., and Huynh, B. H. (1988) Isolation and characterization of rubrerythrin, a non-heme iron protein from *Desulfovibrio vulgaris* that contains rubredoxin centers and a hemerythrin-like binuclear iron cluster, *Biochemistry* **27**(5), 1636-1642
 11. Parkhill, J., Wren, B. W., Mungall, K., Ketley, J. M., Churcher, C., Basham, D., Chillingworth, T., Davies, R. M., Feltwell, T., Holroyd, S., Jagels, K., Karlyshev, A. V., Moule, S., Pallen, M. J., Penn, C. W., Quail, M. A., Rajandream, M. A., Rutherford, K. M., van Vliet, A. H., Whitehead, S., and Barrell, B. G. (2000) The genome sequence of the food-borne pathogen *Campylobacter jejuni* reveals hypervariable sequences, *Nature* **403**(6770), 665-668
 12. Benes, V., Hostomsky, Z., Arnold, L., and Paces, V. (1993) M13 and pUC vectors with new unique restriction sites for cloning, *Gene* **130**(1), 151-152
 13. Bradford, M. M. (1976) A rapid and sensitive method for the quantitation of microgram quantities of protein utilizing the principle of protein-dye binding, *Anal Biochem* **72**, 248-254
 14. Fischer, D. S., and Price, D. C. (1964) A Simple Serum Iron Method Using the New Sensitive Chromogen Tripyridyl-S-Triazine, *Clin Chem* **10**, 21-31
 15. Susin, S., Abian, J., Sanchez-Baeza, F., Peleato, M. L., Abadia, A., Gelpi, E., and Abadia, J. (1993) Riboflavin 3'- and 5'-sulfate, two novel flavins accumulating in the roots of iron-deficient sugar beet (*Beta vulgaris*), *J Biol Chem* **268**(28), 20958-20965
 16. Blattner, F. R., Plunkett, G., 3rd, Bloch, C. A., Perna, N. T., Burland, V., Riley, M., Collado-Vides, J., Glasner, J. D., Rode, C. K., Mayhew, G. F., Gregor, J., Davis, N. W., Kirkpatrick, H. A., Goeden, M. A., Rose, D. J., Mau, B., and Shao, Y. (1997) The complete genome sequence of *Escherichia coli* K-12, *Science* **277**(5331), 1453-1474
 17. Jones, D. T. (1999) GenTHREADER: an efficient and reliable protein fold recognition method for genomic sequences, *J Mol Biol* **287**(4), 797-815
 18. LeGall, J., Liu, M. Y., Gomes, C. M., Braga, V., Pacheco, I., Regalla, M., Xavier, A. V., and Teixeira, M. (1998) Characterisation of a new rubredoxin isolated from *Desulfovibrio desulfuricans* 27774: definition of a new family of rubredoxins, *FEBS Lett* **429**(3), 295-298
 19. Le Brun, N. E., Wilson, M. T., Andrews, S. C., Guest, J. R., Harrison, P. M., Thomson, A. J., and Moore, G. R. (1993) Kinetic and structural characterization of an intermediate in the biomineralization of bacterioferritin, *FEBS Lett* **333**(1-2), 197-202
 20. Romao, C. V., Regalla, M., Xavier, A. V., Teixeira, M., Liu, M. Y., and Le Gall, J. (2000) A bacterioferritin from the strict anaerobe *Desulfovibrio desulfuricans* ATCC 27774, *Biochemistry* **39**(23), 6841-6849

21. Eidsness, M. K., Burden, A. E., Richie, K. A., Kurtz, D. M., Jr., Scott, R. A., Smith, E. T., Ichiye, T., Beard, B., Min, T., and Kang, C. (1999) Modulation of the redox potential of the [Fe(SCys)(4)] site in rubredoxin by the orientation of a peptide dipole, *Biochemistry* **38**(45), 14803-14809
22. Moura, I., Moura, J. J., Santos, M. H., Xavier, A. V., and Le Gall, J. (1979) Redox studies on rubredoxins from sulphate and sulphur reducing bacteria, *FEBS Lett* **107**(2), 419-421
23. Xiao, Z., Maher, M. J., Cross, M., Bond, C. S., Guss, J. M., and Wedd, A. G. (2000) Mutation of the surface valine residues 8 and 44 in the rubredoxin from *Clostridium pasteurianum*: solvent access versus structural changes as determinants of reversible potential, *J Biol Inorg Chem* **5**(1), 75-84
24. Swartz, P. D., Beck, B. W., and Ichiye, T. (1996) Structural origins of redox potentials in Fe-S proteins: electrostatic potentials of crystal structures, *Biophys J* **71**(6), 2958-2969
25. Maher, M. J., Xiao, Z., Wilce, M. C., Guss, J. M., and Wedd, A. G. (1999) Rubredoxin from *Clostridium pasteurianum*. Structures of G10A, G43A and G10VG43A mutant proteins. Mutation of conserved glycine 10 to valine causes the 9-10 peptide link to invert, *Acta Crystallogr D Biol Crystallogr* **55**(Pt 5), 962-968
26. Chen, L., Liu, M. Y., Legall, J., Fareleira, P., Santos, H., and Xavier, A. V. (1993) Purification and characterization of an NADH-rubredoxin oxidoreductase involved in the utilization of oxygen by *Desulfovibrio gigas*, *Eur J Biochem* **216**(2), 443-448
27. Fareleira, P., Legall, J., Xavier, A. V., and Santos, H. (1997) Pathways for utilization of carbon reserves in *Desulfovibrio gigas* under fermentative and respiratory conditions, *J Bacteriol* **179**(12), 3972-3980

4

A novel type of nitric oxide reductase: *Escherichia coli* flavorubredoxin ‡

4.1	Introduction	97
4.2	Materials and Methods	99
4.3	Results and Discussion	100
4.4	Conclusions	103
4.5	References	105

SUMMARY

Escherichia coli flavorubredoxin is a member of the family of the A-type Flavoproteins (ATF), which are built by two core domains: a metallo- β -lactamase like domain, at the N-terminal region, harbouring a non-heme di-iron site, and a flavodoxin-like domain, containing one FMN moiety. The enzyme from *E. coli* has an extra module at the C-terminus, containing a rubredoxin-like centre. The A-type Flavoproteins are widespread among strict and facultative anaerobes, as deduced from the analysis of the complete prokaryotic genomes. In this report we show that the recombinant enzyme purified from *E. coli*, has nitric oxide reductase activity with a turnover number of $\sim 15 \text{ mol NO} \cdot \text{mol enzyme}^{-1} \cdot \text{s}^{-1}$, which is well within the range of those determined for the canonical heme b_3 -Fe_B containing nitric oxide reductases (i.e. $\sim 10 - 50 \text{ mol NO} \cdot \text{mol NOR}^{-1} \cdot \text{s}^{-1}$ for the *Paracoccus denitrificans* NOR). Furthermore, it is shown that the activity is due to the ATF-core, as the rubredoxin domain alone exhibits no activity. Thus, a novel family of prokaryotic NO reductases, with a non-heme di-iron site as the catalytic centre, is established.

‡This Chapter was published in the following article:

Gomes, C.M., Giuffrè, A., Forte, E., Vicente, J.B., Saraiva, L.M., Brunori, M., and Teixeira, M. (2002) "A novel type of nitric oxide reductase: *Escherichia coli* flavorubredoxin", *Journal of Biological Chemistry* 277(28): 25273-6

The work herein reported results from a longstanding collaboration between the group of Prof. Miguel Teixeira at ITQB and the group of Prof. Maurizio Brunori at the Dipartimento di Scienze Biochimiche "A. Rossi Fanelli" from the Università degli Studi "La Sapienza" di Roma, Italy. Cláudio M. Gomes visited Prof. Brunori's lab to perform amperometric NO consumption assays with flavorubredoxin. Construction of the truncated flavorubredoxin consisting solely of the rubredoxin domain was performed in the Lab of Dr. Lígia M. Saraiva at ITQB.

4.1 INTRODUCTION

Nitric oxide (NO) plays a key role in a wide variety of physiological and pathological processes in eukaryotes, namely cell signalling and host-pathogen responses. In prokaryotes, NO is encountered as an intermediate in the global nitrogen cycle, namely in the process of denitrification, i.e. reduction of nitrate/nitrite to dinitrogen. Prokaryotes not directly involved in these metabolic pathways, may nevertheless be exposed to high fluxes of NO, produced either abiotically or biotically (for example by macrophages,(1)). In denitrifying bacteria, NO is reduced to N₂O by nitric oxide reductase (NOR), a membrane-bound enzyme containing at the catalytic subunit a heme *b*₃-Fe_B binuclear centre (2,3). NORs have been proposed to be evolutionarily related to the large family of heme-copper oxygen reductases on the basis of structural homologies (4,5); consistently, two prokaryotic oxidases were recently reported to be endowed with NO-reductase activity (6,7). So far, only a second type of nitric oxide reductases has been found, in fungi, of the cytochrome P450 family (2).

The A-type flavoproteins are a large family of enzymes, widespread among Bacteria and Archaea, either strict or facultative anaerobes (8). The major distinctive feature of this large family is the common core unit, built by two independent structural modules: the N-terminal one characterized by a β -lactamase like fold, and the second domain, having a short chain flavodoxin-like fold (9). Only a few members of this family have been so far purified from its natural host: the enzymes from *Desulfovibrio (D.) gigas* (10), *Rhodobacter capsulatus* (11), and *Methanobacterium thermoautotrophicum* (12). The first to be extensively studied, was the rubredoxin:oxygen oxidoreductase (ROO) from the sulfate reducing bacterium *D. gigas*. This enzyme reduces O₂ to water receiving electrons from a type-I rubredoxin, which in turn is reduced by an NADH:rubredoxin oxidoreductase (13). The 3D crystal structure of ROO (9) revealed its modular

architecture and, quite strikingly, showed that the β -lactamase domain harbours a non-heme di-iron site, consistent with the O_2 reductase activity of this enzyme. The flavodoxin domain contains one FMN molecule, which receives electrons from the rubredoxin (14). The homologous enzymes from cyanobacteria *Synechocystis* (15) and *Anabaena* (16), from enterobacteria (*E. coli* (17), *Salmonella enterica* serovar Typhimurium LT2 (18) and *Salmonella enterica* serovar Typhi CT18 (19)), and from *Clostridium perfringens* (20) contain one extra domain at the C-terminus: whereas the cyanobacterial enzymes contain one NADH:oxidoreductase domain (condensing into a single protein the complete electron transfer chain from NADH to O_2), the enterobacterial enzymes have a rubredoxin-like domain (Rd), i.e. they bear the direct electron donor fused to the core catalytic domain (8,21). Interestingly, in these enterobacteria, downstream to the gene encoding for the A-type flavoprotein, there is a gene encoding for a NADH:rubedoxin oxidoreductase, both genes possibly forming a dicistronic transcriptional unit.

The recombinant enzyme from *E. coli* (named flavorubredoxin, FIRd), purified and characterised, was shown to contain one rubredoxin-like centre, one FMN and one di-iron centre. It was further shown that indeed it receives electrons from the NADH:oxidoreductase (FIRd-red) encoded in the same gene locus (21).

As for the enzyme from *D. gigas*, it was also proven that the enzyme is able to reduce O_2 to water; moreover, the di-iron centre was shown to bind NO (21). Recently, Gardner *et al.* (22) reported that *E. coli* grown anaerobically and exposed (for a certain period of time) to NO, develops a NO-reductase activity, which is lost by knocking out the gene encoding for the flavorubredoxin. However, the same authors were unable to show that the flavorubredoxin is responsible for NO reduction, attributing this failure to enzyme instability. In this article, we show that recombinant *E. coli* flavorubredoxin is a NO reductase, with a turnover number ($14.9 \pm 6.7 \text{ mol NO} \cdot \text{mol FIRd}^{-1} \cdot \text{s}^{-1}$) similar to that of canonical heme b_3 -Fes

containing NOR enzymes (2,3). Thus we demonstrate the existence of a novel family of NO reductases, which is likely to be widespread among strict and facultative anaerobes.

4.2 MATERIALS AND METHODS

Protein expression and purification – Recombinant Flavorubredoxin (FIRd) and Flavorubredoxin-reductase (FIRd-red) were expressed and purified as previously described (8,21). Amplification of the Rd domain of *E. coli* FIRd was achieved by means of a PCR reaction using *Pfu* polymerase (Stratagene), the recombinant plasmid pME2543 (that contains the complete *E. coli* orf479 (8)) and the following oligonucleotides: sense primer, (5'-GTCATATGGGCCACGGAT-3'), that introduced a *Nde*I site changing the codon of the residue 422 to the initiation codon ATG; antisense primer, T7 22-mer (5'-GTAATACGACTCACTATAGGGC-3'). The amplicon was digested with *Nde*I and *Hind*III, ligated into compatible sites on pT7-7, and transformed into *E. coli* DH5 α cells. The cloned insert was then sequenced in both strands by using vector-specific oligonucleotide primers and fluorescent dideoxy terminators and an ABI model 377 DNA sequencer. After confirming that the correct nucleotide sequence was amplified, the recombinant plasmid was transformed in BL21-Gold(DE3). Overnight cultures, grown aerobically at 37°C in minimal medium M9 containing ampicillin (100 μ g/ml), were diluted 1/100 into the same medium, grown to an OD₆₀₀ of 0.8, induced with 0.4 mM IPTG and harvested by centrifugation after 4 hours. After cell disruption in a French Press at 7000 PSI (in two cycles), and soluble extract separation from the membranes through 16-hour ultracentrifugation at 100.000g (at 5°C), the rubredoxin domain of flavorubredoxin was purified in a two-step procedure, in a HiLoad Pharmacia system. The soluble extract was dialysed overnight against 10 mM Tris-HCl pH 7.6 (buffer A), and then loaded into a 60-ml

Q-Sepharose column previously equilibrated with buffer A. The rubredoxin domain of flavorubredoxin eluted at approximately 400 mM NaCl, was concentrated in a Diaflo cell with a YM3 cut off membrane and further applied to a Superdex S-75 gel filtration column, previously equilibrated with 150 mM NaCl in buffer A. The eluted protein was found to be pure, as assayed by SDS-gel electrophoresis (23).

Total protein was determined using the BCA procedure (24) and iron quantitated by the TPTZ method (25). Total FMN content of FIRd was assessed after protein denaturation with 8% TCA, using an extinction coefficient of $12500 \text{ M}^{-1} \cdot \text{cm}^{-1}$ at $\lambda=450 \text{ nm}$ to quantify the flavin. Recombinant FIRd was found to contain 1 mol Flavin/mol protein and $\sim 3.3 \text{ mol Fe/mol protein}$, while FIRd-reductase contained 1 mol FAD/mol protein and the FIRd rubredoxin domain 1 mol Fe / mol protein. The detailed characterisation of the Rubredoxin domain will be published elsewhere.

Kinetic assays - Nitric oxide consumption measurements were carried out using a World Precision Instruments ISO-NOP 2mm electrode, at room temperature. Assays were carried out under anaerobic conditions in 50 mM Tris/HCl buffer at pH = 7.6, in the presence of EDTA (20 μM), glucose (3 mM), glucose oxidase (4 units/ml) and catalase (130 units/ml). Oxygen consumption rates were measured using a Yellow Springs micro O_2 electrode, in 50 mM Tris/HCl buffer at pH 7.6 and room temperature.

4.3 RESULTS AND DISCUSSION

Flavorubredoxin is a novel NO reductase with high affinity for NO.

The NO reductase activity of *E. coli* FIRd was investigated measuring NO consumption in the presence of the physiological partner, FIRd-reductase, and

NADH. It was observed that FIRd catalyses efficiently the NO consumption (Fig. 1); the rate of $14.9 \pm 6.7 \text{ mol NO} \cdot \text{mol FIRd}^{-1} \cdot \text{s}^{-1}$ was estimated by averaging 26 independent measurements carried out at different concentrations of FIRd-red (Fig. 4.2) and at saturating NADH concentration ($> 200 \text{ } \mu\text{M}$). The activity is linearly dependent on FIRd concentration, but is essentially independent of NO concentration from $\leq 1 \text{ } \mu\text{M}$ (approx. the physiological levels) to $\sim 10 \text{ } \mu\text{M}$. This shows that the enzyme has high affinity for NO ($K_M < 1 \text{ } \mu\text{M}$), consistent with the zero-order kinetics of the observed NO consumption (Fig. 4.1).

Control experiments showed that the observed NO consumption is exclusively attributable to FIRd-mediated catalysis: (i) in the absence of FIRd, NO consumption mediated by the NADH/FIRd-reductase pair was much lower

(even at different FIRd-red concentrations) than in the presence of FIRd; (ii) FIRd denaturation by boiling the protein for 10 min in the

presence of 10% SDS totally abolishes NO consumption, thus excluding that contaminant inorganic compounds in the medium are responsible for the observed NO degradation. Altogether, these results clearly establish that *E. coli* FIRd operates as a *bona fide* NOR, with a measured turnover number comparable to that published for NOR from *Paracoccus denitrificans* (in the range $\sim 10 - 50 \text{ mol NO} \cdot \text{mol NOR}^{-1} \cdot \text{s}^{-1}$, (2,3)).

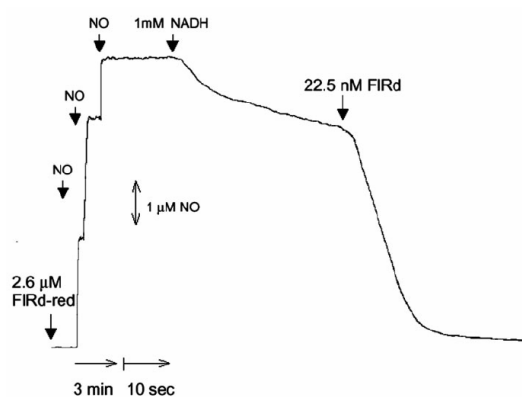


Figure 4.1 - NO reductase activity of *E. coli* FIRd. To an anaerobic buffer, containing $2.6 \text{ } \mu\text{M}$ FIRd-red, three aliquots of NO (yielding a final concentration of $6.8 \text{ } \mu\text{M}$) were sequentially added. After raising the chart-speed, 1 mM NADH was added. Following the addition of 22.5 nM FIRd at about $4.7 \text{ } \mu\text{M}$ NO, a fast consumption of NO was observed whose time course followed a zero-order kinetics. Analysis of this trace yields a NO-reductase activity for FIRd corresponding to $14.6 \text{ mol NO} \cdot \text{mol FIRd}^{-1} \cdot \text{s}^{-1}$.

The di-iron cluster is the active site.

The *E. coli* FIRd contains two different metal centres, integrated into distinct structural domains: the rubredoxin (Rd) centre in a rubredoxin-like fold, and the non-heme di-iron site. Several evidences show that the di-iron centre is the site of NO reduction in FIRd. We previously observed by EPR spectroscopy that the di-iron centre of FIRd is able to bind NO (21). In this work we have tested a truncated form of FIRd, consisting solely of the rubredoxin domain, that proved to be unable to process NO (data not shown), despite being still efficiently reduced by the NADH/FIRd-reductase couple (*our own unpublished observations*). Furthermore, the NO reductase activity is not inhibited by cyanide (even after 1 day-incubation, both at 4 °C or at room temperature, and 3 mM cyanide), which is consistent with the fact that the di-iron site has low affinity for cyanide.

Flavorubredoxin is a bifunctional NO and O₂ reductase, albeit with distinct affinities.

The FIRd di-iron site is capable of reducing O₂ to water, in the presence of NADH and FIRd-reductase (21). Within experimental errors, the NO and O₂ consumption

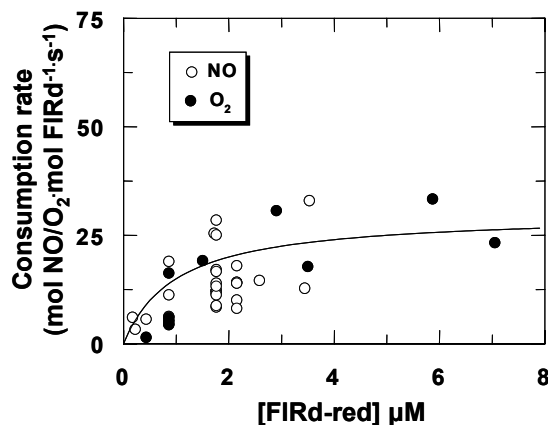


Figure 4.2 - *E. coli* FIRd is a bifunctional NO and O₂ reductase. NO and O₂ reductase activity of *E. coli* FIRd (7.5 or 22.5 nM) measured in the presence of NADH (> 200 μM), at increasing concentration of FIRd-reductase. NO consumption was measured at [NO] = 1 ÷ 10 μM, whereas O₂ consumption was estimated from initial rate at high [O₂], i.e. in air-equilibrated buffer.

rates are similar (Fig. 4.2), as estimated from the initial rate at high O₂ concentration, i.e. in air-equilibrated buffer. NO and O₂ consumption may be thus rate-limited by the same event (for instance by internal electron transfer to the di-iron site). However, whereas NO is processed with a high affinity, O₂ reduction does not follow a zero-order kinetics, as the

apparent rate starts to slowdown at $\sim 200 \mu\text{M O}_2$. This points to a relatively low affinity for O_2 , compared to the much higher affinity for NO ($K_M < 1 \mu\text{M}$). It is interesting that a similar observation has been described for the *P. denitrificans* NOR (see Fig. 7 in (26)).

4.4 CONCLUSIONS

The results reported in this article demonstrate that *in vitro* *E. coli* flavorubredoxin (FIRd) has NO reductase activity, comparable to that of canonical heme b_3 -Fe_B containing NORs. Although at this stage it was not possible to measure this activity in other A-type Flavoproteins, the large overall similarity in amino acid sequence among most members of this family, and the conservation of residues binding the di-iron site, strongly suggests that the NO-reductase activity will be found in many other (if not all) A-Type Flavoproteins. These enzymes clearly display a bifunctional activity, in so far as they are also able to catalyse the reduction of O_2 to water. This behaviour parallels that described for the heme-copper oxygen reductases and for NORs, providing evidence for a widespread bifunctional versatile prokaryotic response to environmental conditions (detoxification of O_2 or NO).

This enzyme family is present in a large variety of prokaryotes, phylogenetically and metabolically as diverse as hyperthermophilic anaerobic archaea (such as *Pyrococcus* species, e.g. (27)), strict and facultative anaerobic bacteria (including enterobacteria, ((17,18)), photosynthetic cyanobacteria (15,16), nitrogen fixing organisms (such as *Rhodobacter capsulatus* (11)), sulfate reducing archaea (28) and bacteria (10,14), and *Clostridia* species (20,29) (Fig. 4.3). The genomic organisation of the A-type Flavoproteins is however quite diversified. In fact, among the known genomes, only enterobacteria have a genomic organisation whereby the gene encoding for the FIRd is adjacent to that encoding for its reductase (17,18),

and both are close to a putative NO regulator. In other micro-organisms, the genes encoding for A-type Flavoproteins are close to sequences encoding for quite diverse or still unknown proteins. Especially interesting cases are those

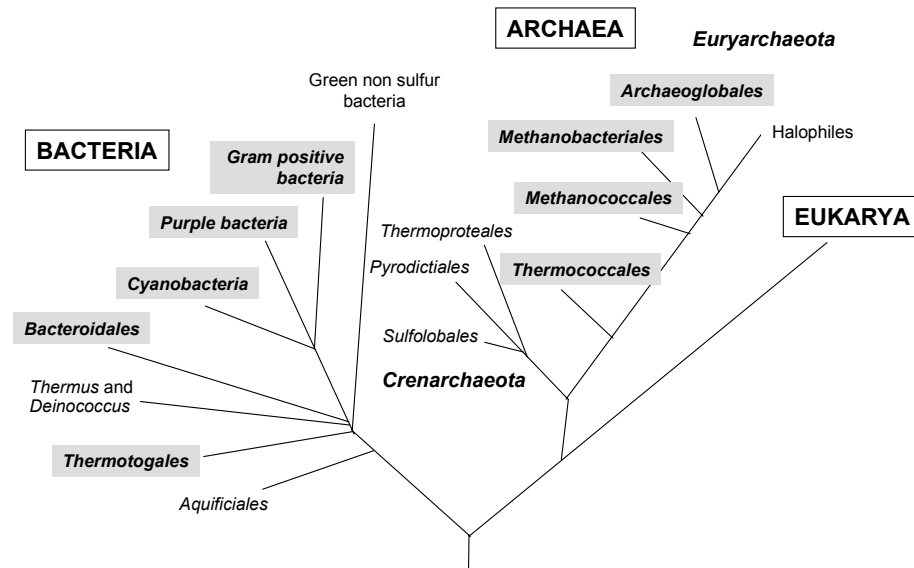


Figure 4.3 - Distribution of A-type Flavoproteins among prokaryotes. Schematic representation of the 16S RNA tree of life, showing the presence of A-type flavoproteins among bacterial and archaeal groups (grey shaded boxes): Archaeoglobales (eg. *Archaeoglobus fulgidus*), Methanobacteriales (eg. *Methanobacterium thermoautotrophicum*), Methanococcales (eg. *Methanococcus jannaschii*), Thermococcales (eg. *Pyrococcus furiosus*), Thermotogales (eg. *Thermotoga maritima*), Bacteroidales (eg. *Porphyromonas gingivalis*), Cyanobacteria (eg. *Synechocystis* sp.), Purple bacteria (eg. the proteobacteria *Escherichia coli*, *Salmonella thyphimurium*, *Desulfovibrio gigas*), Gram-positive bacteria (eg. *Clostridium perfringens*).

found in the genomes of *Clostridium perfringens* (20) and *acetobutylicum* (29), *Methanobacterium thermoautotrophicum* (30), *Methanococcus jannaschii* (31), *Pyrococcus horikoshi* (27) and *Moorella thermoacetica* (32), in which the A-type Flavoproteins are in clusters containing genes coding for proteins involved in oxidative stress responses, such as alkyl hydroperoxide reductases, superoxide reductases or superoxide dismutases. Thus, although there is no simple and direct correlation between the genomic organisation of these enzymes and their physiological functions, examination of the available genome organizations suggests strong physiological links between O₂ and NO metabolisms. Furthermore, while in organisms such as *Desulfovibrio gigas*, *Rhodobacter capsulatus* and *Methanobacterium*

thermoautotrophicum the A-type Flavoproteins are expressed constitutively under sulfate reducing, nitrogen fixing and methanogenic growth conditions, respectively, in *E. coli* the FIRd endowed with NO reductase activity was proposed to be induced by exposure to NO (22).

In summary, we have shown that the purified recombinant *E. coli* A-type Flavoprotein has a high NO reductase activity, which allows to propose a novel family of NO reducing enzymes that may play a key role in NO detoxification by prokaryotes. The relationships between the two functions of this family related to NO and O₂ detoxification, and the understanding of the intricate regulation of the expression and activities of these enzymes, is a challenge for the near future.

4.5 REFERENCES

1. MacMicking, J., Xie, Q. W., and Nathan, C. (1997) Nitric oxide and macrophage function, *Annu Rev Immunol* **15**, 323-350
2. Zumft, W. G. (1997) Cell biology and molecular basis of denitrification, *Microbiol Mol Biol Rev* **61**(4), 533-616
3. Hendriks, J., Warne, A., Gohlke, U., Haltia, T., Ludovici, C., Lubben, M., and Saraste, M. (1998) The active site of the bacterial nitric oxide reductase is a dinuclear iron center, *Biochemistry* **37**(38), 13102-13109
4. Saraste, M., and Castresana, J. (1994) Cytochrome oxidase evolved by tinkering with denitrification enzymes, *FEBS Lett* **341**(1), 1-4
5. van der Oost, J., de Boer, A. P., de Gier, J. W., Zumft, W. G., Stouthamer, A. H., and van Spanning, R. J. (1994) The heme-copper oxidase family consists of three distinct types of terminal oxidases and is related to nitric oxide reductase, *FEMS Microbiol Lett* **121**(1), 1-9
6. Giuffre, A., Stubauer, G., Sarti, P., Brunori, M., Zumft, W. G., Buse, G., and Soulimane, T. (1999) The heme-copper oxidases of *Thermus thermophilus* catalyze the reduction of nitric oxide: evolutionary implications, *Proc Natl Acad Sci U S A* **96**(26), 14718-14723
7. Forte, E., Urbani, A., Saraste, M., Sarti, P., Brunori, M., and Giuffre, A. (2001) The cytochrome cbb3 from *Pseudomonas stutzeri* displays nitric oxide reductase activity, *Eur J Biochem* **268**(24), 6486-6491
8. Wasserfallen, A., Ragetti, S., Jouanneau, Y., and Leisinger, T. (1998) A family of flavoproteins in the domains Archaea and Bacteria, *Eur J Biochem* **254**(2), 325-332
9. Frazao, C., Silva, G., Gomes, C. M., Matias, P., Coelho, R., Sieker, L., Macedo, S., Liu, M. Y., Oliveira, S., Teixeira, M., Xavier, A. V., Rodrigues-Pousada, C., Carrondo, M. A., and Le Gall, J. (2000) Structure of a dioxygen reduction enzyme from

- Desulfovibrio gigas, *Nat Struct Biol* **7**(11), 1041-1045
10. Chen, L., Liu, M. Y., LeGall, J., Fareleira, P., Santos, H., and Xavier, A. V. (1993) Rubredoxin oxidase, a new flavo-hemo-protein, is the site of oxygen reduction to water by the "strict anaerobe" *Desulfovibrio gigas*, *Biochem Biophys Res Commun* **193**(1), 100-105
 11. Jouanneau, Y., Meyer, C., Asso, M., Guigliarelli, B., and Willison, J. C. (2000) Characterization of a nif-regulated flavoprotein (FprA) from *Rhodobacter capsulatus*. Redox properties and molecular interaction with a [2Fe-2S] ferredoxin, *Eur J Biochem* **267**(3), 780-787
 12. Wasserfallen, A., Huber, K., and Leisinger, T. (1995) Purification and structural characterization of a flavoprotein induced by iron limitation in *Methanobacterium thermoautotrophicum* Marburg, *J Bacteriol* **177**(9), 2436-2441
 13. Chen, L., Liu, M. Y., Legall, J., Fareleira, P., Santos, H., and Xavier, A. V. (1993) Purification and characterization of an NADH-rubredoxin oxidoreductase involved in the utilization of oxygen by *Desulfovibrio gigas*, *Eur J Biochem* **216**(2), 443-448
 14. Gomes, C. M., Silva, G., Oliveira, S., LeGall, J., Liu, M. Y., Xavier, A. V., Rodrigues-Pousada, C., and Teixeira, M. (1997) Studies on the redox centers of the terminal oxidase from *Desulfovibrio gigas* and evidence for its interaction with rubredoxin, *J Biol Chem* **272**(36), 22502-22508
 15. Kaneko, T., Tanaka, A., Sato, S., Kotani, H., Sazuka, T., Miyajima, N., Sugiura, M., and Tabata, S. (1995) Sequence analysis of the genome of the unicellular cyanobacterium *Synechocystis* sp. strain PCC6803. I. Sequence features in the 1 Mb region from map positions 64% to 92% of the genome, *DNA Res* **2**(4), 153-166, 191-158
 16. Kaneko, T., Nakamura, Y., Wolk, C. P., Kuritz, T., Sasamoto, S., Watanabe, A., Iriguchi, M., Ishikawa, A., Kawashima, K., Kimura, T., Kishida, Y., Kohara, M., Matsumoto, M., Matsuno, A., Muraki, A., Nakazaki, N., Shimpo, S., Sugimoto, M., Takazawa, M., Yamada, M., Yasuda, M., and Tabata, S. (2001) Complete genomic sequence of the filamentous nitrogen-fixing cyanobacterium *Anabaena* sp. strain PCC 7120, *DNA Res* **8**(5), 205-213; 227-253
 17. Blattner, F. R., Plunkett, G., 3rd, Bloch, C. A., Perna, N. T., Burland, V., Riley, M., Collado-Vides, J., Glasner, J. D., Rode, C. K., Mayhew, G. F., Gregor, J., Davis, N. W., Kirkpatrick, H. A., Goeden, M. A., Rose, D. J., Mau, B., and Shao, Y. (1997) The complete genome sequence of *Escherichia coli* K-12, *Science* **277**(5331), 1453-1474
 18. McClelland, M., Sanderson, K. E., Spieth, J., Clifton, S. W., Latreille, P., Courtney, L., Porwollik, S., Ali, J., Dante, M., Du, F., Hou, S., Layman, D., Leonard, S., Nguyen, C., Scott, K., Holmes, A., Grewal, N., Mulvaney, E., Ryan, E., Sun, H., Florea, L., Miller, W., Stoneking, T., Nhan, M., Waterston, R., and Wilson, R. K. (2001) Complete genome sequence of *Salmonella enterica* serovar Typhimurium LT2, *Nature* **413**(6858), 852-856
 19. Parkhill, J., Dougan, G., James, K. D., Thomson, N. R., Pickard, D., Wain, J., Churcher, C., Mungall, K. L., Bentley, S. D., Holden, M. T., Sebaihia, M., Baker, S., Basham, D., Brooks, K., Chillingworth, T., Connerton, P., Cronin, A., Davis, P., Davies, R. M., Dowd, L., White, N., Farrar, J., Feltwell, T., Hamlin, N., Haque, A., Hien, T. T., Holroyd, S., Jagels, K., Krogh, A., Larsen, T. S., Leather, S., Moule, S., O'Gaora, P.,

- Parry, C., Quail, M., Rutherford, K., Simmonds, M., Skelton, J., Stevens, K., Whitehead, S., and Barrell, B. G. (2001) Complete genome sequence of a multiple drug resistant *Salmonella enterica* serovar Typhi CT18, *Nature* **413**(6858), 848-852
20. Shimizu, T., Ohtani, K., Hirakawa, H., Ohshima, K., Yamashita, A., Shiba, T., Ogasawara, N., Hattori, M., Kuhara, S., and Hayashi, H. (2002) Complete genome sequence of *Clostridium perfringens*, an anaerobic flesh-eater, *Proc Natl Acad Sci U S A* **99**(2), 996-1001
21. Gomes, C. M., Vicente, J. B., Wasserfallen, A., and Teixeira, M. (2000) Spectroscopic studies and characterization of a novel electron-transfer chain from *Escherichia coli* involving a flavorubredoxin and its flavoprotein reductase partner, *Biochemistry* **39**(51), 16230-16237
22. Gardner, A. M., Helmick, R. A., and Gardner, P. R. (2002) Flavorubredoxin, an inducible catalyst for nitric oxide reduction and detoxification in *Escherichia coli*, *J Biol Chem* **277**(10), 8172-8177
23. Garfin, D. E. (1990) One-dimensional gel electrophoresis, *Methods Enzymol* **182**, 425-441
24. Smith, P. K., Krohn, R. I., Hermanson, G. T., Mallia, A. K., Gartner, F. H., Provenzano, M. D., Fujimoto, E. K., Goeke, N. M., Olson, B. J., and Klenk, D. C. (1985) Measurement of protein using bicinchoninic acid, *Anal Biochem* **150**(1), 76-85
25. Fischer, D. S., and Price, D. C. (1964) A Simple Serum Iron Method Using the New Sensitive Chromogen Tripyridyl-S-Triazine, *Clin Chem* **10**, 21-31
26. Fujiwara, T., and Fukumori, Y. (1996) Cytochrome cb-type nitric oxide reductase with cytochrome c oxidase activity from *Paracoccus denitrificans* ATCC 35512, *J Bacteriol* **178**(7), 1866-1871
27. Kawarabayasi, Y., Sawada, M., Horikawa, H., Haikawa, Y., Hino, Y., Yamamoto, S., Sekine, M., Baba, S., Kosugi, H., Hosoyama, A., Nagai, Y., Sakai, M., Ogura, K., Otsuka, R., Nakazawa, H., Takamiya, M., Ohfuku, Y., Funahashi, T., Tanaka, T., Kudoh, Y., Yamazaki, J., Kushida, N., Oguchi, A., Aoki, K., and Kikuchi, H. (1998) Complete sequence and gene organization of the genome of a hyper-thermophilic archaeobacterium, *Pyrococcus horikoshii* OT3, *DNA Res* **5**(2), 55-76
28. Klenk, H. P., Clayton, R. A., Tomb, J. F., White, O., Nelson, K. E., Ketchum, K. A., Dodson, R. J., Gwinn, M., Hickey, E. K., Peterson, J. D., Richardson, D. L., Kerlavage, A. R., Graham, D. E., Kyrpides, N. C., Fleischmann, R. D., Quackenbush, J., Lee, N. H., Sutton, G. G., Gill, S., Kirkness, E. F., Dougherty, B. A., McKenney, K., Adams, M. D., Loftus, B., Peterson, S., Reich, C. I., McNeil, L. K., Badger, J. H., Glodek, A., Zhou, L., Overbeek, R., Gocayne, J. D., Weidman, J. F., McDonald, L., Utterback, T., Cotton, M. D., Spriggs, T., Artiach, P., Kaine, B. P., Sykes, S. M., Sadow, P. W., D'Andrea, K. P., Bowman, C., Fujii, C., Garland, S. A., Mason, T. M., Olsen, G. J., Fraser, C. M., Smith, H. O., Woese, C. R., and Venter, J. C. (1997) The complete genome sequence of the hyperthermophilic, sulphate-reducing archaeon *Archaeoglobus fulgidus*, *Nature* **390**(6658), 364-370
29. Nolling, J., Breton, G., Omelchenko, M. V., Makarova, K. S., Zeng, Q., Gibson, R., Lee, H. M., Dubois, J., Qiu, D., Hitti, J., Wolf, Y. I., Tatusov, R. L., Sabathe, F., Doucette-Stamm, L., Soucaille, P., Daly, M. J., Bennett, G. N., Koonin, E. V., and Smith, D. R. (2001) Genome sequence and comparative analysis of the solvent-producing bacterium *Clostridium acetobutylicum*, *J Bacteriol* **183**(16), 4823-4838
30. Smith, D. R., Doucette-Stamm, L. A., Deloughery, C., Lee, H., Dubois, J., Aldredge, T., Bashirzadeh, R., Blakely, D., Cook, R., Gilbert, K., Harrison, D., Hoang, L., Keagle,

- P., Lumm, W., Pothier, B., Qiu, D., Spadafora, R., Vicaire, R., Wang, Y., Wierzbowski, J., Gibson, R., Jiwani, N., Caruso, A., Bush, D., Reeve, J. N., and et al. (1997) Complete genome sequence of *Methanobacterium thermoautotrophicum* deltaH: functional analysis and comparative genomics, *J Bacteriol* **179**(22), 7135-7155
31. Bult, C. J., White, O., Olsen, G. J., Zhou, L., Fleischmann, R. D., Sutton, G. G., Blake, J. A., FitzGerald, L. M., Clayton, R. A., Gocayne, J. D., Kerlavage, A. R., Dougherty, B. A., Tomb, J. F., Adams, M. D., Reich, C. I., Overbeek, R., Kirkness, E. F., Weinstock, K. G., Merrick, J. M., Glodek, A., Scott, J. L., Geoghagen, N. S., and Venter, J. C. (1996) Complete genome sequence of the methanogenic archaeon, *Methanococcus jannaschii*, *Science* **273**(5278), 1058-1073
32. Das, A., Coulter, E. D., Kurtz, D. M., Jr., and Ljungdahl, L. G. (2001) Five-gene cluster in *Clostridium thermoaceticum* consisting of two divergent operons encoding rubredoxin oxidoreductase- rubredoxin and rubrerythrin-type A flavoprotein-high-molecular-weight rubredoxin, *J Bacteriol* **183**(5), 1560-1567

5

Redox and Spectroscopic Properties of the *Escherichia coli* Nitric Oxide Detoxifying System Involving Flavorubredoxin and its NADH Oxidizing Redox Partner ‡

5.1	Introduction	111
5.2	Materials and Methods	114
5.3	Results and Discussion	115
5.4	Conclusions	128
5.5	References	130

SUMMARY

Under anaerobic conditions, the flavodiiron NO-reductase from *Escherichia coli* (flavorubredoxin, FIRd) constitutes one of the major protective enzymes against nitric oxide. The redox and spectroscopic properties of the rubredoxin (Rd), non-haem diiron and FMN sites of flavorubredoxin were determined, which was complemented by the study of truncated versions of FIRd: one consisting only of its rubredoxin module, and another consisting of its flavodiiron structural core (lacking the Rd domain). The studies here reported were performed by a combination of potentiometry with visible and EPR spectroscopies. Moreover, we present the first direct EPR evidence for the presence of the non-haem diiron site in the flavodiiron proteins family. Also, the redox properties of the FIRd physiological partner, the NADH:flavorubredoxin oxidoreductase (FIRd-Red), were determined. It is further shown that the redox properties of this complex electron transfer system are finely tuned upon interaction of the two enzymes.

‡This Chapter was published in the following article:

Vicente, J.B. and Teixeira, M. (2005) "Redox and Spectroscopic Properties of the *Escherichia coli* Nitric Oxide-detoxifying System Involving Flavorubredoxin and its NADH-oxidizing Redox Partner", *Journal of Biological Chemistry* 280 (41): 34599-34608

5.1 INTRODUCTION

The relevance of nitric oxide (NO) biology grows alongside its complexity. The physiological aspects of NO lie within a balance between beneficial and deleterious, both in the eukaryotic and prokaryotic worlds. The production and release of NO by macrophages' inducible NO synthases (iNOS) constitutes one of the major defence mechanisms from eukaryotic immune systems against pathogen invasion and infection. However, pathogenic organisms have developed subversive mechanisms to counteract the hosts' immune systems. The discovery of an anaerobic nitric oxide detoxification system in *Escherichia (E.) coli* (1,2) appears to complement the role of flavohemoglobin (HMP) as an NO scavenger both in aerobic (3,4) and anaerobic conditions (5). This anaerobic NO detoxification system is constituted by flavorubredoxin (FIRd) (2,6), a terminal complex modular protein of the Flavodiiron Protein (FDP) family (7,8), and its reductase partner (FIRd-Red), an NADH oxidase flavoprotein of the rubredoxin reductase family. The widespread family of flavodiiron proteins shares a common structural core, built by an N-terminal β -lactamase module harbouring a non-haem diiron site, fused to a FMN-binding flavodoxin module (9,10).

The first evidence for the presence of the diiron site arose from the determination of the crystallographic structure of the FDP from *Desulfovibrio gigas*, named rubredoxin:oxygen oxidoreductase (ROO) (9). The centre is coordinated by three histidines, two aspartates and one glutamate, in a H⁷⁹-X-E⁸¹-X-D⁸³-X₆₁-H¹⁴⁶-X₁₈-D¹⁶⁵-X₆₀-H²²⁶ motif, which is common to almost all FDPs, with some variability in the spacing between the ligands (8). The irons are bridged by the carboxylate group from Asp¹⁶⁵ and by a μ -oxo (or μ -hydroxo) species. The distinctive feature of this novel type of diiron centre resides in the structural fold where the ferric ions are embedded. Recently, the crystallographic structure of *Moorella thermoacetica* FDP revealed an almost identical coordination sphere, with the exception that the

highly conserved His⁸⁶ (His⁸⁴ in ROO) is a ligand to the diiron centre, whereas in the structure of ROO a water molecule is a ligand in this position (10). This structural difference cannot be immediately assigned with any mechanistic relevance since NO binding (revealed in the same work) appears to occur in the *trans* position to these ligands (10). The first coordination sphere of the diiron site in the FDPs family places this metal centre in the family of the carboxylate/histidine diiron centres, found in several proteins, like ribonucleotide reductases (RNR), methane monooxygenase hydroxylase (MMOH), hemerythrin, (bacterio)ferritins, and rubrerythrin, (reviewed in (11)), which have in common the activation of oxygen at the diiron centre, coupled to various other reactions (12). Since the two iron atoms are antiferromagnetically coupled, these centres are EPR silent in their fully oxidized Fe^{III}-Fe^{III} state, but have distinctive features at $g < 2$ in their mixed-valence Fe^{III}-Fe^{II} state and a low intensity signal at $g \sim 11-15$, in parallel mode EPR, in the fully reduced Fe^{II}-Fe^{II} state (11,13). EPR is thus a powerful and useful tool to identify and characterize this type of metal centres.

The complexity observed in the modular arrangements of flavodiiron proteins, concerning the presence of extra C-terminal modules, led to their division in subclasses (8). As all the FDPs found in the genomes of enterobacteria (Class B FDPs), *E. coli* flavorubredoxin bears an extra C-terminal rubredoxin module, which is the entry point to accept electrons from the reduced flavorubredoxin reductase (6), for the subsequent intra-molecular electron transfer steps. This constitutes a specially interesting feature, since in *Desulfovibrio gigas*, rubredoxin is the redox partner for ROO, this organism's FDP (14). Rubredoxins are small redox proteins generally ranging from 45 to 54 aminoacid residues in length, bearing as the sole cofactor one iron atom tetrahedrally coordinated to the sulphur atoms of 4 cysteinyl residues in two separate C-X₍₁₋₄₎-C-G segments (15). Rubredoxins are found mostly in archaea and bacteria, mainly anaerobes, although recently eukaryotic rubredoxins have been found in *Guillardia theta* (16) and in the genome

of the rodent malaria vector *Plasmodium yoelii* (17). Available biochemical and genetic data suggest the involvement of rubredoxins as redox components of electron transfer chains in processes such as alkane hydroxylation in *Pseudomonads* (18-20), detoxification of reactive oxygen species in *Desulfovibrio* species (14,21,22), *Archaeoglobus fulgidus* (23) and *Moorella thermoacetica* (24), iron metabolism in *Desulfovibrio* sp. (25) and also in photosynthetic related processes (16). The redox properties of rubredoxins from several sources have been the subject of many studies, including site directed mutagenesis on specific residues thought to be relevant for the modulation of the reduction potential of the [Fe-Cys₄] centre, namely specific conserved residues close to the ligating cysteine residues (26,27). As in FIRd, rubredoxin motifs are also found as structural modules in other proteins, as is the case of rubrerythrin (28) and *Moorella thermoacetica* high molecular weight rubredoxin (29). In most physiological processes where rubredoxins are proposed to act as electron transfer mediators, their reduction is accomplished by NAD(P)H-dependent FAD-binding flavoproteins, therefore named NAD(P)H:rubredoxin oxidoreductases. These are generally 40-45 kDa monomers, with specific sequence fingerprints, both for FAD and NAD(P) binding (30,31). Studies have been reported on rubredoxin reductases (RdRed) from *Pseudomonads* (19,31), *Clostridia* (32) and from *Pyrococcus furiosus* (33,34). The *Pseudomonas oleovorans* electron transfer chain involving a RdRed, a Rd and a terminal alkane hydroxylase has been thoroughly characterized in terms of the RdRed/Rd redox pair electron transfer kinetics (19), thus providing a comparison model towards the system studied in this work. Here we present the biochemical characterisation of the truncated rubredoxin module from flavorubredoxin and a complete redox characterisation of the flavorubredoxin-flavorubredoxin reductase system as essential steps for a further kinetical characterization. We also present the first direct EPR evidence for the non-haem diiron centre for the Flavodiiron Protein family.

5.2 MATERIALS AND METHODS

Protein expression and Purification – *Escherichia coli* flavorubredoxin (FIRd), flavorubredoxin reductase (FIRd-Red) and the truncated forms of FIRd, consisting of the rubredoxin domain (Rd-D) and of the flavodiiron domain (FDP-D), were over-expressed in *Escherichia coli* and purified as previously described (2,6), except for the following modifications: all buffers in the purification of FIRd contained 500 μ M of phenylmethanesulfonylfluoride and 18% of glycerol, and the same amount of glycerol was added to all buffers in the FIRd-Red and FDP-D purifications.

Cofactor analysis – the flavin cofactors from FIRd, FDP-D and FIRd-Red were analysed and quantified after acid extraction with trichloroacetic acid (35). The iron content was determined by the 2,4,6-tripyridyl-1,3,5-triazine method (36).

Spectroscopic methods – All UV-visible spectra were recorded in Shimadzu (UV-1603 or Multispec-1501 diode array) spectrophotometers. When required, the spectrophotometers were connected to temperature baths and cell-stirring systems. EPR spectra were collected on a Bruker ESP 380 spectrometer equipped with an ESR 900 continuous-flow helium cryostat from Oxford Instruments.

Redox titrations – Redox titrations followed by UV-visible spectroscopy were performed as in (6), using the same set of redox mediators, and at the same concentration. For the redox titrations of FIRd and FDP-D followed by EPR spectroscopy, the same mediators were used, although at a concentration of approximately 80 μ M. A Pt and Ag/AgCl electrodes were used, calibrated at 25°C with a saturated quinhydrone solution at pH 7.0. All potentials are quoted against the standard hydrogen electrode. The titrations were carried out at 25°C in 50 mM Tris-HCl, 18% glycerol, pH 7.5. Experimental data analysis was performed using MATLAB (Mathworks, South Natick, MA) for Windows. For the Rd-domain titration analysis a single one electron Nernst curve was used to fit the

experimental data. Two consecutive one-electron steps were considered for the $\text{FAD}_{\text{ox}} \leftrightarrow \text{FAD}_{\text{sq}} \leftrightarrow \text{FAD}_{\text{red}}$ transitions in the FIRd-Red titration analysis, corresponding to the three possible redox states of the flavin cofactor. For each of the three redox states the molar extinction coefficients used at 456 nm were: $\epsilon^{\text{FAD}_{\text{oxidized}}}=14,500 \text{ M}^{-1}\cdot\text{cm}^{-1}$, $\epsilon^{\text{FAD}_{\text{red semiquinone}}}= 4,500 \text{ M}^{-1}\cdot\text{cm}^{-1}$, $\epsilon^{\text{FAD}_{\text{blue semiquinone}}}=4,300 \text{ M}^{-1}\cdot\text{cm}^{-1}$ and $\epsilon^{\text{FAD}_{\text{reduced}}}= 2,700 \text{ M}^{-1}\cdot\text{cm}^{-1}$ (37). The same extinction coefficients and analysis strategy were used for the spectral changes of the FMN cofactor in the FIRd titrations. The data obtained by monitoring the non-haem diiron centre EPR-active species (the mixed-valence $\text{Fe}^{\text{III}}\text{-Fe}^{\text{II}}$ centre) was fitted as the intermediate species of two consecutive one-electron step processes.

5.3 RESULTS AND DISCUSSION

The several recombinant intact and truncated proteins were successfully purified. The addition of glycerol enhanced the stability of the flavin moieties, leading to higher FMN and FAD contents of the respective enzymes, namely $\sim 0.7 \text{ mol FMN / mol of FIRd}$ and $\sim 1 \text{ mol FAD / mol FIRd-Red}$. The iron content of the proteins was $\sim 3 \text{ mol Fe / mol FIRd}$, $\sim 2 \text{ mol Fe / mol FDP-D}$ and $\sim 1 \text{ mol Fe / mol Rd-D}$, indicating a complete iron load in each protein.

EPR spectroscopy on the iron centres of flavorubredoxin

To characterise the rubredoxin module (Rd-D) of flavorubredoxin isolated from the other cofactors (the FMN and the non-haem diiron centre), a truncated version of FIRd was obtained, consisting of its C-terminal 79 residues. The EPR spectrum of Rd-D (*not shown*) is identical to the one obtained for the whole protein in its fully oxidised state, with resonances at $g=9.4$, $g=4.8$ and $g=4.3$ (Fig. 2, A, line b), which were previously assigned to two slightly different conformations of the high-spin ($S=5/2$) ferric Rd centre (6). Although the shape and properties of the FIRd EPR spectrum have already been discussed, the fact that it is identical to

the Rd-D one suggests that no significant change in the [Fe-Cys₄] centre structure is produced upon truncating FIRd. Direct EPR evidence for the diiron centre in

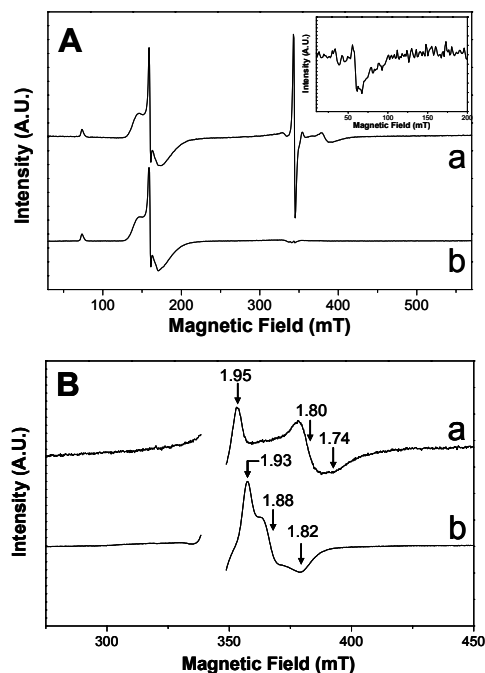


Figure 5.1 - EPR spectra of *E. coli* flavorubredoxin in different redox states. Panel A – EPR spectrum of as isolated FIRd (line b) and at -80 mV (line a), in the course of a redox titration with sodium dithionite. FIRd at 270 μ M was titrated anaerobically at 25°C, in 50 mM Tris-HCl, 18% glycerol, pH 7.5; Inset – Spectrum of reduced 190 μ M FIRd (in 50 mM Tris-HCl, 18% glycerol, pH 7.5, with sodium dithionite) in parallel mode EPR. **Panel B** – EPR spectra of FDP-D, the flavodiiron core of FIRd, obtained in the course of a redox titration (line a) and by mild chemical reduction (line b) with sodium dithionite, focusing on the $g < 2$ region, where mixed-valence non-haem diiron centres are EPR active. Spectra were collected in the same conditions as described for the spectra in Panel A. FDP-D at 250 μ M was titrated anaerobically at 25°C, in 50 mM Tris-HCl, 18% glycerol, pH 7.5. Arrows indicate the g values assigned to each signal. Spectra collected at 7K (lines a and b) and 5K (inset); microwave power: 2.4 mW (lines a and b) and 2.2 mW (inset); microwave frequency: 9.64 GHz; modulation amplitude: 1 mT.

chemical reduction, by anaerobically incubating FDP-D with sub-stoichiometric

flavodiiron proteins was never before obtained, due to the anti-ferromagnetic coupling of the iron nuclei, confirmed by Mössbauer spectroscopy (29). In their fully oxidised and fully reduced states, these centres have integer spins, and are thus EPR silent in perpendicular field. However, the fully reduced species can be identified by a low intensity signal at $g \sim 11-15$ in parallel field EPR, characteristic of an $S=4$ spin ground state (11,13).

It was thus expected that the detection of a mixed-valence $\text{Fe}^{\text{III}}\text{-Fe}^{\text{II}}$ species could

provide direct EPR evidence for the presence of the diiron centre in FIRd.

This was investigated both in the intact FIRd and in a truncated form of FIRd, consisting of the flavodiiron structural core (FDP-D), i.e., structurally similar to ROO and all Class A FDPs. The first EPR evidence was obtained through mild

amounts of sodium dithionite, in the absence of redox mediators. Anaerobic conditions were maintained by continuous argon flushing on surface and by the oxygen-scavenging glucose oxidase / catalase system. A rhombic signal was observed with g values at 1.93, 1.88 and 1.82, very similar in shape and g values (Table 5.1) to those observed for S=1/2 mixed-valence non-haem diiron centres from the hydroxylase component of methane monooxygenase (MMOH). By varying

Table 5.1 – Spectroscopic and redox parameters of non-haem diiron centres.

m.v. – mixed-valence state ([Fe(II)/Fe(III)])

Protein	Organism	EPR spectra	Redox Potentials	Observations	Ref.s
FIRd	<i>Escherichia coli</i>	m.v.: g = 1.95, 1.80 and 1.74 red.: g = 11.3	-20 mV; -90 mV +20 mV; -50 mV (w/ FIRd-Red)	Observed only in the course of redox titration with sodium dithionite, in the presence of redox mediators	This work
FDP-D	<i>Escherichia coli</i>	m.v.: g = 1.92, 1.88 and 1.82 red.: g = 11.3	0 mV; -50 mV	Obtained by mild chemical reduction with sodium dithionite	This work
AOX	<i>Arabidopsis thaliana</i>	m.v.: g = 1.86, 1.67 and 1.53 red.: g = 15		Obtained with 2mM dithionite, 1mM PMS, and reoxidation by O ₂	(41)
MMOH	<i>Methylococcus capsulatus</i> (Bath)	m.v.: g = 1.95, 1.88 and 1.78 red.: g = 15	+48 mV; -135 mV	Obtained with dithionite at room temperature, signal appears after 2 minutes Components B and C decrease the potential of +48 mV to -200 mV; with propylene, the potentials shift to over +150 mV	(42,43)
MMOH	<i>Methylosinus trichosporium</i>	m.v.: g = 1.94, 1.86 and 1.75 red.: g = 15	+76 mV; +21 mV -52 mV; -115 mV (w/MMOB)	Partially reduced by anaerobic addition of dithionite +MMOR and the other components, the potentials are slightly upshifted	(44,45) (46)

the temperature (*not shown*), it was observed that the signal displays its maximal intensity at ~7 K, and that it virtually disappears above 25 K, due to the increasing population of the higher energy spin states and line broadening. Anaerobic redox titrations followed by EPR were carried out, both with intact FIRd and the FDP-D, in order to study the diiron centre reduction potentials and their modulation by the other cofactors and/or the presence of the redox partner (FIRd-Red). Regarding the FDP-D titration, an immediate observation was the different shape and g values of the diiron centre spectrum (Figure 5.1, B), with respect to the one obtained by mild chemical reduction. In this condition, the g values are 1.95, 1.80

and 1.74. This difference in the relaxation properties may be the result of the presence of redox mediators in the redox titrations. Heterogeneity in the shape of diiron centres' spectra has often been observed (38), either for a single protein or among orthologues, arising essentially from differences in the way the mixed-valence species was obtained. Nevertheless, the temperature dependence of the signal from the samples of the FDP-D redox titration displayed identical features as the one described above (*not shown*), which indicates that the intrinsic relaxation properties of the diiron centre remains unaltered in the presence of redox mediators.

The mixed-valence diiron centre from intact flavorubredoxin was detected only by performing the above mentioned redox titration but not by mild chemical reduction. In figure 5.1 (Panel A, line b) are presented the EPR signals for the metal centres of partially reduced FIRd. Whereas the signal from the rubredoxin module still corresponds to its fully oxidised state, an extra signal is displayed with g values < 2 corresponding to the mixed-valence diiron centre spectrum. The g values and shape for the latter signal are identical to the signal of the truncated flavodiiron domain, FDP-D.

Further EPR evidence for the non-haem diiron centre arises from the low intensity signal observed by parallel mode EPR in the fully reduced di-ferrous ($\text{Fe}^{\text{II}}\text{-Fe}^{\text{II}}$) state, at $g \sim 11.3$. (Figure 5.1, A, Inset). Under the same conditions, resonances for the reduced (S=2) rubredoxin site were not observed.

Redox properties of FIRd-Red (NADH:flavorubredoxin oxidoreductase)

The characterisation of the redox parameters of the system here described was performed both with the isolated components and with stoichiometric mixtures of the latter. Anaerobic redox titrations of FIRd-Red (NADH:flavorubredoxin oxidoreductase) were performed using a chemical reductant, sodium dithionite, or the physiological electron donor for this enzyme, NADH. Reduction of the

protein resulted in a bleaching of its spectroscopic features, namely the two flavin bands with maxima at 380 nm and 454 nm (Figure 5.2). Both with dithionite and NADH as reductants, the experimental data, representing absorbance at 454 nm versus reduction potential, were fitted with a Nernst curve

for two consecutive one-electron steps (Figure 5.2, inset). With dithionite as reductant, the fitted potentials were -255 ± 15 mV for FAD_{ox}/FAD_{sq} and -285 ± 15 mV for FAD_{sq}/FAD_{red} (E_m -270 ± 15 mV), whereas for the NADH titration, the reduction potentials were -220 ± 15 mV for FAD_{ox}/FAD_{sq} and -260 ± 15 mV for FAD_{sq}/FAD_{red} (E_m -240 ± 15 mV). In both cases, the

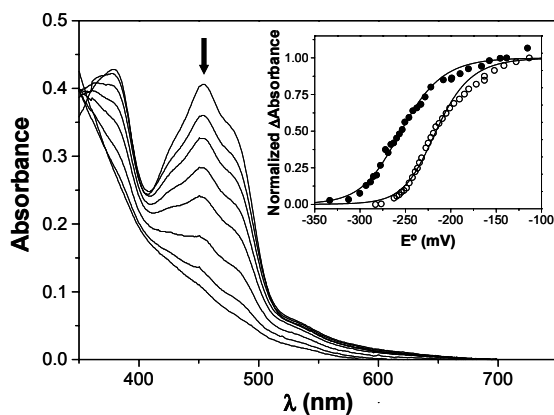


Figure 5.2 – Redox properties of *Escherichia coli* NADH:flavorubredoxin oxidoreductase (FIRd-Red). FIRd-Red (30 μ M, in 50 mM Tris-HCl, 18% glycerol, pH 7.5) reduced either with sodium dithionite or the physiological electron donor NADH, at 25°C. Arrow depicts the absorbance decrease at 455 nm used for the analysis of the redox process. **Inset** – Absorbance at 455 nm measured for the titrations with sodium dithionite (full circles ●) and NADH (hollow circles ○) as reductants. Data were fitted with Nernst curves with -255 mV and -285 mV (●) and -220 mV and -260 mV (○).

potentials for the two consecutive one-electron steps are so close, that no intermediary semiquinone species was significantly stabilized and detected. The determined E_m values are close to the one observed for *P. oleovorans* NADH:rubredoxin oxidoreductase (31). The fact that the E_m value with NADH is approximately 30 mV upshifted with respect to the potential measured with dithionite suggests that NAD binding may slightly modulate the reduction potential of the FAD cofactor. As above described, FIRd-Red appears to have specific sequence motifs for NAD-binding, and this specificity may contribute to an increase of the driving force for electron transfer from the physiological reductant. The values here reported are quite different from the ones previously

obtained for FIRd-Red (6), purified in the absence of glycerol. As stated above, the addition of glycerol has contributed to the obtainment of FIRd-Red batches fully loaded with FAD and stabilised the flavin moiety throughout the purification procedures. Therefore, we assign this difference of the redox potentials to the higher homogeneity of the protein batches here studied in comparison to the other previously reported.

Redox properties of the rubredoxin domain of flavorubredoxin

As previously discussed, the overlapping spectral features of flavorubredoxin's flavin and rubredoxin cofactors hamper the deconvolution of their isolated redox properties. The redox behaviour of the Fe-Cys₄ centre from the rubredoxin domain of flavorubredoxin was initially studied in the intact protein, by performing redox titrations, followed both by visible and EPR spectroscopies (6). The unusually low reduction potential of -140 mV was assigned to a series of amino-acid substitutions in key residues which appear to modulate the reduction potentials of rubredoxins. To analyse the extent of these substitutions on the reduction potential of the centre, i.e., apart from the influence of the other redox centres and the whole protein environment, we have constructed a truncated form of FIRd consisting of its C-terminal 79 a.a. long rubredoxin module (Rd-D). The spectral features of Rd-D (Figure 5.3, A) are almost identical to those observed for rubredoxins, with maxima at 380 nm and 484 nm, and a broad shoulder around 570 nm. Data from an anaerobic redox titration of the Rd module were best fitted with a Nernst curve for a one-electron process with a reduction potential of -123 ± 15 mV (Figure 5.3, A, Inset). This value confirms the exceptionally low reduction potential for this rubredoxin module, and a minor influence of the FIRd modules on this potential. This observation enforces the proposed effect of point natural substitutions in redox relevant residues, in lowering the potential of the Rd centre from FIRd, with respect to canonical

rubredoxins. Taking into account that the global charge of the Rd centre changes

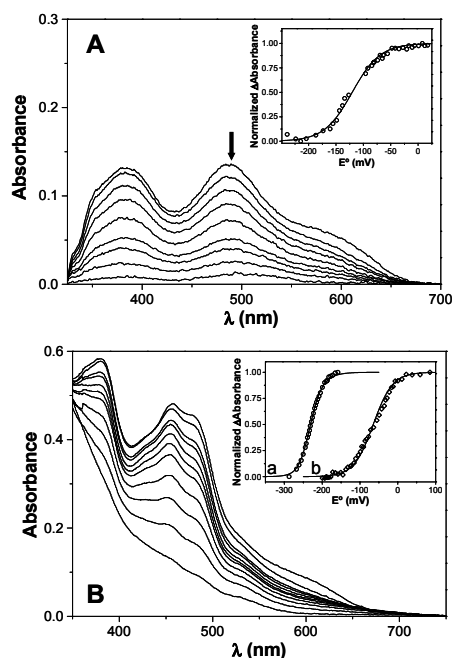


Figure 5.3 - Redox properties of the rubredoxin domain (Rd-D) of *Escherichia coli* flavorubredoxin. Panel A - Optical transitions measured upon reduction of 20 μM Rd-D with sodium dithionite (in 50 mM Tris-HCl, 18% glycerol, pH 7.5). Arrow points the absorbance bleach at 484 nm used for the analysis of the redox process. Inset - Absorbance at 484 nm fitted with a reduction potential of -123 mV. Panel B - Changes in the visible spectra of a stoichiometric mixture of Rd-D and FIRd-Red (in 50 mM Tris-HCl, 18% glycerol, pH 7.5, each protein at 20 μM) upon reduction with NADH, at 25°C. Inset - Normalized absorbance versus measured reduction potential for each redox active species: hollow circles (\circ) for FIRd-Red and hollow diamonds (\diamond) for Rd-D. Lines **a** and **b** were calculated with reduction potentials of -250 mV and -220 mV (a) and -65 mV (b).

from -1 to -2 upon reduction, a decrease in the potential of the truncated domain would be expected if the centre was buried and hidden from the solvent in the intact FIRd. The fact that this reduction potential is almost identical both in the truncated and native proteins suggests that the level of solvent exposure must be similar in the intact and in the truncated Rd modules.

Since we demonstrated previously that the electron entry point of FIRd is its Rd module (6), we went on to check whether the presence of the redox partner FIRd-Red changed the redox properties of the Rd domain, suggesting the formation of an electron transfer complex. For that purpose we titrated anaerobically a 1:1 mixture of FIRd-Red and Rd-D (Figure 5.3, B), using NADH as reductant and, since both FIRd and Rd-D do not accept electrons directly from NADH, their

reduction is exclusively accomplished by reduced FIRd-Red. Although the spectral features of FIRd-Red (containing FAD) and Rd-D are again overlapping, the large separation of their reduction potentials allowed the deconvolution of each redox curve, as observed in the Inset in Figure 5.3, Panel B. To assess the

formation of the eT complex, we ran the two proteins (separately and in a 1:1 mixture) through an analytical gel filtration column (not shown). Despite of the poor resolution inherent to this method, we were able to observe an increase in the high molecular weight area, concomitant with a decrease in the isolated protein bands. Although this does not account for 100% eT complex formation, these results are biased by the fact that the proteins were run through the column in their fully oxidised states, whereas in the redox titrations NADH is present (the eT complex is expected to occur between NADH-reduced FIRd-Red and oxidized FIRd). The data for FIRd-Red were fitted with a Nernst plot for two consecutive one-electron processes, as described for the isolated FIRd-Red titrations. However, although the fitted mean potential is almost identical to the isolated protein (-238 ± 15 mV against -240 ± 15 mV), the potentials appear to be inverted for each transition, i.e., the best fit is obtained with a potential for the first transition lower ($\text{FAD}_{\text{ox}}/\text{FAD}_{\text{sq}}$, -250 ± 15 mV) than that of the second ($\text{FAD}_{\text{sq}}/\text{FAD}_{\text{red}}$, -220 ± 15 mV). This means in fact that the electron transfer process from NADH to FIRd-Red occurs most probably as a two electron process, and that this effect is enhanced by the presence of the redox partner, Rd-D in this case. We thus checked for the best fit with two identical reduction potentials (-245 mV), although the fitted curve was not as adequate as the one described above (data not shown). More striking was the redox upshift from -123 ± 15 mV to -65 ± 15 mV observed for the Rd-D, when titrated in the 1:1 mixture with FIRd-Red. Many redox partners form more or less stable complexes, in which the reduction potentials of the cofactors are changed solely by the presence of one another (39,40).

Effect of the NADH:flavorubredoxin oxidoreductase on the redox properties of its redox partner flavorubredoxin

With the previous observations in mind, we pursued to complete the redox

characterisation with the intact flavorubredoxin. FIRd was titrated anaerobically (Figure 5.4, A) as previously (6) with the exception that 18% of glycerol were present in the work here described. With the complete knowledge of the visible features of the Rd centre, we were able to deconvolute the data for the Fe-Cys4 centre in the Rd domain, which were fitted with a Nernst plot for a one-electron transition (Figure 5.4, A, Inset), with a reduction potential of -123 ± 15 mV. Since this value is identical to the one measured for the truncated Rd-domain, it was possible to subtract the spectra of the Rd-D titration to the ones of the intact FIRd titration, where the corresponding experimental redox values matched. In this manner, it became possible to obtain a matrix comprising solely the spectral features of the flavodiiron core of FIRd (Figure 5.4, B), clearly dominated by the FMN moiety. The three lines clearly show the formation of the red semiquinone upon one-electron reduction of the FMN, characterized by the drop in the absorbance at ~ 450 nm accompanied by an increase at ~ 390 nm, and its disappearance resulting from full reduction to hydroquinone, i.e., the two-electron reduced flavin. This observation is confirmed by the bell-shaped curve of the data corresponding to the absorbance at 390 nm as a function of the redox potential. Whereas the semiquinone radical had already been observed in the previous report (6), the fitted potentials (Figure 5.4, B, Inset), are markedly different from the ones then observed (-40 ± 15 mV against -140 mV for the $\text{FMN}_{\text{ox}}/\text{FMN}_{\text{sq}}$ step and -130 ± 15 mV against -180 mV for the $\text{FMN}_{\text{sq}}/\text{FMN}_{\text{red}}$ step, in this work and the previous (6), respectively). This may result from several factors, such as the inclusion of 18% glycerol in the buffers (which may contribute to the stabilization of the semiquinone radical), or a higher iron incorporation in the present work with respect to previous protein batches. These values are closer to the reduction potentials measured for *D. gigas* ROO, and altogether approximately 80 mV higher than those for *M. thermoacetica* FDP (29).

To complete the characterisation of FIRd's redox properties, we titrated the non-haem diiron centre, following by EPR spectroscopy the rhombic signal at $g < 2$ characteristic of the mixed-valence $\text{Fe}^{\text{III}}\text{-Fe}^{\text{II}}$ centres (Figure 5.1, B). The measured data yield bell-shaped curves, corresponding to the appearance (one electron reduction of fully oxidized $\text{Fe}^{\text{III}}\text{-Fe}^{\text{III}}$ to $\text{Fe}^{\text{III}}\text{-Fe}^{\text{II}}$) of the $g < 2$ EPR signal and its subsequent disappearance (one electron reduction of $\text{Fe}^{\text{III}}\text{-Fe}^{\text{II}}$ to the fully reduced $\text{Fe}^{\text{II}}\text{-Fe}^{\text{II}}$). The fitted potentials for FIRd (-20 ± 20 mV for the $\text{Fe}^{\text{III}}\text{-Fe}^{\text{III}}/\text{Fe}^{\text{III}}\text{-Fe}^{\text{II}}$ step and -90 ± 20 mV for the $\text{Fe}^{\text{III}}\text{-Fe}^{\text{II}}/\text{Fe}^{\text{II}}\text{-Fe}^{\text{II}}$ step, Figure 5.5, C, solid circles) are slightly lower than the ones observed for FDP-D (0 ± 20 mV and -50 ± 20 mV, *not shown*), the truncated form of FIRd consisting of its flavodiiron core (i.e., lacking the rubredoxin domain). This observation reflects the fact that the rubredoxin module influences the redox properties of the diiron centre, possibly due to several factors, such as blockage of solvent accessibility, electrostatic interactions, conformational changes, or a combination of these

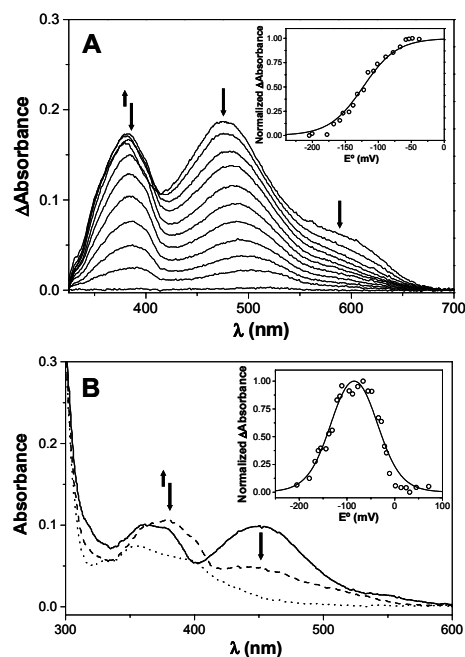


Figure 5.4 - Redox properties of *Escherichia coli* flavorubredoxin. **Panel A** - Optical transitions measured upon reduction of 20 μM FIRd (in 50 mM Tris-HCl, 18% glycerol, pH 7.5) with sodium dithionite, at 25°C. Arrows point the absorbance changes at different wavelengths used for the analysis of the redox process. In the region close to 390 nm, absorbance increases upon formation of the one-electron reduced flavin semiquinone and finally decreases with full reduction to the hydroquinone form. Inset - Deconvoluted data for the rubredoxin module normalized and fitted with a reduction potential of -123 mV. **Panel B** - Representative changes in the visible spectra of the flavodiiron core obtained by subtracting the rubredoxin contribution from the whole flavorubredoxin titration. Solid line - Oxidized FMN moiety (+45 mV); Dashed line - partially reduced FMN moiety (-77 mV); Dotted line - Reduced FMN moiety (-179 mV). Arrows depict the absorbance changes used to monitor the redox changes. Inset - Normalized absorbance at 390 nm minus 458 nm as a function of the reduction potential, fitted with reduction potentials of -40 mV and -130 mV.

factors.

Having established the redox properties of all cofactors in FIRd, we tested the effect of the FIRd-Red on the latter, by titrating both proteins combined in

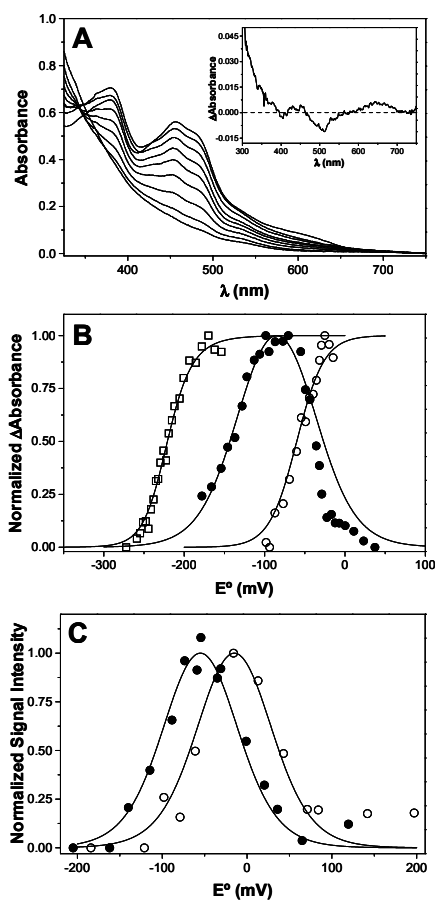


Figure 5.5 - Modulation of the redox properties of *Escherichia coli* flavorubredoxin by its partner NADH:flavorubredoxin oxidoreductase. **Panel A** - Changes in the visible spectra of a stoichiometric mixture of FIRd and FIRd-Red (in 50 mM Tris-HCl, 18% glycerol, pH 7.5, each protein at 20 μ M) upon titration with NADH, at 25°C. Inset - Spectrum of the stoichiometric mixture of FIRd and FIRd-Red minus the sum of their isolated spectra. **Panel B** - Normalized absorbance vs. reduction potential data for the FAD moiety from FIRd-Red (hollow squares \square) and the Rd (hollow circles \circ) and FMN (solid circles \bullet) centres of FIRd. Fitted curves corresponding to Nernst plots with -250 and -220 mV (fit for hollow squares \square), -40 mV and -130 mV (fit for solid circles \bullet) and -65 mV (fit for hollow circles \circ). **Panel C** - Normalized EPR signal intensities (averaged from g_{max} and g_{med}) corresponding to the appearance of the mixed-valence non-heme diiron centre in FIRd upon one-electron reduction and its disappearance upon full reduction to the diferrous state. Solid circles (\bullet): isolated FIRd; hollow circles (\circ): FIRd stoichiometrically mixed with FIRd-Red. Data fitted with -20 mV and -90 mV (solid circles \bullet) and +20 mV and -50 mV (hollow circles \circ).

stoichiometric amounts, and following the redox active species both by visible and EPR spectroscopy. In the titration followed by visible spectroscopy, the data comprise absorption features from three almost overlapping redox centres: the FAD from FIRd-Red, the FMN from the flavodoxin module and the [Fe-Cys₄] centre from the Rd module (Figure 5.5, A). In this titration the spectrum of the oxidized mixture of the two components is slightly different from the sum of their isolated spectra (Figure 5.5, A, Inset). Interestingly, this slight spectral change has been observed for the mixture of rubredoxin reductase and rubredoxin from

Pseudomonas oleovorans, and Lee *et al* (19) propose that this could result from minor structural perturbations of the combined partner proteins. As in the titration of FIRd-Red with the Rd domain, deconvolution of the FIRd-Red data was immediate (Figure 5.5, B, hollow squares) as its reduction potential is significantly lower than those of the FIRd centres. In fact, the reduction potentials used to fit the data with two consecutive one-electron Nernst curves were identical to the ones for the titration of FIRd-Red with Rd-D (FAD_{ox}/FAD_{sq} : -250 ± 15 mV and FAD_{sq}/FAD_{red} : -220 ± 15 mV). Using the reduction potential for FIRd-Red and the spectra of its oxidized and reduced forms (Figure 5.2), it was possible to create a matrix of the FIRd-Red spectra as part of the titration of the mixture. For this purpose, a fraction of oxidized and reduced FIRd-Red was assigned to each experimental potential of the mixture titration, and concomitantly a spectrum with the contribution of FIRd-Red to the overall spectrum. After subtraction of the FIRd-Red matrix to the one corresponding to the mixture titration, we obtained a matrix consisting solely of the FIRd spectra in the course of the titration. In the same manner as in the FIRd titration, we were able to isolate the data for the Rd domain and to fit it with a one-electron Nernst curve with a reduction potential of -65 ± 15 mV (Figure 5.5, B, hollow circles), identical to the reduction potential of the Rd-D measured in the presence of FIRd-Red. With identical reduction potentials for the Rd-D, both in the intact and truncated FIRd (in the presence of the partner FIRd-Red) we proceeded to isolate the reduction potentials of the FMN in the FIRd-Red / FIRd titration by subtracting a matrix with the exclusive contribution of the Rd-D to the one containing the FIRd data (the latter already obtained after subtraction of the FIRd-Red contribution, as described above). To obtain the isolated Rd-D matrix, we took the data from Panel B in Figure 5.3, and subtracted the FIRd-Red contribution, as described above for the FIRd-Red / FIRd titration. By subtracting the Rd-D matrix to the FIRd matrix (both obtained after subtracting the FIRd-Red component out of their

mixed titrations), we obtained a matrix comprising solely the flavodiiron core spectral features dominated by the FMN moiety, identical to the one observed in Panel B from Figure 5.4, for the isolated FIRd titration. Interestingly, in both titrations of FIRd (isolated and in the presence of FIRd-Red), the fitted potentials for the one-electron reduced semiquinone and fully reduced flavin hydroquinone (Figure 5.5, B, full circles) were identical. This result contrasts with the observation that the reduction potential of Rd-D changes substantially in the presence of FIRd-Red, which led us to finally study the influence of the presence of FIRd-Red on the reduction potentials of the non-haem diiron site of FIRd, by repeating the (1:1) FIRd/FIRd-Red titration followed by EPR spectroscopy. The determined values (Table 5.1) are upshifted with respect to the isolated FIRd, namely +40 mV for each transition.

Mechanistical implications of the redox shifts observed upon formation of the electrostatic complex between flavorubredoxin and its reductase partner

One of the most striking observations here reported concerns the shifts in the reduction potentials of the iron centres - but not of the FMN moiety - of flavorubredoxin, arisen from the presence of the redox partner flavorubredoxin reductase. The molecular nature of these modifications in the thermodynamic properties of the redox cofactors remains to be determined, although distinct effects can be envisaged in terms of the intra-molecular electron transfer mechanism within flavorubredoxin's centres (Figure 5.6). Being rubredoxin the entry point for electrons coming from reduced FIRd-Red, the observed upshift in its reduction potential (from -123 mV to -65 mV) makes it much less favourable to reduce the flavin semiquinone to the fully reduced hydroquinone. On the other hand, since also the two transitions of the diiron centre are upshifted approximately 40 mV each, the reduction potential of the flavin semiquinone suffices to provide electrons to the diiron centre, where NO reduction occurs.

Altogether, these modifications point to a possible intra-molecular electron transfer mechanism in which the two-electron reduction of the diiron centre can

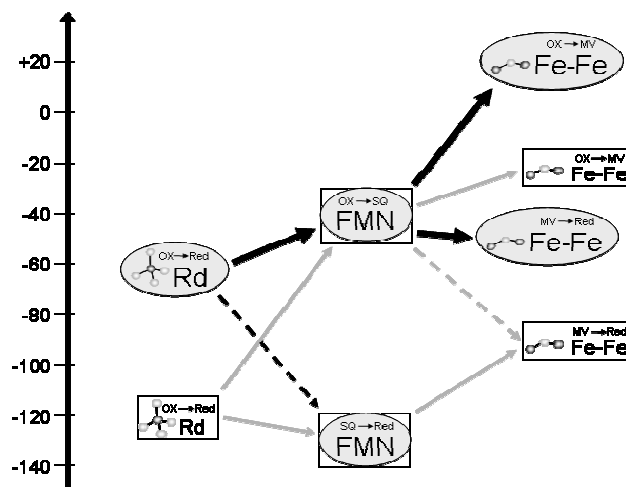


Figure 5.6 - Electron transfer mechanistic insights derived from the redox properties of the interacting partners of *Escherichia coli* NO detoxification system. Reduction potentials of the cofactors in flavorubredoxin represented by Rd-[Fe-Cys₄] rubredoxin, FMN – flavin moiety, and Fe-Fe – diiron site. Centres within grey oval boxes, FIRd stoichiometrically mixed with FIRd-Red; centres within square white boxes: isolated FIRd. Thick black arrows – most likely electron transfer pathways within the cofactors of FIRd, when its redox partner (FIRd-Red) is present. Thin gray arrows – possible electron transfer steps between the redox centres in isolated FIRd. Dashed arrows depict less favourable eT steps.

occur without full reduction of the FMN cofactor, since the semiquinone state can sequentially reduce the oxidized Fe^{III}-Fe^{III} forms of the diiron centre and then the Fe^{III}-Fe^{II} mixed-valence state.

5.4 CONCLUSIONS

The nitric oxide detoxification system from *Escherichia coli*, consisting of flavorubredoxin (FIRd) and its NADH oxidizing partner, was studied in terms of its redox properties, contributing to the proposal of inter- and intra-molecular eT mechanisms, coupling NADH oxidation to NO reduction. Besides studying the intact proteins, we used truncated versions of FIRd, namely one form lacking the C-terminal rubredoxin (Rd) module, and another consisting solely of the Rd

domain. Moreover, we used EPR spectroscopy to monitor the redox properties of the non-haem diiron centre from FIRd, a novelty for the flavodiiron proteins family.

The NADH:flavorubredoxin oxidoreductase (FIRd-Red) is here established as a member of the rubredoxin reductases (RdReds) family. The determined redox properties are consistent with this protein to accept consecutively two electrons from NADH, without the formation of a partially reduced semiquinone species. In the presence of its partner (FIRd), this two-electron eT character is enforced by a possible inversion of its reduction potentials.

More striking are the changes in reduction potentials of the iron centres (but not of the flavin moiety) in flavorubredoxin upon formation of a complex with the partner FIRd-Red. As depicted in Figure 5.6, the reduction potential of the rubredoxin site is upshifted due to the presence of FIRd-Red, still allowing eT to the oxidized FMN but hampering eT to the one-electron reduced FMN semiquinone, as ΔE° then becomes much larger (approximately -60 mV). With the parallel upshift observed in the reduction potentials for the two consecutive transitions of the non-haem diiron centre, the flavin semiquinone then has an effective reduction potential that allows eT to the diiron centre to occur without the need of having the fully reduced flavin hydroquinone to transfer electrons to the mixed-valence diiron site. It is commonly observed that interaction between redox partners often results in the formation of more or less stable electrostatic complexes. Upon formation of these complexes, efficient electron transfer (eT) will benefit from a favourable thermodynamic drive provided by an upward directionality of the reduction potentials of each eT species, from the donor to the acceptor side.

The observations reported in this work indicate that fast and effective electron transfer appears to be ensured through a bypass of the second transition of the flavin (from the semiquinone to the hydroquinone forms), since the semiquinone

species appears to be sufficiently functional to reduce both irons, as judged by the thermodynamic data. This effect seems to be enforced by the upshift observed in the reduction potential of the electron entry point, the rubredoxin module, which creates a barrier for eT from Rd to the flavin semiquinone. The fine tuning which appears to impose electrons to be delivered (via the flavin semiquinone) one at a time onto the non-haem diiron centre, the site of nitric oxide reduction, may be related with the complex chemistry of NO or simply to avoid the plausible formation of even more reactive species. Further studies will aim to understand the nature of the redox modifications imposed on the redox cofactors of FIRd by the presence of FIRd-Red and how this fine tuning of the thermodynamic parameters may affect the NO reduction mechanism.

5.5 REFERENCES

1. Gardner, A. M., Helmick, R. A., and Gardner, P. R. (2002) Flavorubredoxin, an inducible catalyst for nitric oxide reduction and detoxification in *Escherichia coli*, *J Biol Chem* **277**(10), 8172-8177
2. Gomes, C. M., Giuffre, A., Forte, E., Vicente, J. B., Saraiva, L. M., Brunori, M., and Teixeira, M. (2002) A novel type of nitric-oxide reductase. *Escherichia coli* flavorubredoxin, *J Biol Chem* **277**(28), 25273-25276
3. Poole, R. K., and Hughes, M. N. (2000) New functions for the ancient globin family: bacterial responses to nitric oxide and nitrosative stress, *Mol Microbiol* **36**(4), 775-783
4. Frey, A. D., Farres, J., Bollinger, C. J., and Kallio, P. T. (2002) Bacterial hemoglobins and flavohemoglobins for alleviation of nitrosative stress in *Escherichia coli*, *Appl Environ Microbiol* **68**(10), 4835-4840
5. Justino, M. C., Vicente, J. B., Teixeira, M., and Saraiva, L. M. (2005) New genes implicated in the protection of anaerobically grown *Escherichia coli* against nitric oxide, *J Biol Chem* **280**(4), 2636-2643
6. Gomes, C. M., Vicente, J. B., Wasserfallen, A., and Teixeira, M. (2000) Spectroscopic studies and characterization of a novel electron-transfer chain from *Escherichia coli* involving a flavorubredoxin and its flavoprotein reductase partner, *Biochemistry* **39**(51), 16230-16237.
7. Wasserfallen, A., Ragetti, S., Jouanneau, Y., and Leisinger, T. (1998) A family of flavoproteins in the domains Archaea and Bacteria, *Eur J Biochem* **254**(2), 325-332
8. Saraiva, L. M., Vicente, J. B., and Teixeira, M. (2004) The role of the flavodiiron proteins in microbial nitric oxide detoxification, *Adv Microb Physiol* **49**, 77-129

9. Frazao, C., Silva, G., Gomes, C. M., Matias, P., Coelho, R., Sieker, L., Macedo, S., Liu, M. Y., Oliveira, S., Teixeira, M., Xavier, A. V., Rodrigues-Pousada, C., Carrondo, M. A., and Le Gall, J. (2000) Structure of a dioxygen reduction enzyme from *Desulfovibrio gigas*, *Nat Struct Biol* **7**(11), 1041-1045
10. Silaghi-Dumitrescu, R., Kurtz, D. M., Jr., Ljungdahl, L. G., and Lanzilotta, W. N. (2005) X-ray Crystal Structures of *Moorella thermoacetica* FprA. Novel Diiron Site Structure and Mechanistic Insights into a Scavenging Nitric Oxide Reductase(), *Biochemistry* **44**(17), 6492-6501
11. Solomon, E. I., Brunold, T. C., Davis, M. I., Kemsley, J. N., Lee, S. K., Lehnert, N., Neese, F., Skulan, A. J., Yang, Y. S., and Zhou, J. (2000) Geometric and electronic structure/function correlations in non-haem iron enzymes, *Chem Rev* **100**(1), 235-350
12. Kurtz, D. J. (1997) Structural similarity and functional diversity in diiron-oxo proteins, *J Biol Inorg Chem* **2**, 159-167
13. Hendrich, M. P., Munck, E., Fox, B. G., and Lipscomb, J. D. (1990) Integer-Spin Epr Studies of the Fully Reduced Methane Monooxygenase Hydroxylase Component, *J Am Chem Soc* **112**(15), 5861-5865
14. Gomes, C. M., Silva, G., Oliveira, S., LeGall, J., Liu, M. Y., Xavier, A. V., Rodrigues-Pousada, C., and Teixeira, M. (1997) Studies on the redox centers of the terminal oxidase from *Desulfovibrio gigas* and evidence for its interaction with rubredoxin, *J Biol Chem* **272**(36), 22502-22508
15. Meyer, J., and Moulis, J. M. (2001) Rubredoxin. In: Messerschmidt, A., Huber, R., Poulos, T., and Wieghardt, K. (eds). *Handbook of Metallproteins*, 1 Ed., John Wiley & Sons, Chichester
16. Wastl, J., Sticht, H., Maier, U. G., Rosch, P., and Hoffmann, S. (2000) Identification and characterization of a eukaryotically encoded rubredoxin in a cryptomonad alga, *FEBS Lett* **471**(2-3), 191-196
17. Carlton, J. M., Angiuoli, S. V., Suh, B. B., Kooij, T. W., Perlea, M., Silva, J. C., Ermolaeva, M. D., Allen, J. E., Selengut, J. D., Koo, H. L., Peterson, J. D., Pop, M., Kosack, D. S., Shumway, M. F., Bidwell, S. L., Shallom, S. J., van Aken, S. E., Riedmuller, S. B., Feldblyum, T. V., Cho, J. K., Quackenbush, J., Sedegah, M., Shoaibi, A., Cummings, L. M., Florens, L., Yates, J. R., Raine, J. D., Sinden, R. E., Harris, M. A., Cunningham, D. A., Preiser, P. R., Bergman, L. W., Vaidya, A. B., van Lin, L. H., Janse, C. J., Waters, A. P., Smith, H. O., White, O. R., Salzberg, S. L., Venter, J. C., Fraser, C. M., Hoffman, S. L., Gardner, M. J., and Carucci, D. J. (2002) Genome sequence and comparative analysis of the model rodent malaria parasite *Plasmodium yoelii yoelii*, *Nature* **419**(6906), 512-519
18. Lee, N. R., Hwang, M. O., Jung, G. H., Kim, Y. S., and Min, K. H. (1996) Physical structure and expression of alkBA encoding alkane hydroxylase and rubredoxin reductase from *Pseudomonas maltophilia*, *Biochem Biophys Res Commun* **218**(1), 17-21
19. Lee, H. J., Basran, J., and Scrutton, N. S. (1998) Electron transfer from flavin to iron in the *Pseudomonas oleovorans* rubredoxin reductase-rubredoxin electron transfer complex, *Biochemistry* **37**(44), 15513-15522
20. van Beilen, J. B., Neuenschwander, M., Smits, T. H., Roth, C., Balada, S. B., and Witholt, B. (2002) Rubredoxins involved in alkane oxidation, *J Bacteriol* **184**(6), 1722-1732

21. Coulter, E. D., and Kurtz, D. M., Jr. (2001) A role for rubredoxin in oxidative stress protection in *Desulfovibrio vulgaris*: catalytic electron transfer to rubrerythrin and two-iron superoxide reductase, *Arch Biochem Biophys* **394**(1), 76-86
22. Lumpio, H. L., Shenvi, N. V., Summers, A. O., Voordouw, G., and Kurtz, D. M., Jr. (2001) Rubrerythrin and rubredoxin oxidoreductase in *Desulfovibrio vulgaris*: a novel oxidative stress protection system, *J Bacteriol* **183**(1), 101-108
23. Rodrigues, J. V., Abreu, I. A., Saraiva, L. M., and Teixeira, M. (2005) Rubredoxin acts as an electron donor for neelaredoxin in *Archaeoglobus fulgidus*, *Biochem Biophys Res Commun* **329**(4), 1300-1305
24. Das, A., Coulter, E. D., Kurtz, D. M., Jr., and Ljungdahl, L. G. (2001) Five-gene cluster in *Clostridium thermoaceticum* consisting of two divergent operons encoding rubredoxin oxidoreductase- rubredoxin and rubrerythrin-type A flavoprotein-high-molecular-weight rubredoxin, *J Bacteriol* **183**(5), 1560-1567
25. da Costa, P. N., Romao, C. V., LeGall, J., Xavier, A. V., Melo, E., Teixeira, M., and Saraiva, L. M. (2001) The genetic organization of *Desulfovibrio desulphuricans* ATCC 27774 bacterioferritin and rubredoxin-2 genes: involvement of rubredoxin in iron metabolism, *Mol Microbiol* **41**(1), 217-227
26. Eidsness, M. K., Burden, A. E., Richie, K. A., Kurtz, D. M., Jr., Scott, R. A., Smith, E. T., Ichiye, T., Beard, B., Min, T., and Kang, C. (1999) Modulation of the redox potential of the [Fe(SCys)₄] site in rubredoxin by the orientation of a peptide dipole, *Biochemistry* **38**(45), 14803-14809
27. Kummerle, R., Zhuang-Jackson, H., Gaillard, J., and Moulis, J. M. (1997) Site-directed mutagenesis of rubredoxin reveals the molecular basis of its electron transfer properties, *Biochemistry* **36**(50), 15983-15991
28. deMare, F., Kurtz, D. M., Jr., and Nordlund, P. (1996) The structure of *Desulfovibrio vulgaris* rubrerythrin reveals a unique combination of rubredoxin-like FeS₄ and ferritin-like diiron domains, *Nat Struct Biol* **3**(6), 539-546
29. Silaghi-Dumitrescu, R., Coulter, E. D., Das, A., Ljungdahl, L. G., Jameson, G. N., Huynh, B. H., and Kurtz, D. M., Jr. (2003) A flavodiiron protein and high molecular weight rubredoxin from *Moorella thermoacetica* with nitric oxide reductase activity, *Biochemistry* **42**(10), 2806-2815
30. Wierenga, R. K., Terpstra, P., and Hol, W. G. (1986) Prediction of the occurrence of the ADP-binding beta alpha beta-fold in proteins, using an amino acid sequence fingerprint, *J Mol Biol* **187**(1), 101-107.
31. Eggink, G., Engel, H., Vriend, G., Terpstra, P., and Witholt, B. (1990) Rubredoxin reductase of *Pseudomonas oleovorans*. Structural relationship to other flavoprotein oxidoreductases based on one NAD and two FAD fingerprints, *J Mol Biol* **212**(1), 135-142
32. Petitdemange, H., Blusson, H., and Gay, R. (1981) Detection of NAD(P)H--rubredoxin oxidoreductases in Clostridia, *Anal Biochem* **116**(2), 564-570
33. Ma, K., and Adams, M. W. (1999) A hyperactive NAD(P)H:Rubredoxin oxidoreductase from the hyperthermophilic archaeon *Pyrococcus furiosus*, *J Bacteriol* **181**(17), 5530-5533
34. Ma, K., and Adams, M. W. (2001) NAD(P)H:rubredoxin oxidoreductase from *Pyrococcus furiosus*, *Methods Enzymol* **334**, 55-62
35. Susin, S., Abian, J., Sanchez-Baeza, F., Peleato, M. L., Abadia, A., Gelpi, E., and Abadia, J. (1993) Riboflavin 3'- and 5'-sulfate, two novel flavins accumulating in the roots

- of iron-deficient sugar beet (*Beta vulgaris*), *J Biol Chem* **268**(28), 20958-20965.
36. Fischer, D. S. a. P., D.C. (1964) A simple serum iron method using the new sensitive chromogen tripyridyl-triazine, *Clinical Chemistry* **10**, 21-25
 37. Ghisla, S., and Edmondson, D. A. (2001) Flavin Coenzymes. In. *Encyclopedia of Life Sciences*, Nature Publishing Group
 38. Atta, M., Andersson, K. K., Ingemarson, R., Thelander, L., and Graslund, A. (1994) Epr Studies of Mixed-Valent [(Fefiii)-Fe-Ii] Clusters Formed in the R2 Subunit of Ribonucleotide Reductase from Mouse or Herpes-Simplex Virus - Mild Chemical-Reduction of the Diferric Centers, *J Am Chem Soc* **116**(14), 6429-6430
 39. Alric, J., Cuni, A., Maki, H., Nagashima, K. V., Vermeglio, A., and Rappaport, F. (2004) Electrostatic interaction between redox cofactors in photosynthetic reaction centers, *J Biol Chem* **279**(46), 47849-47855
 40. Teixeira, V. H., Baptista, A. M., and Soares, C. M. (2004) Modeling electron transfer thermodynamics in protein complexes: interaction between two cytochromes c(3), *Biophys J* **86**(5), 2773-2785
 41. Berthold, D. A., Voevodskaya, N., Stenmark, P., Graslund, A., and Nordlund, P. (2002) *J Biol Chem* **277**(46), 43608-14
 42. Woodland, M. P., Patil, D. S., Cammack, R., and Dalton, H. (1986) *Biochimica et Biophysica Acta* **873**, 237-242
 43. Liu, K. E., and Lippard, S. J. (1991) *J Biol Chem* **266**(20), 12836-9
 44. Fox, B. G., and Lipscomb, J. D. (1988) *Biochem Biophys Res Commun* **154**(1), 165-70
 45. Fox, B. G., Surerus, K. K., Munck, E., and Lipscomb, J. D. (1988) *J Biol Chem* **263**(22), 10553-6
 46. Paulsen, K. E., Liu, Y., Fox, B. G., Lipscomb, J. D., Munck, E., and Stankovich, M. T. (1994) *Biochemistry* **33**(3), 713-22

6

Kinetics of Electron Transfer from NADH to the *Escherichia coli* Nitric Oxide Reductase Flavorubredoxin ‡

6.1	Introduction	137
6.2	Materials and Methods	139
6.3	Results	141
6.4	Discussion	148
6.5	References	152

SUMMARY

Escherichia coli flavorubredoxin (FIRd) belongs to the family of flavodiiron proteins (FDPs), microbial enzymes that are expressed to scavenge nitric oxide (NO) under anaerobic conditions. To degrade NO, FIRd has to be reduced by NADH via the FAD-binding protein flavorubredoxin reductase, thus the kinetics of electron transfer along this pathway was investigated by stopped-flow absorption spectroscopy.

We found that NADH, but not NADPH, quickly reduces the FIRd-reductase ($k = 5.5 \pm 2.2 \times 10^6 \text{ M}^{-1}\text{s}^{-1}$ at 5°C), with a limiting rate of $255 \pm 17 \text{ s}^{-1}$. The reductase in turn quickly reduces the rubredoxin (Rd) center of FIRd, as assessed at 5 °C working with the native FIRd enzyme ($k = 2.4 \pm 0.1 \times 10^6 \text{ M}^{-1}\text{s}^{-1}$) and with its isolated Rd-domain ($k \sim 1 \times 10^7 \text{ M}^{-1}\text{s}^{-1}$); in both cases the reaction was found to be dependent on pH and ionic strength. In FIRd the fast reduction of the Rd center occurs synchronously with the formation of FMN semiquinone. Our data provide evidence that i) FIRd-reductase rapidly shuttles electrons between NADH and FIRd, a pre-requisite for NO reduction in this detoxification pathway, and ii) the electron accepting site in FIRd, the Rd center, is in very fast redox equilibrium with FMN.

‡ **This Chapter was published in the following article:**

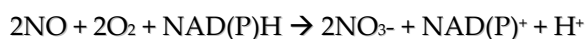
Vicente, J.B., Scandurra, F.M., Rodrigues, J.V., Brunori, M., Sarti, P., Teixeira, M., and Giuffrè, A. (2006) "Kinetics of Electron Transfer from NADH to the *Escherichia coli* Nitric Oxide Reductase Flavorubredoxin", *FEBS Journal*, *in press*

Most of the work described in this chapter, namely the kinetics studies, was performed during visits to the Dipartimento di Scienze Biochimiche "A. Rossi Fanelli" from the Università degli Studi di Roma "La Sapienza", Rome, Italy, to work with Francesca M. Scandurra, Dr. Alessandro Giuffrè, Prof. Paolo Sarti and Prof. Maurizio Brunori.

6.1 INTRODUCTION

In humans and other higher organisms, nitric oxide (NO) is produced by the inducible isoform of NO-synthase (iNOS) in several cell types, including macrophages, as part of the immune response to counteract microbial infection (1, 2). NO production is enhanced at the site of infection (2) leading to the formation of highly reactive species, such as peroxynitrite (ONOO⁻; (3)), all of which are cytotoxic towards the invading microbes.

As a strategy to evade the host immune attack, pathogenic microorganisms have evolved biochemical pathways to resist to such a stress condition (generally termed “nitrosative stress”), and particularly to degrade NO. Many microorganisms express flavohemoglobin (4, 5), an enzyme that efficiently catalyzes the oxidation of NO to nitrate (NO₃⁻) in the presence of O₂, according to the following reaction:



The flavodiiron proteins (FDPs, originally named A-type flavoproteins (6)), are a different class of microbial enzymes that were recently proposed to be involved in NO detoxification, particularly under microaerobic conditions (7). In the absence of O₂, FDPs are indeed endowed with NO-reductase activity (8-10), being capable of degrading NO most probably to nitrous oxide (N₂O):



Flavodiiron proteins are widespread among prokaryotes (6, 11); based on genomic and functional analysis they were more recently identified also in a restricted number of anaerobic, pathogenic protozoa (11-14). As a distinctive feature, FDPs are characterized by two structural domains: the N-terminal one, with a metallo-β-lactamase like fold, harbouring a non-heme diiron site, and the flavodoxin-like domain with a FMN moiety (15). The 3D structure is now available for two FDPs, i.e. the enzyme isolated from *Desulfovibrio gigas* (originally named rubredoxin: oxygen oxidoreductase, (16)) and that one from *Moorella*

thermoacetica (17). In both cases, the two redox centers (FMN and Fe-Fe) are at a relatively long distance ($\sim 35\text{\AA}$), but the enzyme displays a homodimeric assembly in a head-to-tail configuration, bringing the FMN of one monomer in close proximity to the Fe-Fe site of the other monomer. It is therefore likely, though not proven yet, that the dimer is the functional unit of this enzyme, ensuring fast electron equilibration between the redox cofactors.

The FDP expressed by *Escherichia coli* contains in addition a rubredoxin-like domain with an iron-sulfur center, fused at the C-terminus of the flavodiiron core; thus this protein was named flavorubredoxin (FIRd) (6). *E. coli* FIRd is the terminal component of an electron transport chain (see Fig. 6.1) that involves

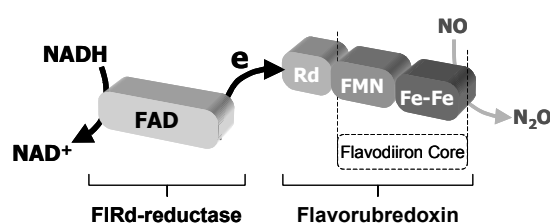


Figure 6.1 - Schematic representation of the *Escherichia coli* electron transfer chain coupling NADH oxidation to NO reduction.

NADH and flavorubredoxin reductase, a FAD-binding protein of the NAD(P)H: rubredoxin oxidoreductase family. The genes coding for FIRd (*norV*) and its redox

partner FIRd-reductase (*norW*) form a single dicistronic transcriptional unit (18).

In *E. coli*, the involvement of FIRd in the anaerobic NO detoxification was originally proposed by Gardner et al. (7) on the basis of molecular genetic evidence and confirmed by measuring the NO consumption catalyzed by the purified recombinant FIRd (8) and by other bacterial FDPs (9, 10). The protective role of FIRd towards nitrosative stress is further supported by the finding that after exposing *E. coli* cells to NO under anaerobic conditions, the transcriptional levels of the *norVW* genes raise considerably and the FIRd protein is promptly expressed (7, 19). It is not clear whether the capability of degrading NO is a common and distinctive feature among all the members of the FDPs family. Every FDP characterized so far seems to be capable of reacting with O₂ as well, though to different extents. Moreover, recently it was reported the case of one FDP,

the ROO from *Desulfovibrio gigas*, which *in vivo* protects from nitrosative stress, but *in vitro* as purified it consumes O₂ possibly more efficiently than NO (20).

Although FDPs might be the targets for novel drugs designed to counteract microbial infection, the information on the mechanism whereby FDPs degrade NO is as yet very poor. Likely, the active site is the Fe-Fe binuclear center, since substitution of Zn for Fe abolishes the activity (9). Consistently, we have previously shown that the Rd-domain of FIRd, a genetically truncated version of the enzyme lacking the flavodiiron domain, is unable to catalyze the anaerobic NO degradation in the presence of excess reductants (8). Also based on the redox potentials determined for FIRd (21), it is likely that electrons donated to FIRd enter the enzyme at the [Fe-Cys₄] center in the Rd-domain to be subsequently transferred *via* FMN to the Fe-Fe site where the reaction with NO is expected to occur; however, essentially no information is available as yet on the kinetics of electron transfer to (as well as within) this enzyme. Since the efficiency of NO detoxification by FIRd (and FDPs in general) clearly depends on the availability of electrons at the site of reaction with NO, this prompted us to use *E. coli* FIRd as a model to study the kinetics of eT along the NADH → FIRd-reductase → FIRd chain (Fig.1), which is herein investigated by time-resolved spectroscopy working on the purified recombinant proteins.

6.2 MATERIALS AND METHODS

Materials – NADH, glucose oxidase and catalase were purchased from Sigma (St. Louis, Mo). The concentration of NADH in stock solutions was determined spectrophotometrically using the extinction coefficient $\epsilon^{340\text{nm}} = 6.2 \text{ mM}^{-1} \text{ cm}^{-1}$. Unless otherwise specified, experiments were performed at 5 °C in 50 mM Tris-HCl, 18 % glycerol, pH 8.0. The low temperature was chosen in order to slow down the reactions otherwise too fast to be time-resolved. Glycerol was used to enhance the stability of purified FIRd and FIRd-reductase in solution, an effect

already documented for *Pseudomonas oleovorans* rubredoxin reductase (RR) and rubredoxin (22, 29). Anaerobic conditions were achieved by N₂-equilibration of the buffers and by scavenging residual contaminant oxygen using glucose oxidase (17 units/ml), glucose (2 mM) and catalase (130 units /ml).

Escherichia coli flavorubredoxin (FIRd), flavorubredoxin reductase (FIRd-reductase) and a truncated version of FIRd consisting of the only rubredoxin domain (Rd-domain) were over-expressed in *E. coli*, purified as previously described (8, 15) and stored at -80 °C until use. The concentration of oxidized FIRd-reductase and Rd-domain was determined spectrophotometrically using the extinction coefficients $\epsilon^{455\text{nm}} = 12 \text{ mM}^{-1}\cdot\text{cm}^{-1}$ and $\epsilon^{484\text{nm}} = 7 \text{ mM}^{-1}\text{cm}^{-1}$, respectively. The protein concentration of FIRd, was determined by the bicinchoninic acid method (30), iron and FMN contents were quantitated as in (31) and (32), respectively. As purified, FIRd contained the expected amount of iron (~3 Fe/monomer), but sub-stoichiometric FMN (0.5 – 0.6 instead of 1 FMN/monomer), pointing to partial loss of flavin during the purification procedure or incomplete incorporation of flavin during expression.

Absorption spectroscopy and data analysis – UV/visible static spectra were recorded by using a Shimadzu spectrophotometer (UV-1603). Stopped-flow experiments were carried out with a thermostated instrument (DX.17MV, Applied Photophysics, Leatherhead, UK) equipped with either a monochromator or a diode-array (light path = 1 cm). When the instrument was used in the multiwavelength mode (diode-array), time-resolved absorption spectra were recorded with an acquisition time of 2.56 ms per spectrum and a wavelength resolution of 2.1 nm. Typically, three independent traces were collected to be averaged before analysis.

Kinetic data were analyzed by nonlinear least-squares regression analysis using the software MATLAB (MathWorks, South Natick, NA). The reaction of FIRd-reductase with NADH, whenever it was not probed under pseudo-first order

conditions, was modeled according to a scheme of the type $A + B \xrightarrow{k} C$. The apparent second order rate constant k was thus obtained by fitting the experimental time courses to the equation:

$$\ln\left(\frac{B_0(A_0 - x)}{A_0(B_0 - x)}\right) = kt(A_0 - B_0) \quad (1)$$

where A_0 and B_0 are the initial concentrations of A and B and x is the amount of A and B reacted at the time t . The time courses of both Rd-domain and FIRd reduction by FIRd-reductase were fitted to single exponential decays. In the case of FIRd, observed rate constants were linearly dependent on the concentration of the FIRd-reductase and the apparent second-order rate constant was thus estimated by linear regression analysis. The observed rate constants for Rd-domain reduction showed a hyperbolic dependence on the concentration of FIRd-reductase. In this case, the apparent second-order rate constant was estimated by kinetic simulations performed using the software FACSIMILE (AEA Technology, United Kingdom).

6.3 RESULTS

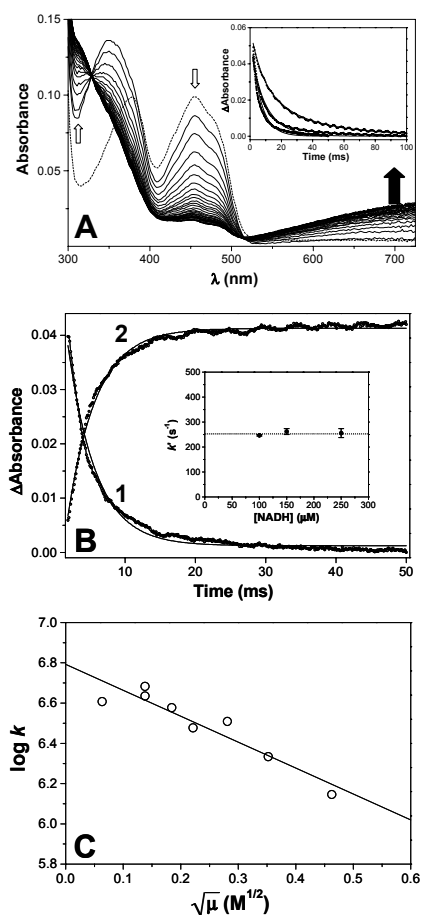
Reduction of flavorubredoxin reductase by NADH.

The kinetics of the reduction of flavorubredoxin reductase (FIRd-reductase) by NADH was investigated by time-resolved spectroscopy under anaerobic conditions and at 5°C. Upon mixing with NADH, oxidized FIRd-reductase is fully reduced within 100 ms, as inferred from the absorption bleaching detected in the 400 – 500 nm range and the absorption increase at ~ 310 nm (Fig. 6.2A). Synchronously, a broad band appears at $\lambda > 520$ nm (see thick arrow in Fig. 6.2A); as previously proposed by Lee et al. (22) for the *Pseudomonas oleovorans* rubredoxin reductase (RR), we assign the latter band to the formation of a charge-transfer complex between NAD⁺ and reduced FIRd-reductase.

Figure 6.2 - Reduction of flavorubredoxin reductase by NADH.

Panel A - Time-resolved absorption spectra collected every 2.56 ms up to 100 ms after mixing oxidized FIRd-reductase with NADH under anaerobic conditions. Concentrations after mixing: [FIRd-reductase] = 7.6 μM ; [NADH] = 16.5 μM . Dotted line: spectrum of fully oxidized FIRd-reductase ($\lambda_{\text{max}} = 455 \text{ nm}$, see arrow). $T = 5^\circ\text{C}$. Buffer: 50 mM Tris-HCl, 18 % glycerol, pH 8.0. Inset: Time courses of the reaction as measured at [NADH] = 10, 30 and 50 μM

(concentrations after mixing), fitted according to equation (1) in Materials and Methods. $\lambda = 455 \text{ nm}$. **Panel B** - Time course of FIRd-reductase reduction probed under pseudo-first order conditions, followed at 455 nm (line 1) and 310 nm (line 2). Concentrations after mixing: [NADH] = 100 μM ; [FIRd-reductase] = 7.6 μM . $T = 5^\circ\text{C}$. Buffer: 50 mM Tris-HCl, 18 % glycerol, pH 8.0. Inset: Observed rate constants measured at three different concentrations of NADH $\geq 100 \mu\text{M}$. **Panel C** - Ionic strength dependence of the second order rate constant of FIRd-reductase reduction by NADH. Data were modeled according to the Bronsted-Bjerrum equation yielding $Z_A Z_B = -1.3$ (see Results and Discussion). $T = 5^\circ\text{C}$. In these experiments FIRd-reductase was desalted by gel filtration and ionic strength adjusted by addition of KCl to the buffer (5 mM Tris-HCl, 18 % glycerol, pH 8.0).



The reduction of FIRd-reductase was followed at 455 and 310 nm (see thin arrows in Fig. 6.2A) at increasing NADH concentrations. At [NADH] $< 100 \mu\text{M}$, pseudo-first order conditions were not attained and the reaction was thus modelled according to the scheme $A+B \rightarrow C$. By fitting the experimental time courses to equation (1) (see Materials and Methods), we estimated a second-order rate constant $k = 5.5 \pm 2.2 \times 10^6 \text{ M}^{-1} \cdot \text{s}^{-1}$ (see inset to Fig 6.2A). At [NADH] $\geq 100 \mu\text{M}$, i.e. under pseudo-first order conditions, within the experimental error the reaction followed a single exponential time course, proceeding at $k' = 255 \pm 17 \text{ s}^{-1}$ (Fig. 6.2B). In this [NADH] range, the observed rate constant was independent of [NADH], suggesting a limiting rate for eT within the NADH/FIRd-reductase complex. Under identical experimental conditions, NADPH reduces FIRd-

reductase at an approximately 100-fold slower rate (not shown).

The rate of FIRd-reductase reduction by NADH decreased constantly with increasing ionic strength (Fig. 6.2C). Data were analyzed according to the Brønsted-Bjerrum equation, whereby $\log k$ is expected to be linearly dependent on the square root of the ionic strength with a slope equal to $2AZ_AZ_B$, ($A \sim 0.49$ at 5°C and Z_A and Z_B are the charges involved). From the data in Fig. 6.2C we estimated $Z_AZ_B \sim -1.3$, which is consistent with a slight effect of ionic strength on this reaction. Finally, the reduction of FIRd-reductase by NADH was found to be essentially independent of pH in the range 5.0 – 8.0 (not shown).

Reduction of the rubredoxin domain of FIRd (Rd-domain) by flavorubredoxin reductase.

The isolated, genetically truncated rubredoxin domain (Rd-domain) of flavorubredoxin (FIRd) is characterized in the oxidized state by a typical absorption spectrum (Fig. 6.3A) that is bleached upon reduction (not shown). The kinetics of the anaerobic reduction of Rd-domain by FIRd-reductase (pre-reduced by a large excess of NADH) was investigated by stopped-flow spectroscopy.

As monitored at 484 nm (see arrow in Fig. 6.3A), the Rd-domain is rapidly ($< 1\text{s}$) reduced by FIRd-reductase in a concentration-dependent manner, following a single exponential time course (Fig. 6.3B). This is consistent with the fact that FIRd-reductase is kept fully reduced during the whole time course by the excess NADH. After mixing the oxidized Rd-domain with NADH only, i.e. in the absence of FIRd-reductase, no absorbance changes are observed even over several seconds (not shown), thus proving that NADH is unable to directly reduce the Rd-domain. When FIRd-reductase is present to shuttle electrons, the observed rate constant for the reduction of the Rd-domain shows a hyperbolic dependence on the FIRd-reductase concentration (see inset to Fig. 6.3B). Data were modeled

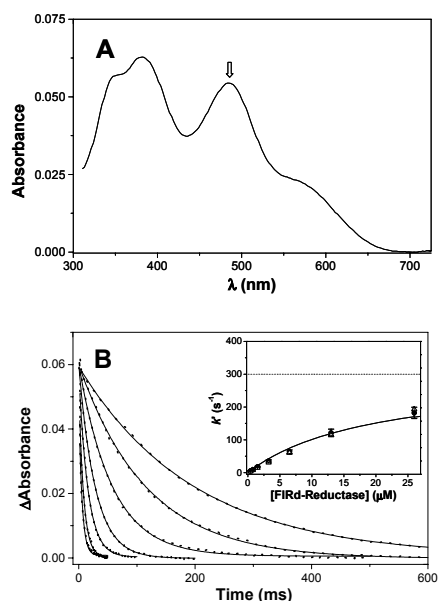
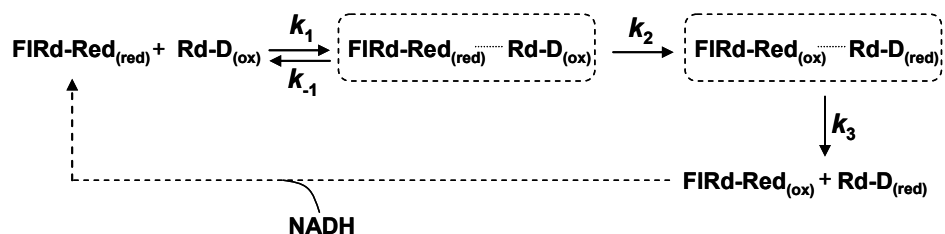


Figure 6.3 – Reduction of the rubredoxin domain of FIRd (Rd-domain) by FIRd-reductase. Oxidized Rd-domain was anaerobically mixed with FIRd-reductase at increasing concentrations, pre-reduced by excess NADH. Concentrations after mixing: [Rd-domain] = 7.7 μM ; [FIRd-reductase] = 0.38, 0.75, 1.5, 3.3, 6.5, 13 or 26 μM ; [NADH] = 375 μM . T = 5 $^{\circ}\text{C}$. Buffer: 50 mM Tris-HCl, 18 % glycerol, pH 8.0. **Panel A** – Absorption spectrum of 7.7 μM oxidised Rd-domain ($\lambda_{\text{max}} = 484$ nm, see arrow).

Panel B – Best fit to single exponential decays of the time courses measured at 484 nm at increasing FIRd-reductase concentrations. Inset: Observed rate constant as a function of FIRd-reductase concentration. Experimental data (closed symbols) were modeled (open symbols) according to Scheme 1, by assuming $k_1 = 1.3 \times 10^7 \text{ M}^{-1}\text{s}^{-1}$, $k_2 = 300 \text{ s}^{-1}$ and $k_3 \geq 5000 \text{ s}^{-1}$.

according to scheme 6.1, whereby complex formation between oxidized Rd-domain and reduced FIRd-reductase (k_1 , k_{-1}) is associated with intracomplex electron transfer (k_2). This is followed by fast dissociation of the partners ($k_3 \gg k_2$) and re-reduction of oxidized FIRd-reductase by NADH at 255 s^{-1} , as independently determined (see inset to Fig. 6.2B). As an over-simplification, in this model intramolecular eT is assumed to be an irreversible process, based on the information that the reduction of Rd-domain by FIRd-reductase is largely



Scheme 1

avored thermodynamically, according to the redox potentials determined by Vicente et al. (21). As shown in the inset to Fig. 6.3B, experimental rates (closed symbols) are suitably fitted by kinetic simulations (open symbols), by assuming $k_1 = 1.3 \times 10^7 \text{ M}^{-1}\text{s}^{-1}$, $k_{-1} \leq 13 \text{ s}^{-1}$, $k_2 = 300 \text{ s}^{-1}$ and $k_3 \geq 5000 \text{ s}^{-1}$ in Scheme 1.

Reduction of flavorubredoxin (FIRd) by flavorubredoxin reductase

Spectral analysis of FIRd is complex due to the partial overlap of the optical contribution of its redox cofactors. Fig. 6.4 shows the absorption spectrum of FIRd in the oxidized state (spectrum a) and after reduction by an excess of NADH in

the presence of catalytic amounts of FIRd-reductase (spectrum b). In the visible region, the spectrum of oxidized FIRd is characterized by a broad band centered at 474 nm and a shoulder at ~ 560 nm (see arrow); this spectrum is contributed by [Fe-Cys4] in the Rd-domain (spectrum c) and by FMN with a possible contribution of the Fe-Fe center (spectrum d). The spectrum of reduced FIRd (Fig. 6.4, line b) displays a low

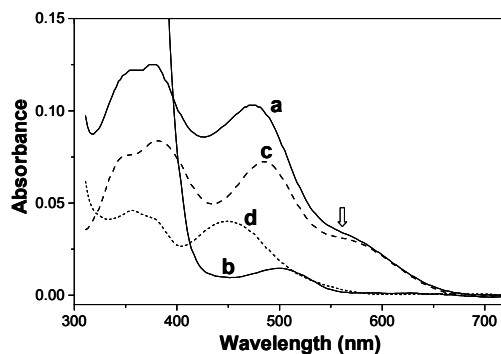


Figure 6.4 – Spectral features of flavorubredoxin (FIRd) and its individual cofactors. Spectrum a: oxidized FIRd (arrow indicates the shoulder at ~560 nm). Spectrum b: reduced FIRd (a few seconds after mixing with 0.25 μ M FIRd-reductase in the presence of 375 μ M NADH). Spectrum c: oxidized Rd-domain. Spectrum d: optical contribution of the oxidized flavodiiron (FMN/Fe-Fe) domain of FIRd estimated by subtracting spectrum c from spectrum a. Protein concentration: 10 μ M.

intensity band centered at ~500 nm, which cannot be directly assigned solely from analyzing these spectra, as it could either result from partially reduced FMN or from the Fe-Fe centre. From these spectra, it is evident that at $\lambda > 550$ nm the absorption changes are almost exclusively dominated by the Rd-domain, making this an adequate wavelength range to monitor redox changes of the Rd centre in the whole enzyme.

The kinetics of FIRd reduction was investigated by anaerobically mixing the oxidized protein with FIRd-reductase pre-incubated with excess NADH. Also in the case of FIRd, no direct reduction by NADH was observed over several seconds. The absolute absorption spectra collected from 2.56 ms to 10 s after

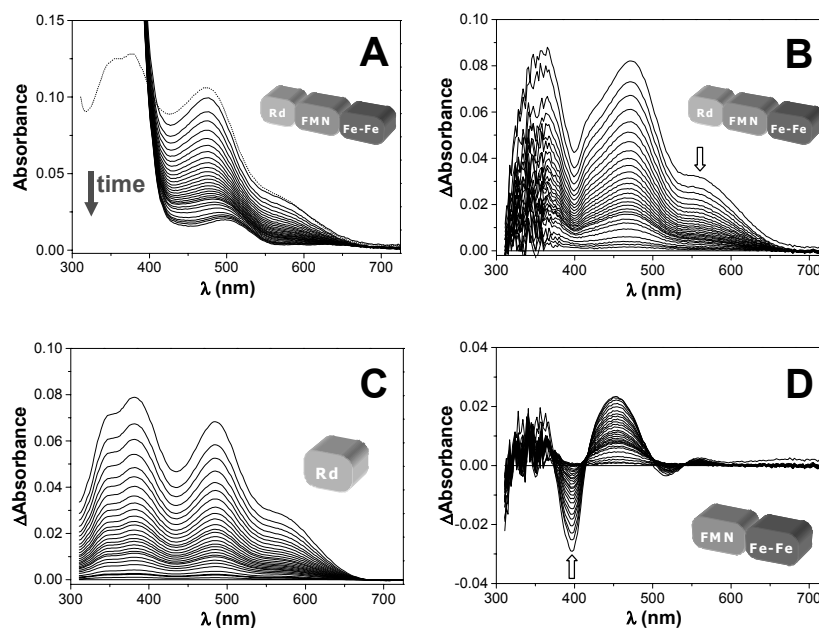


Figure 5 – Reduction of flavorubredoxin (FIRd) by FIRd-reductase. **Panel A** – Absolute spectra collected after mixing oxidized FIRd with FIRd-reductase pre-reduced by excess NADH. Concentrations after mixing: [FIRd] = 10 μ M; [FIRd-reductase] = 0.25 μ M; [NADH] = 375 μ M. Spectra acquired in a logarithmic time mode, from 2.56 ms up to 10 s (arrow depicts the direction of the absorption changes with time). Buffer: 50 mM Tris-HCl, 18 % glycerol, pH 8.0. T = 5^o C. **Panel B** – Difference spectra obtained by subtracting the final spectrum in Panel A (t = 10 s) from the remainders. Arrow depicts 560 nm as a suitable wavelength to monitor the redox changes of the [Fe-Cys₄] centre in FIRd. **Panel C** – Optical contribution of the Rd-domain to the difference spectra depicted in panel B. These spectra were reconstructed by estimating the Rd_{ox}/Rd_{red} ratio at every time point from the absorption changes detected at 560 nm along the reaction (see arrow in panel B). **Panel D** – Optical contribution of the flavodiiron domain estimated by subtracting the contribution of the Rd-domain (panel C) from the difference spectra depicted in panel B. Spectra reveal the formation of flavin red semiquinone, as indicated by the increase at 390 nm (see arrow).

mixing are depicted in Figure 6.5A, together with the initial spectrum of FIRd in the oxidized state (dotted line); absorption at $\lambda < 400$ nm is dominated by NADH in excess. The difference spectra are shown in Fig. 6.5B. The Rd_{ox}/Rd_{red} ratio at each time point was estimated at 560 nm (see arrow in Fig. 6.5B), which allowed us to re-construct the optical contribution of [Fe-Cys₄] (Fig. 6.5C) to the difference spectra in Fig. 6.5B. By subtraction we estimated the optical contribution of the FIRd flavodiiron domain, that is dominated by the FMN moiety (Fig. 6.5D). Inspection of the latter data reveals the formation of a red flavin semiquinone, characterized by an absorbance increase at ~ 390 nm and a synchronous

absorbance decrease at ~450 nm (23).

Summing up, after mixing oxidized FIRd with reduced FIRd-reductase in the

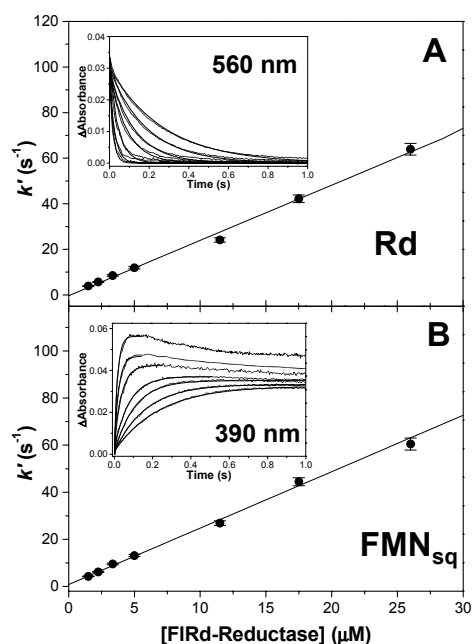


Figure 6.6 – Kinetics of electron transfer between FIRd-reductase and flavorubredoxin. Concentrations after mixing: [FIRd] = 10 μM; [FIRd-reductase] = 0.25, 0.5, 1.5, 2.3, 3.4, 5, 11.5, 17.5 and 26 μM; [NADH] = 375 μM. T = 5°C. Buffer: 50 mM Tris-HCl, 18% glycerol, pH 8.0. Data collected after anaerobically mixing oxidized FIRd with increasing concentrations of FIRd-reductase pre-reduced by excess NADH. Observed rate constants obtained by fitting to single exponential decays the absorption changes collected at 560 nm (panel A) and at 390 nm (panel B).

presence of an excess of NADH, two events can be deconvoluted: the reduction of [Fe-Cys4] (monitored at 560 nm) and the formation of semiquinone FMN (monitored at 390 nm after subtraction of the optical contribution of [Fe-Cys4]). As shown in Fig. 6.6, both processes appear to be synchronous, following a single exponential time course with a rate constant linearly dependent on FIRd-reductase concentration; the calculated apparent second order rate constant is $k = 2.4 \pm 0.1 \times 10^6 \text{ M}^{-1} \text{ s}^{-1}$. To be noted that at the highest concentrations of FIRd-reductase (inset to Fig. 6.6B), the faster accumulation of FMN_{sq} is followed by a slower partial decay presumably

to 2e-reduced FMN.

The effect of ionic strength and pH on the reduction of Rd-domain and FIRd

The effect of ionic strength and pH on the reduction of either the Rd-domain or FIRd was also investigated, upon mixing at 20 °C these proteins in the oxidized state with FIRd-reductase pre-reduced by excess NADH. Figure 6.7 shows that in the cases of FIRd (panel A) and Rd-domain (panel B), the observed rates follow a bell-shaped dependence on ionic strength, with a maximum at around 40 – 50

mM. As shown in Fig. 6.8, the kinetics of FIRd reduction was found to be strongly pH dependent with an apparent $pK_a \sim 7.3$, the asymptotic value at acidic pH being $k' \sim 0.04 \text{ s}^{-1}$. A very similar pH dependence was also observed for the reduction of the isolated Rd-domain.

6.4 DISCUSSION

Flavodiiron proteins (FDPs), expressed in many prokaryotes (6, 11) and in a restricted group of pathogenic amitochondriate protozoa (12-14), are responsible for NO detoxification under anaerobic conditions (7, 8), thus helping microbes to survive in NO-

enriched microaerobic environments. Since FDPs catalyze the reduction of NO at the level of their non-heme di-iron site, their catalytic efficiency clearly depends on the availability of reducing equivalents at this bimetallic site. In *E. coli* NADH is the source of these electrons, which are then transferred to FIRd via FIRd-reductase ((15), see Fig. 6.1). The results herein presented show that *E. coli* FIRd-reductase is highly specific for NADH, that acts as a very efficient electron donor ($k = 5.5 \pm 2.2 \times 10^6 \text{ M}^{-1}\text{s}^{-1}$, at 5 °C) contrary to NADPH. This specificity can be possibly understood based on the protein engineering studies on glutathione reductase (24) and dihydrolipoamide dehydrogenase (25) from *E. coli*, which are

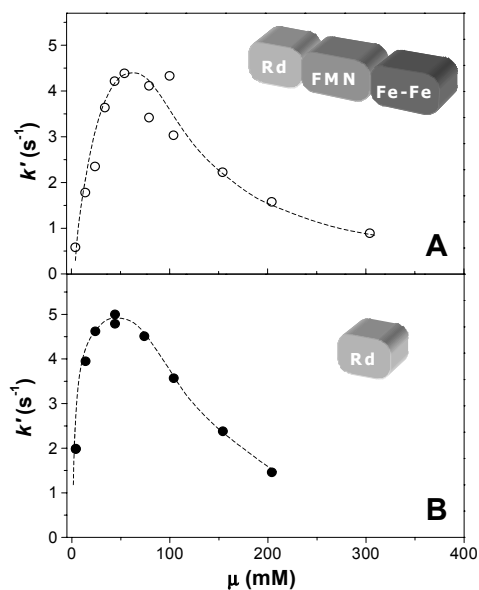


Figure 7 – Effect of ionic strength. Ionic strength dependence of the rate constants observed for the anaerobic reduction of FIRd by FIRd-reductase of FIRd (**Panel A**) or the isolated Rd-domain (**Panel B**). Concentrations after mixing: 8.5 μM FIRd, 2 μM FIRd-reductase, 375 μM NADH (Panel A) or 10.5 μM Rd-domain, 0.5 μM FIRd-reductase, 375 μM NADH (Panel B). T= 20 °C. Rd-domain and FIRd were previously desalted and equilibrated with 5 mM Tris-HCl, 18% glycerol, pH 7.6, by gel permeation chromatography. Ionic strength was then adjusted by addition of KCl to the buffer. The dashed lines are merely shown to represent the observed bell-shaped behaviour.

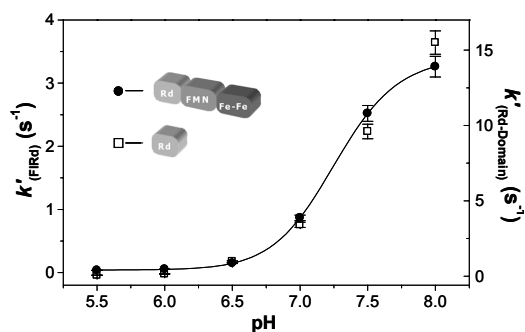


Figure 8 – Effect of pH. Rate constants obtained by measuring FIRd anaerobic reduction by FIRd-reductase, at different pH values. Concentrations after mixing: 8.5 μM FIRd, 2 μM FIRd-reductase, 375 μM NADH. $T = 20^\circ\text{C}$. Buffer: 5 mM Tris-HCl, 18% glycerol, pH 7.6. FIRd was previously desalted and equilibrated in 5 mM Tris-HCl, 18% glycerol, pH 7.6, by gel permeation chromatography, whereas NADH and FIRd-reductase were diluted into concentrated buffers (100 mM) at different pH values. Ionic strength ~ 145 mM after mixing.

specific for NADPH and NADH, respectively. Sequence analyses and homology modeling of FIRd-reductase (not shown) suggest: 1) the presence of the residues competent to form H-bonds with the ribose 2'-OH and 3'-OH groups of NADH, and 2) the absence of a nest of positively charged residues to stabilize the extra phosphate group in NADPH.

In the present study, we have observed several analogies between *E. coli* FIRd-reductase and the rubredoxin reductase (RR) from *Pseudomonas oleovorans* (22). The latter is a FAD-binding protein sharing a significant aminoacid sequence similarity with *E. coli* FIRd-reductase (27% identity, 50% similarity); its physiological role is to shuttle electrons between NADH and rubredoxin, the electron donor of a membrane bound diiron ω -hydroxylase required for the hydroxylation of alkanes (26). Comparing *E. coli* FIRd-reductase and *P. oleovorans* RR, we notice that: i) the FAD moiety accepts the two electrons from NADH as a single kinetic step with no evidence for flavin radical accumulation; ii) at saturating NADH concentrations ($> 100 \mu\text{M}$), flavin is reduced at comparable limiting rates ($255 \pm 17 \text{ s}^{-1}$ in FIRd-reductase, see inset to Fig 6.2B, to be compared with $180 - 190 \text{ s}^{-1}$ measured for RR); iii) upon reduction by NADH, a charge transfer complex with NAD^+ is formed, identified by a broad absorption band at $\lambda > 520 \text{ nm}$ (Fig. 6.2A in the present study to be compared with Fig. 4 in (22)).

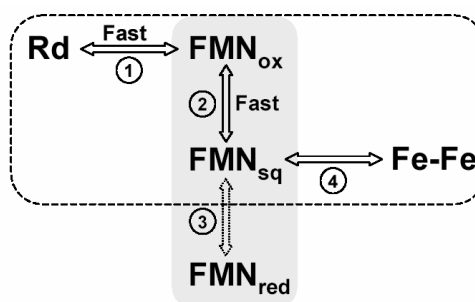
Based on the structural and functional similarities with *P. oleovorans* RR, it may be

expected that the physiological function of *E. coli* FIRd-reductase is to shuttle electrons between NADH and the Rd center in FIRd, as originally proposed by Gomes et al. (15). Consistently, we observed that NADH is unable to directly reduce [Fe-Cys₄] in the Rd-domain, either isolated or as part of FIRd, unless FIRd-reductase is present to catalyze this eT process (Fig. 6.3B and Fig. 6.6A). In the latter case, the Rd center is promptly reduced by FIRd-reductase and this reaction was found to be highly dependent both on pH and ionic strength (Fig. 6.7 and Fig. 6.8). Namely, we found that the reaction i) speeds up at alkaline pH (apparent pK ~ 7.3), a finding that appears physiologically relevant as in the cytosol of *E. coli*, where FIRd-reductase and FIRd are found, pH is ~ 7.5 and ii) displays a bell-shaped dependence on ionic strength, a fairly common feature for inter-protein electron transfer (27), with maximum rate at around 40 – 50 mM.

Under optimal eT conditions (pH = 8.0 and μ ~ 40 mM), kinetic data could be modeled according to scheme 1 (Fig. 6.3B); we observe that FIRd-reductase and the Rd domain form a tight complex rapidly ($k \sim 1 \times 10^7$ M⁻¹s⁻¹; $K_d \leq 1$ μ M), followed by an intra-complex eT (from FAD to [Fe-Cys₄]) proceeding at a limiting rate of ~300 s⁻¹. With the whole FIRd, electrons donated by FIRd-reductase enter the protein at the Rd center (with an apparent k of 2.4×10^6 M⁻¹s⁻¹) and clearly re-equilibrate with FMN, leading to formation of FMN_{sq} (detected by spectral analysis detailed in Fig. 6.5). Such a finding is consistent with the reduction potentials of FMN/FMN_{sq} and [Fe³⁺-Cys₄]/[Fe²⁺-Cys₄] being very similar ($E_0 = -40$ mV and -60 mV, respectively (21)). These two events were observed to proceed synchronously even at the highest FIRd-reductase concentration, thus strongly suggesting that [Fe-Cys₄] and FMN are in very fast redox equilibrium (scheme 2). It is interesting that also in the flavocytochrome P450BM3 (from *Bacillus megaterium*), the flavin semiquinone shuttles one electron at a time to the heme active site, whereas the fully (2 electron) reduced flavin contributes to inactivation of the enzyme (28).

The lack of a UV-visible spectral fingerprint for the Fe-Fe site hampers the detection of this site's prompt reduction via FMN_{sq}. However, we notice that if

the reduction of the Fe-Fe site was not occurring synchronously with [Fe-Cys₄] and FMN 1e-reduction, only 2 electrons would quickly equilibrate within FIRd. Since the redox potentials of both [Fe³⁺-Cys₄]/[Fe²⁺-Cys₄] and FMN/FMN_{sq}



Scheme 2

are similar (21), in the absence of other effects the observed apparent rate constant for the reduction of [Fe-Cys₄] and FMN should be approximately 2-fold smaller than that measured with the isolated Rd-domain (accepting only 1 electron). Taking this into account, it is relevant that the second order rate constants for eT from FIRd-reductase to isolated Rd-domain ($\sim 1 \times 10^7 \text{ M}^{-1}\text{s}^{-1}$) or FIRd ($2.4 \times 10^6 \text{ M}^{-1}\text{s}^{-1}$) actually differ by a factor significantly greater than 2. This leads to hypothesize that electrons entering FIRd at the Rd center quickly equilibrate also with the Fe-Fe site via FMN_{sq}. In conclusion, we have thoroughly investigated the eT kinetics to flavorubredoxin, the crucial enzyme in the *E. coli* anaerobic NO-detoxification pathway. We found that FIRd-reductase acts as an efficient electron shuttle between NADH and the [Fe-Cys₄] center of FIRd, where electrons quickly equilibrate intra-molecularly with FMN_{sq} and most probably Fe-Fe, to become available for the reduction of NO to N₂O.

6.5 REFERENCES

- 1 MacMicking, J., Xie, Q. W. and Nathan, C. (1997) Nitric oxide and macrophage function. *Annu Rev Immunol* **15**, 323-50
- 2 Bogdan, C. (2001) Nitric oxide and the immune response. *Nat Immunol* **2**, 907-16
- 3 Beckman, J. S. and Koppenol, W. H. (1996) Nitric oxide, superoxide, and peroxynitrite: the good, the bad, and ugly. *Am J Physiol* **271**, C1424-37
- 4 Poole, R. K., Anjum, M. F., Membrillo-Hernandez, J., Kim, S. O., Hughes, M. N. and Stewart, V. (1996) Nitric oxide, nitrite, and Fnr regulation of hmp (flavo-hemoglobin)

- gene expression in *Escherichia coli* K-12. *J Bacteriol* **178**, 5487-92
- 5 Gardner, P. R., Gardner, A. M., Martin, L. A. and Salzman, A. L. (1998) Nitric oxide dioxygenase: an enzymic function for flavohemoglobin. *Proc Natl Acad Sci U S A* **95**, 10378-83
 - 6 Wasserfallen, A., Ragetti, S., Jouanneau, Y. and Leisinger, T. (1998) A family of flavoproteins in the domains Archaea and Bacteria. *Eur J Biochem* **254**, 325-32
 - 7 Gardner, A. M., Helmick, R. A. and Gardner, P. R. (2002) Flavorubredoxin, an inducible catalyst for nitric oxide reduction and detoxification in *Escherichia coli*. *J Biol Chem* **277**, 8172-7
 - 8 Gomes, C. M., Giuffre, A., Forte, E., Vicente, J. B., Saraiva, L. M., Brunori, M. and Teixeira, M. (2002) A novel type of nitric-oxide reductase. *Escherichia coli* flavorubredoxin. *J Biol Chem* **277**, 25273-6
 - 9 Silaghi-Dumitrescu, R., Coulter, E. D., Das, A., Ljungdahl, L. G., Jameson, G. N., Huynh, B. H. and Kurtz, D. M., Jr. (2003) A flavodiiron protein and high molecular weight rubredoxin from *Moorella thermoacetica* with nitric oxide reductase activity. *Biochemistry* **42**, 2806-15
 - 10 Silaghi-Dumitrescu, R., Ng, K. Y., Viswanathan, R. and Kurtz, D. M., Jr. (2005) A flavodiiron protein from *Desulfovibrio vulgaris* with oxidase and nitric oxide reductase activities. Evidence for an in vivo nitric oxide scavenging function. *Biochemistry* **44**, 3572-9
 - 11 Saraiva, L. M., Vicente, J. B. and Teixeira, M. (2004) The role of the flavodiiron proteins in microbial nitric oxide detoxification. *Adv Microb Physiol* **49**, 77-129
 - 12 Andersson, J. O., Sjogren, A. M., Davis, L. A., Embley, T. M. and Roger, A. J. (2003) Phylogenetic analyses of diplomonad genes reveal frequent lateral gene transfers affecting eukaryotes. *Curr Biol* **13**, 94-104
 - 13 Sarti, P., Fiori, P. L., Forte, E., Rappelli, P., Teixeira, M., Mastronicola, D., Sanciu, G., Giuffre, A. and Brunori, M. (2004) *Trichomonas vaginalis* degrades nitric oxide and expresses a flavorubredoxin-like protein: a new pathogenic mechanism? *Cell Mol Life Sci* **61**, 618-23
 - 14 Loftus, B., Anderson, I., Davies, R., Alsmark, U. C., Samuelson, J., Amedeo, P., Roncaglia, P., Berriman, M., Hirt, R. P., Mann, B. J., Nozaki, T., Suh, B., Pop, M., Duchene, M., Ackers, J., Tannich, E., Leippe, M., Hofer, M., Bruchhaus, I., Willhoeft, U., Bhattacharya, A., Chillingworth, T., Churcher, C., Hance, Z., Harris, B., Harris, D., Jagels, K., Moule, S., Mungall, K., Ormond, D., Squares, R., Whitehead, S., Quail, M. A., Rabinowitsch, E., Norbertczak, H., Price, C., Wang, Z., Guillen, N., Gilchrist, C., Stroup, S. E., Bhattacharya, S., Lohia, A., Foster, P. G., Sicheritz-Ponten, T., Weber, C., Singh, U., Mukherjee, C., El-Sayed, N. M., Petri, W. A., Jr., Clark, C. G., Embley, T. M., Barrell, B., Fraser, C. M. and Hall, N. (2005) The genome of the protist parasite *Entamoeba histolytica*. *Nature* **433**, 865-8
 - 15 Gomes, C. M., Vicente, J. B., Wasserfallen, A. and Teixeira, M. (2000) Spectroscopic studies and characterization of a novel electron-transfer chain from *Escherichia coli* involving a flavorubredoxin and its flavoprotein reductase partner. *Biochemistry* **39**, 16230-7
 - 16 Frazao, C., Silva, G., Gomes, C. M., Matias, P., Coelho, R., Sieker, L., Macedo, S., Liu, M. Y., Oliveira, S., Teixeira, M., Xavier, A. V., Rodrigues-Pousada, C., Carrondo, M. A. and Le Gall, J. (2000) Structure of a dioxygen reduction enzyme from *Desulfovibrio gigas*. *Nat Struct Biol* **7**, 1041-5

- 17 Silaghi-Dumitrescu, R., Kurtz, D. M., Jr., Ljungdahl, L. G. and Lanzilotta, W. N. (2005) X-ray crystal structures of *Moorella thermoacetica* FprA. Novel diiron site structure and mechanistic insights into a scavenging nitric oxide reductase. *Biochemistry* **44**, 6492-501
- 18 da Costa, P. N., Teixeira, M. and Saraiva, L. M. (2003) Regulation of the flavorubredoxin nitric oxide reductase gene in *Escherichia coli*: nitrate repression, nitrite induction, and possible post-transcription control. *FEMS Microbiol Lett* **218**, 385-93
- 19 Justino, M. C., Vicente, J. B., Teixeira, M. and Saraiva, L. M. (2005) New genes implicated in the protection of anaerobically grown *Escherichia coli* against nitric oxide. *J Biol Chem* **280**, 2636-43
- 20 Lee, H. J., Basran, J. and Scrutton, N. S. (1998) Electron transfer from flavin to iron in the *Pseudomonas oleovorans* rubredoxin reductase-rubredoxin electron transfer complex. *Biochemistry* **37**, 15513-22
- 21 Perry, A., Tambyrajah, W., Grossmann, J. G., Lian, L. Y. and Scrutton, N. S. (2004) Solution structure of the two-iron rubredoxin of *Pseudomonas oleovorans* determined by NMR spectroscopy and solution X-ray scattering and interactions with rubredoxin reductase. *Biochemistry* **43**, 3167-82
- 22 Smith, P. K., Krohn, R. I., Hermanson, G. T., Mallia, A. K., Gartner, F. H., Provenzano, M. D., Fujimoto, E. K., Goeke, N. M., Olson, B. J. and Klenk, D. C. (1985) Measurement of protein using bicinchoninic acid. *Anal Biochem* **150**, 76-85
- 23 Fischer, D. S. and Price, D. C. (1964) A Simple Serum Iron Method Using the New Sensitive Chromogen Tripyridyl-S-Triazine. *Clin Chem* **10**, 21-31
- 24 Susin, S., Abian, J., Sanchez-Baeza, F., Peleato, M. L., Abadia, A., Gelpi, E. and Abadia, J. (1993) Riboflavin 3'- and 5'-sulfate, two novel flavins accumulating in the roots of iron-deficient sugar beet (*Beta vulgaris*). *J Biol Chem* **268**, 20958-65
- 25 Ghisla, S. and Edmondson, D. A. (2001) in *Encyclopedia of Life Sciences*, Nature Publishing Group
- 26 Zumft, W. G. (2005) Nitric oxide reductases of prokaryotes with emphasis on the respiratory, heme-copper oxidase type. *J Inorg Biochem* **99**, 194-215
- 27 Mittl, P. R., Berry, A., Scrutton, N. S., Perham, R. N. and Schulz, G. E. (1994) Anatomy of an engineered NAD-binding site. *Protein Sci* **3**, 1504-14
- 28 Bocanegra, J. A., Scrutton, N. S. and Perham, R. N. (1993) Creation of an NADP-dependent pyruvate dehydrogenase multienzyme complex by protein engineering. *Biochemistry* **32**, 2737-40
- 29 McKenna, E. J. and Coon, M. J. (1970) Enzymatic omega-oxidation. IV. Purification and properties of the omega-hydroxylase of *Pseudomonas oleovorans*. *J Biol Chem* **245**, 3882-9
- 30 McLendon, G. and Hake, R. (1992) Interprotein Electron Transfer. *Chem Rev* **92**, 481-490
- 31 Vicente, J. B. and Teixeira, M. (2005) Redox and spectroscopic properties of the *Escherichia coli* nitric oxide-detoxifying system involving flavorubredoxin and its NADH-oxidizing redox partner. *J Biol Chem* **280**, 34599-608
- 32 Warman, A. J., Roitel, O., Neeli, R., Girvan, H. M., Seward, H. E., Murray, S. A., McLean, K. J., Joyce, M. G., Toogood, H., Holt, R. A., Leys, D., Scrutton, N. S. and Munro, A. W. (2005) Flavocytochrome P450 BM3: an update on structure and mechanism of a biotechnologically important enzyme. *Biochem Soc Trans* **33**, 747-53

7

Functional properties of *Desulfovibrio gigas* Flavodiiron Protein: interaction with rubredoxin and NO vs. O₂ reduction †

7.1	Introduction	157
7.2	Materials and Methods	159
7.3	Results and Discussion	164
7.4	Conclusions	170
7.5	References	171

SUMMARY

This chapter encompasses developments in the understanding of the functional properties of *Desulfovibrio (D.) gigas* Flavodiiron Protein (ROO; the initial designation of rubredoxin:oxygen oxidoreductase will be held in this chapter). The work here reported focuses on two main aspects of *D. gigas* ROO: its interaction with its rubredoxin (Rd) redox partner, and the functional properties as an oxygen and/or nitric oxide reductase, investigated both *in vitro* and *in vivo*. The interaction and electron transfer (eT) between Rd and ROO was studied by molecular modelling techniques. Kinetic assays using recombinant proteins show that Rd re-oxidation by ROO displays a bell-shape dependence on ionic strength, suggesting a non-trivial electrostatic type of interaction. Rigid docking studies reveal prevalence for Rd to specifically interact with the surface of the ROO near its FMN cofactors. Molecular dynamics simulations show a tight interaction at the proteins' surfaces, with a probability for Rd residues (but not its Fe centre directly) to be in direct contact with the FMN of ROO. Although the major contributions for complex formation are polar interactions, between acidic residues of Rd and basic residues of ROO, substantial non-polar interactions are also relevant. Estimates of rates for eT (using the Pathways model) suggest that the optimised lowest energy complexes are efficient for eT.

With the number of flavodiiron proteins shown to be endowed with NO reductase activity, the functional properties of *D. gigas* ROO were probed *in vivo*, by complementation studies of an *E. coli flrd*-deleted strain, by phenotypical analysis of a *D. gigas roo*-deleted strain and by transcriptional studies of the gene encoding ROO upon exposure of *D. gigas* to nitrosative stress and oxygen. The constitutively expressed ROO affords *in vivo* protection against nitrosative stress and the recombinant protein is, *in vitro*, endowed with both NO and oxygen reductase activities.

‡Parts of this Chapter were published in the following articles:

Victor, B.L., Vicente, J.B., Rodrigues, R., Oliveira, S., Rodrigues-Pousada, C., Frazão, C., Gomes, C.M., Teixeira, M., and Soares, C.M. (2003) "Docking and electron transfer studies between rubredoxin and rubredoxin:oxygen oxidoreductase" *Journal of Biological Inorganic Chemistry* 8 (4): 475-88

Rodrigues, R., Vicente, J.B., Felix, R., Oliveira, S., Teixeira, M., and Rodrigues-Pousada, C. (2002) "*Desulfovibrio gigas* flavodiiron protein affords protection against nitrosative stress in vivo", *Journal of Bacteriology* 188(8): 2745-51

The work here reported results from an ongoing and longstanding collaboration between the groups of Prof. Miguel Teixeira, Prof. Claudina Rodrigues-Pousada and Dr. Cláudio Soares, all at ITQB, involving a number of members of their groups, namely Rute Rodrigues (molecular genetics of *D. gigas* ROO) and Bruno Victor (Modelling of the interaction between Rd and ROO), respectively.

7.1 INTRODUCTION

7.1.1 - Electron transfer (eT) between redox proteins is an ubiquitous process in multiple biochemical pathways. Several theories attempt to rationalize eT reactions. In many cases, the formation of an efficient interacting complex is required for eT to occur. However, it is still under discussion whether the eT process is performed by a single productive complex (1), or by multiple efficient conformations (2,3). A characterization of the interaction surface is anyway essential to understand eT processes between redox proteins. The present study focuses on the interaction between *D. gigas* flavodiiron protein (ROO) (4,5) and its redox partner rubredoxin (6)¹. In the absence of detailed experimental data about protein-protein associations, one viable route is the use of theoretical methodologies to predict them. One of the methods describing the interaction of eT partners is the Brownian Dynamics (BD) method (2). This technique is capable of simulating a series of diffusional dynamic trajectories, mimicking the association process between two proteins (through time). Specific electrostatic interactions and important residues can be studied using this method (7,8). Another strategy in the search of protein-protein complexes uses shape complementarity as a target function (9), which has been further developed to incorporate electrostatic interactions, solvation terms, and other biochemical information.

In the present study AUTODOCK 2.4 (10) was used to perform rigid-body docking studies, which searches for interaction solutions in real space, using common force field terms for the interaction energy between the two proteins. Specifically, this program uses a Monte Carlo Simulated Annealing technique for

¹ Detailed properties of *D. gigas* ROO are described in Chapter 2 and therefore omitted from this chapter.

configurational exploration with a rapid energy evaluation using molecular affinity grids. However, the lack of protein flexibility imposed by the rigid-body docking methods may become a problem. Interacting side-chains are usually in unnatural positions for the complex, preventing a close association and yielding an apparently lower eT efficiency. One efficient way to overcome this problem is to perform a refinement of the complexes obtained by rigid-body docking with Molecular Dynamics/Mechanics simulations (MD/MM).

This combined approach, of complementing rigid-body docking simulations with MD optimization, was undertaken to study eT from *D. gigas* Rd to the ROO. The resulting observations were rationalized in agreement with the experimental results from the experimentally determined ionic strength dependence of eT from Rd to ROO. The modelling results showed a clear preference for Rd to interact with the ROO dimer near the FMN cofactors. These MD refined complexes were analysed together with the experimental results, aiming at the characterisation of the interactions between these two proteins, suggesting representative eT complexes, and making an evaluation of the structural factors that influence the ET efficiency in this system.

7.1.2 - Although a role in oxygen reduction was initially assigned to the ROO family, recent reports contributed to the establishment of members of this protein family as NO reductases. The first evidence of NO reduction activity concerned *E. coli* flavorubredoxin (FIRd). A role in anaerobic NO reduction was proposed for FIRd on the basis of an increased sensitivity to NO of an *E. coli* *norV* (the gene coding for FIRd) mutant (11), which was further confirmed by the NO reductase activity of the enzyme *in vitro* (12) and by transcriptional analysis of *E. coli* grown under nitrosative stress, both aerobically (13) and anaerobically (14). Subsequently, the same NO reductase activity was determined for the FDPs from *M. thermoacetica* (15) and *Desulfovibrio vulgaris* (16). The presence of protective mechanisms against NO in *Desulfovibrio* species (besides *D. gigas* and *D. vulgaris*,

other *Desulfovibrio* species have FDP orthologues present in their genomes) raises the possibility that these organisms may face nitrosative stress in their living environments. They may indeed have to cope with NO formed and released in the process of nitrite reduction by coexisting denitrifying organisms. On the other hand, as some of these organisms inhabit the mammalian digestive tract, associated to chronic inflammatory diseases (17), at the onset of infection and inflammatory processes they may locally be subjected to the immune response mechanisms of their hosts, including NO production and release by activated macrophages. The existence of FDPs in *Desulfovibrio* species thus appears to constitute another stress resistance strategy of these versatile organisms.

The present work aims to investigate the role of FDP in the protection of *D. gigas* against NO, using a combination of approaches *in vitro* and *in vivo*. The NO and O₂ reductase activities of recombinant ROO *in vitro* were measured by amperometric methods, and the *in vivo* approach involved complementation studies performed in an *E. coli norV* mutant strain as well as construction and phenotypic analysis of a *D. gigas roo*- mutant strain. The results are discussed in the light of the versatility of ROO to act either as an NO or an oxygen reductase.

7.2 MATERIALS AND METHODS

Protein cloning, expression and purification – Recombinant *Escherichia coli* flavorubredoxin reductase (FlRd-red) and recombinant *D. gigas* Rd were expressed and purified as previously described (18). *D. gigas* ROO was cloned in the expression vector pET-30a (Novagene), using restriction sites for *Nde*I and *Xho*I. The clone obtained was confirmed by sequencing, performed with Thermo Sequenase Cycle Sequencing Kit (Amersham) and with ABI Prism 373A Automatic Sequencer using ABI Prism DyeDeoxy Terminator Cycle Sequencing Kit. Recombinant expression of ROO was performed in *E. coli* strain BL21 (DE3) (Novagene), using M9 minimal medium with kanamycin (30 mg/mL)

supplemented with FeSO₄ (10 μM), at 30°C. Isopropyl-beta-D-thiogalactopyranoside (IPTG, 1mM) was used as inducer at OD_{600nm}~0.6, and cultures were allowed to grow for 7 hours before harvest of the cells by centrifugation. *E. coli* cells over-expressing ROO were disrupted in two cycles in a French Press mini-cell at 1.000 PSI. The soluble extract was separated from the membrane fraction through ultra-centrifugation for 2 hours at 100.000 g and analysed by SDS-PAGE, using molecular mass markers (Fermentas). The obtained soluble extract was dialysed overnight at 4°C, against 5 mM Tris-HCl, pH 7.6 with 9% glycerol (buffer A), and then loaded onto a 60 ml Q-Sepharose Fast Flow column (Amersham Pharmacia) previously equilibrated with 20 mM Tris-HCl, 18% glycerol, pH 7.5 (buffer B). An NaCl gradient of 8 column volumes (from buffer B to buffer C, i.e., bufferB with 1 M NaCl) was applied at a flow rate of 2.5 ml/min, and ROO eluted at approximately 350 mM NaCl, as indicated by the mild yellow colour and confirmed by UV-visible spectroscopy. The pooled fractions were then dialysed overnight against buffer A and subsequently applied to a 50 ml Fractogel TMAE column (Merck), previously equilibrated with buffer B. ROO eluted at approximately 250 mM NaCl, at a flow rate of 1.5 ml/min, using an eight column volumes gradient of buffer B to buffer C. This step yielded pure ROO, as judged by SDS-PAGE.

Biochemical analysis of recombinant ROO

The purity of recombinant ROO was assessed by 12% SDS-PAGE. ROO flavin cofactor analysis was performed as in (19), and its iron content determined by the 2,4,6-tripyridyl 1,3,5-triazine method (20). Total protein was quantified using the bicinchoninic acid assay method (21).

Kinetic assays

Kinetic assays were performed in a Shimadzu UV-1603 spectrophotometer

D. gigas Flavodiiron Protein: interaction with rubredoxin and NO vs. O₂ reduction

thermostated at 25°C. *D. gigas* Rd (16 µM) was aerobically incubated with 40 µM NADH in TrisHCl 1 mM, pH 7.0 at the tested ionic strength, and reduced by *E. coli* FIRd-reductase (final concentration, 560 nM), as observed by the complete absorbance bleaching at 490 nm. Recombinant ROO (final concentration, 3.8 nM) was added to the reaction mixture and the Rd reoxidation rate was followed also at 490 nm ($\epsilon^{490 \text{ nm}}: 6970 \text{ M}^{-1}\cdot\text{cm}^{-1}$). Ionic strength was adjusted using a 1M NaCl stock solution.

Amperometric NO and oxygen consumption measurements

NO consumption measurements were carried out using a World Precision Instruments ISO-NOP 2 mm electrode, at room temperature, as described in (12). Reduced *D. gigas* rubredoxin was prepared separately by anaerobically incubating 415 µM Rd with 48 nM *E. coli* FIRd-reductase and 1 mM NADH. Oxygen consumption rates were measured using a Clark-type O₂ electrode plugged to a Biological Oxygen Monitor (Model 5300, Yellow Springs). Rubredoxin was reduced in situ with 400 nM of *E. coli* flavorubredoxin reductase (FIRd-reductase) and 1 mM NADH, prior to addition of ROO to the reaction mixture. Catalase (SIGMA) was added to the reaction mixture to test the production of hydrogen peroxide upon oxygen consumption. The experiments were carried out at 25°C in air-equilibrated buffer (50 mM Tris-HCl, pH 7.5, containing 18% glycerol), i.e., with approximately 240 µM O₂. Since full reduction of oxygen to water requires four electrons, ROO will oxidize four Rd (one-electron carrier) molecules to catalyse this reaction to completeness. To check whether the O₂ or NO reductase activities were limited by electron donation from reduced Rd, the concentration of the latter was varied and the O₂ and NO consumption rates measured.

Modelling of molecular interactions between Rd and ROO

The program AUTODOCK 2.4 (10) was used to study rigid body molecular interactions between the ROO dimer (that remains static in a grid) and Rd (that moves randomly about the ROO surface). Crystallographic structures of Rd (6) (PDB entry 1RDG) and of the ROO dimer (5) (PDB entry 1E5D) at 1.4 and 2.5 Å resolution respectively, were used in this work. To simulate the interaction of reduced Rd with oxidised ROO, i. e. the moment just before the first eT step takes place, both FMN molecules were set to their quinone form, while for the diiron centres a global charge of +1 was assigned (iron atoms were assigned a partial charge of +3). In the case of Rd, a simple charge set for the Fe-Cys₄ metal cluster was used (global charge -2 for reduced Rd).

To optimize the complexes obtained by rigid body modelling, MD simulations were performed, by creating a modified version of the PROMD program from the GROMOS 96 package.

Electron transfer calculations

The non-adiabatic ET rate can be defined according to equation 7.1,

$$K_{ET} = \frac{2\pi}{h} [T_{DA}]^2 FC \quad \text{Equation 7.1}$$

where h is the Planck constant, T_{DA} is the electron tunnelling coupling factor between donor and acceptor and FC the Franck-Condon factor, that includes the re-organizational energy λ for the eT process. This term should be constant when the interacting partners are the same, as in this work (reviewed in (22)). Taking into account equation 7.1 and these considerations, it is possible to assume that the eT rate (k_{eT}) is directly proportional to the square of the eT coupling (T_{DA}). T_{DA} can be evaluated with the Pathways model developed by Beratan and others (23,24). According to this model, an electron pathway is defined as a combination of interactions, such as space jumps and hydrogen or covalent bonds, connecting

a specified donor and acceptor. To each connection, a specific decay is assigned. The product of all connection decays is an approximation of the total decay of a certain pathway. Therefore, the ET efficiency can be evaluated according to the T_{DA} obtained for the pathway. GREENPATH v.0.971 was used to perform these studies in Rd-ROO complexes optimised by MD simulations. This program, based on the Tunnelling Pathways theory, calculates every possible pathway between a specified electron donor and acceptor. The one with higher T_{DA} is selected as representative of the eT process.

Assessment of D. gigas ROO functional properties in vivo

To probe *D. gigas* ROO's functional properties, different approaches were undertaken, using a broad combination of molecular biology techniques, which are described in the original article by Rodrigues et al, which is part of this chapter (25). A mutated *E. coli* strain deleted in the *norV* gene (11) (encoding the flavorubredoxin NO reductase), was the subject of complementation studies using a plasmid with the *D. gigas* ROO-encoding gene (here called *roo* (26), for historical reasons). The *E. coli norV* strain was transformed with the *roo*-bearing plasmid and a phenotypical analysis was carried out testing the comparative sensitivities to NO and nitrosative stress of transformed vs. non-transformed cells. Cultures were challenged either with 50 μ M NO from a 2 mM stock solution or with 1 mM GSNO. Moreover, a mutated *D. gigas* strain was obtained, deleted in *roo*, through insertion of a kanamycin resistance gene between the flanking regions of *roo*. This mutated strain was assayed for its phenotype in response to nitrosative stress in comparison with wild-type *D. gigas*. Cultures of both strains were challenged at the appropriate times with either 10 μ M NO or 10 μ M GSNO. The expression of *D. gigas* ROO in response to nitrosative and oxidative stress was probed by real-time reverse-transcription PCR (RT-PCR) analysis of cultures exposed to 150 μ M NO, 1mM GSNO or 60 μ M O₂.

7.3 RESULTS AND DISCUSSION

7.3.1 – Interaction between Rubredoxin and the Flavodiiron Protein

Reaction rate ionic strength dependence

The reoxidation rate of Rd by ROO, in the presence of oxygen, was determined as

a function of the ionic strength in order to investigate the type of interaction between the two proteins. For this purpose, a hybrid *in vitro* assay was designed, in which Rd was enzymatically reduced by *E. coli* FIRd-red, a protein which was shown to efficiently reduce *D. gigas* Rd at the expense of NADH oxidation (18): upon addition of catalytic amounts of FIRd-red in the presence of NADH, Rd is reduced as monitored at 490 nm (Figure 7.1,

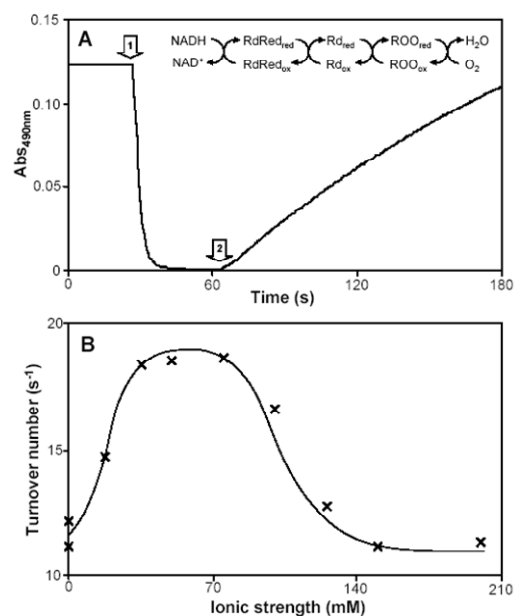


Figure 7.1 - *D. gigas* Rd/ROO interaction studies followed by UV/visible spectroscopy. Panel A – Representative assay performed at 50 mM ionic strength, as described in Materials and Methods. See text for details; Panel B – Ionic strength dependence of the ROO-mediated Rd reoxidation rates.

panel A, block arrow 1). Under the conditions used, the rate of reduction of Rd by FIRd-red is independent of the ionic strength, having a constant value of $0.6 \pm 0.1 \mu\text{M Rd} \cdot \text{s}^{-1}$, in the range studied. As assessed by the flat absorbance line after reduction, Rd is not efficiently reoxidised by oxygen. When catalytic amounts of ROO are added to the reaction mixture (Figure 7.1, panel A, block arrow 2), Rd reoxidation by ROO is triggered, at the expense of oxygen reduction. Due to the large excess of Rd over ROO (4000 fold), the initial rate of Rd oxidation, measured from the initial linear slope of the reoxidation curve, is independent of its re-

reduction by FlRd-red. The Rd reoxidation rates vary with ionic strength in a bell shape fashion (Figure 7.1, Panel B), which suggests that electrostatic interactions are important for complex formation (further discussed below).

Simulation of the interaction, complex optimization by MD and eT calculations

Overall, the modelling studies strongly favour an interaction of reduced Rd with

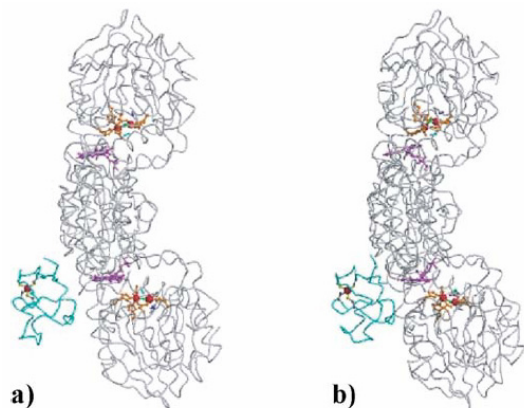


Figure 7.2 - Representation of the lowest energy complex obtained in the docking of reduced Rd with oxidised ROO, before (4.a) and after (4.b) MD simulations. The figures were prepared with programs Molscrip and Raster3D.

oxidized ROO, with the Rd docking to the ROO dimer on the FMN moiety region (Fig. 7.2A), which is enforced by the MD complex optimization (Fig 7.2B). This observation is in accordance with the previous proposal that Rd donates electrons directly to the FMN from *D. gigas* ROO (27).

The simulations point out the relevant groups involved in the interaction. Acidic residues from Rd and basic residues from ROO play an important role, but other non-polar interactions are also relevant. As suggested by the eT calculations, specific residues at the surface of reduced Rd may directly interact with the FMN moiety. The experimental bell-shaped dependence of eT rates on ionic strength is not a simple phenomenon to interpret, and we put forward two possible explanations for it. In one case, the binding of one Rd molecule would make the binding of another Rd molecule (ROO can accommodate a maximum of 4 electrons, 2 in the FMN and 2 in the diiron centre) considerably more difficult, by electrostatic repulsion (as shown by our modelling results). This repulsion would be higher for lower ionic strengths but, with increasing concentration of salt, this repulsion would be diminished, allowing a

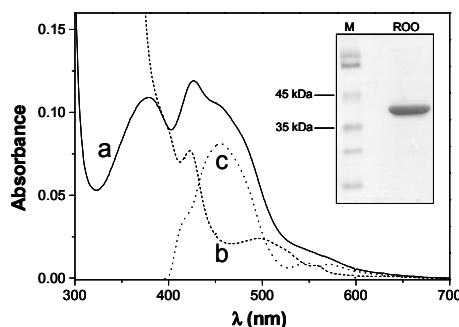
more stable 2:1 complex formation. A second hypothesis considers electrostatic locking of unproductive complexes that become unstable with increasing ionic strength, allowing the two proteins to interact with each other in more productive configurations. Both hypotheses are amenable to experimental testing, and work is in progress to clarify this issue.

7.3.1 – Functional properties of *D. gigas* Flavodiiron Protein

Biochemical and spectroscopic analyses of recombinant ROO

ROO was successfully over-expressed in *E. coli* and purified to homogeneity, as revealed by the SDS-PAGE analysis which displays a single band of about 43 kDa (inset in Fig. 7.3), as predicted. Recombinant ROO was isolated with ~2 irons and ~0.8 FMN per monomer, as expected. The spectrum of recombinant oxidized *D. gigas* ROO (Fig. 7.3) is dominated by the flavin moiety, with two major bands around 380 nm and 450 nm. The band at 424 nm appears to be due to a sub-stoichiometric b-type haem. The low-absorbance band at approximately 500 nm observed in the spectrum of the reduced enzyme (Fig. 7.3, line b) remains to be assigned. The dominance of the flavin moiety is confirmed by subtracting the reduced ROO spectrum to the oxidized one (Fig. 7.3, line a). The redox spectrum thus obtained (Fig. 7.3, line c) displays the features of the oxidized flavin moiety, with a maximum at 454 nm, and the α and β bands at 548 and 571 nm, characteristic of reduced haem moieties. From the redox spectrum it was also possible to estimate a haem content of about 0.02-0.04 mol haem/mol ROO. It should be noted that wt ROO also contains sub-stoichiometric amounts of haem (27). It is still not known the significance, if any, of the haem co-purification, also observed for the *D. vulgaris* enzyme (16). Nevertheless, the very low amount of

haem (less than 0.05 haem per protein molecule) present in the purified recombinant protein precludes any significant contribution to the NO reaction.



Oxygen consumption by recombinant D. gigas ROO

The oxygen reductase activity of recombinant *D. gigas* ROO was measured using reduced recombinant *D. gigas* rubredoxin as the

Figure 7.3 - Biochemical and spectroscopic analyses of recombinant *D. gigas* ROO. Visible spectra of pure ROO recorded in different redox states. Line a (full) – spectrum of as isolated ROO; Line b (dashed) – spectrum of reduced ROO (the sample from line a reduced with sodium dithionite); Line c (dotted) – redox spectrum obtained by subtracting line a to line b. **Inset** – SDS-PAGE analysis of purified recombinant *D. gigas* ROO.

electron donor (Fig. 7.4, Panel A). In the tested range of Rd concentrations, the oxygen reduction activity of ROO was shown to depend hyperbolically on the concentration of Rd (Fig. 7.4, Panel B). From the data, a maximal oxygen reductase activity can be estimated as $50.5 \pm 10 \mu\text{M O}_2 \cdot \text{s}^{-1} \cdot \mu\text{M ROO}^{-1}$. However, the observation that a great fraction of the Rd was immediately oxidized upon addition of ROO and remained so in the course of the assays, suggested that re-reduction of Rd by FIRd-reductase could be limiting the overall reaction. This was further investigated by performing a set of experiments where the Rd concentration was kept constant and the FIRd-reductase concentration was varied. The inset in Panel B, Fig. 7.4 displays the linear increase of the O₂ reductase activity of ROO with increasing FIRd-reductase concentration, up to 1 μM . The feasibility of these assays at higher FIRd-reductase concentrations is impaired by the O₂ reductase activity of the FIRd-reductase (17). The slow O₂ consumption observed upon addition of FIRd-reductase (Panel A in Fig. 7.3) becomes steeper with the increasing FIRd-reductase concentration, enough to

compromise the correct assignment of the O₂ reductase activity to ROO. With these observations in mind, we envisage that the maximal oxygen reductase activity of recombinant ROO may be significantly higher than the rates reported here, i.e., when not limited by electron donation from its redox partners.

Nitric oxide reductase activity of recombinant D. gigas Flavodiiron Protein

Nitric oxide consumption by recombinant ROO was measured anaerobically using excess reduced Rd as the electron donor to ROO. In the absence of oxygen, the expected NO reduction product is nitrous oxide (N₂O), as corroborated by the NADH/NO stoichiometries observed for other ROOs ((15) and our own unpublished results). In comparison with the O₂ reduction measurements, two major differences reside in the fact that i) NO reduction to nitrous oxide (N₂O) requires only two electrons (one per NO molecule) and ii) the NO concentrations tested here are much lower (maximally 10 μM) than those of oxygen (~240 μM). Thus, electron donation from reduced Rd should not pose the same experimental difficulties as for the O₂ reduction assays, i.e., the slow re-reduction of Rd by catalytic amounts of FIRd-reductase.

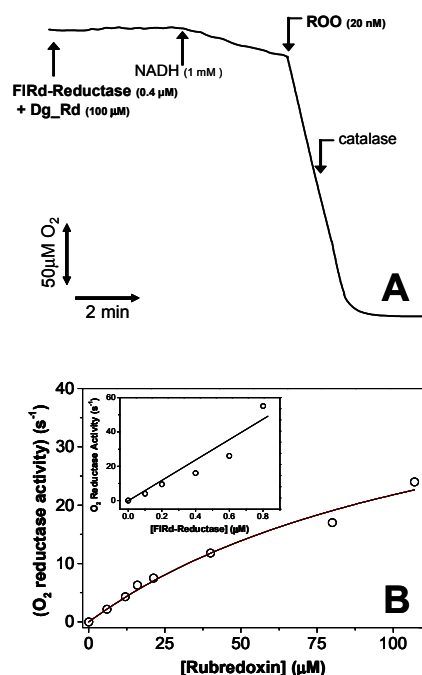


Figure 7.4 - Oxygen consumption by recombinant *D. gigas* ROO. Panel A – representative oxygen consumption assay by *D. gigas* ROO monitored with a Clark-type electrode: FIRd-reductase – *E. coli* flavorubredoxin reductase; Dg_Rd – *D. gigas* recombinant rubredoxin. Panel B - hyperbolic dependence of the oxygen reductase activity of ROO on the concentration of rubredoxin. Inset – linear dependence of the oxygen reductase activity of ROO on the concentration of *E. coli* FIRd-reductase (tested range: 100 – 800 nM), at a fixed rubredoxin concentration of 16 μM.

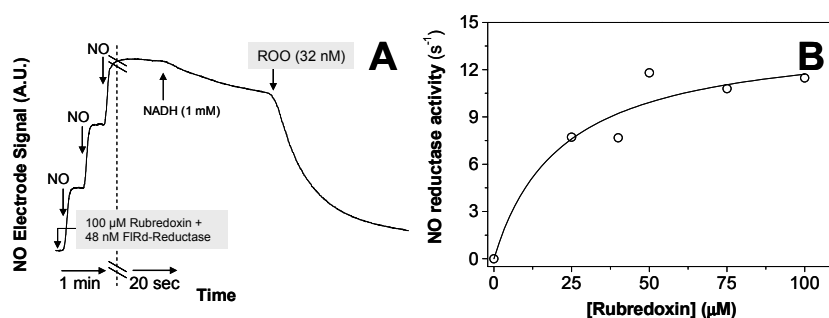


Figure 7.5 - Nitric Oxide consumption by recombinant *D. gigas* ROO. Panel A – representative NO consumption anaerobic assay by *D. gigas* ROO monitored with a NO-specific electrode. Panel B - hyperbolic dependence of the NO reductase activity of ROO on the concentration of reduced Rd.

The NO reductase activity was thus studied as a function of reduced Rd concentration, by anaerobically incubating Rd with FIRd-reductase and excess NADH prior to its addition to the reaction mixture. Upon addition of aliquots of a saturated NO solution (1.9 mM at 25°C) a slow NO consumption rate was observed, due to the unspecific reduction of NO by NADH, mediated by FIRd-reductase (Fig. 7.5, Panel A). The NO reduction rates were shown to vary hyperbolically with increasing reduced Rd concentration (Fig. 7.5, Panel B) with an estimated maximal NO consumption rate of $14.9 \pm 3.2 \text{ mol NO} \cdot \text{s}^{-1} \cdot \text{mol ROO}^{-1}$. From the observation of the NO consumption traces, an apparent K_M can be estimated to be higher than that reported for *E.coli* FIRd and within the order of the ones for the *M. thermoacetica* and *D. vulgaris* ROOs (15,16), i.e., slightly over 5 μM .

Assessment of D. gigas ROO functional properties in vivo

Complementation studies were performed with a mutant *E. coli* strain where the *norV* gene (encoding a flavorubredoxin NO reductase) has been knocked-out through insertion of a kanamycin cassette. This strain has been shown to have impaired growth profiles in anaerobic conditions upon exposure to low NO

concentrations. Transforming this mutant *E. coli* strain with a plasmid encoding for *D. gigas* ROO restores growth of the mutated strain under the aforementioned conditions, indicating that *D. gigas* ROO succeeds in mimicking flavorubredoxin's role as an NO reductase involved in NO detoxification.

To further assess a possible role of *D. gigas* ROO in NO detoxification, a *D. gigas* *roo*⁻ strain mutant was generated. Whereas the growth profiles of the mutated and non-mutated strains are identical under standard growth conditions (for *D. gigas*), a relatively low NO or GSNO concentrations (10 μM) create significant differences in the growth profiles of both strains. Although the wild-type *D. gigas* suffers from a temporary growth arrest upon exposure to nitrosative agents, it eventually resumes its growth. Conversely, the mutated *roo*⁻ strain suffers a growth arrest that is prolonged in time and fails to recover as fast as the wild-type strain, with a more pronounced effect from GSNO than NO. Sensitivity of both *D. gigas* strains to oxygen exposure (up to full aeration) displayed no differences between the two strains in the tested conditions, which precludes any conclusion from this observation.

The levels of *roo* expression were tested as a function of nitrosative stress and oxygen exposure. Whereas exposure to oxygen and NO produced no changes in the levels of *roo* expression, 1 mM GSNO induce a twofold increase in *roo* mRNA levels. It should be noted that *D. gigas* ROO is a constitutive enzyme and is in fact one of the few non-recombinant ROOs so far isolated and studied, which may explain an apparent lack of regulation by two putative substrates of this enzyme.

7.4 CONCLUSIONS

Altogether, the results reported in this chapter provide some light on the functional properties of *Desulfovibrio gigas* flavodiiron protein, leaving room for pending questions, which are currently the subject of ongoing studies.

Modelling the interaction of oxidized *D. gigas* ROO with its redox partner reduced rubredoxin leads to the proposal of an efficient electron transfer mechanism, where reduced Rd docks on the surface of the ROO dimer close to its FMN cofactors. A number of Rd's acidic residues and basic residues from ROO enforce the surface complementarity, although non-polar interactions may play a significant role. These observations can be rationalized by the bell-shaped ionic strength dependence of eT from Rd to ROO (measured indirectly through the ROO-mediated oxidation of reduced Rd by oxygen).

The function of *D. gigas* ROO remains elusive, as it appears to be able to scavenge both NO and oxygen, the latter being a much more robust activity. However, there is solid evidence for *D. gigas* ROO to afford *in vivo* protection against nitrosative stress. The constitutive nature of *D. gigas* ROO suggests that this enzyme may be a bifunctional first line of defence both against nitrosative stress and oxygen exposure.

7.5 REFERENCES

1. Lange, C., and Hunte, C. (2002) Crystal structure of the yeast cytochrome bc₁ complex with its bound substrate cytochrome c, *Proc Natl Acad Sci U S A* **99**(5), 2800-2805
2. Northrup, S. H., Boles, J. O., and Reynolds, J. C. (1988) Brownian dynamics of cytochrome c and cytochrome c peroxidase association, *Science* **241**(4861), 67-70
3. Ubbink, M., Ejdeback, M., Karlsson, B. G., and Bendall, D. S. (1998) The structure of the complex of plastocyanin and cytochrome f, determined by paramagnetic NMR and restrained rigid-body molecular dynamics, *Structure* **6**(3), 323-335
4. Chen, L., Liu, M. Y., LeGall, J., Fareleira, P., Santos, H., and Xavier, A. V. (1993) Rubredoxin oxidase, a new flavo-hemo-protein, is the site of oxygen reduction to water by the "strict anaerobe" *Desulfovibrio gigas*, *Biochem Biophys Res Commun* **193**(1), 100-105
5. Frazao, C., Silva, G., Gomes, C. M., Matias, P., Coelho, R., Sieker, L., Macedo, S., Liu, M. Y., Oliveira, S., Teixeira, M., Xavier, A. V., Rodrigues-Pousada, C., Carrondo, M. A., and Le Gall, J. (2000) Structure of a dioxygen reduction enzyme from *Desulfovibrio gigas*, *Nat Struct Biol* **7**(11), 1041-1045
6. Frey, M., Sieker, L., Payan, F., Haser, R., Bruschi, M., Pepe, G., and LeGall, J. (1987) Rubredoxin from *Desulfovibrio gigas*. A molecular model of the oxidized form at 1.4 Å resolution, *J Mol Biol* **197**(3), 525-541

7. Castro, G., Boswell, C. A., and Northrup, S. H. (1998) Dynamics of protein-protein docking: cytochrome c and cytochrome c peroxidase revisited, *J Biomol Struct Dyn* **16**(2), 413-424
8. Pearson, D. C., Jr., and Gross, E. L. (1998) Brownian dynamics study of the interaction between plastocyanin and cytochrome f, *Biophys J* **75**(6), 2698-2711
9. Katchalski-Katzir, E., Shariv, I., Eisenstein, M., Friesem, A. A., Aflalo, C., and Vakser, I. A. (1992) Molecular surface recognition: determination of geometric fit between proteins and their ligands by correlation techniques, *Proc Natl Acad Sci U S A* **89**(6), 2195-2199
10. Morris, G. M., Goodsell, D. S., Huey, R., and Olson, A. J. (1996) Distributed automated docking of flexible ligands to proteins: parallel applications of AutoDock 2.4, *J Comput Aided Mol Des* **10**(4), 293-304
11. Gardner, A. M., Helmick, R. A., and Gardner, P. R. (2002) Flavorubredoxin, an inducible catalyst for nitric oxide reduction and detoxification in *Escherichia coli*, *J Biol Chem* **277**(10), 8172-8177
12. Gomes, C. M., Giuffre, A., Forte, E., Vicente, J. B., Saraiva, L. M., Brunori, M., and Teixeira, M. (2002) A novel type of nitric-oxide reductase. *Escherichia coli* flavorubredoxin, *J Biol Chem* **277**(28), 25273-25276
13. Mukhopadhyay, P., Zheng, M., Bedzyk, L. A., LaRossa, R. A., and Storz, G. (2004) Prominent roles of the NorR and Fur regulators in the *Escherichia coli* transcriptional response to reactive nitrogen species, *Proc Natl Acad Sci U S A* **101**(3), 745-750
14. Justino, M. C., Vicente, J. B., Teixeira, M., and Saraiva, L. M. (2005) New genes implicated in the protection of anaerobically grown *Escherichia coli* against nitric oxide, *J Biol Chem* **280**(4), 2636-2643
15. Silaghi-Dumitrescu, R., Coulter, E. D., Das, A., Ljungdahl, L. G., Jameson, G. N., Huynh, B. H., and Kurtz, D. M., Jr. (2003) A flavodiiron protein and high molecular weight rubredoxin from *Moorella thermoacetica* with nitric oxide reductase activity, *Biochemistry* **42**(10), 2806-2815
16. Silaghi-Dumitrescu, R., Ng, K. Y., Viswanathan, R., and Kurtz, D. M., Jr. (2005) A flavo-diiron protein from *Desulfovibrio vulgaris* with oxidase and nitric oxide reductase activities. Evidence for an in vivo nitric oxide scavenging function, *Biochemistry* **44**(9), 3572-3579
17. Loubinoux, J., Valente, F. M., Pereira, I. A., Costa, A., Grimont, P. A., and Le Faou, A. E. (2002) Reclassification of the only species of the genus *Desulfomonas*, *Desulfomonas pigra*, as *Desulfovibrio piger* comb. nov., *Int J Syst Evol Microbiol* **52**(Pt 4), 1305-1308
18. Gomes, C. M., Vicente, J. B., Wasserfallen, A., and Teixeira, M. (2000) Spectroscopic studies and characterization of a novel electron-transfer chain from *Escherichia coli* involving a flavorubredoxin and its flavoprotein reductase partner, *Biochemistry* **39**(51), 16230-16237
19. Susin, S., Abian, J., Sanchez-Baeza, F., Peleato, M. L., Abadia, A., Gelpi, E., and Abadia, J. (1993) Riboflavin 3'- and 5'-sulfate, two novel flavins accumulating in the roots of iron-deficient sugar beet (*Beta vulgaris*), *J Biol Chem* **268**(28), 20958-20965
20. Fischer, D. S., and Price, D. C. (1964) A Simple Serum Iron Method Using the New Sensitive Chromogen Tripyridyl-S-Triazine, *Clin Chem* **10**, 21-31
21. Smith, P. K., Krohn, R. I., Hermanson, G. T., Mallia, A. K., Gartner, F. H., Provenzano,

D. gigas Flavodiiron Protein: interaction with rubredoxin and NO vs. O₂ reduction

- M. D., Fujimoto, E. K., Goeke, N. M., Olson, B. J., and Klenk, D. C. (1985) Measurement of protein using bicinchoninic acid, *Anal Biochem* **150**(1), 76-85
22. Nocek, J. M., Zhou, J. S., De Forest, S., Priyadarshy, S., Beratan, D. N., Onuchic, J. N., and Hoffman, B. M. (1996) Theory and Practice of Electron Transfer within Proteinminus signProtein Complexes: Application to the Multidomain Binding of Cytochrome c by Cytochrome c Peroxidase, *Chem Rev* **96**(7), 2459-2490
 23. Beratan, D., and Skourtis, S. (1998) Electron transfer mechanisms, *Curr Opin Chem Biol* **2**(2), 235-243
 24. Winkler, J. R. (2000) Electron tunneling pathways in proteins, *Curr Opin Chem Biol* **4**(2), 192-198
 25. Rodrigues, R., Vicente, J. B., Felix, R., Oliveira, S., Teixeira, M., and Rodrigues-Pousada, C. (2006) Desulfovibrio gigas flavodiiron protein affords protection against nitrosative stress in vivo, *J Bacteriol* **188**(8), 2745-2751
 26. Silva, G., Oliveira, S., LeGall, J., Xavier, A. V., and Rodrigues-Pousada, C. (2001) Analysis of the Desulfovibrio gigas transcriptional unit containing rubredoxin (rd) and rubredoxin-oxygen oxidoreductase (roo) genes and upstream ORFs, *Biochem Biophys Res Commun* **280**(2), 491-502
 27. Gomes, C. M., Silva, G., Oliveira, S., LeGall, J., Liu, M. Y., Xavier, A. V., Rodrigues-Pousada, C., and Teixeira, M. (1997) Studies on the redox centers of the terminal oxidase from Desulfovibrio gigas and evidence for its interaction with rubredoxin, *J Biol Chem* **272**(36), 22502-22508



Module fusion in an A-Type Flavoprotein from the cyanobacterium *Synechocystis* condenses a multiple component pathway in a single polypeptide chain ‡

8.1	Introduction	177
8.2	Materials and Methods	179
8.3	Results and Discussion	181
8.4	Conclusions	188
8.5	References	189

SUMMARY

The A-type flavoproteins (ATF) are modular proteins involved in multi-component electron transfer pathways, having oxygen reductase activity. They are complex flavoproteins containing two distinct structural domains, one having an FMN in a flavodoxin-like fold and the other a binuclear iron centre within a metallo- β -lactamase like fold. Here we report the purification and characterisation of a recombinant ATF from the cyanobacterium *Synechocystis* sp. PCC 6803, which has the unique feature of comprising an additional third domain with similarities towards flavin:NAD(P)H reductases. The latter was expressed independently as a truncated protein form and found to be capable of receiving electrons from NADH as well as to indiscriminately bind either one FAD or one FMN with equivalent affinities. Further kinetic studies have shown that the intact ATF is an NADH:oxygen oxidoreductase, with the catalytic ability to fully reduce oxygen to water. Thus, this constitutes an example on how structural modules found within partner proteins from an electron transfer pathway can be combined in a single polypeptide chain achieving identical catalytic activities.

‡This Chapter was published in the following article:

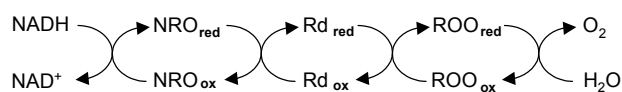
Vicente, J.B., Gomes, C.M., Wasserfallen, A. and Teixeira, M. (2002) "Module fusion in an A-Type Flavoprotein from the cyanobacterium *Synechocystis* condenses a multiple component pathway in a single polypeptide chain", *Biochem Biophys Res Commun* 294 (1): 82-87

The molecular biology procedures undertaken to clone the target proteins for over-expression were performed in the Institut für Mikrobiologie, Eidgenössische Technische Hochschule, ETH, Zürich, Switzerland, with the help of S. Ragetti.

8.1 INTRODUCTION

The A-type flavoproteins (ATF) are a family of soluble enzymes, with dioxygen reductase activity, so far exclusively found in anaerobes and facultative aerobes. The family was originally defined solely on the basis of amino acid sequence comparisons (1), but recent biochemical and structural data obtained for some of its members allowed a significant progress towards the overall understanding of the family (2-5). The ATF are modular proteins, having a flavodoxin and a metallo-β-lactamase domains as core modules (4). Whereas the former is closely related to canonical flavodoxins, containing one FMN, the second is quite distinct from the metallo-β-lactamases, as the catalytic zinc centre found in these proteins has been replaced by a diiron site, and the substrate binding groove was eliminated (4). This accounts for the observed catalytic activity of these proteins, which are able to reduce molecular oxygen to water (2,3,6). The best studied ATF is the rubredoxin:oxygen oxidoreductase (ROO) from the sulfate reducing bacterium *Desulfovibrio gigas*. This protein was found to be the terminal element of a three component electron transfer pathway that operates when this anaerobe is exposed to oxygen (6-8). In these conditions, polyglucose is consumed and the electrons from NADH produced in the early steps of glycolysis are transferred through an NADH oxidoreductase to a type I rubredoxin, which finally donates electrons to ROO (Scheme 8.1). This enzyme fully reduces dioxygen to water, thus scavenging it.

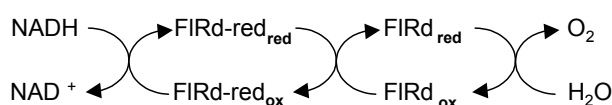
The crystal structure of ROO was recently determined



Scheme 8.1

which allowed the identification of the family composing structural modules (4). Whereas most of the composing members of this family solely consist of the two ATF core modules, inspection of amino acid sequence alignments shows that there are two exceptions in which additional modules are present in the same polypeptide chain. One case is found in *Escherichia coli*, whose ATF core is fused

to a rubredoxin domain at the C-terminus side (1,3). This protein was named Flavorubredoxin (FIRd) and its characterisation showed that it contains a rubredoxin FeS centre apart from the FMN and diiron sites (3). This is particularly interesting considering that *D. gigas* ROO was shown to receive electrons directly from a rubredoxin, which is encoded in the same operon as ROO (2,4,9). Thus, the three component pathway observed in the sulfate reducer has been condensed into a two component system operating in *E. coli*, involving a NADH:flavorubredoxin oxidoreductase (FIRd-red) and a flavorubredoxin (3). Interestingly, these two proteins form a putative dicistronic unit (Scheme 8.2).



Scheme 8.2

The other case, which is even more extreme, is observed in the

cyanobacteria *Synechocystis* and *Anabaena*. Analysis of the genomes of these organisms shows that multiple copies of distinct ATFs are encoded: four in *Synechocystis* (1,10) and six in *Anabaena* (11). Analysis of these sequences establishes that there is an additional NAD(P)H:flavin oxidoreductase module fused at the C-terminus side of the ATF core region. This analysis suggests that these cyanobacterial proteins may be able to receive electrons directly from NAD(P)H, transferring them directly to the catalytic diiron site, thus bypassing rubredoxin. If these proteins are capable of mediating electron transfer from NAD(P)H to dioxygen this would indicate a complete condensation of the above mentioned multi-component pathways into a single protein. This hypothesis was tested by studying a recombinant ATF from *Synechocystis* PCC. 6803, which is here reported.

8.2 MATERIALS AND METHODS

Amplification, cloning and expression - The gene coding for *Synechocystis* ATF, SsATF573, was amplified from cosmid cs0236 DNA from the gene bank of

Synechocystis strain PCC 6803 (10) using primers Syne1, 5'-GGAGTACCCATATGTTCAC₃' (*Nde*I site underlined), and Syne2, 5'-CCTTGAAAAGCTTTGCGGT-3' (*Hind*III site underlined). The amplified DNA was cut with *Nde*I and *Hind*III and cloned into plasmid pUC28 (12). After sequence verification, the gene was recloned into expression vector pET24a (Novagen) and named pME2336, and the protein was overexpressed in BL21(DE3) cells at 30°C upon 10h induction with 25 μM IPTG at an OD⁶⁰⁰ of ca.0.3. The gene coding for the C-terminal part of *Ss*ATF573, *Ss*ΔATF171, was amplified from the same source using primers Syne4, 5'-CTTGGCTCATATGCTCATCC-3' (*Nde*I site underlined) and Syne2. The amplified DNA was cut, cloned, sequenced, recloned in pET24a (to give plasmid pME2470), and *Ss*ΔATF171 was overexpressed as described above. Cells were grown as previously described (1,3).

Protein purification – Cell disruption was performed in a French Press cell at 7000 PSI, followed by separation of the soluble extract from membranes through 17 hour ultracentrifugation at 100.000g, at 5°C. Purification of *Ss*ATF573 was performed using a HiLoad Pharmacia system. For this protein, the soluble extract was dialysed against 10 mM Tris-HCl pH 7.6 (buffer A) and subsequently applied to a 34-ml Q-Sepharose column previously equilibrated with buffer A. The protein eluted at ~450 mM NaCl, was concentrated on a Diaflo cell using a YM10 cut off membrane and then applied to a Superdex S-75 gel filtration column, equilibrated and eluted with buffer A plus 150 mM NaCl, at 0.75 ml/min. The truncated *Ss*ΔATF171 protein was purified in two steps using 3.5 ml custom-packed Econo-Pac columns (15 x 20 mm) equilibrated in 20 mM potassium phosphate buffer at pH 6 (buffer B). *Ss*ΔATF171 was collected in the flow-through of a Q-Sepharose Fast Flow column, and was subsequently applied on an SP-Sepharose column which was eluted with a step gradient of potassium chloride in buffer B. *Ss*ΔATF171 eluted with ca. 200 mM KCl in buffer B. Protein purity was evaluated by SDS-gel electrophoresis (13) and pure protein was divided in

aliquots and stored at -70°C .

Spectroscopic methods – Ultra-violet/Visible spectra and kinetic assays were recorded in thermostated spectrophotometers, equipped with cell stirring systems (Shimadzu UV 1603 and Shimadzu Multispec 1501 diode-array).

Biochemical methods – Protein purity along the purification steps was assayed with SDS-PAGE mini-gels as described (13), using a molecular mass standards Kit (Pharmacia) ranging from 14.4 kDa to 97 kDa. Protein concentration was determined with a BCA (2-Bicinchoninic Acid) Protein Assay Kit (Pierce) and by the Bradford (14) method.

Kinetic assays – NAD(P)H oxidation was followed at 340 nm in 10 mM Tris-HCl pH 7.6 ($\epsilon^{340}_{\text{NAD(P)H}} = 6200 \text{ M}^{-1}\cdot\text{cm}^{-1}$) and ferricyanide reduction was followed at 420 nm ($\epsilon^{420}_{\text{Ferricyanide}} = 1020 \text{ M}^{-1}\cdot\text{cm}^{-1}$). NAD(P)H:cytochrome c oxidoreductase assays were performed as previously described (15), except that free flavins were absent from the reaction mixture. For oxygen reduction/consumption assays, a YSI-Micro cell Clark-type oxygen electrode was used, thermostated at 37°C and 40°C for assays with NAD(P)H and ascorbate as electron donors, respectively. Catalase and superoxide dismutase (Sigma) were used to determine if water was the final product of oxygen reduction.

Cofactor analysis and reconstitutions – The iron content of SsATF573 was determined by the 2,4,6-tripyridil-1,3,5-triazine method (16). Flavins were quantified spectrometrically ($\epsilon_{\text{ave}} = 12000 \text{ M}^{-1}\cdot\text{cm}^{-1}$) after extraction with TCA (10%) followed by centrifugation and supernatant neutralization with 1M $\text{NH}_4\text{CH}_3\text{COO}$, pH 7.0. Flavin HPLC analysis was performed as in (17). Flavins were reconstituted either by overnight incubation at 4°C with equimolar amounts of free FAD and FMN followed by dialysis against 10 mM Tris-HCl pH 7.6, or by titration of the apoprotein as in (18). Small aliquots of 30 μM Ss Δ ATF171 apoprotein were added to 3 μM of free flavin (FAD or FMN) in 100 mM KPi, 0.3 mM EDTA, pH 7.0 in a spectrophotometer cell and the UV-visible spectrum was

recorded after each addition. Spectral changes were followed at 512 nm, after observation of differential spectra, and the data were analysed using MATLAB (Mathworks, South Natick, MA, USA).

Sequence analysis tools – Searches for similar proteins in databases were performed using the BLAST, TBLASTN, and PSI-BLAST algorithms) using mainly NCBI-BLAST. The search for conserved domains was done using the CD-browser at NCBI. The 3DPSSM (19) fold recognition server (<http://www.bmm.icnet.uk/~3dpssm/>) carried out sequence threading. Multiple alignments were performed using CLUSTAL X (20) version 1.8.

8.3 RESULTS AND DISCUSSION

Proteomic and genomic analysis – As elucidated from the crystal structure of *D. gigas* ROO, the metallo- β -lactamase and flavodoxin like domains constitute the core architecture of A-type flavoproteins, and are present among all known members of this family. Inspection of sequence databanks and genomic data shows that the cyanobacteria *Synechocystis* sp. PCC 6803 (10) and *Anabaena* sp. PCC 7120 (11) contain respectively four and six distinct copies of ATF genes. Further, these



Figure 8.1 - **Structural modules present in several A-type flavoproteins.** Boxes represent structural domains and the text inside them the redox cofactors present. Light grey box, metallo- β -lactamase domain; medium-grey box, flavodoxin domain; dark-grey box, rubredoxin domain; black box, NAD(P)H:flavin oxidoreductase domain. Fe-Fe, binuclear iron site; FMN, flavin adenine mononucleotide; Rd, rubredoxin-type FeS centre; Flav, Flavin, either FMN or FAD in the case of *Synechocystis* ATF573 protein (see text).

proteins contain a C-terminal extension of about 170 amino acid residues, suggesting the presence of an additional structural module. In fact, analysis of the 10 sequences of the cyanobacterial ATFs, using a database of conserved domains,

confirmed that they harbour three distinct domains: a metallo- β -lactamase, a flavodoxin and an additional flavin reductase-like domain (Fig. 8.1).

An amino acid sequence comparison was carried out between the *Synechocystis* and *Anabaena* proteins, and *D. gigas* ROO, the structural prototype of the family (Fig. 8.2). The cyanobacterial ATFs are very similar between themselves in all their extension, having amino acid identities ranging from 31 to 66% and similarities from 52 to 83%. A direct comparison of the ATF core region (typically between residue 1 and 400) towards *D. gigas* ROO shows a lower degree of conservation, with ~20% identity and ~40% similarity. This does not reflect any major structural difference between these proteins, as threading analysis performed on the cyanobacterial ATFs shows that they all have a high probability of assuming the overall ROO fold. Nevertheless, analysis of the sequence alignment shows that there are some subtle differences in respect to cofactor binding residues. Concerning the di-iron site binding residues, half of the cyanobacterial ATFs do not have all of the ligands of the *D. gigas* motif H⁷⁹-X-E⁸¹-X-D⁸³-X₆₂-H¹⁴⁶-X₁₈-D¹⁶⁵-X₆₀-H²²⁶ conserved (Fig. 8.2, marked with *), thus suggesting that a modified ligation set exists or that those two proteins simply lack the centre. Interestingly, somehow conservative substitutions are observed: H⁸¹-X-(N/S)⁸³-X-N⁸⁵-X₆₄-R¹⁴⁹-X₁₉-K¹⁶⁸-X₅₇-H²²⁵ (SsATF594 numbering). As for the flavodoxin domain, the set of ligands that has been identified in ROO as being involved in contacts with the FMN molecule are, in overall, also found on the cyanobacterial ATFs. Two FMN stabilising regions can be proposed: one involved in contacts with the phosphate group (FMN 1 in Fig. 8.2) and the other with the isoalloxazine ring and ribityl chain (FMN 2 in Fig. 8.2). Two other residues that are also in close contact to the FMN group, and which are present among the compared ATFs are an aromatic residue in the first position of the partly conserved WPD motif and a strictly conserved proline (Fig 8.2, marked with #).

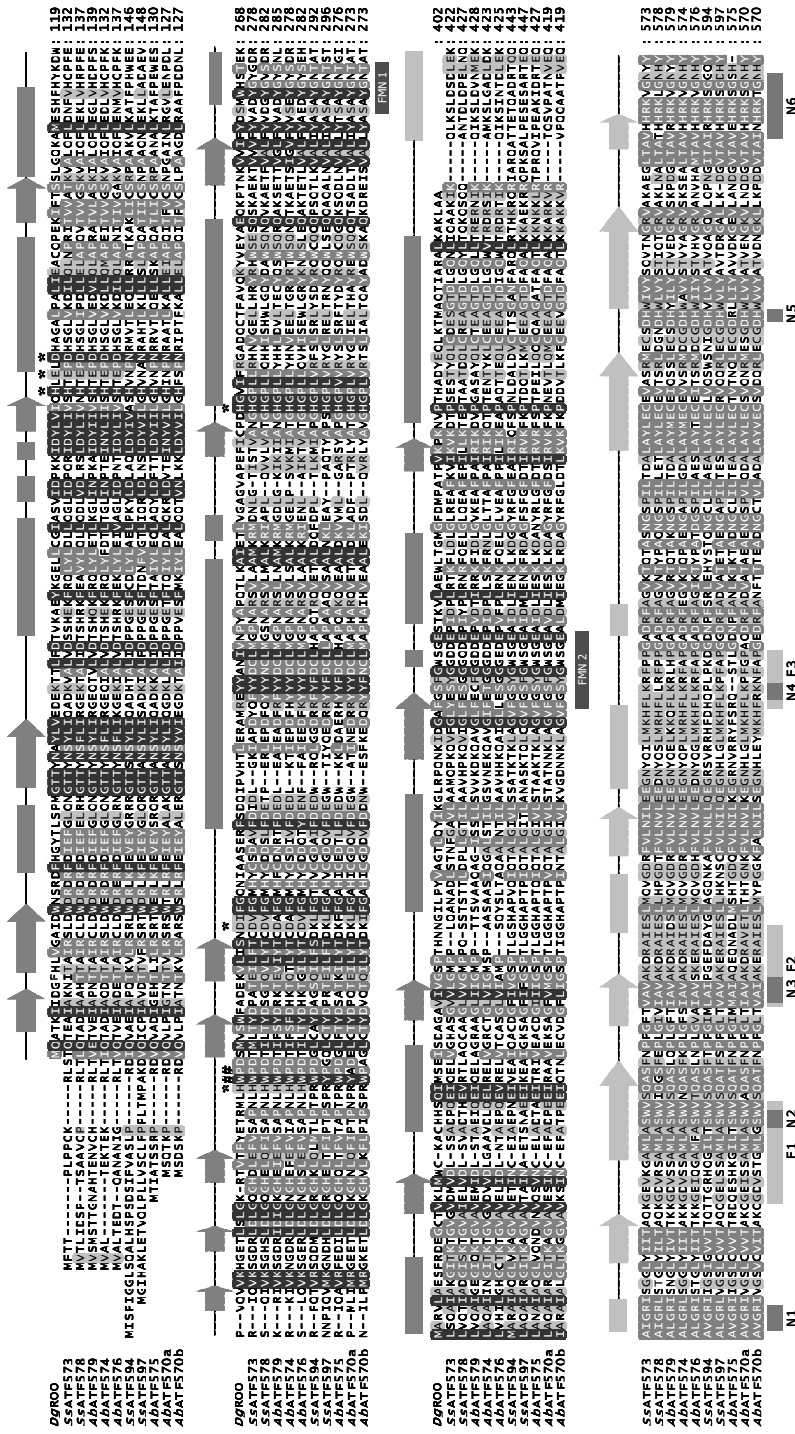
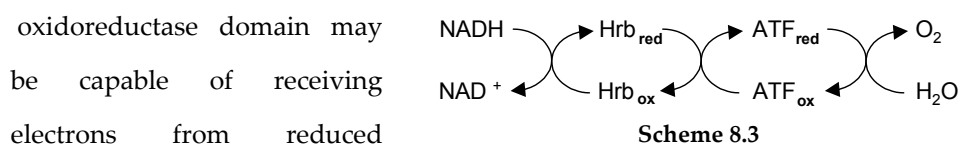


Figure 8.2 - Amino acid sequence alignment of cyanobacterial A-type flavoproteins The ATF from *Synechocystis* PCC. 6803, *Anabaena* sp. PCC 7120 and *D. gigas* ROO were aligned using Clustal X: SsATF573 (S75748), SsATF578 (S74578), SsATF594 (S74576), SsATF597 (S76209), AbATF579 (NP_484222.1), AbATF574 (NP_487935.1), AbATF576 (NP_488486.1), AbATF575 (NP_488484.1), AbATF570a (NP_487931.1), AbATF570b (NP_484221.1), and DgROO (Q9F0J6). The residues involved in binding of the binuclear iron site in *D. gigas* ROO are marked with an asterisk (*), whereas the regions involved in contacts with the FMN are labeled as FMN1 and FMN2, and marked with a cardinal (#). The secondary structure of the C-terminus domain of cyanobacterial ATF was predicted using PISPRED. Arrows denote β -sheets and cylinders α -helices. The three regions proposed to bind flavin are marked in boxes labelled F1...F3 and the five regions involved in stabilising NAD(P)H are marked in boxes labeled N1...N5.

Features of the NAD(P)H:flavin oxidoreductase domain - The presence of the putative NAD(P)H:flavin oxidoreductase domain is uniquely found among the *Synechocystis* and *Anabaena* ATF proteins. This domain is similar to enzymes known to be flavin reductases, ferric reductases as well as various oxidoreductase and monooxygenase components (Pfam entry PF01613). The high molecular weight rubredoxin (Hrb) from *Moorella thermoacetica* (21) is also an interesting case in which a C-terminal NAD(P)H:flavin oxidoreductase domain is found fused to a N-terminal rubredoxin domain (Fig. 8.1). This protein, which exhibits ca. 30% identity and 45% similarity towards the C-terminal domain of the cyanobacterial ATFs, has the particular feature of being the putative redox partner of *Moorella thermoacetica* ATF, both being encoded in the same operon (21) (Scheme 8.3). Altogether, these findings suggest that this NAD(P)H:flavin



dinucleotides and transferring them either to a rubredoxin centre or to an FMN moiety. A detailed analysis of the NAD(P)H:flavin oxidoreductase domain was undertaken in order to identify putative flavin and NAD(P)H binding regions. A fold recognition study performed by the 3D-PSSM server indicated a strong similarity towards the tertiary structure of the *Archaeoglobus fulgidus* ferric reductase (22) (an expectancy value of 5.6E-13 was determined, corresponding to 95% certainty on the fold identification). Based on this similarity, which in terms of amino acid sequence corresponds to 24% identity, a molecular model was built for the *Synechocystis* SsATF573 protein from residue 419 to position 573 using the ferric reductase coordinates (PDB entry: 1ios). At this point it is important to stress that the residues involved in FMN and NAD(P)H binding in the *A. fulgidus* ferric reductase are not conserved in the sequences of its homologues (22), as most of the interactions with these cofactors are made through main chain

nitrogen or oxygen atoms. Thus, the regions putatively involved in cofactor binding (marked on Fig. 8.2) were identified by mapping the residues that are at less than 6 Å from the cofactor. Interestingly, in most cases these regions correspond to highly conserved areas. Nevertheless, an exact description of ligands will require a crystallographically determined structure.

Biochemical studies – In order to study the role of the NAD(P)H:flavin oxidoreductase domain in the cyanobacterial ATF proteins, SsATF573 was selected as a target. A truncated form of this protein, consisting on a 171 amino

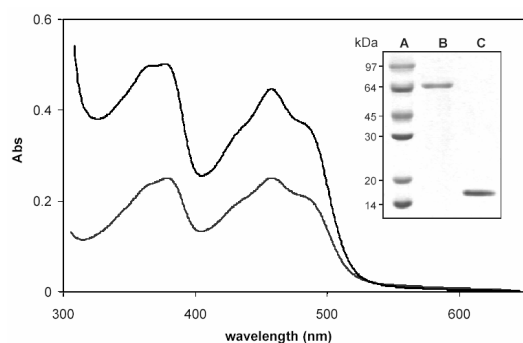


Figure 8.3 - UV-visible spectra of as purified proteins. Proteins are in Tris/HCl buffer, pH 7.6. Trace a: SsATF573 (100 μM); trace b. SsΔATF171 (25 μM). Inset : SDS-PAGE analysis of purified proteins. Lane A, molecular mass markers (Pharmacia); lane B, SsATF573; lane C, SsΔATF171.

acid long peptide comprising the NAD(P)H:flavin oxidoreductase domain was also designed. Both proteins were overexpressed in *E. coli* BL21(DE3)Gold cells and purified to homogeneity, as assayed by 12% SDS-PAGE gel electrophoresis (Fig. 8.3, inset).

The predicted molecular masses for the proteins based on their

sequence, are slightly different from the values calculated from gel electrophoresis. The intact SsATF573 is a 63.5 kDa protein, whereas the truncated form SsΔATF171 has 18.4 kDa, although the apparent masses are 70 kDa and 16 kDa, respectively. The UV/visible spectra of both proteins (Fig. 8.3) show features typical of flavoproteins, having two major bands with maxima at 378 nm and 458 nm.

Cofactor analysis – The selected *Synechocystis* ATF is a complex flavoprotein, containing multiple redox cofactors. The as purified intact SsATF573 was found to contain an amount of flavin substoichiometric in respect to the expected 2 moles of flavin per molecule, a situation which is commonly observed among

flavoproteins. The truncated Ss Δ ATF171 form contains 0.8 mol of flavin per mol of protein. In order to identify and quantify the relative flavin content, an acid extraction was performed and the extracts resolved by HPLC using free FAD and FMN as standards. The intact SsATF573 was found to contain both FMN and FAD, in a 3:1 ratio. On the other hand, the Ss Δ ATF171 form contains equimolar amounts of FMN and FAD. To confirm this, spectrophotometric titrations were done, where apoprotein was added to free flavin solutions and a spectrum was collected after each addition, as in (18). Absorbance changes at 512 nm were plotted against apoprotein/flavin ratio (*data not shown*) and a clear intercept is detected at 1 mol of apoprotein per mol of flavin. The latter result indicates that the NAD(P)H:flavin oxidoreductase domain randomly binds one mol of FAD or FMN. The correct interpretation of the flavin ratio observed for the intact protein lies on an established feature of ATF proteins, which is the fact that the FMN which is found in the flavodoxin fold is very poorly labile. Thus, the FMN/FAD ratio of 3 is explainable assuming that the flavodoxin site is fully loaded, whereas the flavin binding site of the NAD(P)H:flavin oxidoreductase domain either contains FAD or FMN. Considering that in SsATF573 there is a conservation of the motif that accounts for binding of a binuclear iron site in ATF proteins (see above), the amount of iron present on the purified sample was determined. Pure SsATF573 contains approximately 2 moles of iron per protein (1.9 mol Fe/mol of protein) thus indicating that a bimetallic iron site is indeed present in this protein. Iron was found to be absent from the Ss Δ ATF171 protein.

Kinetic properties – Considering the presence of the NAD(P)H:flavin oxidoreductase domain in the *Synechocystis* SsATF573 protein, the ability of this protein to be directly reduced by NADH was tested. An *in vitro* assay was performed, following the NADH:cytochrome c oxidoreductase activity. The measured rate in turnover number units (24 min^{-1} , at 25°C) is very similar to the one determined for the *Escherichia coli* 4-hydroxyphenylacetate 3-monooxygenase

reductase component (33.4 min^{-1} , at 25°C , calculated from (15)). This protein also belongs to the above mentioned family of proteins containing a NAD(P)H:flavin oxidoreductase domain (15), and has a canonical NAD(P)H:flavin oxidoreductase activity. As determined from NAD(P)H:ferricyanide oxidoreductase assays, the SsATF573 protein displays a greater affinity for NADH ($K_M=22.4 \text{ }\mu\text{M}$, 25°C) than for NADPH ($K_M=130 \text{ }\mu\text{M}$, 25°C) (data not shown).

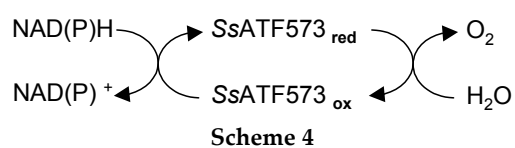
Having established that the SsATF573 protein can receive electrons from reduced nucleotides, its ability to catalyse the reduction of dioxygen to water, a catalytic activity present in all ATF proteins so far studied, remained to be tested. Assays performed on a Clark-type oxygen electrode showed that in the presence of NADH SsATF573 consumes oxygen at a rate of $0.38 \pm 0.05 \text{ min}^{-1}$, and at a rate of $0.20 \pm 0.06 \text{ min}^{-1}$ in the presence of NADPH. Further, as the addition of catalase and superoxide dismutase at the end of the assay had no effect on the observed rate. Thus, it can be concluded that oxygen is completely reduced to water, and that no partially reduced oxygen species are formed during catalysis.

Altogether, these experiments show that the *Synechocystis* SsATF573 is capable of linking NADH oxidation to oxygen reduction, an activity that requires three proteins in *D. gigas* (2,6), and two in *E. coli* (3). In order to compare the oxygen reductase activities of the different A-type flavoproteins, which all have distinct electron donors, a polarographic assay was outlined in which ascorbate was used as electron donor for the ATF proteins. The caveat of this assay is that the rates obtained are underestimated with respect to the physiological ones as ascorbate is an unspecific reductant. However, the great advantage is that it provides a comparable measure of the oxygen reductase activity, without generating partially reduced oxygen species. In fact, with this assay, all ATFs tested have identical oxygen reduction rates of approximately 0.1 min^{-1} .

8.4 CONCLUSIONS

The A-type flavoproteins are modular multi-redox cofactor containing flavoproteins (1). Here we reported the characterisation of one of these proteins from *Synechocystis* sp. PCC 6803, a representative member of the cyanobacterial type ATFs. Unlike all other so far known members of the ATF family, these proteins contain a NADH:flavin oxidoreductase module additionally to the two other core metallo- β -lactamase and flavodoxin structural domains. The studied protein was found to have NADH:oxygen oxidoreductase activity, thus showing that a single polypeptide chain condenses a multiple component pathway as observed in other organisms (2) (Scheme 8.4). This constitutes an excellent

example of module fusion of structurally independent units in a single protein. Future studies aimed



at comparing the inter- and intra- protein electron transfer kinetics of ATF proteins will eventually provide insights allowing to establish what is the extent of the role played by functional factors on driving protein evolution by module arrangement. The presence of these proteins in all of the so far sequenced obligate and facultative anaerobes genomes, co-related to the biochemical data available for some of the members of the ATF family, suggests that these proteins may have a role in the response to transient oxidative stress conditions. Furthermore, it was recently suggested that the enzyme from *E. coli* may be capable of acting as a NO reductase (23). This activity remains to be proven among the purified proteins but, if confirmed, it will strongly enhance the important physiological function of A-type flavoproteins.

8.5 REFERENCES

1. Wasserfallen, A., Ragetti, S., Jouanneau, Y., and Leisinger, T. (1998) A family of flavoproteins in the domains Archaea and Bacteria, *Eur J Biochem* **254**(2), 325-332
2. Gomes, C. M., Silva, G., Oliveira, S., LeGall, J., Liu, M. Y., Xavier, A. V., Rodrigues-Pousada, C., and Teixeira, M. (1997) Studies on the redox centers of the terminal oxidase from *Desulfovibrio gigas* and evidence for its interaction with rubredoxin, *J Biol Chem* **272**(36), 22502-22508
3. Gomes, C. M., Vicente, J. B., Wasserfallen, A., and Teixeira, M. (2000) Spectroscopic studies and characterization of a novel electron-transfer chain from *Escherichia coli* involving a flavorubredoxin and its flavoprotein reductase partner, *Biochemistry* **39**(51), 16230-16237
4. Frazao, C., Silva, G., Gomes, C. M., Matias, P., Coelho, R., Sieker, L., Macedo, S., Liu, M. Y., Oliveira, S., Teixeira, M., Xavier, A. V., Rodrigues-Pousada, C., Carrondo, M. A., and Le Gall, J. (2000) Structure of a dioxygen reduction enzyme from *Desulfovibrio gigas*, *Nat Struct Biol* **7**(11), 1041-1045
5. Gomes, C. M., Frazao, C., Xavier, A. V., Legall, J., and Teixeira, M. (2002) Functional control of the binuclear metal site in the metallo-beta-lactamase-like fold by subtle amino acid replacements, *Protein Sci* **11**(3), 707-712
6. Chen, L., Liu, M. Y., LeGall, J., Fareleira, P., Santos, H., and Xavier, A. V. (1993) Rubredoxin oxidase, a new flavo-hemo-protein, is the site of oxygen reduction to water by the "strict anaerobe" *Desulfovibrio gigas*, *Biochem Biophys Res Commun* **193**(1), 100-105
7. Chen, L., Liu, M. Y., Legall, J., Fareleira, P., Santos, H., and Xavier, A. V. (1993) Purification and characterization of an NADH-rubredoxin oxidoreductase involved in the utilization of oxygen by *Desulfovibrio gigas*, *Eur J Biochem* **216**(2), 443-448
8. Santos, H., Fareleira, P., Xavier, A. V., Chen, L., Liu, M. Y., and LeGall, J. (1993) Aerobic metabolism of carbon reserves by the "obligate anaerobe" *Desulfovibrio gigas*, *Biochem Biophys Res Commun* **195**(2), 551-557
9. Silva, G., Oliveira, S., LeGall, J., Xavier, A. V., and Rodrigues-Pousada, C. (2001) Analysis of the *Desulfovibrio gigas* transcriptional unit containing rubredoxin (rd) and rubredoxin-oxygen oxidoreductase (roo) genes and upstream ORFs, *Biochem Biophys Res Commun* **280**(2), 491-502
10. Kaneko, T., Tanaka, A., Sato, S., Kotani, H., Sazuka, T., Miyajima, N., Sugiura, M., and Tabata, S. (1995) Sequence analysis of the genome of the unicellular cyanobacterium *Synechocystis* sp. strain PCC6803. I. Sequence features in the 1 Mb region from map positions 64% to 92% of the genome, *DNA Res* **2**(4), 153-166, 191-158
11. Kaneko, T., Nakamura, Y., Wolk, C. P., Kuritz, T., Sasamoto, S., Watanabe, A., Iriguchi, M., Ishikawa, A., Kawashima, K., Kimura, T., Kishida, Y., Kohara, M., Matsumoto, M., Matsuno, A., Muraki, A., Nakazaki, N., Shimpo, S., Sugimoto, M., Takazawa, M., Yamada, M., Yasuda, M., and Tabata, S. (2001) Complete genomic sequence of the filamentous nitrogen-fixing cyanobacterium *Anabaena* sp. strain PCC 7120, *DNA Res* **8**(5), 205-213; 227-253
12. Benes, V., Hostomsky, Z., Arnold, L., and Paces, V. (1993) M13 and pUC vectors with new unique restriction sites for cloning, *Gene* **130**(1), 151-152

13. Garfin, D. E. (1990) One-dimensional gel electrophoresis, *Methods Enzymol* **182**, 425-441
14. Bradford, M. M. (1976) A rapid and sensitive method for the quantitation of microgram quantities of protein utilizing the principle of protein-dye binding, *Anal Biochem* **72**, 248-254
15. Galan, B., Diaz, E., Prieto, M. A., and Garcia, J. L. (2000) Functional analysis of the small component of the 4-hydroxyphenylacetate 3-monooxygenase of *Escherichia coli* W: a prototype of a new Flavin:NAD(P)H reductase subfamily, *J Bacteriol* **182**(3), 627-636
16. Fischer, D. S., and Price, D. C. (1964) A Simple Serum Iron Method Using the New Sensitive Chromogen Tripyridyl-S-Triazine, *Clin Chem* **10**, 21-31
17. Susin, S., Abian, J., Sanchez-Baeza, F., Peleato, M. L., Abadia, A., Gelpi, E., and Abadia, J. (1993) Riboflavin 3'- and 5'-sulfate, two novel flavins accumulating in the roots of iron-deficient sugar beet (*Beta vulgaris*), *J Biol Chem* **268**(28), 20958-20965
18. Haines, D. C., Sevrioukova, I. F., and Peterson, J. A. (2000) The FMN-binding domain of cytochrome P450BM-3: resolution, reconstitution, and flavin analogue substitution, *Biochemistry* **39**(31), 9419-9429
19. Kelley, L. A., MacCallum, R. M., and Sternberg, M. J. (2000) Enhanced genome annotation using structural profiles in the program 3D-PSSM, *J Mol Biol* **299**(2), 499-520
20. Thompson, J. D., Gibson, T. J., Plewniak, F., Jeanmougin, F., and Higgins, D. G. (1997) The CLUSTAL_X windows interface: flexible strategies for multiple sequence alignment aided by quality analysis tools, *Nucleic Acids Res* **25**(24), 4876-4882
21. Das, A., Coulter, E. D., Kurtz, D. M., Jr., and Ljungdahl, L. G. (2001) Five-gene cluster in *Clostridium thermoaceticum* consisting of two divergent operons encoding rubredoxin oxidoreductase- rubredoxin and rubrerythrin-type A flavoprotein-high-molecular-weight rubredoxin, *J Bacteriol* **183**(5), 1560-1567
22. Chiu, H. J., Johnson, E., Schroder, I., and Rees, D. C. (2001) Crystal structures of a novel ferric reductase from the hyperthermophilic archaeon *Archaeoglobus fulgidus* and its complex with NADP⁺, *Structure* **9**(4), 311-319
23. Gardner, A. M., Helmick, R. A., and Gardner, P. R. (2002) Flavorubredoxin, an inducible catalyst for nitric oxide reduction and detoxification in *Escherichia coli*, *J Biol Chem* **277**(10), 8172-8177

9 | DISCUSSION

9.1	Structural and Functional Properties of Flavodiiron Proteins	192
	<i>Primary structure, domain arrangement and electron transfer chains</i>	192
	<i>Molecular properties</i>	193
	<i>Spectroscopic properties</i>	194
	<i>Redox properties</i>	196
	<i>Kinetic properties</i>	198
	<i>Structural properties</i>	200
9.2	Role of <i>Escherichia coli</i> Flavorubredoxin in	
	Nitric Oxide Detoxification	201
	<i>Genetic basis for a role in nitric oxide detoxification</i>	201
	<i>Nitric oxide reductase activity of flavodiiron proteins</i>	203
	<i>Nitric oxide reduction mechanism</i>	204
	<i>Nitric oxide vs. oxygen reduction by flavodiiron proteins</i>	206
	References	209

9.1 Structural and Functional Properties of Flavodiiron Proteins

Primary structure, domain arrangement and electron transfer chains

The family of flavodiiron proteins (FDPs) was primarily established on the basis of common sequence motifs that altogether constituted the flavodiiron core (1). This core comprises two structural domains, as first revealed by crystallographic studies on *Desulfovibrio gigas* rubredoxin:oxygen oxidoreductase (Dg_ROO) (2). FDPs have as their prototypical domain arrangement a C-terminal FMN-binding flavodoxin domain fused to a metallo- β -lactamase-like fold. An important development in the understanding of the functional properties of this protein was the finding of a novel type of non-haem diiron centre nested in the lactamase domain, with carboxylate and histidine residues in the first coordination sphere. Despite the conservation of the structural core, some members of this protein family bear extra C-terminal domains, which led to the division of the FDPs in three classes (3). Class A FDPs are the simplest, comprising solely the flavodiiron core. Class B FDPs – mainly found in enterobacteria – have a C-terminal rubredoxin (Rd) domain fused to the flavodiiron core, an interesting evolutionary event, since Rds are the redox partners of FDPs from several organisms (4-6). In cyanobacteria, another class of FDPs has been identified – Class C – bearing a C-terminal NAD(P)H:flavin oxidoreductase domain (7).

To accomplish NO or oxygen reduction, FDPs use the reducing equivalents derived from NAD(P)H, that are transported along *electron transfer (eT) chains*. The modular arrangement of FDPs reflects itself in the complexity of these eT chains. Whereas the *D. gigas* ROO (class A) requires rubredoxin and an NADH:rubredoxin oxidoreductase (5,8), *E. coli* FIRd (class B) has the Rd fused to the flavodiiron core, therefore requiring only the NADH oxidoreductase partner (9). More extreme is the case of cyanobacterial FDPs (class C), where the fused C-terminal NAD(P)H:flavin oxidoreductase module allows these proteins to couple

NAD(P)H oxidation to oxygen reduction, in a single polypeptide chain (7). It thus appears that the modular complexity of FDPs (or of the redox partners (6)) results in simplicity of the corresponding eT chains. The only exception to this observation is so far the case of methanogenic FDPs, that are proposed to accept electrons directly from $F_{420}H_2$ (10), an organic cofactor which acts as a general source of reducing equivalents in methanogens.

Phylogenetic analyses of available FDP sequences allow to propose that lateral gene transfer is responsible for this protein family to extend from Bacteria and Archaea to anaerobic protozoan pathogens (11,12). Analysing solely the flavodiiron cores, it is interesting to observe that class B FDPs (from enterobacteria) and class C FDPs (from cyanobacteria) each cluster as separate branches. This suggests that the fusion of extra C-terminal modules is an evolutionary event that occurred in primordial organisms that eventually evolved to enterobacteria and cyanobacteria.

Molecular Properties

Flavodiiron proteins of all three classes have been studied, the majority of which belong to class A. Class A FDPs have approximately 400 residues, whereas class B and class C FDPs are longer, due to the C-terminal extensions (~480 residues and ~600 residues, respectively). Quaternary arrangements of these soluble proteins vary between homodimeric and homotetrameric. The cofactor content of studied FDPs - determined by elemental analysis, colorimetric methods or spectroscopic techniques - yields ~1-2 Fe (~3 Fe in *E. coli* flavorubredoxin, one in the rubredoxin domain and two in the diiron site) and ~0.7-1 FMN per monomer. Iron incorporation into the diiron site of heterologously over-expressed FDPs has been optimized by growing the cells in minimal medium, supplemented with ferrous sulphate, with decreased aeration and temperature. By replacing Fe with Zn in the growth medium of cells over-expressing *Moorella thermoacetica* FDP (6), a

binuclear Zn-Zn site is obtained instead of the diiron site, which is accounted for by a significant affinity of the centre for Zn (13). The same metal substitution has been achieved in a truncated version of flavorubredoxin, consisting solely of its flavodiiron core (FDP-D) (*our unpublished observations*).

Spectroscopic Properties

As anticipated from the cofactor content, the **visible** and near UV absorption spectra of FDPs are dominated by the contribution of the flavin cofactor(s). The notable exception is *E. coli* flavorubredoxin, whose spectrum results from an overlap of the contribution of the flavin and rubredoxin [Fe-Cys₄] cofactors. Non-haem diiron proteins (14) have much lower extinction coefficients than flavins (free and protein-bound) (15). The flavin-dominated spectrum of FDPs displays

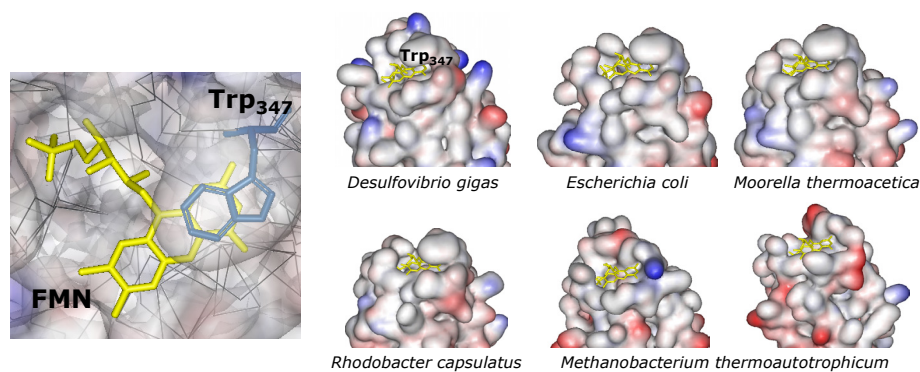


Figure 9.1 – Structural modelling of the FMN pocket. The structures of various FDP that have already been characterised were modelled in SwissModel, with *D. gigas* ROO structure (PDB entry 1e5d) as the template. Here, the FMN pocket is highlighted for the *D. gigas* ROO, stressing the superposition of the Trp347 aromatic ring over the pyrimidine ring of the FMN isoalloxazine core. The FMN pockets of the other modelled FDPs show that with the exception of the *Methanothermobacter thermoautotrophicus* enzymes, the conserved Trp residue is in the same position as for the ROO structure.

some heterogeneity among the proteins isolated from different sources: whereas the flavin band centered at ~450 nm is broad and smooth in some cases, in others this band has two shoulders. This band is commonly assigned to charge transfer transitions from the xylene ring to the pyrimidine ring, in the isoalloxazine core of the flavin cofactor. Based on structural modelling of the flavin pocket of different

FDPs with Dg_ROO structure as the template (Fig. 9.1), it is proposed that the conserved tryptophan residue (Trp347 in Dg_ROO) contributes to this spectral heterogeneity, being coplanar with the flavin isoalloxazine ring. As mentioned above, the visible spectrum of *E. coli* FIRD comprises also features from the [Fe-Cys₄] centre in its rubredoxin domain. Rubredoxins have unique spectral features, namely two major bands at approximately 380 nm and 490 nm, and a low absorption broad band around 570 nm (16).

Electron paramagnetic resonance (EPR) spectroscopy has been used to characterize the flavin cofactor in *D. gigas* ROO (5) and the iron centres in *E. coli* flavorubredoxin (17). In the case of Dg_ROO, a radical signal at $g \sim 2.0$ obtained under reductive conditions was attributed to the one-electron reduced semiquinone state of the flavin, which was determined to be a red anionic radical, from the 1.6 mT line width (5), in accordance with the data from visible spectroscopy. EPR studies on *E. coli* flavorubredoxin provided the spectroscopic fingerprints of each cofactor as probes for their redox state. Whereas the rubredoxin [Fe-Cys₄] centre is the only cofactor with an EPR signature in oxidized FIRD, upon reduction this signal decreases in intensity (spin changes from $S=5/2$ to $S=2$) (9,17). Due to the antiferromagnetic coupling of the two ferric ions, the diiron centre is only clearly EPR detectable in its one electron reduced mixed-valence ($\text{Fe}^{\text{III}}\text{-Fe}^{\text{II}}$) state, with a rhombic signal with g values at $g < 2.0$ (17). Upon full reduction this signal disappears and the only evidence for the diferrous state is a $g \sim 1.1$ signal in parallel-mode EPR. Besides the diiron centre, the signal for the one electron reduced FMN semiquinone is observed at $g \sim 2.0$.

Shilaghi-Dumitrescu and co-workers (6) have used **Mössbauer** spectroscopy to study the properties of the diiron centre from *M. thermoacetica* FDP. The data analysis for the ⁵⁷Fe-enriched recombinant protein showed that in the oxidized diferric state the iron ions were anti-ferromagnetically coupled, yielding a diamagnetic ground state. The different quadrupole splittings and asymmetry

parameters for the two quadrupole doublets used to fit the data, are assigned to two different iron environments of the centre, consistent with the distinct coordination spheres of each iron of the centre (18).

Redox Properties

The redox properties of FDPs have been determined only for a few cases, and focusing mainly on the flavin moiety (5,6,17). An interesting observation is the proximity of the two reduction potentials of the FMN moiety in at least three FDPs, which contrasts with the typical redox behaviour of flavodoxins. Due to the large separation of the reduction potentials ($E_{\text{FMN}_{\text{ox}}/\text{FMN}_{\text{sq}}}$ between -229mV and +121mV; $E_{\text{FMN}_{\text{sq}}/\text{FMN}_{\text{red}}}$ between -522mV and -372mV), flavodoxins stabilize the semiquinone state, which is accounted for by conformational rearrangements and a number of hydrogen bonds. Besides that, canonical flavodoxins tend to form the blue neutral semiquinone radical whereas FDP-bound flavodoxin modules stabilize the red anionic semiquinone. The fact that a red radical is formed in FDPs may correlate with a prevalence of basic over acidic residues in the FMN pocket (2). The pK_a of 8.3 for the equilibrium between the red and blue semiquinone forms of free FMN (15) could be lowered in the FDPs due to the presence of the excess basic residues, and thus result in the formation of a red semiquinone. It must be taken into account that the diiron centre is in close contact with the FMN moiety and thus an electrostatic influence in the redox potentials of each other is to be expected. At this point, there is not enough information to attribute a physiological relevance to this difference between canonical flavodoxins and the flavodoxin modules in FDPs.

A thorough redox characterisation was undertaken with *E. coli* flavorubredoxin and its reductase, combining potentiometric methods with visible and EPR spectroscopies. FIRd and FIRd-Red were titrated as isolated and in a stoichiometric mixture, to understand the role of each interacting partner on the

redox properties of the other. The obtained results are summarized in figure 9.2. In general terms, it was observed that the reduction potentials of the iron cofactors are upshifted upon interaction of the two redox partners, whereas those of the flavin moieties in FIRd (FMN) and its reductase (FAD) remain essentially

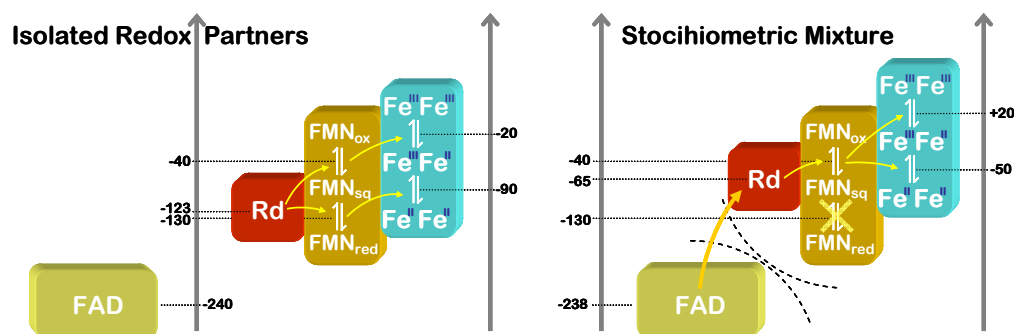


Figure 9.2 – Scheme summarizing the redox properties of flavorubredoxin and its reductase, as isolated (left) or in a stoichiometric mixture (right). Yellow arrows depict proposed electron transfer steps inferred from the thermodynamic parameters.

unaltered. This modulation of FIRd's reduction potentials by its cognate reductase poses the possibility of intra-molecular eT steps to be inferred differently, with respect to the reduction potentials of the isolated FIRd. In the isolated protein the more favourable intra-molecular eT mechanism involves full reduction of FMN, to further allow two electron reduction of the diiron site (fig. 9.2, left). However, upon interaction of the two redox partners, two significant redox shifts change the situation regarding possible eT mechanisms. On the one hand, the upshift in the Rd potential creates a thermodynamic barrier for full reduction (two electrons) of FMN. On the other hand, the upshift observed in the redox properties of the diiron centre allows the flavin semiquinone to act as a one-electron shuttle to the diiron, without the need to reach the hydroquinone state (fig. 9.2, right).

Assuming this eT mechanism on a pure thermodynamic basis, the “fully” reduced FIRd under “normal” operative conditions would have a total of four electrons available for reductive chemistry, sufficient to catalyze the reduction of

four NO to two N₂O or full reduction of oxygen to water.

Kinetic Properties

Data on the electron transfer kinetics of flavodiiron proteins are still scarce. The nature of the interaction between *D. gigas* ROO and its electron donor reduced rubredoxin was studied by a combination of steady-state kinetics and protein modelling studies (19). Pre-steady-state kinetics studies on FDPs have been performed for *E. coli* FIRd, focusing on the reactions that mediate FIRd reduction by NADH-derived reducing equivalents (20). By stopped-flow absorption spectroscopy, two distinct reactions were studied separately: the reaction of NADH with oxidized flavorubredoxin reductase (FIRd-Red) and the reaction of

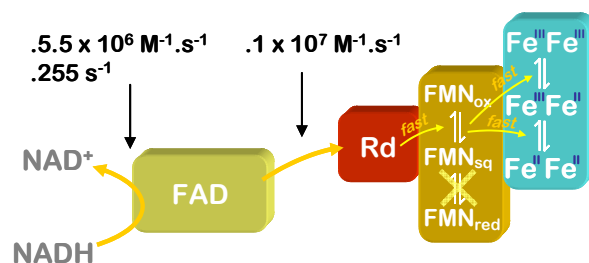


Figure 9.3 - Scheme depicting electron transfer mechanisms inferred from kinetics studies performed with *E. coli* flavorubredoxin and its reductase partner.

pre-reduced FIRd-Red with oxidized flavorubredoxin. The results are summarized in figure 9.3. In these studies, NADH – but not NADPH – was shown to efficiently reduce FIRd-Red ($k=5.5 \times 10^6 \text{ M}^{-1} \cdot \text{s}^{-1}$), in a reaction that apparently does

not involve partially reduced flavin semiquinone, thus resulting in an apparent two electron reduction, which in formal terms still has to be regarded as a two consecutive one-electron steps. The selectivity for NADH can be assigned - on the basis of studies with glutathione reductase (21) and dihydrolipoamide dehydrogenase (22) - to the presence of competent residues to form H-bonds with the ribose 2'-OH and 3'-OH groups of NADH and the absence of a nest of positively charged residues to stabilize the extra phosphate group in NADPH. The reaction of reduced FIRd-Red with FIRd was studied both with the intact FIRd and a truncated version consisting solely of its rubredoxin domain (Rd-D),

which is the electron entry point of FIRd (9). For the reduction of FIRd by its reductase, an apparent bimolecular rate constant of $\sim 2.4 \times 10^6 \text{ M}^{-1} \cdot \text{s}^{-1}$, whereas a rate of $\sim 1 \times 10^7 \text{ M}^{-1} \cdot \text{s}^{-1}$ was determined for the reduction of Rd-D. The strong pH and ionic strength dependences suggest a contribution of electrostatics for the formation of the eT complex, including protonable groups presumably at the interacting surfaces. The observed absorption changes upon reduction of FIRd reveal that the kinetic end-point has optical features of a flavin semiquinone, and that formation of this semiquinone (by one electron reduction of FMN) is synchronous with Rd reduction. Taking into account the proximity of the reduction potentials from the three cofactors in FIRd (fig. 9.2), a total of four electrons should equilibrate among the latter, when rubredoxin reduction is observed synchronously to the formation of the flavin semiquinone. Therefore, it may be proposed that the apparent rate of FIRd reduction ($\sim 2.4 \times 10^6 \text{ M}^{-1} \cdot \text{s}^{-1}$) is in fact in the order of $\sim 1 \times 10^7 \text{ M}^{-1} \cdot \text{s}^{-1}$ (as obtained for the Rd-D) and that four electrons quickly equilibrate among the three cofactors. The observation that the kinetic end-point of FIRd reduction is the flavin semiquinone is in agreement with the mechanistic proposal based on the redox properties of the system, which precludes the full reduction of the flavin to its hydroquinone state. This proposed mechanism finds resemblances in the reductive mechanism of modular flavocytochromes such as P450BM3, where FMN semiquinone also acts as a one electron shuttle to the haem active site. Furthermore, full reduction of the FMN moiety results in enzyme inactivation (23). The intra-molecular eT steps are currently under investigation by micro-second hyper freeze-quench coupled to visible and EPR spectroscopies (in collaboration with Prof. Simon de Vries, University of Delft, The Netherlands).

Structural Properties

Reports on structures of FDPs so far concern only the *D. gigas* ROO (Dg_ROO) (2) and *M. thermoacetica* FDP (Mt_FDP) (18). The two structures retain the “head-to-tail” homodimeric quaternary structure (described in Chapter 2), which ensures close proximity of the FMN moiety from one monomer with the diiron centre from the other monomer. The most significant difference is found in the first coordination sphere of the diiron centre. A histidine residue (His84 in Dg_ROO, His86 in Mt_FDP) that is conserved throughout the whole protein family is a ligand to the diiron site in Mt_FDP, but is replaced by a water molecule in Dg_ROO (Fig. 9.4). In fact, in the structure of Dg_ROO this His84 is displaced

from the centre. This difference could also be accounted for by slightly different redox states of the diiron site, due to the X-ray radiation. A physiological relevance to this difference has not yet been attributed, and more structures of FDPs must be elucidated before understanding which of the presently known cases is the exception in terms of the conserved His residue being or not a ligand. Moreover, this may contribute to understand substrate selectivity in the FDP family (see below). Structural studies are underway with *E. coli* FIRd, by a combination of structural biology techniques, with different aims. Crystals of the flavodiiron domain of *E. coli* FIRd (FDP-D) have been obtained in collaboration with the Protein Crystallography Laboratory (ITQB), led by Prof. Maria Arménia Carrondo, which were successfully measured at the European Synchrotron Radiation Facility (ESRF, Grenoble, France) with a resolution of 2.6 and 2.9 Å. Although FDP-D lacks the rubredoxin domain present in the full-length FIRd, it retains the flavodiiron minimal operative unit. In collaboration with Dr. Wolfram Meyer-Klaucke

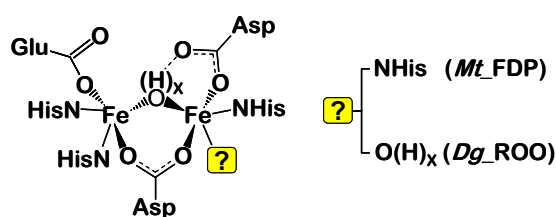


Figure 9.4 – Coordination sphere of *D. gigas* ROO and *M. thermoacetica* FDP.

(EMBL, Hamburg, Germany), Extended X-ray Absorption Fine Structure (EXAFS) studies have been performed with FDP-D in different redox states and reacted with possible substrates and inhibitors. Since crystals of full-length FIRd were never obtained, an alternative strategy was undertaken to understand the spatial arrangement of the different modules in FIRd, which is being done by Small Angle X-ray Scattering (SAXS), in collaboration with the group of Dr. Dmitri Svergun (EMBL, Hamburg, Germany). Altogether, the different approaches for structural studies on *E. coli* FIRd and its truncated domains will add more information to this protein family, possibly clarifying the role of the bound/unbound (?) conserved His residue (XR, EXAFS), providing the structure of redox and reaction intermediates of the diiron centre (EXAFS), and/or allowing to envisage the structure of full-length FIRd, even in the absence of a crystallographic structure (SAXS). The bulk of this work is in the phase of data analysis.

10.2 Role of *Escherichia coli* Flavorubredoxin in Nitric Oxide Detoxification

Genetic basis for a role in nitric oxide metabolism

The seminal work of Gardner and co-workers (24) provided the first clues for a role of flavorubredoxin in the protection of anaerobically-grown *E. coli* from NO-induced stress. By searching for putative regulators of NO metabolism in the genome of *E. coli*, it was observed that a homologue of *Rashtonia eutropha* NorR was adjacent to the flavorubredoxin-encoding gene, being that FIRd had been demonstrated to bind NO at the diiron centre (9). The FIRd-encoding gene, renamed to *norV* (from nitric oxide reductase), was shown to be induced by NO (24) and to contribute to the protection of important metabolic enzymes from NO stress, specially those harbouring Fe-S centres, common targets of NO-induced damages. *norV* was also induced by the nitrosative agent nitroprusside (25), in a

regulatory process involving *norR*. Regulation of *norV* expression by the *norR*-encoded product NorR has been the subject of extensive studies attempting to understand the molecular basis of this regulatory process (26-29). It has been demonstrated that NorR has an NO-sensing mononuclear Fe centre that upon NO binding induces a conformational change that de-represses the transcriptional activity of NorR with respect to *norV* (29).

Further evidence for a role of flavorubredoxin in NO detoxification has been retrieved from DNA microarray studies of *E. coli* cultures challenged with NO or/and the nitrosative agent GSNO, under various conditions, namely batch aerobic in rich medium (30), batch anaerobic in defined medium (31), and continuous in defined medium (32). *norV* and the gene encoding flavohaemoglobin (*hmpA*) are among the few common genes shown to be up-regulated in all three microarray conditions (33). Altogether, the molecular genetics studies place flavorubredoxin in a prominent place of NO-detoxifying enzymes as an NO reductase, alongside flavohaemoglobin (Hmp), with possible complementary roles, depending on several factors, such as oxygen availability, response times, growth media, etc. (34). Aside from other possible NO-detoxifying routes, many organisms have both Hmp(s) and FDP(s) in their genomes, whereas some appear to rely solely on either Hmp or FDP as possible NO scavengers. Notably, the regulation of FIRd (the only FDP whose regulation has been studied) and of Hmp are apparently independent of each other, having no common branches (35). As mentioned in chapter 1, microbes may encounter NO as an intermediate of neighbouring denitrifiers, or as a product of macrophage NO synthases as part of the host immune response to invading/infecting microbes. Therefore, the presence of two lines of defence (FDPs and Hmp) against the cytotoxic effects of NO confers robustness to microorganisms colonizing habitats with neighbouring denitrifiers, and/or may allow invading pathogens to subvert the host immune system. Recently, cells of

the protozoan pathogen *Trichomonas vaginalis* were shown to be endowed with NO-degrading activity in anaerobic conditions (36). This activity was assigned to a flavorubredoxin-like protein, on the basis of NADH dependence, cyanide insensitivity and inhibition by O₂. Moreover, this activity was attributed to a protein immunodetected with antibodies raised against *E. coli* FIRd.

Nitric oxide reductase activity of flavodiiron proteins

The molecular genetics studies suggesting a role of *E. coli* FIRd in NO detoxification (24) were followed by testing the NO reductase activity *in vitro* (37). By amperometric assays using an NO-specific electrode, the eT chain comprising FIRd-Red and FIRd was reconstituted *in vitro*, with NADH as the source of reducing equivalents. Flavorubredoxin was thus shown to reduce NO with a turnover of $\sim 15\text{ s}^{-1}$, in the order of the activities of *bona fide* respiratory NORs (see chapter 1). The K_m of FIRd for NO was predicted to be low on the basis of the NO consumption traces and further shown to be 1.2 μM (*our own unpublished data*). In the same report, the oxygen consumption of this system was misleadingly assigned to FIRd, whereas it resulted in fact from a direct reduction by FIRd-Red. Subsequently, other FDPs have been studied in terms of their NO and oxygen reductase activities, by similar amperometric methods. *Moorella thermoacetica* FDP (Mt_FDP) has comparable NO and O₂ reductase activities (respectively, 48 s⁻¹ and 50 s⁻¹), although the K_m for NO is lower than that of oxygen (5 μM and 26 μM , respectively) (6). In this report, the oxygen activity is considered as inhibitory towards the NO reductase activity. Complementation studies with a *norV*-deleted *E. coli* strain showed that Mt_FDP afforded *in vivo* protection against NO-induced stress. Similar measurements have been performed with FDPs from two *Desulfovibrio* strains, *D. gigas* and *D. vulgaris*. *D. vulgaris* FDP catalyses NO and O₂ reduction with similar efficiency (12 s⁻¹ and 17 s⁻¹, respectively) and affords the same protection as Mt_FDP to an *E. coli norV*⁻ strain against NO stress (38).

Recombinant *D. gigas* ROO has also a considerable NO reductase activity ($\sim 15 \text{ s}^{-1}$), and several molecular genetics results point to a role in NO detoxification in *D. gigas* (39) (Chapter 7). A mutant strain of *D. gigas* knocked-out in the *roo* gene displays greater sensitivity to NO and to the nitrosative agent GSNO (39) and transcriptional studies reveal induction of *roo* by GSNO (39). It should be noted, however, that even under limiting electron delivery conditions, the oxygen reductase activity of Dg_ROO is higher than the NO reductase activity ($\sim 50 \text{ s}^{-1}$), which opens the possibility of a dual role for these proteins in anaerobic organisms (discussed below).

Nitric oxide reduction mechanism

Presently, clues for a nitric oxide reduction mechanism lack a satisfactory amount of spectroscopical and kinetic information to provide an unequivocal reaction mechanism. However, several scattered pieces of information can be put together to get a clearer picture. Firstly, the reaction product of NO reduction by *M. thermoacetica* FDP has been proposed to be N_2O , on the basis of the stoichiometry of 2 NO molecules reduced per consumed NADH molecule (6). Although N_2O is the likely expected product of NO reduction by FDPs, the NADH:NO stoichiometry does not ensure that the reaction product is directly N_2O . It could be argued that in steady-state conditions, NO reduction to nitroxyl anion (NO^-) can result in dimerization of the latter and ultimately lead to N_2O . To further confirm N_2O as the reaction product of FDPs, two methods were applied, one to directly measure N_2O production upon NO reduction, and another to definitely exclude generation of nitroxyl (NO^-) (done in collaboration with F.M. Scandurra, P. Sarti, M. Brunori and A. Giuffrè, University of Roma, La Sapienza). Gas-inlet mass spectrometry was used to confirm N_2O production upon NO reduction by *E. coli* FIRd and after calibrating the apparatus with N_2O stock solutions. Nitroxyl production was assayed with metmyoglobin present in the reaction mixture.

Metmyoglobin promptly reacts with nitroxyl (faster than it dimerizes), which results in that the bound nitroxyl reduces the haem-bound Fe^{3+} to Fe^{2+} , forming an iron-nitrosyl with a characteristic spectrum. By mixing metmyoglobin with the reaction mixture whereby FIRD is reducing NO, it was possible to exclude the production of nitroxyl and thus confirm the gas-inlet mass spectrometry results (*our own unpublished data*).

Recently, a mechanism of NO reduction by *M. thermoacetica* FDP has been proposed on the basis of theoretical studies using as template the structure of Mt_FDP (40). In this mechanism, reaction with NO occurs with the diiron centre in the diferrous “resting” state (① in fig. 9.5). Regardless of the NO reduction mechanism, the calculations firmly suggest that the μ -(hydr)oxo bridge between the two irons is a μ -hydroxo, clearing the pending doubt from the crystallographic structure. An overall striking proposal of this reaction mechanism is that one N_2O product can be released prior to inclusion of the two protons and two electrons that complete the reaction scheme: $2\text{NO} + 2\text{H}^+ + 2\text{e}^- \rightarrow \text{N}_2\text{O} + \text{H}_2\text{O}$. The reaction scheme in fig. 9.5 argues against

the proposal that the diiron centre of Mt_FDP could bind two NO molecules, each one binding *end-on* to each Fe (18). It is proposed instead that one of the irons is used to stabilize the formation of a hyponitrite dianion (③ in fig. 9.5). Before this takes place, the bound NO is slightly reduced to a state between NO and nitroxyl anion (② in fig. 9.5), whereas the

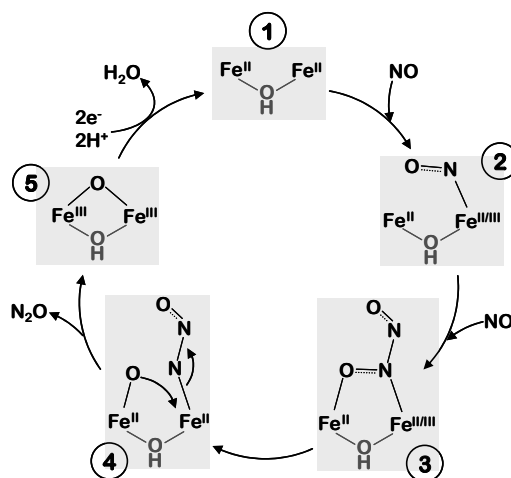


Figure 9.5 – Reaction mechanism proposed for NO reduction by *Moorella thermoacetica* flavodiiron protein.

respective Fe is in an intermediate state between ferric and ferrous. Furthermore,

cleaving the hyponitrite dianion N-O bond is proposed to be the rate-determining step (④ in fig. 9.5), which leaves a transient Fe(IV)=O state, very short-lived due to the highly exergonic formation of a bridging oxo group (⑤ in fig. 9.5). The final step in the proposed reaction mechanism is reduction of the oxo-bridged diiron centre with the two electrons and two protons, releasing water and re-establishing the diferrous “resting” state. Great emphasis is given in this reaction scheme to the relevance of the His25 residue, in stabilizing reaction intermediates. Indeed, mutating this residue resulted in a decrease of activity around 85% (18). Although convincing, this theory-derived mechanism requires confirmation from experimental data.

Nitric oxide vs. oxygen reduction by flavodiiron proteins

Although this dissertation focuses on the growing evidence for a role of flavodiiron proteins in microbial NO detoxification, it must be recalled that this protein family was initially thought to be involved in oxygen detoxification in anaerobes, with special emphasis on the *Desulfovibrio* genus (41). Although several of these enzymes retain oxygen reductase activity, the corresponding molecular genetics studies suggest a role in NO detoxification (6,38,39). Moreover, these organisms have been shown to encode and express canonical respiratory oxidases (42-45), which should account for the greater part of oxygen consumption, with energetic profit. One possible explanation is that FDPs can scavenge oxygen that finds its way to the cytoplasm, or simply to act as a first line of defence against O₂, while the oxygen respiring machinery is being turned-on. If this is the case, it may confer FDPs with a bifunctional role as NO reductases and oxygen scavengers in anaerobes. It should be noted that one of the cyanobacterial FDPs has *in vitro* oxygen NADH:oxygen oxidoreductase activity (the FDP from *Synechocystis* sp. PCC6803 FDP, named SsATF573) (7), which was suggested to be related with oxygen photoreduction, by molecular genetics studies (46).

However, the nitric oxide reductase activity of cyanobacterial FDPs has not yet been measured, which precludes any conclusion about this class of FDPs (class C). Other recent reports propose a role for FDPs in oxygen exposure / oxidative stress alleviation in the corresponding organisms, namely methanogens (10) and *Clostridium acetobutylicum* and *Clostridium aminovalericum* (47).

Promiscuity of substrates regarding the intertwining between NO and oxygen has been observed for the structurally related families of NORs and haem-copper oxidases. Indeed, some NORs are endowed with oxygen reductase activity (48) and some oxidases are able to reduced NO to N₂O (49,50).

In summary, a bi-functional role for flavodiiron proteins as NO and oxygen reductases may be argued, although many more research efforts are required to clarify this ambiguity. It is however clear that flavorubredoxin has a definite role in alleviation of anaerobically-grown *E. coli* against NO-derived stress, with a relative weight in the overall response, depending on several factors. Whether FDPs are NO, O₂ or bifunctional reductases, it is clear that their contribution in the response to either type of stress is only part of the scenario, since the microbial stress response usually involves a multitude of molecular strategies to scavenge the stress-inducing agents (detoxification machinery) and to cope with

the resulting damages to the cellular targets (Fe-S centres, DNA, lipids, haems, thiol groups, etc.).

This panoply of response systems is illustrated in figures 9.6 and 9.7. The transcriptional responses of anaerobically-grown *E. coli* challenged with NO (31)

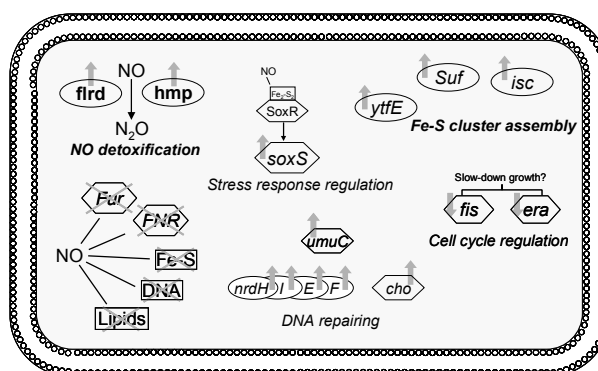


Figure 9.6 – Cellular responses of anaerobically-grown *E. coli* exposed to NO-induced stress, determined by DNA microarray studies (31).

are depicted in fig. 9.6. The scheme displays some of the cellular targets of NO and includes some of the up-regulated genes, namely those encoding NO detoxification systems, Fe-S centre assembly machinery, cell cycle regulators and DNA-repairing enzymes. Figure 9.7 (the same as figure 2.3) displays known detoxification and repair systems proposed to afford protection of *Desulfovibrio* strains against oxidative stress (43).

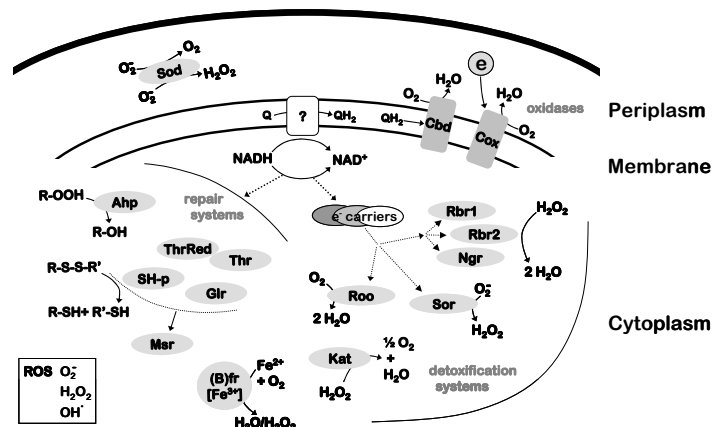


Figure 9.7 - Schematic model of oxygen defence systems in *Desulfovibrio* (43).

Both cases clearly illustrate that FDPs are part of the nitrosative and/or oxidative stress response machineries, which are composed by many other systems, thus conferring robustness (often through redundancy) to microbial survival to these challenges.

Regarding the role of FDPs in nitric oxide detoxification, the physiological relevance of these proteins in the subversion of the host immune system by pathogenic protozoans is a challenging field for future studies.

I find this the appropriate place to share my *personal* thoughts on the work herein described and the field of flavodiiron proteins in general. As a research apprentice, it was a real lesson to grow alongside a new field of research. Now, it is with some amazement that I find many parallels in the way that the research fields of flavohaemoglobins and flavodiiron proteins have evolved. Both were

initially considered to be related with oxygen metabolism and later shown to be involved in the alleviation of NO-induced stress. Presently, it may be observed that possibly the two functions (as well as possibly others) are not mutually exclusive. In conclusion, it is my personal conviction – mostly from discussions with the people I have had the pleasure to work with – that the Flavodiiron Proteins still hold some surprises with regard to their function, in the multitude of organisms where they are present.

REFERENCES

1. Wasserfallen, A., Ragetli, S., Jouanneau, Y., and Leisinger, T. (1998) A family of flavoproteins in the domains Archaea and Bacteria, *Eur J Biochem* **254**(2), 325-332
2. Frazao, C., Silva, G., Gomes, C. M., Matias, P., Coelho, R., Sieker, L., Macedo, S., Liu, M. Y., Oliveira, S., Teixeira, M., Xavier, A. V., Rodrigues-Pousada, C., Carrondo, M. A., and Le Gall, J. (2000) Structure of a dioxygen reduction enzyme from *Desulfovibrio gigas*, *Nat Struct Biol* **7**(11), 1041-1045
3. Saraiva, L. M., Vicente, J. B., and Teixeira, M. (2004) The role of the flavodiiron proteins in microbial nitric oxide detoxification, *Adv Microb Physiol* **49**, 77-129
4. Nolling, J., Ishii, M., Koch, J., Pihl, T. D., Reeve, J. N., Thauer, R. K., and Hedderich, R. (1995) Characterization of a 45-kDa flavoprotein and evidence for a rubredoxin, two proteins that could participate in electron transport from H₂ to CO₂ in methanogenesis in *Methanobacterium thermoautotrophicum*, *Eur J Biochem* **231**(3), 628-638
5. Gomes, C. M., Silva, G., Oliveira, S., LeGall, J., Liu, M. Y., Xavier, A. V., Rodrigues-Pousada, C., and Teixeira, M. (1997) Studies on the redox centers of the terminal oxidase from *Desulfovibrio gigas* and evidence for its interaction with rubredoxin, *J Biol Chem* **272**(36), 22502-22508
6. Silaghi-Dumitrescu, R., Coulter, E. D., Das, A., Ljungdahl, L. G., Jameson, G. N., Huynh, B. H., and Kurtz, D. M., Jr. (2003) A flavodiiron protein and high molecular weight rubredoxin from *Moorella thermoacetica* with nitric oxide reductase activity, *Biochemistry* **42**(10), 2806-2815
7. Vicente, J. B., Gomes, C. M., Wasserfallen, A., and Teixeira, M. (2002) Module fusion in an A-type flavoprotein from the cyanobacterium *Synechocystis* condenses a multiple-component pathway in a single polypeptide chain, *Biochem Biophys Res Commun* **294**(1), 82-87
8. Chen, L., Liu, M. Y., Legall, J., Fareleira, P., Santos, H., and Xavier, A. V. (1993) Purification and characterization of an NADH-rubredoxin oxidoreductase involved in the utilization of oxygen by *Desulfovibrio gigas*, *Eur J Biochem* **216**(2), 443-448
9. Gomes, C. M., Vicente, J. B., Wasserfallen, A., and Teixeira, M. (2000) Spectroscopic

- studies and characterization of a novel electron-transfer chain from *Escherichia coli* involving a flavorubredoxin and its flavoprotein reductase partner, *Biochemistry* **39**(51), 16230-16237
10. Seedorf, H., Dreisbach, A., Hedderich, R., Shima, S., and Thauer, R. K. (2004) F420H2 oxidase (FprA) from *Methanobrevibacter arboriphilus*, a coenzyme F420-dependent enzyme involved in O₂ detoxification, *Arch Microbiol* **182**(2-3), 126-137
 11. Andersson, J. O., Hirt, R. P., Foster, P. G., and Roger, A. J. (2006) Evolution of four gene families with patchy phylogenetic distributions: influx of genes into protist genomes, *BMC Evol Biol* **6**, 27
 12. Andersson, J. O., Sjogren, A. M., Davis, L. A., Embley, T. M., and Roger, A. J. (2003) Phylogenetic analyses of diplomonad genes reveal frequent lateral gene transfers affecting eukaryotes, *Curr Biol* **13**(2), 94-104
 13. Schilling, O., Vogel, A., Kostecky, B., Natal da Luz, H., Spemann, D., Spath, B., Marchfelder, A., Troger, W., and Meyer-Klaucke, W. (2005) Zinc- and iron-dependent cytosolic metallo-beta-lactamase domain proteins exhibit similar zinc-binding affinities, independent of an atypical glutamate at the metal-binding site, *Biochem J* **385**(Pt 1), 145-153
 14. Solomon, E. I., Brunold, T. C., Davis, M. I., Kemsley, J. N., Lee, S. K., Lehnert, N., Neese, F., Skulan, A. J., Yang, Y. S., and Zhou, J. (2000) Geometric and electronic structure/function correlations in non-heme iron enzymes, *Chem Rev* **100**(1), 235-350
 15. Ghisla, S., and Edmonson, D. E. (2001) Flavin Coenzymes. In: *Encyclopedia of Life Sciences*, MacMillan Publishers Ltd, Nature Publishing Group / www.els.net
 16. Meyer, J., and Moulis, J. M. (2001) Rubredoxin. In: Messerschmidt, A., Huber, R., Poulos, T., and Wiegardt, K. (eds). *Handbook of Metalloproteins*, 1 Ed., John Wiley & Sons, Chichester
 17. Vicente, J. B., and Teixeira, M. (2005) Redox and spectroscopic properties of the *Escherichia coli* nitric oxide-detoxifying system involving flavorubredoxin and its NADH-oxidizing redox partner, *J Biol Chem* **280**(41), 34599-34608
 18. Silaghi-Dumitrescu, R., Kurtz, D. M., Jr., Ljungdahl, L. G., and Lanzilotta, W. N. (2005) X-ray crystal structures of *Moorella thermoacetica* FprA. Novel diiron site structure and mechanistic insights into a scavenging nitric oxide reductase, *Biochemistry* **44**(17), 6492-6501
 19. Victor, B. L., Vicente, J. B., Rodrigues, R., Oliveira, S., Rodrigues-Pousada, C., Frazao, C., Gomes, C. M., Teixeira, M., and Soares, C. M. (2003) Docking and electron transfer studies between rubredoxin and rubredoxin:oxygen oxidoreductase, *J Biol Inorg Chem* **8**(4), 475-488
 20. Vicente, J. B., Scandurra, F. M., Rodrigues, J. V., Brunori, M., Sarti, P., Teixeira, M., and Giuffre, A. (2006) Kinetics of electron transfer from NADH to the *Escherichia coli* nitric oxide reductase flavorubredoxin, *Febs J*
 21. Mittl, P. R., Berry, A., Scrutton, N. S., Perham, R. N., and Schulz, G. E. (1994) Anatomy of an engineered NAD-binding site, *Protein Sci* **3**(9), 1504-1514
 22. Bocanegra, J. A., Scrutton, N. S., and Perham, R. N. (1993) Creation of an NADP-dependent pyruvate dehydrogenase multienzyme complex by protein engineering, *Biochemistry* **32**(11), 2737-2740
 23. Warman, A. J., Roitel, O., Neeli, R., Girvan, H. M., Seward, H. E., Murray, S. A., McLean, K. J., Joyce, M. G., Toogood, H., Holt, R. A., Leys, D., Scrutton, N. S., and

- Munro, A. W. (2005) Flavocytochrome P450 BM3: an update on structure and mechanism of a biotechnologically important enzyme, *Biochem Soc Trans* **33**(Pt 4), 747-753
24. Gardner, A. M., Helmick, R. A., and Gardner, P. R. (2002) Flavorubredoxin, an inducible catalyst for nitric oxide reduction and detoxification in *Escherichia coli*, *J Biol Chem* **277**(10), 8172-8177
 25. Hutchings, M. I., Mandhana, N., and Spiro, S. (2002) The NorR protein of *Escherichia coli* activates expression of the flavorubredoxin gene *norV* in response to reactive nitrogen species, *J Bacteriol* **184**(16), 4640-4643
 26. Justino, M. C., Goncalves, V. M., and Saraiva, L. M. (2005) Binding of NorR to three DNA sites is essential for promoter activation of the flavorubredoxin gene, the nitric oxide reductase of *Escherichia coli*, *Biochem Biophys Res Commun* **328**(2), 540-544
 27. Tucker, N., D'Autreaux, B., Spiro, S., and Dixon, R. (2005) DNA binding properties of the *Escherichia coli* nitric oxide sensor NorR: towards an understanding of the regulation of flavorubredoxin expression, *Biochem Soc Trans* **33**(Pt 1), 181-183
 28. Tucker, N. P., D'Autreaux, B., Spiro, S., and Dixon, R. (2006) Mechanism of transcriptional regulation by the *Escherichia coli* nitric oxide sensor NorR, *Biochem Soc Trans* **34**(Pt 1), 191-194
 29. D'Autreaux, B., Tucker, N. P., Dixon, R., and Spiro, S. (2005) A non-haem iron centre in the transcription factor NorR senses nitric oxide, *Nature* **437**(7059), 769-772
 30. Mukhopadhyay, P., Zheng, M., Bedzyk, L. A., LaRossa, R. A., and Storz, G. (2004) Prominent roles of the NorR and Fur regulators in the *Escherichia coli* transcriptional response to reactive nitrogen species, *Proc Natl Acad Sci U S A* **101**(3), 745-750
 31. Justino, M. C., Vicente, J. B., Teixeira, M., and Saraiva, L. M. (2005) New genes implicated in the protection of anaerobically grown *Escherichia coli* against nitric oxide, *J Biol Chem* **280**(4), 2636-2643
 32. Pullan, S. T., Gidley, M. A., Jones, R. A., Barrett, J., Stevanin, T. M., Read, R. C., Green, J., and Poole, R. K. (2006) Nitric Oxide in Chemostat-Cultured *Escherichia coli* is Sensed by Fnr and Other Global Regulators; Unaltered Methionine Biosynthesis Indicates Lack of S-Nitrosation, *J Bacteriol*
 33. Spiro, S. (2006) Nitric oxide-sensing mechanisms in *Escherichia coli*, *Biochem Soc Trans* **34**(Pt 1), 200-202
 34. Poole, R. K. (2005) Nitric oxide and nitrosative stress tolerance in bacteria, *Biochem Soc Trans* **33**(Pt 1), 176-180
 35. Spiro, S. (2007) Regulators of bacterial responses to nitric oxide, *FEMS Microbiol Rev*
 36. Sarti, P., Fiori, P. L., Forte, E., Rappelli, P., Teixeira, M., Mastronicola, D., Sancier, G., Giuffre, A., and Brunori, M. (2004) *Trichomonas vaginalis* degrades nitric oxide and expresses a flavorubredoxin-like protein: a new pathogenic mechanism?, *Cell Mol Life Sci* **61**(5), 618-623
 37. Gomes, C. M., Giuffre, A., Forte, E., Vicente, J. B., Saraiva, L. M., Brunori, M., and Teixeira, M. (2002) A novel type of nitric-oxide reductase. *Escherichia coli* flavorubredoxin, *J Biol Chem* **277**(28), 25273-25276
 38. Silaghi-Dumitrescu, R., Ng, K. Y., Viswanathan, R., and Kurtz, D. M., Jr. (2005) A flavo-diiron protein from *Desulfovibrio vulgaris* with oxidase and nitric oxide reductase activities. Evidence for an in vivo nitric oxide scavenging function,

Biochemistry **44**(9), 3572-3579

39. Rodrigues, R., Vicente, J. B., Felix, R., Oliveira, S., Teixeira, M., and Rodrigues-Pousada, C. (2006) Desulfovibrio gigas flavodiiron protein affords protection against nitrosative stress in vivo, *J Bacteriol* **188**(8), 2745-2751
40. Blomberg, L. M., Blomberg, M. R., and Siegbahn, P. E. (2007) Theoretical study of the reduction of nitric oxide in an A-type flavoprotein, *J Biol Inorg Chem* **12**(1), 79-89
41. Fareleira, P., Santos, B. S., Antonio, C., Moradas-Ferreira, P., LeGall, J., Xavier, A. V., and Santos, H. (2003) Response of a strict anaerobe to oxygen: survival strategies in Desulfovibrio gigas, *Microbiology* **149**(Pt 6), 1513-1522
42. Lemos, R. S., Gomes, C. M., Santana, M., LeGall, J., Xavier, A. V., and Teixeira, M. (2001) The 'strict' anaerobe Desulfovibrio gigas contains a membrane-bound oxygen-reducing respiratory chain, *FEBS Lett* **496**(1), 40-43
43. Dolla, A., Kurtz, D. M., Jr., Teixeira, M., and Voordow, G. (2007) Biochemical, proteomic and genetic characterization of oxygen survival mechanisms in sulphate-reducing bacteria of the genus Desulfovibrio. In: Barton, L. L., and Hamilton, W. A. (eds). *Sulphate-Reducing Bacteria: Environmental and Engineered Systems*, Cambridge Univ. Press
44. Das, A., Silaghi-Dumitrescu, R., Ljungdahl, L. G., and Kurtz, D. M., Jr. (2005) Cytochrome bd oxidase, oxidative stress, and dioxygen tolerance of the strictly anaerobic bacterium Moorella thermoacetica, *J Bacteriol* **187**(6), 2020-2029
45. Machado, P., Felix, R., Rodrigues, R., Oliveira, S., and Rodrigues-Pousada, C. (2006) Characterization and expression analysis of the cytochrome bd oxidase operon from Desulfovibrio gigas, *Curr Microbiol* **52**(4), 274-281
46. Helman, Y., Tchernov, D., Reinhold, L., Shibata, M., Ogawa, T., Schwarz, R., Ohad, I., and Kaplan, A. (2003) Genes encoding A-type flavoproteins are essential for photoreduction of O₂ in cyanobacteria, *Curr Biol* **13**(3), 230-235
47. Kawasaki, S., Watamura, Y., Ono, M., Watanabe, T., Takeda, K., and Niimura, Y. (2005) Adaptive responses to oxygen stress in obligatory anaerobes Clostridium acetobutylicum and Clostridium aminovalericum, *Appl Environ Microbiol* **71**(12), 8442-8450
48. Flock, U., Watmough, N. J., and Adelroth, P. (2005) Electron/proton coupling in bacterial nitric oxide reductase during reduction of oxygen, *Biochemistry* **44**(31), 10711-10719
49. Butler, C., Forte, E., Maria Scandurra, F., Arese, M., Giuffre, A., Greenwood, C., and Sarti, P. (2002) Cytochrome bo(3) from Escherichia coli: the binding and turnover of nitric oxide, *Biochem Biophys Res Commun* **296**(5), 1272-1278
50. Forte, E., Urbani, A., Saraste, M., Sarti, P., Brunori, M., and Giuffre, A. (2001) The cytochrome cbb3 from Pseudomonas stutzeri displays nitric oxide reductase activity, *Eur J Biochem* **268**(24), 6486-6491